Development of a coronary artery bypass graft with the aid of tissue engineering: *Investigation of gene expression on seeded compliant nanocomposite conduits*

A thesis submitted for the degree of
Doctor of Philosophy (Ph.D)

By

Dina Shantilal Vara B.sc (Hons)

University College London
Biomaterial & Tissue Engineering Centre
University Department of Surgery

2009

Abstract

Background: Coronary artery bypass graft surgery is a commonly performed procedure. The internal thoracic or mammary artery is gaining widespread preference as the bypassing conduit. Synthetic grafts used for large diameter substitutes are successful but have dismal patency as small diameter (< 6mm) grafts due to compliance mismatch and thrombogeniecity. To overcome this, cell adhesion to synthetic scaffolds is used to construct tissue engineered grafts. For this to be successful a precise understanding of the behaviour of cells at the synthetic graft surface is required under static and haemodynamic conditions.

The aim of this research was to investigate gene expression of seeded human umbilical vein endothelial cells (HUVEC) on the novel compliance conduit under physiological flow condition; furthermore various physiological shear stress preconditioning was used to investigate adhesion of HUVEC on the conduit.

Methods: HUVEC seeding of a novel polymer nanocomposite was undertaken. An optimal method for extracting mRNA from HUVEC seeded onto conduits was then validated. The optimal seeding conditions for the conduits were delineated. Haemodynamic conditions were applied to the seeded conduits and gene expression was investigated using polymerase chain reaction (PCR). Shear stress was used to assess the ideal preconditioning environment.

Results: Studies of nanocomposite graft material and cultured HUVEC proved that the novel nanocomposite polymer was non-toxic to cells and supported good rates of growth. To provide useful flow studies an extrusion-phase inversion method was used to reproducibly fabricate conduits of this nanocomposite with compliance similar to the native artery. The optimal seeding density of the conduits was found to be 1.2×10^4 cells/cm^2. It was demonstrated that RNA can be extracted from seeded conduits and I succeeded in showing the optimal technique.

This study culminates in the combination of all these techniques when the gene expression of HUVEC under flow was studied after physiological shear stress was applied on the conduits. Genes significantly upregulated included TGF-β1, COL-1 and PECAM-1. Low shear stress demonstrated the optimal preconditioning environment with increasing expression of VEGFR-1 and VEGFR-2 genes.

Conclusion: This thesis demonstrated that novel nanocomposite small diameter bypass graft can be seeded with human endothelial cells.

Table of contents

List of figures

Chapter 1: Cardiovascular tissue engineering

Chapter 2: Molecular aspects of haemodynamics and vascular tissue engineering: An overview

Chapter 3: Materials and methods

Chapter 5: In vitro cytotoxicity analysis of nanocomposite

Chapter 7: EC & nanocomposite hybrid grafts: seeding and culture

Chapter 8: The effect of shear stress on human endothelial cells seeded on cylindrical conduits: An investigation of gene expression

Figure 9-5. Typical ScEM of nanocomposite conduits: A (unseeded conduit), B (Pre-flow conduit), C (S_1 conduit), D (S_4 conduit), E (P_1 conduit), F (P_4 conduit), G (SR_1 conduit), H (SR_4 conduit), I (PR_1 conduit) and J (PR_4 conduit). 257

List of Tables

Chapter 1: Cardiovascular tissue engineering

Chapter 2: Molecular aspects of haemodynamics and vascular tissue engineering: An overview

Chapter 3: Materials and methods

Chapter 6: Fabrications of a small diameter compliant nanocomposite coronary artery bypass graft

Chapter 7: EC & nanocomposite hybrid grafts: seeding and culture

Chapter 8: The effect of shear stress on human endothelial cells seeded on cylindrical conduits: An investigation of gene expression

Chapter 9: Shear stress preconditioning of human endothelial cell seeded on compliant nanocomposite conduits: A study of gene expression

Publications

Vara DS, Punshon G, Sales KM, Hamilton G, Seifalian AM. Endothelial cell retention on a viscoelastic nanocomposite vascular conduit is improved by exposure to shear stress preconditioning prior to physiological flow. Artificial Organs, In press December 2008

Vara DS, Punshon G, Sales KM, Hamilton G, Seifalian AM. The effect of shear stress on human endothelial cells seeded on cylindrical viscoelastic conduits: an investigation of gene expression. Biotechnol Appl Biochem. 2006 Nov;45(Pt 3):119-30.

Kannan RY, Salacinski HJ, Vara DS, Odlyha M, Seifalian AM. Review paper: principles and applications of surface analytical techniques at the vascular interface. J Biomater Appl. 2006 Jul;21(1):5-32.

Vara DS, Salacinski HJ, Kannan RY, Bordenave L, Hamilton G, Seifalian AM. Cardiovascular tissue engineering: state of the art. Pathol Biol (Paris). 2005 Dec;53(10):599-612.

Punshon G, Vara DS, Sales KM, Kidane AG, Salacinski HJ, Seifalian AM. Interactions between endothelial cells and a poly(carbonate-silsesquioxane-bridge-urea)urethane.Biomaterials. 2005 Nov;26(32):6271-9.

Vara DS, Punshon G, Sales KM, Salacinski HJ, Dijk S, Brown RA, Hamilton G, Seifalian AM. Development of an RNA isolation procedure for the characterisation of human endothelial cell interactions with polyurethane cardiovascular bypass grafts. Biomaterials. 2005 Jun;26(18):3987-93.

Presentations

Oral presentation

Vara DS, Punshon G, Sales K.M, Salacinski H.J, Hamilton G, Seifalian AM.
Investigation of the effects of flow on human endothelial cells seeded in cylindrical conduits representing vascular grafts. International Meeting on Tissue Engineered Blood Vessels, Academicum, Göteborg University, Sweden, *April 23-24, 2005.*

Vara DS, Punshon G, Sales K.M, Salacinski H.J, Brown R, Hamilton G, Seifalian AM.
Development of a hybrid cardiovascular graft for coronary applications. EPSRC Summer School in Tissue Engineering, University of Nottingham, UK. *September 6-10 2004.*

Vara DS, Punshon G, Sales K.M, Salacinski H.J, Hamilton G, Seifalian AM.
Fabrication of small-diameter vascular grafts for coronary bypass surgery. Queen Mary University, Department of Materials, UK, *June 8 2004.*

Vara DS, Punshon G, Sales K.M, Salacinski H.J, Hamilton G, Seifalian AM.
Development of an RNA extraction procedure from human endothelial cells seeded onto the surface of a polymer used in bypass grafts. International Society for Applied Cardiovascular Biology, 9th Biennial Meeting, Savannah, Georgia, USA, *March 10-13 2004.*

Vara DS, Sales K.M, Hamilton G, Seifalian AM.
The effect of MGF on human umbilical vein smooth muscle cell proliferation. Royal Free Hospital Surgical Grand Round, UK, *March 5 2004.*

Poster presentation

Vara DS, Punshon G, Sales K.M, Salacinski H.J, Hamilton G, Seifalian AM.
A model study of the alterations in gene expression that occurs following the application of shear stress in cylindrical conduits representing vascular grafts. 19th European Conference on Biomaterials including the 4th Young Scientists Forum and Consensus Meeting, Hilton Sorrento Palace, Sorrento Naples Italy, *September 11-16 2005.*

Abbreviations

AB	Alamar Blue™
ADS	Acquisition Recording System
AIF	Allograft Inflammatory Factor
ANOVA	Analysis Of Variance
AU	Arbitrary Units
AVS	Arterioveneous Shunt
BAEC	Bovine Aortic Endothelial Cells
BASMC	Bovine Aortic Smooth Muscle Cells
bFGF	Basic Fibroblast Growth Factor
BPMEC	Bovine Pulmonary Microvascular Endothelial Cells
BrdU	Bromodeoxyuridine
CABG	Coronary Artery Bypass Graft
CCM	Cell Culture Medium
cDNA	Complementary Deoxyribonucleic Acid
COL-1	Collagen type 1
CYP	Cytochromes
Dacron	Polyethylene-terephthalate
DMAC	Dimethylacetamide
DNA	Deoxyribonucleic Acid
EC	Endothelial Cells
ECM	Extracellular Matrix
EDTA	Ethylenediamine Tetraacetic Acid
EGF	Epidermal Growth Factor
eNOS	Endothelial Nitric Oxide Synthase
ePTFE	Expanded Polytetraflouroethylene
Fb	Fibroblasts
FBS	Foetal Bovine Serum
FGF	Fibroblast Growth Factor
FWC	Flow Waveform Conditioner
GAPDH	Glyderaldehyde-3-Phosphate Dehydrogenase
GITC	Guanidine Isothiocyanate
HAEC	Human Aortic Endothelial Cells
HAMVEC	Human Adipose Microvessel Endothelial Cells
HCAEC	Human Coronary Artery Endothelial Cells
HSPG	Heparan Sulphate Proteoglycan
HUASMC	Human Umbilical Artery Smooth Muscle Cells
HUVEC	Human Umbilical Vein Endothelial Cells
ICAM	Intracellular Adhesion Molecule
IGF	Insulin Growth Factor
iNOS	Inducible Nitric Oxide Synthase
LAD	Left anterior descending artery
LCA	Left Coronary Artery
LDH	Lactate Dehydrogenase
LDI	Lysine-di- isocyanate
LITA	Left Internal Thoracic Artery
MCP	Monocyte Chemotactic Protein
MDI	Methylene diisocyanate

MIH	Myointimal Hyperplasia
mmHg	Millimeter of mercury
MMP	Matrix Metalloproteinase
mRNA	Messenger RNA
MYD88	Myeloid Differentiation Primary Response Gene 88
NO	Nitric Oxide
NOS	Nitric oxide synthase
PAR	Protease Activator Receptor
PBS	Phosphate Buffer Saline
PCU	Poly(Carbonate-Urea)Urethane
PCR	Polymersase Chain Reaction
PDGF	Platelet Derived Growth Factor
PDGFR	Platelet Derived Growth Factor Receptor
PDMS	Poly(dimethylsiloxane)
PDV	Pulse Doppler Velocitimeter
PECAM	Platelet Endothelial Cell Adhesion Molecule
PET	Polyethylene terephthalate
PG	Pico green
PGA	Polyglycolic Acid
PLLA	Poly-L-Lactic Acid
POSS	Polyhedral Oligomeric Silsesquioxane
RAEC	Rat Aortic Endothelial Cells
RBMSC	Rabbit Bone Marrow Stromal Cells
RCA	Right Coronary Artery
RNA	Ribonucleic Acid
RPD	Right Posterior Descending Artery
RT-PCR	Reverse Transcriptase-Polymerase Chain Reaction
ScEM	Scanning Electron Microscopy
SD	Standard Deviation
SEM	Standard Error Mean
SI	International System
SMC	Smooth Muscle Cells
SV	Sapheneous Vein
TAE	Tris Acetate-EDTA
TCP	Tissue Culture Plastic/Plates
TGF	Transforming Growth Factor
TMF	Transonic Medical Flowmeter
tPA	Tissue plasminogen activator
uPA	Urokinase-type Plasminogen Activator
US	Ultrasound Duplex
VCAM	Vascular Cellular Adhesion Molecule
VEGF	Vascular Endothelial Growth Factor
VEGFR	Vascular Endothelial Growth Factor Receptor
VOR	Variable Outflow Resistance
VSECP	Variable Speed Electromagnetic Pump
WSS	Wall Shear Stress
WTS	Wall Tracking System

Glossary

Anastomosis: The connection between the native artery and a vascular graft

Angioplasty: The repair of a blood vessel by inserting a balloon-tipped catheter to unclog it

Aorta: Largest artery in the body. Runs from the heart

Arterioles: Smaller type of arteries, found before capillaries in the vascular tree

Arteriosclerosis: Arterial disease causing stiffening and dilation of the major arteries

Atherosclerosis: Arterial disease causing the narrowing of one or more major artery

Autologous: From the same organism

Biocompatability: is the ability of a material to perform with an appropriate host response in a specific application

Biodegradable: is the process by which organic substances are broken down by other living organisms

Cardiac Cycle: One complete heartbeat, consisting of one complete contraction and relaxation of the heart muscle

Collagen: An extracellular protein found in blood vessel walls, exhibited as fibres of high stiffness

Compliance: Measure of radial dissention with respect to pressure change

Coronary artery bypass graft: is a surgical procedure performed to relieve angina and reduce the risk of death from coronary artery disease

Cytotoxicity: is the quality of being toxic to cells. Examples of toxic agents are a chemical substance or an immune cell

Dacron (PET): Polymer used to create woven or knitted vascular grafts

Dynamic Test: When a material is stretched and effects caused by movement, such as viscoelasticity, occur

Elastic: An object's ability to return to its original shape after the removal of a deforming load

Endothelial cells: Cells lining the luminal surface of blood vessels, making up the endothelium

Extracellular matrix: is the defining feature of connective tissue

Gastroepiploic Artery: Artery lying close to the stomach, sometimes used as a vascular bypass graft

Gene expression: or simply expression is the process by which a gene's DNA sequence is converted into functional proteins of the cell. Non-protein coding genes (e.g. rRNA genes, tRNA genes) are not translated into protein

Haemodynamics: The study of blood flow

Heterologous: Derived from a different specie

Hydrolysis: is a chemical reaction or process in which a chemical compound reacts with water. This is the type of reaction that is used to break down polymers.

Internal Mammary Artery: Artery situated close to the heart, sometimes used as a vascular graft in coronary artery bypass surgery

Intima: Inner layer of a blood vessel

Intimal hyperplasia: Wall thickening of a vascular graft, especially at the anastomosis

In vitro: Performed experimentally in a controlled environment, not in an organism

In vivo: Performed in an organism

Left coronary artery: arises from the aorta above the left cusp of the aortic valve.

Luminal: Lying radially internal in a blood vessel or graft

Millimeter of mercury (mmHg): is a non-SI unit of pressure. It is the atmospheric pressure that supports a column of mercury 1 millimeter high

Morphology: The study of the form and structure of an object

Myointimal: Concerning the intima and media of a blood vessel

Neo-adventitia: The adventitial layer forming on a vascular graft after implantation

Neo-intima: The intimal layer forming on the luminal surface of a vascular graft after implantation

Occlusion: Closing/blocking of blood vessel or graft

Patency: State of open

Pathologic: Involving disease

Peripheral: Further from the heart

Plaque: Fatty build up on the luminal surface of a vascular wall

Platelets: Red blood cells

Polymer: Molecules with large molecular mass composed of repeating structural units, or monomers, connected by covalent chemical bonds

Polyurethane: is any polymer consisting of a chain of organic units joined by urethane links

Prosthetic: A device, either external or implanted, that substitutes for or supplements a missing or defective part of the body

Proximal: Close to heart

Pulse Pressure: The difference between systolic and diastolic pressure

Radial Artery: Artery found in the arm

Right coronary artery: originates above the right cusp of the aortic valve

Sapheneous Vein: Vein found in the leg

Shear Stress: is a stress state where the stress is parallel or tangential to a face of the material, as opposed to normal stress when the stress is perpendicular to the face

Stenosis: A constriction of a duct or passage

Stent: A small, expandable wire form or perforated tube used for opening a blocked vessel

Strain: Measure of the deformation of a body in response to an applied force

Stroke Volume: The amount of blood that gets released from the heart into the arterial system during one cardiac cycle

Suture: A joining of the edges of a wound or the like by stitching or some similar process

Systole: The normal rhythmical contraction of the heart, during which the blood in the chambers is forced onward

Teflon (PTFE): Polymer used to create vascular grafts

Thrombus: A fibrous clot that forms in and obstructs a blood vessel

Tissue Engineering: is the use of a combination of cells, engineering and materials methods, and suitable biochemical and physio-chemical factors to improve or replace biological functions

Tunica Adventitia: External layer of a blood vessel

Tunica Intima: Internal (luminal) layer of a blood vessel

Tunica Media: Middle layer of a blood vessel that resides between the intima and the media

Vascular Bypass Graft: Conduit used to bypass a diseased blood vessel

Vasoconstriction: Narrowing of blood vessel

Vasodilation: Dilation of blood vessel

Venules: Small veins joining capillaries and larger veins

Viscoelastic: Pertaining to a substance having both viscous and elastic properties

Viscosity: The property of a fluid that resists the force tending to cause the fluid to flow

Young's Modulus: A coefficient of elasticity of a substance, expressing the ratio between a stress that acts to change the length of a body and the fractional change in length caused by this force

Statement of originality

I, Dina Shantilal Vara, confirm that the work presented in this thesis is my own but had help with specific areas. All assistance was from other members of the University Department of Surgery except where information has been derived from other sources, I confirm that this has been indicated in the thesis.

Calculations of shear stress were performed by Professor Alexander Seifalian using an ultrasound device with a wall tracking system. Innes Clatworthy from the Department of Electron Microscopy within the Department of Pathology was responsible for all the ScEM pictures. The automated bio-processor employed in Chapter 6 for extruding conduits was devised by Mr Sandip Sarkar, fellow Ph.D. student and the electrospraying procedure was carried out at Queen Mary University of London, Materials Dept., Mile End Road, London E1 4NS. Dr. Henryk Salacinski and Arnold Derbyshire were responsible for the nanocomposite polymer design.

The physiological flow circuit have a long history in the department with contributions to their development from Professor Alexander Seifalian, Mrs Karen Cheetham and amongst others. More recent refinements have critically allowed them to achieve long-term sterility and were from Mr. Geoff Punshon and myself.

Acknowledgements

First, my sincerest thanks go to supervisor Professor Alexander M Seifalian, whose unending supervision, help and patience have been invaluable. Thank you for giving me the opportunity to carry out this project and for the constant encouragement.
I would like to also thank my co-supervisor, Professor Parvin Shamlou.

I would like to express my appreciation to Professor George Hamilton for his encouragement and the support especially at the conferences that I have attended to present my work.

Sincerest thanks also go to Mr. Geoffrey Punshon and Dr. Kevin Sales for all the help in the laboratory. This thesis would not have been possible without all their help and advice. I am very grateful for the constant support but most of all for their friendship.

I would also like to thank Mr. Sandip Sarkar for the ceaseless help with Chapter 6. It would not have been possible to produce conduits without your expertise.

There are many others who have given me constant support and encouragement within the Department of Surgery. Special thanks to Bernard Cousins, Valerie Wilson, Arnold Derbyshire, Professor Mohan Edirisinghe, Professor Barry Fuller, Professor Kirk, but most particularly Karen Cheetham and the rest of my colleagues at the department.

I would also like to thank EPSRC for the financial support.

Finally, I would like to thank Ozan Gundogdu, who has been put through every high and low this Ph.D. has thrown at me. Thank you to my dearest mother, for her patience and encouragement. Thanks also to my sisters, Kiran and Shital I cannot even begin to express my gratitude to you both, you have helped and supported me in so many ways. Finally I cannot forget my younger brother, Vinay for the laughter; it wouldn't have been the same without you!

This thesis is dedicated in its entirety to my beloved late father (1950-2003) who sadly suffered from coronary artery disease

1

Cardiovascular tissue engineering

1.1 Introduction

Occlusive cardiovascular disease of the blood vessel is the main cause of death in the aged western population (1). The symptoms and treatment depend on which set (or sets) of arteries are affected. However, the symptomatic prevalence is mainly in vessels that are smaller than 6 mm internal diameter. In coronary disease, atherosclerotic plaques (inflamed fatty deposits in the blood vessel wall) obstruct the coronary arteries (2). If interventional procedures (angioplasty and stenting) are not successful the only therapeutic option left is to carry out reconstructive or bypass surgery (3). Veins or arteries from elsewhere in the patient's body are grafted from the aorta to the coronary arteries, bypassing coronary artery narrowing's thereby improving myocardial blood supply. Coronary artery bypass graft (CABG) surgery was originally performed using saphenous vein (SV) (4) from the leg to carry blood around the obstruction. In the 1970's and 1980's, cardiothoracic surgeons discovered that an artery from the inside of the chest wall, the internal thoracic artery (also called the internal mammary artery), could be used instead of vein for the bypass grafts. It was shown that these grafts stayed open longer than SV grafts (5). Today most CABG operations are performed using a combination of bypass grafts including this artery and some SV. The main problem is that many patients do not have veins or arteries suitable for grafting due to preexisting vascular disease or

previous surgery. Hence the development of small diameter vascular grafts has been a rapidly growing area of research (6).

Prosthetic materials that are currently used clinically are expanded polytetrafluoroethylene (ePTFE) or knitted/woven poly(ethylene)terephthalate (Dacron) and have been successful as large vessel substitutes in peripheral artery disease, but have not proven useful for long-term application as small diameter arterial conduits (7;8). This is accentuated in less than 6 mm grafts or in areas of low-flow. Failure has occurred in both infrainguinal and coronary circulations where very high-flow rates are essential. Graft failure is associated with a number of critical factors. Both material mismatch between the graft and the host artery and junction haemodynamics are cited as being major factors in disease formation at the junction (9). Baird and Abbott's hypothesis that a difference in circumferential compliance of a vascular graft and the host artery is detrimental to graft performance (10;11). The nature of compliance mismatch is complex, as it is determined by the compliance differences of the host artery, the anastomosis, and the graft itself. Such failures are often seen primarily at the downstream end of the graft. This asymmetry suggests that a flow mechanism of some sort is responsible. The haemodynamic consequences of mismatch include increased impedance and decreased distal perfusion as well as disturbed flow, turbulence and low shear stress rates (12). These changes lead to the development of myointimal hyperplasia and thrombosis around the anastomosis, finally resulting in graft failure, particularly in small diameter vessels (13). Previous experimental and numerical studies have shown that lower than normal wall shear stresses (WSSs) and trapping of particles (such as cells and other blood elements) are observed at junctions between a stiff graft and compliant artery (14). Some efforts have been made over the years to engineer prosthetic grafts with compliance similar to that found in human artery, so that the pulsating blood can flow from the viscoelastic graft into the compliant artery (15). To date these attempts have still failed due to a variety of reasons; highly noncompliant and inferior graft materials.

The absence of EC at the luminal surface of prosthetic vascular grafts potentates' thrombosis and neointimal hyperplasia, which are common causes of graft failure in humans. Because adding functional endothelium to artificial grafts potentially could overcome these problems, endothelialisation of prosthetic vascular grafts has been a goal in clinical medicine for well over two decades. Up to now, this goal has not been

achieved. Autologous cells grown in culture tend to lose their differentiated phenotype and therefore lack the adhesive strength to resist the force of flowing blood when the graft is implanted *in vivo*. Hence, loss of the cells from the implanted graft is one of the most vexing problems in this field.

This chapter gives an overview of the conduits clinically used for CABG surgery, history of patency and graft failure. A crucial factor for the development of a successful vascular graft is the ability of the artificial device to undergo endothelialisation. Therefore, in this Chapter the biology of ECs has been described in detail, with particular attention to their importance in more than just a lining of blood vessels.

1.1.1 Coronary artery structure

Oxygenated blood is distributed to the heart via the coronary arteries that are on the surface of the heart. The two primary coronary arteries are the left main coronary artery and the right coronary artery. These originate near the cusps of the aortic valve. The left coronary artery (LCA), which divides into the left anterior descending (LAD) artery and the circumflex branch, supplies blood to the left ventricle and left atrium. The right coronary artery (RCA), which divides into the right posterior descending (RPD) and acute marginal arteries, supplies blood to the right ventricle, right atrium, and sinoatrial node (cluster of cells in the right atrial wall that regulates the heart's rhythmic rate). Additional arteries branch off the two main coronary arteries to supply the heart muscle with blood. Since coronary arteries deliver blood to the heart muscle, any coronary artery disorder or disease can have serious implications by reducing the flow of oxygen and nutrients to the heart, which may lead to myocardial infarction and possibly death.

1.1.2 Conduits used for bypass

With the rise in the number of bypass surgeries, more patients are undergoing repeat coronary revascularisation. Veins that are used either have their valves removed or are reversed so that the valves in them do not occlude blood flow in the graft. Vein grafts are not the preferred choice as arterial substitutes. They are fragile and sometimes damaged when transplanted into the arterial system. Over time they undergo structural

and functional changes that can lead to thrombosis, calcification and premature occlusion of the graft.

Typically, the left internal thoracic artery (LITA) (previously referred to as left internal mammary artery or LIMA) and right internal thoracic artery (RITA) are used for coronary bypass surgery (16). In the most common situation the LITA was used as a graft to the LAD coronary artery (Figure 1-1 A) and SV grafts were used from the aorta to the other coronary vessels (Figure 1-1 B). LITA grafts are longer lasting than vein grafts, both because the artery is more robust than a vein and because, being already connected to the arterial tree, the LITA need only be grafted at one end (17). Alternatively, an artery such as the radial artery from the arm or gastroepiploic artery (GEA) from the stomach may be used in place of a vein. The latter choice is a difficult operation to perform and it has not become the bypass graft of choice (18). The radial artery graft has an advantage as they are easy to prepare but has the occurrence of graft occlusions (19).

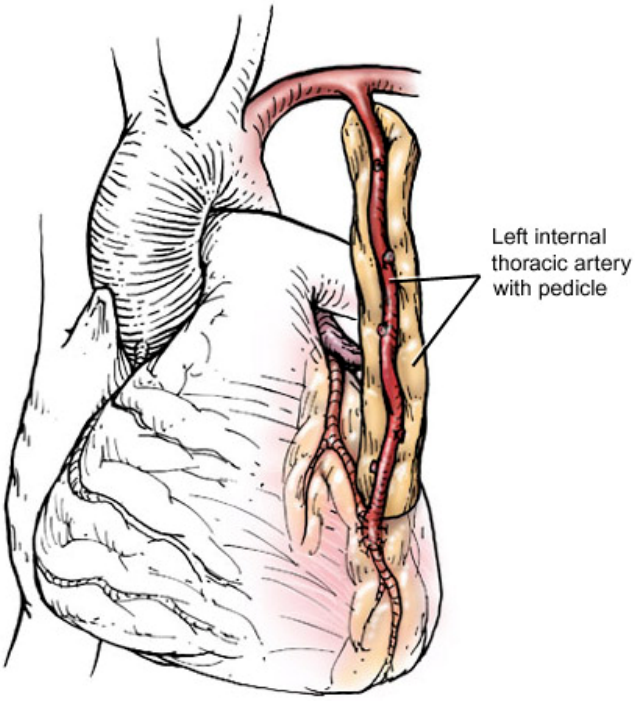

A

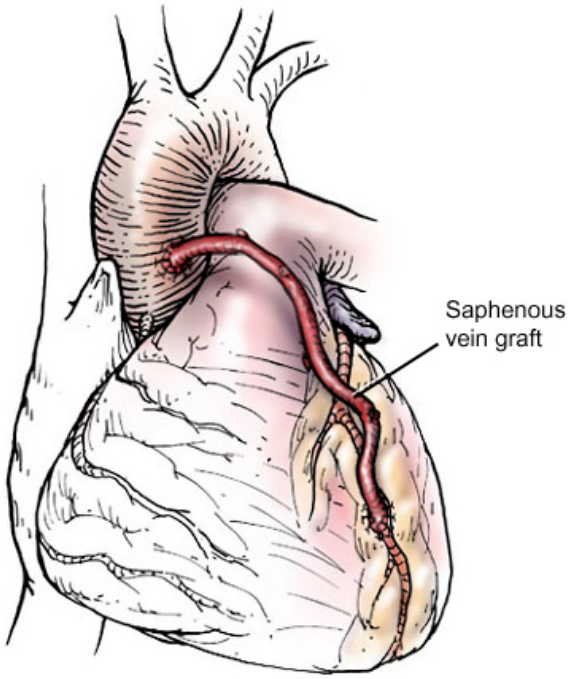

B

Figure 1-1. This illustration shows a heart with A) the left internal thoracic artery (LITA) grafted to the anterior descending coronary artery (bottom right) and B) a saphenous vein graft connected to the aorta (upper left) and to the coronary artery at the (lower right) (20)

1.1.3 Graft patency

Grafts can become diseased and may occlude in the months to years after bypass surgery is performed. Patency is a term used to describe the chance that a graft remains open. Graft patency is dependant on a number of factors, including the type of graft used (internal thoracic artery, radial artery, or great SV) and the size or the artery that the graft is anastomosing with. Occlusions can develop in SV to coronary bypass grafts and that the likelihood of obstructions developing is related to time. Within 5 years of surgery approximately 20 % of SV grafts developed partial or total obstructions, and between 5 and 10 years after operation these processes continued to progress such that by 10 years after operation almost half of SV grafts were either totally obstructed or showed some angiographic evidence of pathologic changes (21).

The best patency rates are achieved with the LITA, when the distal end being anastomosed with the coronary artery (typically the LAD artery or a diagonal branch artery). Studies of angiograms performed after bypass surgery have shown that not only did the LITA to LAD graft have a more than 90% chance of functioning well early after operation, but that these grafts continued to function well for many years and that even 20 years after operation the development of obstructions in these grafts is extremely uncommon (21). Over time, patients with a LITA-LAD graft are less likely to die or to need a re-operation when compared with patients who received only vein grafts (22). Since these studies have been completed the LITA-LAD graft has become a standard part of operations for coronary bypass grafting.

It is very clear that the internal thoracic arteries are the best bypass grafts to use for coronary bypass surgery. However not all patients can be completely treated with just the internal thoracic arteries, the search continues to go on for other arterial bypass conduits and/or total arterial revascularization.

1.1.4 Prosthetic vascular grafts

In the early phases of the use of prostheses as vascular grafts, the establishment of flow without leakage or thrombosis and the survival of flow-dependent tissues were the main objectives. As long-term survival of grafted patients became the norm, other

problems presented themselves and it became clear that the mechanical and haemodynamic properties of the prosthesis were very significant. The importance of differing mechanical properties of different parts of the arterial tree is referred to later (see review Chapter 2).

By the early 1950s, a number of polymeric materials such as polyethylene and methacrylate had been tried as arterial substitutes in animal experiments (23). It was hoped that their smooth and impermeable surfaces might help to minimize the formation of thrombus. In 1952, Vorhees *et al.* reported that a silk suture exposed for several months to flowing blood became covered by a glistening film of tissue free of microscopic thrombi (24) and this observation inspired the idea that a woven rather than a smooth material, by stimulating the formation of this layer, would provide a non-thrombogenic surface suitable for an arterial prosthesis. The first clinical use of hand-woven fabric made from Vinyon N as an arterial prosthesis showed all detectable leakage of blood through the weave had ceased within 1 minute after the prosthesis was filled with blood at arterial pressure (25). Once the idea of porous woven fabrics was introduced, a variety of materials including nylon, Teflon, Orlon, Dacron, and polyurethane were tested (26). Nylon was unsuccessful as it was found to degenerate rapidly following implantation. However, early clinical comparisons of graft success suggested that Dacron was the most promising material (27).
Although Dacron is still widely used as a graft material it remains the most widely used for aortic and iliac grafts. Dacron used especially in cardiovascular applications seems to cause an adverse reaction towards blood and the surrounding tissue resulting in inflammation and MIH (28;29). A number of other compounds have been developed, the most important being ePTFE (30) and polyurethane (31). PTFE is widely used due to its high bio-stability and reasonable tolerance by the body but as with Dacron there is a high adherence of platelets and blood proteins to the surface (32).

Polyurethane grafts have characteristics that would be ideal for use in bypass procedures namely similar compliance to native arteries and a surface that is conducive for seeding (33-36). Several variations of polyurethane graft have been investigated (37) (38), (39), (40) and are available commercially (41). But these have been associated with a significant rate of thrombosis and infection, with patency rates sometimes worse than PTFE grafts (42;43); also, they suffer from aneurysm formation (44). This has led to the

development of a compliant polyurethane graft based on poly(carbonate-urea)urethane (PCU). For longstanding implantation without biodegradation, PCU is currently considered to be much more stable than either polyester or polyether. The PCU graft eliminates ester and ether links (45) and thus improving biostability. It is an elastic graft making it potentially suitable for vascular access and small vessel bypass (46). Compared with other polyurethanes it has favourable haemocompatability (40), although its thrombogenecity can be lowered further by surface modification (47-49) or EC seeding (50). Unfortunately, even polycarbonate-based polyurethanes show biodegradation and aneurismal changes after just 10 weeks implantation in sheep model (47). As might be expected from their chemical structure, the polycarbonate soft segments are susceptible to hydrolysis. However, it is the enhanced hard segment interaction with polycarbonate that can render the overall structure resistant to degradation (51). The challenge in our department has been to optimise this interaction to yield a non-biodegradable graft (52).

The physical and mechanical properties of commercially available grafts vary widely, but a number of characteristics common to all successful vascular prostheses may be identified (26;53;54). Table 1-1 shows the current and the possible future plethora of bypass grafts that are or will be in used in cardiac and peripheral vascular bypass procedures.

Table 1-1. Current and possible future choices for cardiac and peripheral vascular bypass grafting

Graft Type	Applied experimentally	Under clinical trial	Used routinely
Autogenous vein [b]	√	√	√
Radial artery (55)	√	√	√
Internal mammary artery (56)	√	√	√
Gastro-epiploic artery (28)	√	√	√
ePTFE*	√	√	√
Dacron*	√	√	√
PCU*	√	√	[a]
Tissue engineering			
Seeded/hybrid	√	√	[c]
Living graft	√	[c]	[c]

ePTFE: expanded polytetrafluoroethylene (29); Dacron: polyethylene terephtalate (32;33); PCU: compliant polyurethane graft (57).
[a] Clinical trial imminent.
[b] Saphenous or arm vein.
[c] Not to date.
* Prosthetic grafts not of choice in CABG surgery.

1.1.5 The requirement for coronary bypass grafts

Even now, there is no synthetic small calibre vascular prosthesis that has been clinically proven to improve on ePTFE. Prosthetic conduits for CABG surgery are rarely in use because they have far lower patency rates compared to autologous vein or artery grafts. This is supported by a study that compared ePTFE and SV grafts. At 1 year follow up, 86% of the vein grafts were patent while only 59% of ePTFE grafts were patent (29). Chard and colleagues found that ePTFE coronary bypass grafts were 86% patent at 1 week, 64% at 12 months, 32% at 24 months, 21% at 36 months, and 14% at 45 months (34). Other evidence for artificial CABG is Dacron, for instance, has been utilized as a polymeric graft (3-4 mm) in a few case reports with patent vessels at 17 months (32;33).

Compliance mismatch aside, thrombogenicity is the major cause of prosthetic coronary graft failure. The low medium-term patency rates of prosthetic grafts have

restricted primarily to patients with inadequate autologous conduits or to selected emergencies. This can be reduced by either coating these grafts with EC (as discussed in depth later in this chapter) and RGD-peptide sequences (36) or ensuring high blood flow rates within the graft. A small vessel prosthesis that better emulates normal arterial walls would greatly improve the treatment of both peripheral vascular disease and coronary artery disease. Over 20,000 peripheral bypass and over 25,000 coronary artery bypass grafts are implanted annually in the United Kingdom: the potential annual market value is for synthetic CABG (58).

An ideal vascular graft (Table 1-2) would be biocompatible in that the graft should be resistant to both thrombosis and infection and possess sufficient mechanical strength that when the graft is placed in the arterial circulation it must be capable of withstanding long-term haemodynamic stress without material failure (14;59). The prosthesis should allow the leakage of a small amount of blood. This leads to a tightly adherent thrombus, permitting its subsequent replacement by fibrin and fibrous tissue. The end result of this process is the formation of a non-thrombogenic surface resembling that of the native vessel (13). Availability, suturability and durability are also desirable for minimising operating time, risk and expense.

Table 1-2. Characterisation and desirable features of the ideal cardiovascular graft.

1) Biocompatibility
No healing disturbances
Non-toxic
Non-allergenic
No induction of malignancies
Minimally traumatic to blood compounds
Non-thrombogenic
Resistance to infection
2) Compliant
Flexible, elastic, without kinking
Ability to stretch
Tensile and shear strength sufficient to resist fraying
Circumferential strength sufficient to withstand arterial pressures
Mechanical properties approximate to those of the native vessels to which they are attached
Resistant to MIH
3) Easy Processing
Adequate physical and chemical properties, mechanical durability
Readily available in a variety of sizes and lengths
No need for special storage
Easy to suture
Sterilisation (Radiation)
4) Optional
Capable of local drug delivery
Low costs

1.1.6 Possible role of nanocomposite for CABG

Nanotechnology is concerned with manipulation at the molecular or atomic level to provide useful applications (60;61). The main unifying theme is the control of matter on a scale smaller than 1 micrometer, normally between 0.1-100 nanometers, as well as the fabrication of devices on this same length scale. One nanometer (nm) is one billionth, or 10^{-9} of a meter. Materials reduced to the nanoscale can suddenly show very different properties compared to what they exhibit on a macroscale, enabling unique applications (60). For instance, inert materials become catalysts (platinum); solids turn into liquids at room temperature (gold); insulators become conductors (silicon). A material such as gold, which is chemically inert at normal scales, can serve as a potent chemical catalyst at

nanoscales. Much of the fascination with nanotechnology stems from these unique quantum and surface phenomena that matter exhibits at the nanoscale.

The difficulties involved in fulfilling the numerous ideal characteristics using traditional synthetic materials have lead biomaterials research towards the fields of nanotechnology and tissue engineering. Nanotechnology is concerned with the incorporation of man-made molecules into traditional materials to express novel advantageous properties such as anti-thrombogenecity and biostability (62).
Hybrid inorganic–organic composites are an emerging class of new materials that hold significant promise. Materials are being designed with the good physical properties and the excellent choice of functional group chemical reactivity associated with organic chemistry. Nano-engineered materials integrated with its constituents at the nanoscale level result in a 'supermaterial' with numerous enhanced properties: greater strength, higher resistance to permeability and higher heat stability.

1.1.7 Poly(carbonate-urea)urethane (PCU) incorporating polyhedral oligomeric silsesquioxane (POSS) nanocomposite

Our group has concentrated on the use of PCU. As discussed earlier the polymer is relatively biostable. However, specific hydrolytic enzymes such as cholesterol esterase as well as exposure to oxidative solutions have shown *in vitro* degradation. Monocyte-derived macrophages could hydrolyse PCU as predicted by *in vitro* cholesterol esterase action (63). Although *in vivo*, macrophage-derived oxidative compounds are also released this may be protective against hydrolytic degradation. To some extent PCU is protected from degradation by the shielding effect of the hard segment. Research in our department has undergone to modify polycarbonate-based polyurethane to improve biostability with a view to using it as a long-term implant material, in particular cases the much need for a CABG.

Using conventional silicon-containing polydimethylsiloxane) (PDMS) as a coating, a surface modifying end group (64;65) and by partial incorporation into the soft segment of the polyurethane backbone (66;67) could reduce biodegradation and the extent of the inflammatory response to the polymer (68). The rationale behind this approach has been that silicon has an unstable surface free energy that would repel protein and platelet

adhesion as well as increase degradative resistance to hydrolysis and oxidation. As PDMS itself is a rigid polymer, efforts have been made to link silicon with more compliant materials such as rubber so as to better mimic the elastic properties of arteries (13). Rubber possesses high elastic extensibility. Crystalline polymers are harder than rubber but not brittle like glass. They comprise rigid polymer chains (crystallites) embedded in an amorphous gel. However, the latter soft phase is vulnerable to biodegradation *in vivo*.

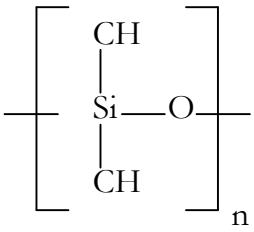

Figure 1-2. Monomer of polydimethylsiloxane (PDMS).

In our laboratory, silsesquioxane technology was targeted due to previous incorporation of siloxane (Si-O chains) in the form of PDMS (Figure 1-2) into polyurethanes. Siloxane groups are biologically inert and have similar bond properties as ether groups within polyurethanes. Silsesquioxane means one silicon atom for 1.5 oxygen atoms. It represents a class of silicon-oxygen compounds that include the polyhedral oligomeric silsesquioxane (POSS). This latter comprises cyclical rings of alternating Si-O atoms in layers. POSS is being used increasingly to synthesise hybrid nanocomposites (69).

PCU-POSS is a nonaocomposite material covalently bonding polyurethane with a silsesquioxane 'nanomolecule'. PCU-POSS contains one of the most widely used POSS structures, namely the Octahedral-Dimeric Silsesquioxane (see Figure 1-3). The initial aim upon development of this nanocomposite was to improve biostability further for long-term biological implant functionality. However, it has also been found to have a very favourable blood compatability as well (52).
The nanocomposite polymer investigated in this thesis is being characterised in our laboratory and has also demonstrated *in vitro* biostability (70).

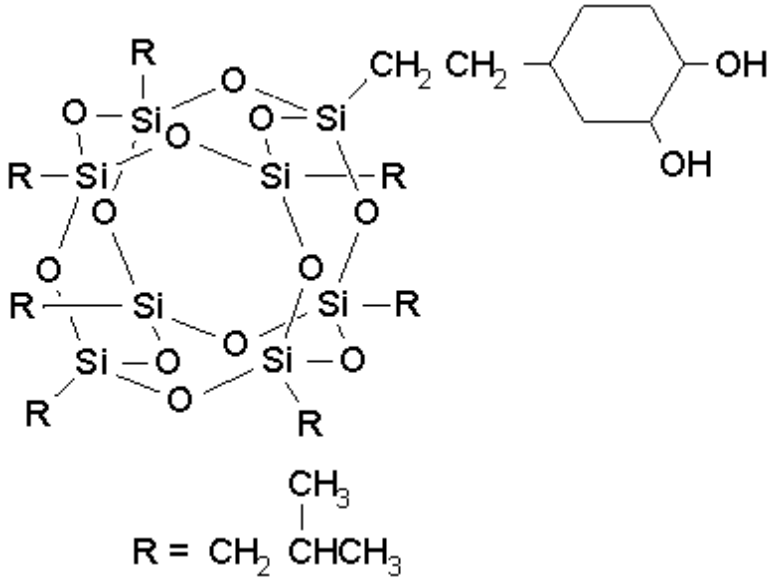

Figure 1-3. Molecular structure of trans-cyclohexanediolisobutylsilsequioxane, the POSS moiety used in PCU-POSS.

1.1.8 Tissue engineering

Tissue engineering is a broad field defined as the use of a combination of cells, engineering materials, and suitable biochemical factors to improve or replace biological functions in an effort to affect the advancement of medicine. The first definition of tissue engineering was by Langer and Vacanti who stated it to be "an interdisciplinary field that applies the principles of engineering and life sciences toward the development of biological substitutes that restore, maintain, or improve tissue function or a whole organ" (71). There are more general definitions such as MacArthur and Oreffo defined tissue engineering as "understanding the principles of tissue growth, and applying this to produce functional replacement tissue for clinical use" (72). These more general definitions are by recent scientific progress with completely autologous approaches. That is, demonstrating functional tissue engineered devices/organs without using synthetic biomaterials/scaffolds. These recent approaches are based more on an understanding of cell biology than materials science.

The important factor implicated in graft failure is the lack of EC lining the lumen of the graft (73). This endothelial monolayer that lines the normal blood vessel serves as a

bioregulator of cardiovascular physiology. The endothelium provides structural integrity to the blood vessel by forming a continuous selectively permeable, thromboresistant barrier between circulating blood and the arterial wall. It also controls blood flow and vessel tone (74), platelet activation, adhesion and aggregation (75), leukocyte adhesion (76) and SMC migration and proliferation (77). This is the key rationale behind utilising autologous EC to make a haemocompatible artificial polymeric surface that will perform the major functions of an intact healthy endothelium that would normally be found in the blood vessel itself.

1.2 Adding endothelium to artificial vascular grafts

1.2.1 Normal vascular anatomy and function

Differentiation of arteries and veins results in the gradual formation of three anatomic layers: the adventitia the media and the intima, (Figure 1-4).

1.2.1.1 Tunica adventitia

The strong outermost layer of arteries and veins is the *tunica adventitia* or the *adventitia*. It is composed of connective tissue and is composed primarily of fibroblasts as well as collagen and elastic fibers. These fibres allow the arteries and veins to stretch whilst preventing overexpansion due to the pressure that is exerted on the walls by blood flow.

1.2.1.2 Tunica media

The *tunica media* or *media* is the middle layer of the wall. It is composed of smooth muscle cells (SMC) and extracellular matrix (ECM), such as collagen types I and III, elastin fibronectin and proteoglycans such as versican. This layer is thicker in arteries than in veins and gives the vessel properties to contract and relax in response to different stimulus. The media of elastic arteries is composed of layers of SMC and elastic laminas. In contrast, muscular arteries have less elastic tissue that organises into laminae only at

the boundaries of intima with the media and the adventitia. Veins develop thinner walls than arteries and have the media composed primarily of SMC with relatively low amounts of elastic tissue.

1.2.1.3 Tunica intima

The innermost layer, which is in direct contact with the flow of blood, is the *tunica intima,* commonly called the *intima*. This layer is made up of mainly EC. This layer is supported by a basement membrane that contains type IV collagen, laminin and heparin sulphate proteoglycans such as perlecan and syndecans. The basement membrane separates endothelium from the underlying layers. EC act as protective barrier and control the exchange of nutrients and fluid between blood and tissue, which is the basis for the maintenance of the stability of the physiological environment essential to cell survival.

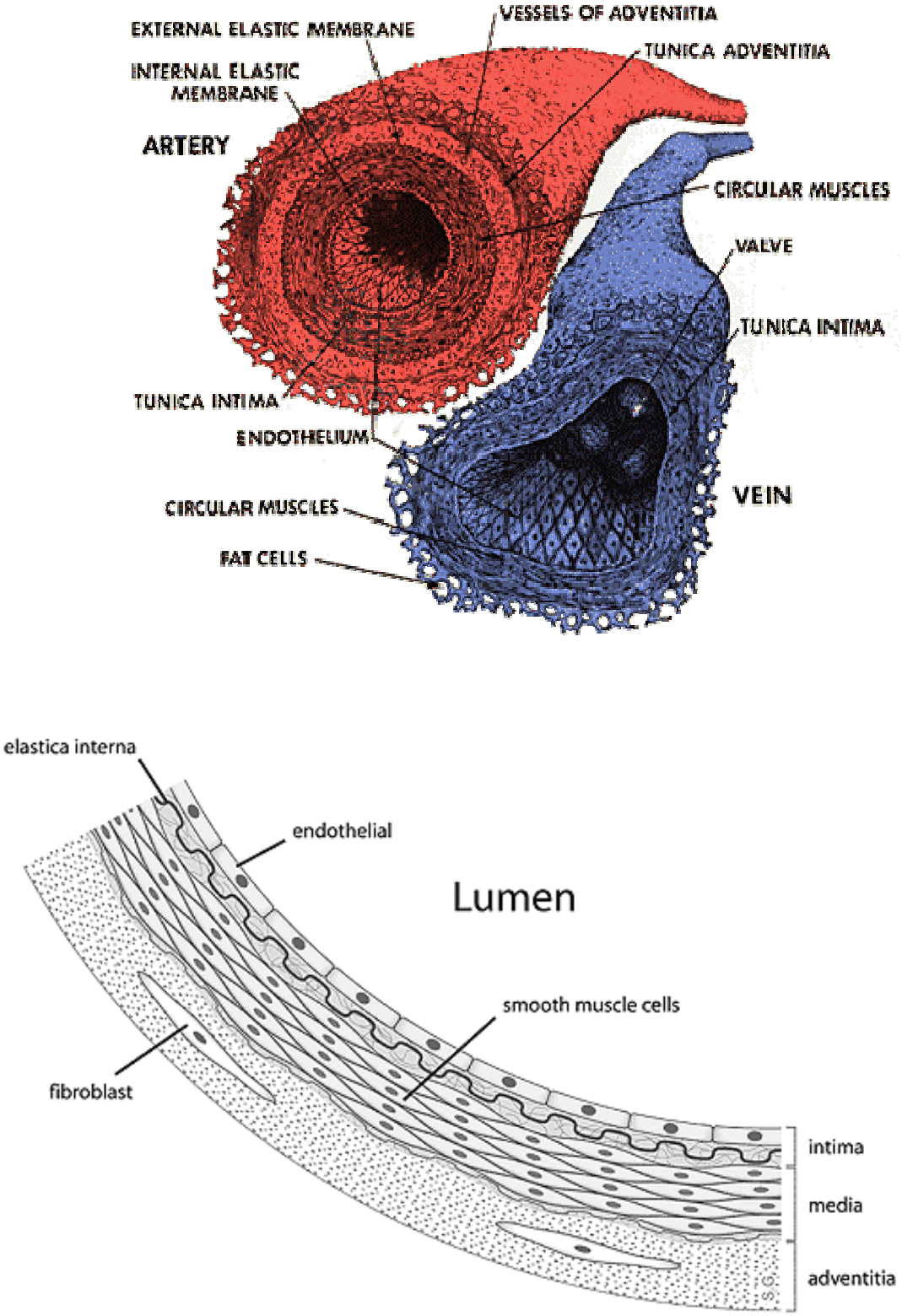

Figure 1-4. Structure of an artery and vein and anatomy of the arterial wall.

1.2.2 Endothelial cell biology

The endothelium is more than a layer lining the blood vessels. The structural and functional integrity of EC is important in the maintenance of the vessel wall function. As a barrier, the endothelium is semi-permeable and controls the transfer of small and large molecules from the bloodstream to the vascular bed (i.e. tunica media, adventitia and perivascular layers). ECs are also capable of conducting a variety of metabolic and synthetic functions. The synthesis and release of paracrine factors (see Figure 1-5) by ECs influences underlying SMCs or circulating blood elements, such as platelets and white blood cells (78;79).

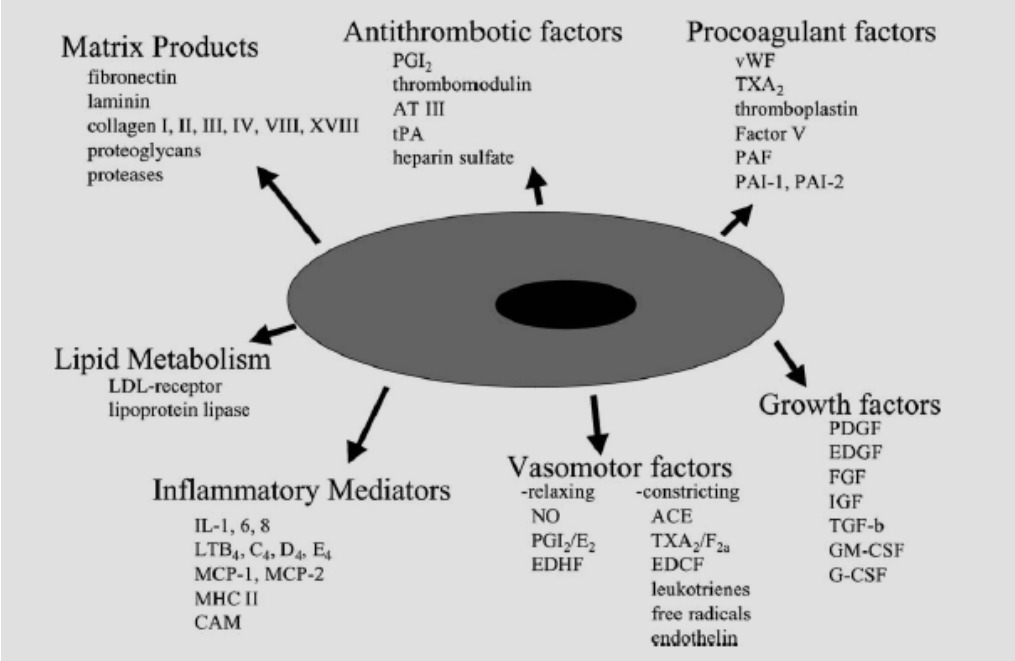

Figure 1-5. Synthesis and release of important mediators in endothelial cells(80).

1.2.3 EC phenotype & structure

Normal EC has a typical 'cobble-stone' morphology at confluence. By contrast, when cells are sparse or intercellular junctions' disrupted, fibroblastoid/mesenchymal morphology predominates (Figure1-6). ECs are about 1-2 μm thick and some 10-20 μm in diameter. They form flat, pavement-like patterns on the inside of the vessels and at the junctions between cells there are overlapping regions which help to seal the vessel(81).

These intercellular junctions are critical for the integrity of the vessel. Toxic substances open up these junctions and allow large molecules to pass through the wall. Thus such toxins can potentiate degenerative changes in blood vessels and lead to serious vascular diseases.

The cytoplasm is relatively simple with few organelles, mostly concentrated in the perinuclear zone (80;82). The most obvious feature is the concentration of small vesicles (pinocytotic vesicles) adjacent to the EC membranes. This is a mechanism for passing materials, especially fluid, across the cells from the blood stream to the underlying tissues. Gases simply diffuse through very rapidly, and this is exemplified in the lung capillaries where there is very efficient movement of gases (carbon dioxide, oxygen and anaesthetics etc).

ECs behave differently in confluent or sparse conditions (see figure; from left to right, respectively).

Confluent cells
•Epithelloid phenotype
•Contact inhibition of growth and motility
•Rearrangement of actin microfillaments
•Protection form apoptosis

Sparse cells
•Fibroblastoid morphology
•Active growth
•Motility

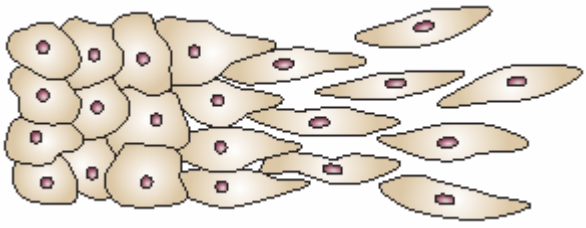

Figure 1-6. Phenotypes of confluent and sparse cells (82).

A typical characteristic of EC is the presence of Weibel-Palade-bodies (WP-bodies). These are large rod-shaped organelles that are specific for EC. WP-bodies store large amounts of von Willebrand Factor (vWF) that can quickly be released upon activation of the cells (83). Secretion of vWF can be constitutive or regulated and also occurs in the absence of WP-bodies. vWF is a large adhesive glycoprotein synthesised in EC and megakaryocytes. Its primary function is binding to other proteins, particularly Factor VIII and it is important in platelet adhesion to wound sites (83).

vWF binds to a number of molecules. The most important ones are:

- Factor VIII is bound to vWF while inactive in circulation and degrades rapidly when not bound to vWF. Factor VIII is released from vWF by the action of thrombin.
- vWF binds to collagen, e.g., when it is exposed in EC due to damage occurring to the blood vessel.
- vWF binds to platelet gpIb when it forms a complex with gpIX and gpV; this binding establishes a transient bond that slows down platelets and thus facilitates their activation (84).

On the surface of EC is a glycocalyx layer. The glycocalyx ("sugar coat") is a complex and highly dynamic polymeric meshwork that coats the surfaces of most cells and consists of proteoglycans, glycosaminoglycans (GAGs), and glycoproteins, as well as adherent plasma proteins (85). The glycocalyx layer on the EC surface plays a critical role in regulating vessel permeability, modulating the dynamics of near-wall movement of red blood cells, and coordinating interactions between leukocytes and the vascular wall during inflammation.
Perturbation of the glycocalyx on the endothelium appears to be associated with vascular damage, as well as increased vulnerability to the development of atherosclerosis (86). A number of studies have demonstrated that the presence of an intact glycocalyx is essential for EC sensitivity and responsiveness to fluid mechanical stimulation, thereby supporting the idea of a central role for the glycocalyx in endothelial cell flow-mediated mechanotransduction (87;88).

1.2.4 Endothelium modulates vascular tone

As ECs are directly exposed to the cellular and molecular components of blood, as well as being exposed to the physical forces inherent in the circulation, they play a major role in modulating vascular wall function (78;80). The EC surface expresses receptors for circulating hormones including catecholamines, angiotensin and vasopressin, and local autacoids, including bradykinin, serotonin and acetylcholine. Furthermore, the cell membrane responds directly to physical stimuli, allowing calcium release from subsarcolemmal storage sites through non-specific cation channels when subjected to stretch, and allowing potassium efflux when shear stress is increased (89).

The result of these various stimuli is to controls vasodilatory mediator synthesis and release.

ECs locally control vascular tone by releasing potent vasodilatory mediators, such as endothelium-derived relaxing factor (EDRF), and vasoconstrictor mediators such as endothelin-1. Furchgott & Zawadzki (74) demonstrated the phenomenon of endothelium-dependent relaxation. It has been described that the vasodilatory actions of acetylcholine are mediated indirectly through release of a mediator from the endothelium. This mediator was initially described as EDRF, however the mediator of endothelium-dependent relaxation is now known to be a nitric oxide (NO) (90).

NO is synthesised by the enzyme NO synthase (NOS) from the amino acid L-arginine. Once synthesised, NO diffuses from endothelium to the underlying smooth muscle where it activates guanylate cyclase to cause a rise in intracellular cyclic GMP and relaxation of the vessel (refer to Figure 1-7). There are two endothelial forms of NOS: constitutive NOS (cNOS; type III) and inducible NOS (iNOS; type II) (91).

Under normal basal conditions in healthy blood vessels, NO is continually produced by cNOS. The activity of cNOS is calcium and calmodulin dependent. There are two pathways for the stimulation of cNOS, both of which involve release of calcium from subsarcolemmal storage sites. 1. Shearing forces acting on the vascular endothelium generated by blood flow causes a release of calcium and subsequent cNOS activation. Therefore, increases in blood flow stimulate NO formation. 2. Endothelial receptors for a variety of ligands (acetylcholine, bradykinin, substance-P and adenosine) stimulate intracellular calcium release and subsequent NO production (78). The NO generated can only act locally, since it has a chemical half-life of a few seconds in biological solutions and is rapidly inactivated upon contact with haemoglobin.

The other isoform of endothelial NOS is iNOS. It differs, in part, from cNOS in that its activation is calcium independent. Under normal, basal conditions, the activity of iNOS is very low. The activity of iNOS is stimulated during inflammation by bacterial endotoxins (e.g., lipopolysaccharide) and cytokines such as tumor necrosis factor (TNF) and interleukins (92).

Certain agents usually thought of as vasoconstrictors, including noradrenaline and serotonin, also stimulate NO synthesis, with the NO released blunting the direct constrictor action on vascular smooth muscle. In the case of serotonin, this indirect effect can override the constriction such that, in vessels with healthy endothelium, serotonin

may cause vasodilatation, whereas when endothelial integrity is breached, it is a potent vasoconstrictor (93).

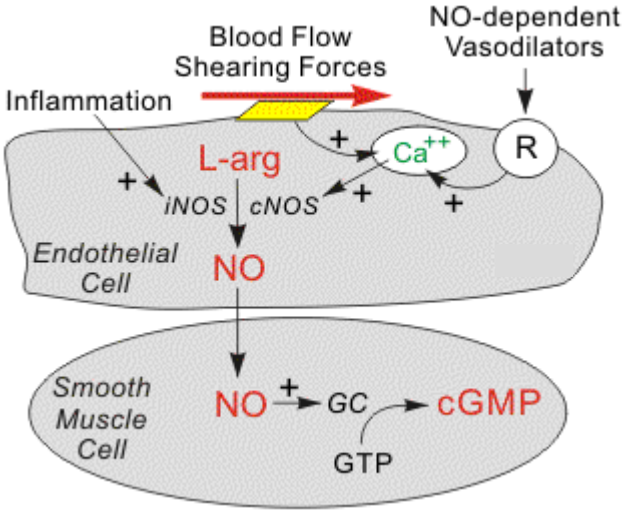

Figure 1-7. Nitric oxide synthesis in endothelial cells to promote vasodilatory effects on the vessel wall.

The endothelium has a major basal dilator influence on the blood vessels by continuously adjusting dilator tone through the release of NO from the luminal side of the vessel, with the sympathetic nervous system as the major basal constrictor influence. The latter achieved by continuously adjusting constrictor tone through the release of noradrenaline, ATP and neuropeptide Y onto the adventitial side of the vessel.

NO is not the only vasoactive mediator produced by ECs. Vasodilator and vasoconstrictor prostanoids are synthesized and released (80). A vasorelaxant, endothelium-derived hyperpolarizing factor (EDHF) has been described (94). ECs also express renin, angiotensin I and angiotensin converting enzyme (95), constrictor superoxide anions (96) and endothelin (97). Endothelin is the most potent vasoconstrictor yet discovered.

How do other endothelium-derived mediators fit into vascular control? Endothelin has a long duration of action and therefore could enhance the action of low background levels of circulating vasoconstrictor hormones (98). Renin-angiotensin has been demonstrated to make contribution to vessel tone and provides a link between the endothelium and nerves, by locally generated angiotensin II diffusing from the endothelium through the vessel wall to increase noradrenaline release from neurones (99). Synthesis and release of

the unstable prostaglandin endoperoxide (PGH_2) may account for the activity of the elusive short acting EDCF (100) but its role in the control of human vasculature is entirely unknown.

1.2.5 Endothelium maintains thromboresistant barrier

One of vascular ECs major role is the prevention of thrombin generation and platelet adhesion to luminal surface of blood vessels. Molecules physiologically important in suppressing platelet activation and platelet-vessel wall interaction include prostacyclin (PGI_2), nitric oxide (NO) and ecto-adenosine diphosphatase (ADPase) (101). Molecules involved in controlling coagulation also include the surface-expressed thrombomodulin, heparin-like molecules, protein S and tissue factor pathway inhibitor (102). Finally, ECs synthesise and secrete tissue-plasminogen activator (tPA) and urokinase-type plasminogen activator (uPA) to promote fibrinolysis (81).

1.2.5.1 Antiplatelet activity

When vessel wall damage occurs, proteins from the subendothelial matrix (vWF, collagen and fibronectin) are exposed and proteins from the circulation (particularly fibrinogen) are absorbed to the subendothelial matrix. Platelets adhere to the exposed proteins present in this matrix and become activated (103).
Under normal circumstances, ECs have an antithrombogenic function. Platelets do not adhere to the unperturbed EC luminal membrane. This is due to the large negatively charges sulphate proteoglycans (glycocalyx) bound to EC membrane (85). As well as NO and PGI_2 production inhibit platelet adhesion and aggregation and cause blood vessel dilation (104).

Most studies have focused on PGI_2. It is produced in ECs from PGH_2 by the action of the enzyme prostacyclin synthase. Although prostacyclin is considered an independent mediator, it is called PGI_2 (prostaglandin I2) in eicosanoid nomenclature, and is a member of the prostanoid fasmily (together with the prostaglandins and thromboxane) (105). Its platelet-inhibitory activities are mediated via a guanosine nucleotide binding receptor thus activating adenylate cyclase and the elevation of platelet cyclic adenosine monophosphate (cAMP) levels with resultant inhibition of platelet

activation (106). It also induces vascular SMC relaxation, blocks monocyte-endothelial interaction, and reduces SMC lipid accumulation. The actions of PGI_2 on other cells are thought to be mediated by a similar receptor-mediated signal transduction pathway.

1.2.5.2 Anticoagulant surface

The endothelium serves as an anticoagulant surface in order to maintain a thromboresistant luminal surface. *In vivo*, the initiation of coagulation in response to trauma occurs almost instantly after an injury to the blood vessel damages the endothelium. Platelets immediately form a hemostatic plug at the site of injury (primary hemostasis). Simultaneously, proteins in the blood plasma, called coagulation factors, respond in a cascade to form fibrin strands that strengthen the platelet plug (Secondary haemostasis). The coagulation cascade of secondary hemostasis has two pathways that lead to fibrin formation the contact activation pathway (known as the intrinsic pathway) and the tissue factor pathway (known as the extrinsic pathway). The extrinsic pathway is initiated at the site of injury in response to the release of tissue factor; also called thromboplastin, factor III or CD142 (107).
Although they are initiated by distinct mechanisms, the two converge on a common pathway that leads to clot formation. The pathways are a series of reactions, in which a zymogen (inactive enzyme precursor of a serine protease) and its glycoprotein co-factor are activated to become active components that then catalyse the next reaction in the cascade, ultimately resulting in cross-linked fibrin. Each of these pathway constituents leads to the conversion of factor X (inactive) to factor Xa (active) (108). Factor Xa activates prothrombin (factor II) to thrombin (factor IIa). Clot formation occurs when thrombin, in turn, converts fibrinogen to fibrin. The activation of thrombin occurs on the surface of activated platelets and requires formation of a prothrombinase complex (109).

One important way in which ECs control the clotting system is by regulating the expression of binding sites for anticoagulant and procoagulant factors on the cell surface. In the quiescent state, ECs maintain blood fluidity by promoting the activity of numerous anticoagulant pathways, including the protein C/protein S pathway (110;111). After activation, as can be brought about by cytokines, the balance of endothelial properties can be tipped to favor clot formation through coordinated induction of procoagulant and suppression of anticoagulant mechanisms. Tumor necrosis factor suppresses the

endothelial anticoagulant cofactor thrombomodulin and induces expression of the procoagulant cofactor tissue factor (112). Working in concert, these changes can allow fibrin formation to proceed in an inflamed focus but maintain blood fluidity in the surrounding area of normal vasculature.

1.2.5.3 Fibrinolysis

Fibrinolysis is a process where a fibrin clot, the product of coagulation, is broken down. The enzyme plasmin cuts the fibrin mesh at various places, leading to the production of circulating fragments that are cleared by other proteases. Plasmin is produced in an inactive form, plasminogen. Although plasminogen cannot cleave fibrin, it has a high affinity for it and is incorporated into the clot when it is formed. Tissue plasminogen activator (t-PA) and urokinase-type plasminogen activator (u-PA) convert plasminogen to the active plasmin, thus allowing fibrinolysis to occur (113;114). t-PA is a serine protease normally found on the surface of ECs and is released into the blood very slowly by the damaged endothelium. This enzyme plays a role in cell migration and tissue remodeling. u-PA is present in the ECM. t-PA and u-PA are inhibited by plasminogen activator inhibitor-1 and plaminogen activator inhibitor 2 (PAI-1 and PAI-2). In contrast, plasmin further stimulates plasmin generation by producing more active t-PA and u-PA (114;115).

1.2.6 Regulation of cell growth, survival and apoptosis

Apoptosis is programmed cell death or a physiological cell "suicide" mechanism. It serves to remove supernumerary cells during development and tissue remodelling (116); maintain homeostasis in adult tissues; remove self-reactive or non-reactive immune cells (117) and delete damaged, infected or transformed cells. Throughout the process the cell membrane integrity is maintained to avoid the initiation of an inflammatory response. This contrasts with necrosis in which cells die relatively passively following overwhelming damage, leading to loss of membrane integrity and to inflammation (118).

Within blood vessels, vascular ECs play an especially important role in regulating overall vessel structure. Most ECs in adult blood vessels are relatively quiescent and resistant to apoptosis. However, they are thought to retain the latent capacity for

proliferation and apoptosis to mediate angiogenesis and regression, respectively. In support of this concept, EC apoptosis has been detected within remodelling vessels *in vivo*, and inactivation of EC apoptosis regulators has caused dramatic vascular phenotypes (119).

EC apoptosis may also contribute to angiogenesis. Several EC types spontaneously form vessel-like structures *in vitro* (vascular morphogenesis) when cultured on an extracellular matrix or with matrix-producing cells. Incubation of EC with anti-apoptotic caspase inhibitors or overexpression of the anti-apoptotic protein Bcl-2 appears to inhibit vascular morphogenesis in vitro (120).

As well as supporting vessel regression and possibly promoting angiogenesis, EC apoptosis may in addition play a role in lumen formation. In support of this hypothesis, ECs undergoing apoptosis are seen in the centre of developing vascular structures (121),

To prevent the activation of this conserved "suicide" cascade, most cells must be continuously exposed to survival factors. Basic FGF (bFGF) growth factor modulates cell proliferation and differentiation (122). The responses of vascular EC to bFGF *in vitro* include transient stimulation of the expression of multiple genes including c-fos and c-myc (123), increased production of plasminogen activator and collagenase, cytoskeletal reorganisation (124), and, ultimately, stimulation of cell proliferation as well as migration (125).

1.2.7 EC migration

The migration of ECs plays an important role in vascular remodeling and regeneration. EC migration can be regulated by different mechanisms such as chemotaxis and mechanotaxis. EC migration and mechanotransduction can be modulated by cytoskeleton, cell surface molecules such as integrins and proteoglycans, chemical and physical properties of ECM and cell-cell adhesions. The shear stress applied on the luminal surface of the endothelium can be sensed by cell membrane and associated molecules and transmitted throughout the cell to cell-ECM adhesions and cell-cell adhesions. As a result, shear stress induces directional migration of ECs by promoting lamellipodial protrusion and the formation of focal adhesions (FAs) in the flow direction and the disassembly of FAs at the rear. Persistent EC migration in the flow direction can be driven by polarized activation of signaling molecules and Rho GTPases. Rho GTPases

regulate cytoskeletal organization and cell adhesion, thereby contributing to cell migration (126) and endothelial permeability (127). Given the haemodynamic environment of the vascular system, mechanotransduction during EC migration has a significant impact on vascular development, angiogenesis, and vascular wound healing.

1.2.8 EC role in angiogenesis and vasculogenesis

The vascular endothelium not only forms the innermost multifunctional cell lining and permselective barrier of the entire cardiovascular system, but centrally contributes under disturbed or activated conditions to neovascularization, wound repair and vascular remodelling). Angiogenesis, the growth of new blood vessels from the existing vasculature is associated with physiological (wound healing, endometrial cycle and embryonic development) and pathological processes (tumour growth, rheumatoid arthritis, diabetic retinopathy, and brain and cardiac infarctions) (128;129). During new growth, quiescent EC are stimulated to degrade their basement membrane and to invade the surrounding stroma, initially as solid EC cords. Later, these cords develop a lumen and deposit a new basement membrane, thus resulting in functional new capillaries. Alterations in at least three EC functions occur during this series of events: 1) modulation of interactions with the ECM, which requires alterations in cell-matrix contacts and the production of matrix-degrading proteolytic enzymes; 2) an initial increase and subsequent decrease in migration, which allows cells to translocate towards the angiogenic stimulus and to stop once they reach their destination; and 3) an increase in proliferation, which provides new cells for the growing and elongating vessel, and a subsequent return to the quiescent state once the vessel is formed. Together, these cellular functions contribute to the process of capillary morphogenesis i.e. the formation of three-dimensional tube like structures (see Figure 1-8) (129).

Angiogenesis is mediated by pro-angiogenic factors including vascular endothelial cell growth factor (VEGF), fibroblast growth factor-2 (FGF-2), angiopoietin, and epidermal growth factor (EGF) (130;131). Several platelet-derived anti-angiogenic factors including thrombospondin, platelet factor 4 or transforming growth factor-ß1 (TGF- ß1) have been shown to inhibit endothelial cell proliferation, migration or capillary tube formation (132).

VEGF comprises a family of multifunctional cytokines that include the variants VEGF-A, -B, -C, -D and-E and placental growth factor (PlGF) (133). VEGF-A is mitogenic *in vitro* and angiogenic *in vivo* (134) and its role in angiogenesis and vasculogenesis has been elucidated (135). VEGF is also associated with pathological angiogenesis (136) and exerts its biological action upon binding with two high affinity receptor tyrosine kinases; VEGFR-1 (flt-1) and VEGFR-2 (kinase domain receptor; flk-1) (134;136). VEGFR-1 has a 50 times higher binding affinity for VEGF than VEGFR-2 (137). However, VEGFR-2 has a stronger receptor tyrosine kinase activity than VEGFR-1 and acts as a major mitogenic receptor on ECs (138).

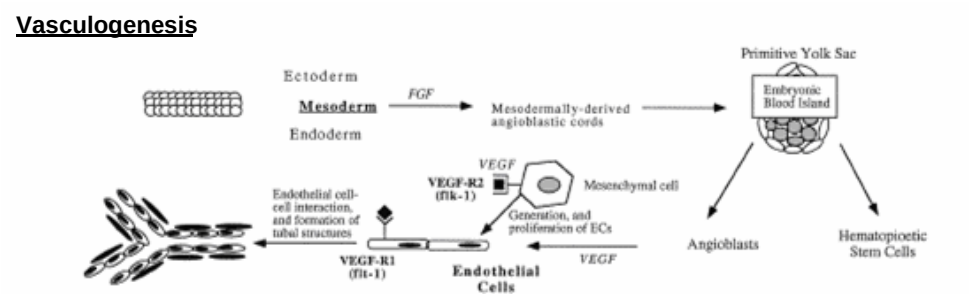

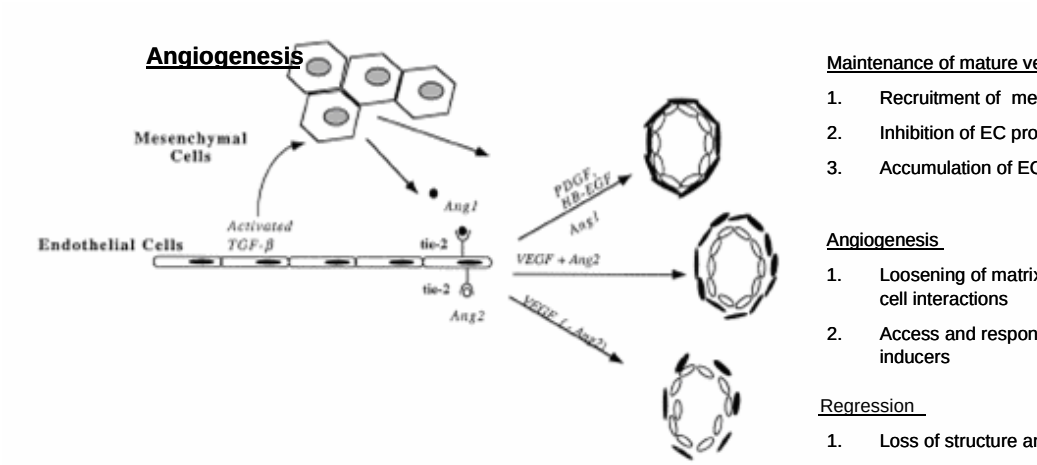

Maintenance of mature vessels

1. Recruitment of mesenchymal cells
2. Inhibition of EC proliferation
3. Accumulation of ECM

Angiogenesis

1. Loosening of matrix contacts and support of cell interactions
2. Access and responsiveness to angiogenic inducers

Regression

1. Loss of structure and matrix contacts
2. Absence of growth of survival signals
3. Apoptosis

Figure 1-8. The formation of new vessels during vasculogenesis and angiogenesis. Vasculogenesis, the de novo organization of EC into vessels in the absence of pre-existing vascular structures, takes place during embryogenesis in the blood islands of the yolk sac (pictured) and in the embryo through expression of growth factors, in particular fibroblast growth factor (FGF) and vascular endothelial growth factor (VEGF). The tyrosine receptor kinases, VEGFR-1 (flk-1) and VEGFR-2 (flt-1), are expressed on mesenchymal cells and newly formed EC, respectively, and are essential for the generation and proliferation of new EC and the formation of tube EC structures. Angiogenesis, the continued expansion of the vascular tree, is mediated through the expression of additional tyrosine kinase receptors, tie-2, which binds to Ang1 and Ang2 (angiopoietins), resulting in the maintenance of mature vessels, the development of new vessels, and the regression of formed vessels (81).

Transforming growth factor-beta (TGF-β) has profound effects on all cell types making up the vasculature, including ECs, SMCs, and adventitial connective tissue. As such, it plays a prominent role not only in the physiologic vasculogenesis and angiogenesis but also in vascular disorders such as the arterial thickening associated with pulmonary hypertension. The actions of TGF-β on these vascular cells *in vitro* and *in vivo* are extremely complex. TGF-β exerts stimulatory effects on cell proliferation, stimulating proliferation and migration at low concentrations, whereas at higher concentrations, it inhibits these processes. It regulates the activation state of ECs via receptors ALK-5 and ALK-1 (139). The TGF-β/ALK-1 pathway stimulates endothelial cell proliferation and migration, whereas the TGF-β/ALK-5 pathway inhibits these processes. TGF-ß1 also affects vascular permeability by upregulating the expression of Claudin-5, an EC–specific component of tight junctions (140), and inhibits the expression of adhesion molecules. TGF-β also inhibits gene that promote inflammation, interleukin-6 (IL-6), monocyte chemoattractant protein-1, and granulocyte–colony-stimulating factor (141).

1.2.9 EC role in inflammation

In inflammation, white blood cells interact with the vascular endothelium by specific cell surface receptors and adhesion molecules. Leukocytes are normally repelled by endothelium, in order to allow the free flow of blood cells over the surface. However, in inflammatory states, the leukocytes are attracted to the endothelium by adhesion molecules. At the site of inflammation, the endothelium recruits circulating white blood cells by inflammatory cytokines and direct cell-cell contact(142). Following arrest at the site of inflammation, leukocytes pass through the endothelial cells by a process called *diapedesis*, which literally means "walking through". Many leukocytes pass through ECs, especially in capillaries as part of their normal life cycle, so that they can monitor foreign agents (antigens) in the tissues.

Leukocytes cross the endothelial barrier in a multistep process involving the capture and rolling of leukocytes on the blood vessel wall, firm adhesion of leukocytes to ECs, and subsequent leukocyte crawling and transmigration. Proinflammatory mediators, such as tumor necrosis factor- (TNF-), interleukin-1 (IL-1), and the lipopolysaccharide (LPS) of bacterial walls, or hemodynamic forces imposed by blood flow increase the surface levels of a variety of molecules on ECs implicated in EC–leukocyte interaction.

Moreover, both these stimuli and EC–leukocyte interaction induce changes in endothelial cell shape, permeability, and gene expression (143).

1.2.10 EC adhesion

Another important property of ECs is to separate blood from underlying tissues. These cells function as gatekeepers, controlling the infiltration of blood proteins and cells into the vessel wall. This is achieved through specialised transcellular systems of transport vesicles and by coordinated opening and closure of cell-cell junctions. These systems must be tightly regulated to maintain endothelial integrity and to protect the vessels from any uncontrolled increase in permeability, which would lead to inflammation or thrombotic reactions.

Cell-cell junctions are not only sites of attachment between ECs; they can also function as signalling structures that communicate cell position, limit growth and apoptosis, and regulate vascular homeostasis. Through their cytoplasmic tail, junctional adhesion proteins bind to cytoskeletal and signalling proteins, which allows the transduction of extracellular signals to the cytoplasm (144;145). The association with actin is required not only for stabilisation of the junctions, but also for the dynamic regulation of junction opening and closure. In addition, the interaction of junctional adhesion proteins with the actin cytoskeleton might be relevant in the maintenance of cell shape and polarity (146).

The development in our understanding of ECs concerns the knowledge of the cell surface molecules. These proteins are transmembrane receptors and are composed of three domains: an intracellular domain that interacts with the cytoskeleton, a transmembrane domain and an extracellular domain that interacts with either other cell adhesion molecules or the ECM. Most of the cell adhesion molecules belong to four protein families; Ig (immunoglobulin) superfamily, the integrins, the cadherins and the selectins (147).

1.2.10.1 Calcium dependent adhesion molecules (Cadherins)

ECs have specialised junctional regions called adherent juctions and tight junctions. Tight junctions in ECs are combined with adherent junctions all the way along the cleft (Figure 1-9). Adherent junctions are cell-cell adhesion complexes that contain

cadherins and catenins. Catenins (α-catenin and β-catenin) are proteins found in complexes with cadherin cell adhesion molecules. α-catenin can bind to β-catenin and can also bind actin. Tight junctions contain claudin-5 (148). Junctional proteins can aso function as scaffolds by binding several effector proteins and facilitating their reciprocal interaction. Example of this includes the tight junction component zona occludens-1 (ZO1), which can associate with many transmembrane proteins, such as claudins, occludin or junctional adhesion molecules (JAMs); with cytoskeletal binding proteins such as α-catenin, vinculin and α-actinin; or with signalling mediators such as ZONAB (ZO1-associated nucleic-acid binding)(149;150).

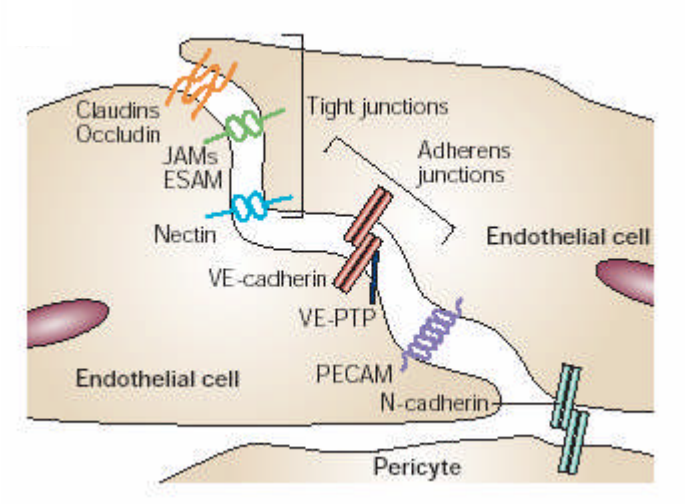

Figure 1-9. The organization of endothelial cell–cell junctions.
Transmembrane adhesive proteins at endothelial junctions. At tight junctions, adhesion is mediated by claudins, occludin, members of the junctional adhesion molecule (JAM) family and EC selective adhesion molecule (ESAM).
At adherens junctions, adhesion is mostly promoted by vascular endothelial cadherin (VE-cadherin), which, through its extracellular domain, is associated with vascular endothelial protein tyrosine phosphatase (VE-PTP). Nectin participates in the organisation of both tight junctions and adherens junctions. Outside these junctional structures, platelet-endothelial cell adhesion molecule (PECAM) contributes to endothelial cell–cell adhesion (151).

Cadherins are a family of adhesion molecules (152) that bind homophilically and heterophilically in a cation-dependent and protease-sensitive manner. ECs express at least three cadherins: N-, P-, and VE-cadherin (Vascular Endothelial Cadherin or CD144). N-cadherin is diffusely spread across the cell (153), P-cadherin is present in trace amounts (154). VE-cadherin is a strictly endothelial specific adhesion molecule located at junctions

between ECs. It is a calcium-dependent EC-EC adhesion glycoprotein functioning by granting the cells with the ability to adhere in a homotypic manner; this protein plays an important role in EC biology through control of the cohesion and organisation of the intercellular junctions. VE-cadherin is linked to the actin cytoskeleton via β-catenin (82). In addition as of vital importance for the maintenance and control of EC contacts, VE-cadherin regulates various cellular processes such as cell proliferation and apoptosis and modulates vascular endothelial growth factor receptor (VEGFR) functions (137). VE-cadherin has been described to mediate contact inhibition of cell growth, thereby negatively interfering with VEGFR-2-stimulated cell proliferation.

1.2.10.2 Cell to cell surface carbohydrate binding proteins (Selectins)

Selectins are a family of transmembrane molecules, expressed on the surface of leukocytes and activated ECs and platelets. The initial attachment of leukocytes, during inflammation, from the blood stream is afforded by the selectin family, and causes a slow downstream movement of leukocytes along the endothelium via transient, reversible, adhesive interactions called leukocyte rolling. L selectin, P-selectin and E-selectin can mediate leukocyte rolling. L-selectin is the smallest of the vascular selectins, and can be found on leukocytes. P-selectin, the largest selectin, is expressed on activated platelets and ECs. E-selectin is expressed on activated endothelium upon chemical stimulation or cytokine-induced inflammation.

P-selectin (CD62P) attaches to the actin cytoskeleton through anchor proteins and extends approximately 40nm from the endothelial surface. It is a component of the membrane of the alpha and dense granules of platelets, and also of the membrane of the WP- bodies of ECs. In common with the other selectins, P-selectin has an epidermal growth factor motif (155). P-selectin plays an essential role in the initial recruitment of leukocytes to the site of tissue injury during inflammation. When ECs are activated by inflammatory mediators such as histamine or thrombin, WP- bodies are mobilised and degranulate their vWF. P-selectin is also expressed at the cell surface as rapidly as two minutes after stimulation (156;157), as a consequence of the exocytosis of WP-bodies. Thrombin is one trigger that can stimulate EC surface translocation of P-selectin. Recent studies suggest an additional Ca2+-independent pathway involved in P-selectin surface expression regulation (156).

Additional synthesis of P-selectin is brought about by cytokines, such as interleukin-1, tumour necrosis factor-, and by thrombin, lipopolysaccharide or oxygen radicals. NO has been shown to be a regulator of P-selectin expression as inhibitors of NO synthase increased P-selectin expression (158). This may be clinically important as Minamino et al (159) suggest that concurrent low NO metabolites and high platelet P-selectin expression are linked. Although P-selectin will bind to heparan sulphate, its primary ligand is P-selectin glycoprotein ligand-1 (PSGL-1). PSGL-1 is found on a number of cells such as platelets, neutrophils, lymphocytes, eosinophils, monocytes and other myeloid progenitor cells (155;160).

1.2.10.3 Cell to cell and cell to matrix binding through Integrins

Integrins are cell surface receptors that interact with the ECM and define cellular shape, mobility, and regulate the cell cycle. These integral membrane proteins are attached to the cellular plasma membrane through a single transmembrane helix (161). Integrins play a role in the attachment of cells to other cells, and also a role in the attachment of ECs to the ECM. Besides the attachment role, integrin also plays a role in signal transduction (162).

The integrins are unusual membrane proteins because they transduce signals in two directions; 1) inside-out by transforming cytoplasmic information into surface conformational changes. 2) outside-in; by transducing from the ECM to the cytoplasm. This allows cells to make rapid and flexible responses (163). There are many types of integrins, and many cells have multiple types on their surface. They appear on the cell surface as heterodimers that comprise two distinct chains, α and β subunits (162). In addition, variants of some of the subunits are formed by differential splicing, for example 4 variants of the β-1 subunit exist. Through different combinations of these alpha and beta subunits, some 24 unique integrins are generated, although the number varies according to different studies. The β subunits are directly involved in coordinating at least some of the ligands that integrin bind (164).

Integrins bind to ECM components such as collagen (e.g. integrins α1 β1, and α2 β1) and fibrinogen (e.g. integrin αIIb β3) or act as cell-cell adhesion molecules (integrins of the β2 family) (165). Laminin, a major glycoprotein component of vessel basement

membranes, is recognized by β1- and β3-integrins expressed on ECs. The integrins VLA-2 (α2/β1-CD49b/CD29), receptor for laminin and collagen (166), VLA-5 (α5/β1-CD49e/CD29), receptor for fibronectin (167), VLA-6 (α6/β1-CD49f/CD29), receptor for laminin (168), and αVβ3-CD51/CD61, receptor for vitronectin (169) have been identified on ECs.

1.2.10.3.1 Attachment of cell to the ECM

The ECM is a complex structural entity surrounding and supporting cells that is found within mammalian tissues. As mentioned earlier the ECM is composed of 3 major classes of biomolecules: 1. Structural proteins; e.g. collagen and elastin, 2. Specialised proteins; e.g. fibrillin, fibronectin, and laminin and 3. Proteoglycans; composed of a protein core to which attached long chains of repeating disaccharide units termed of glycosaminoglycans (GAGs). ECM proteins can induce diverse intracellular signals by providing both mechanical and chemical stimuli to cells (170).

Integrins couple the ECM outside a cell to the cytoskeleton inside the cell. The interactions between the cell and the ECM may help the cell to endure pulling forces without being ripped out of the ECM (171). Integrins are not simply hooks, but give the cell critical signals about the nature of its surroundings. Together with signals arising from receptors for soluble growth factors like VEGF and EGF, they enforce a cellular decision on what biological action to take, be it attachment, movement, death, or differentiation. The attachment of the cells takes place through formation of focal adhesion complexes, which contain integrins and many cytoplasmic proteins that include talin, vinculin, paxillin and alpha-actinin. Focal adhesions act by regulating kinases like FAK (focal adhesion kinase) (172;173) and Src kinase family members to phosphorylate substrates such as p130CAS, thereby recruiting signaling adaptors such as Crk. These adhesion complexes attach to the actin cytoskeleton (Figure 1-10). Activation of FAK leads to subsequent alterations in the cytoskeleton and cell morphology, changes in adhesion strength, and changes in cellular responsiveness to mechanical stimuli (172). Fibronectin and type I collagen binding requires transcription factors (c-Fos and c-Jun) which are important in cell proliferation.

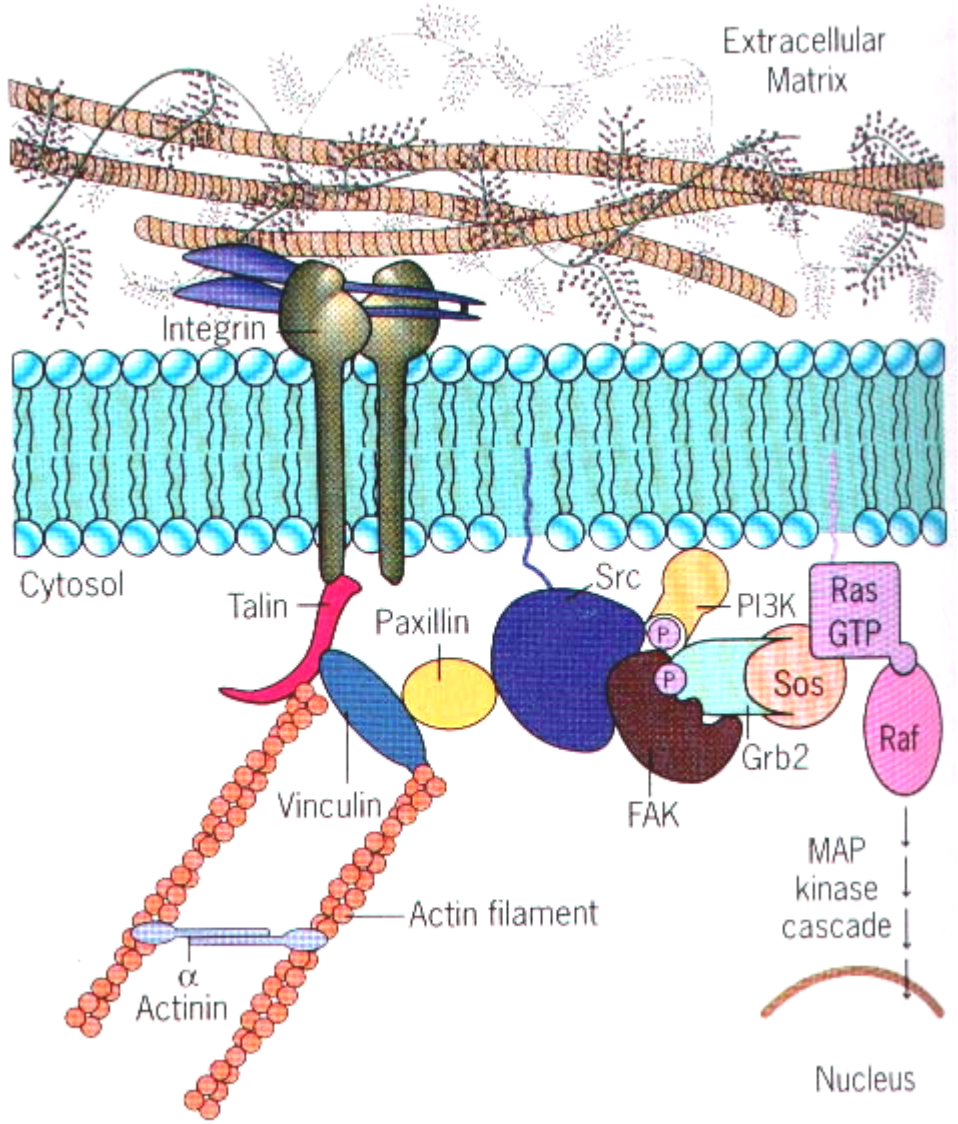

Figure 1-10. Integrins are receptors at sites of cell-substrate and cell-cell contact. Interaction between the extracellular domain of integrin and an extracellular ligand generate a variety of signals. The interaction leads to clustering of integrins and the rapid tyrosine phosphorylation of proteins at the cytoplasmic face of focal adhesions by the tyrosne kinase, Src. Focal adhesion kinase (FAK) is an effector in integrin-mediated responses (173).

One of the most important functions of surface integrins is their role in cell migration (174). Cells adhere to a substrate through their integrins. During movement, the cell makes new attachments to the substrate at its front and concurrently releases those at its rear. When released from the substrate, integrin molecules are taken back into the cell by endocytosis; they are transported through the cell to its front by the endocytic

cycle where they are added back to the cell surface. In this way integrins enable the cell to make fresh attachments at its leading front (175).

1.2.10.4 Non-calcium dependent cell to cell binding (Immunoglobulin)

Adhesion molecules of the immunoglobulin superfamily are involved in cell-cell adhesion, especially important during embryogenesis, wound healing, and the inflammatory response (176). They are transmembrane proteins that bind to the cytoskeletal system inside the cells. Outside the cell, the binding may be homophilic (to each other) or heterophilic (to different molecules)

As discussed above, leukocytes first establish transient interactions with the endothelium that allow them to roll along the endothelial surface. This is achieved primarily through the interaction of members of the selectin family and their ligands. Leukocytes then encounter chemokines on the endothelial surface. This activates leukocyte integrins such as Lß2 (also known as lymphocyte function-associated antigen-1; LFA-1) and 4ß1 (also known as very late antigen-4; VLA-4), allowing them to establish firm adhesions with the EC by interacting with endothelial ICAM-1 and VCAM-1 (177).

ICAM-1 and VCAM-1 are enriched in F-actin-rich structures that extend from the luminal surface of ECs towards leukocytes (178;179). During diapedesis, leukocytes cross the endothelium either through intercellular junctions (paracellular pathway) or through the EC body (transcellular pathway). The paracellular pathway involves platelet-endothelial cell adhesion molecule-1 (PECAM-1) and members of the junctional adhesion molecule (JAM) family (180). Less is known about the mechanism underlying the transcellular route, which is often observed *in vivo* (181). Leukocyte-EC interaction is believed to drive cytoskeleton and membrane rearrangements to "open" a transient channel across the EC for leukocyte transcellular migration (182). ICAM-1 engagement rapidly induces changes in EC morphology and redistribution of cell membrane proteins (178;179). This is followed by changes in gene expression, including modulation of endothelial adhesion molecule expression and production of proinflammatory mediators, which may mark these sites on the endothelium to recruit further leukocytes and prolong the inflammatory response (183).

ECs express other cell-specific homophilic adhesion proteins at intercellular contacts. Platelet endothelial cell molecule (PECAM; also known as CD31) is an Ig superfamily adhesion molecule highly expressed on EC. It was originally described as a protein capable of mediating cell-cell adhesion through homophilic interactions (184;185). In addition to being an adhesive protein, PECAM-1 has important intracellular signalling capacities that function to control cell activation and survival (186;187).

1.3 Clinical relevance: Role of EC in development of tissue engineered bypass graft

1.3.1 Development of hybrid/seeded graft

Prosthetic grafts do not spontaneously endothelialise in humans except for a short peri-anastomotic region, where the anastomosis is made (188;189). It is thought that this lack of EC contributes to the failure of the prosthetic graft by thrombosis in this region devoid of cells (73). Matsuda and co-workers have been investigating the development of hybrid vascular prostheses composed mainly of SMC, collagen with reinforcement onto polyester fibres. These grafts once developed could then be seeded and have shown promising results (190). This group has also been evaluating polyurethane and Dacron scaffolds (191), (192). Polyurethane scaffolds have been used because of their unique properties in tissue engineering. This scaffold has been either seeded with both SMC and EC (193) or lined with an artificial membrane composed of collagen and dermatan sulphate before seeding. SMCs make the scaffold more viscoelastic rather than elastic, thus mimicking the mechanical properties of native vessels. Such grafts were then used in canine models and showed promising results after implantation, with patency rates of up to 75% after 26 weeks (194).

Developing a bio-hybrid vascular graft would require the EC to undergo four phases (see Figure 1-11). These cells have to first remain viable within the culture medium exposed to fragments of the polymer as well as on direct contact with the polymer (Phase I). Next, the EC would have to adhere to the polymer surface, preferably within a short time, to minimise the complications associated with long-term cell cultures

(Phase II). These adherent ECs would then need to proliferate at a steady rate (phase III) in order to achieve a confluent EC monolayer (Phase IV).

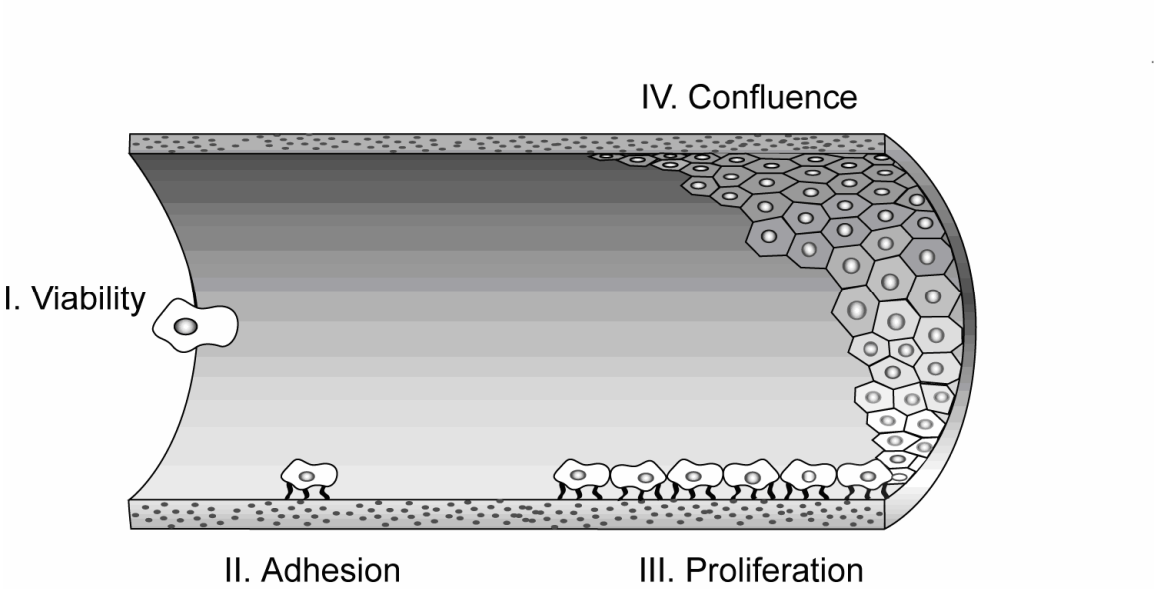

Figure 1.11. Schematic representations of the stages of cell seeding on biomaterials.

A cellular engineering approach called 'seeding' has been used to overcome graft failure. In simple terms, it involves lining the lumen of the graft *in vitro* with EC (195;196). To be successful in a clinical situation, seeding of grafts has required the culturing of EC over a period of weeks to date. As a result of this problem, there have been numerous attempts at creating fully tissue-engineered vessels composed of prosthetic (ePTFE, Dacron or polyurethane), bioresorable (e.g. polyglycolic acid (PGA), poly-L-lactic acid (PLLA)) or fully biological materials together with autologous cells, which can be readily available on the shelf of any operating theatre (197).

1.3.2 Seeding techniques with mature EC

There are currently two strategies in seeding of grafts: a two-stage or a single-stage procedure (195;198;199). Two-stage seeding is the conventional and successful technique used and is discussed below. Single-stage seeding is the technique most aspired for and this is discussed subsequently. The principal sources for EC extraction are vein, artery,

omental or subcutaneous fat, laparotomy washes and blood as progenitor cells. These tissues are relatively easily accessible in clinical practice (200).

1.3.2.1 Two-stage seeding

In two-stage seeding, the EC are extracted and made to undergo a prolonged period of cell culture in the laboratory in order to increase the cell numbers before seeding. The cells are normally cultured for a period of between 2 and 4 weeks (201). The main source of EC in two-stage seeding has been a vein harvested from the patient though arteries are used occasionally. This technique has given rise to excellent patency rates in animal studies: patency rates of 62.5% without antiplatelet drugs and 100% with them (202-204). The high initial density of seeded EC means that even with cell loss on exposure to pulsatile blood flow on implantation, the EC is still functionally effective as a whole since a relatively high number of cells are still left attached. However a confounding factor is that in animals, such constructs tend to show improved results compared to studies in humans. This is due to the inherent ability of many animals to self-endothelialise their vascular lumens (205), a problem which was only realised when initial clinical trials in humans with these seeded grafts showed poor results. This problem may be overcome if older animals are used as a model (206;207). It is for this reason that the authors tend to assess the efficacy of their seeding experiments *in vitro* with the use of physiological blood flow pumps (199;208).

An apparent disadvantage of the two-stage seeding procedure in clinical practise is that it cannot be used in the emergency situation because of the prolonged cell culture time (2 – 4 weeks), the ever-increasing probability of infection within the cell culture medium and the inability of the cells to proliferate effectively with time (209;210). In addition, it incurs the extra cost of a cell culture technician and the need for a culture laboratory.

1.3.2.2 Single-stage seeding

This method also utilises freshly harvested EC of either venous or microvascular origin (200). Microvascular sources include omental and subcutaneous fat (211;212). In the single-stage procedure, the EC are harvested and then immediately seeded onto

grafts. The obvious benefit of this is that it can be performed during a surgical operation, thus avoiding a second procedure and the costs and risk of infection associated with prolonged cell culture.

Herring *et al* introduced the concept of single-stage seeding in 1978 using EC derived from canine veins. They showed that grafts seeded by this way in a canine animal model established an extensive EC lining (195). However for reasons mentioned above, animal models may not be the most suitable method of assessing the efficacy of seeding. The results of the initial clinical trials of single-stage seeding using vein as a source of EC were disappointing (196;198). The reason was thought to be the low seeding density of EC due to the low number of EC that can be extracted from veins using current methods. Therefore when undertaken, these low numbers exert a minimal effect on the endothelialisation of the PTFE graft (209). This is because a proportion of seeded cells are lost when exposed to pulsatile blood flow (213). This could be overcome by improving the cell density.

1.3.3 Improving cell adherence and retention to the graft lumen

For both tissue engineers and biomaterial researchers, precise control of cell interactions with the prosthetic or biomaterial surface is critical. To this end, the tissue engineer requires the interaction of specific cell types with the material surface used in the vascular construct in order to promote tissue ingrowth as well as regeneration of the construct. In bio-hybrid tissue constructs, the tissue engineer seeks to obtain very specific cells such as ECs to place into biomaterial based scaffolds. Optimal cell–polymer interaction would allow the host tissue to integrate with the graft and allow for the development of actual tissue formation. The development of bio-hybrid or fully tissue-engineered biological vascular grafts requires the very selective adhesion of actual donor/patient cells onto the implanted vascular graft in such a way that these cells optimally integrate and most importantly adhere onto the surface with limited inflammatory cell-mediated encapsulation (214).

Numerous research groups have examined whether modifications to the luminal surface of the prosthetic graft can stimulate self-endothelialisation or allow improved adherence of pre-seeded cells when exposed to arterial flow (215). This lack of adherence

as discussed earlier is an important cause of the problems associated with low density seeding; the major cause of graft failure so far in clinical trials. The majority of the work on promoting EC adherence and growth to permanent non-biodegradable polymers has involved the modification of the surface with a single coating of endothelial cell-specific adhesion proteins. These substances include albumin (216), albumin–heparin conjugates (217), collagen (218-220), collagen–elastin matrices (221), fibronectin, gelatin (222), fibrin-gelatin (223), laminin (224), extracellular matrix (225), dipyridamole (47), granulocyte-stimulating factor (G-CSF) (226), peptide fragments (227), preclotting with blood, plasma, fibrin glue (228) and serum (229). Fibrin glue is the commonest substrate used in trials of two-stage seeding in humans (230). Non-ligand based techniques have included carbon deposition, photo discharge, chemical vapour deposition (231) and plasma discharge technology (232) in order to deposit reactive groups onto polymer surfaces or to directly influence the proteins adsorbed to the surface. These methods to encourage cell attachment have met with limited success owing to the lack of specificity and poor control over protein orientation. Physical methods to improve the development of a pseudointima on the surface have involved altering the porosity and nano-texture (233) of luminal surfaces to promote tissue ingrowths into the graft and allowing it to act as a three-dimensional scaffold for cell seeding and tissue engineering (219).
Haemodynamics flow is a way of increasing cell retention to the graft surface. This method is the main consideration in this thesis and is further discussed in Chapter 2.

1.4 Conclusion

The success of current clinical grafts such as Dacron in large calibre high flow vessel replacement has not been replicated when considering small diameter vessels with low flow. The non-clinical studies in cardiovascular tissue engineering have led to important advances in the progression to a blood vessel substitute that can serve as a living graft. These should be responsive to the surrounding biological environment, be self-replicating and have an inherent healing potential. It is now been shown to be possible to develop cellular engineered grafts composed purely of human cells. The mechanical strength of biomaterials derived from the ECM, the production of the matrix and the integrity of the cellular sheets themselves could be significantly enhanced by simple alterations in cell culture conditions. The optimal biological coronary or vascular

graft can only be used *in vitro* if they are incubated within bioenvironmental conditions that they would confront *in vivo* or during their natural formation. For example, studies have shown that culturing SMC within a pulsatile flow model similar to *in vivo* arterial systems helped mimic nature's vessels. Seliktar *et al.* (234) have discovered that gene expression is enhanced when such constructs are subjected to *in vivo* cyclic strain. Chello *et al,* (235) have found that *in vitro* pressure distension markedly increases expression of adhesion molecules like inter-cellular adhesion molecule (ICAM-1) while earlier studies showed that haemodynamic forces were able to stimulate the expression of platelet-derived growth factor (PDGF), an SMC mitogen (236) and (237).

The problems associated with graft thrombosis and neointimal hyperplasia are most prevalent in small calibre (<6 mm) prosthesis, leading to their poor medium and long term results, so the development of these conduits from the nanocomposite would have the highest impact. The multiple demands placed on a small calibre CABG grafts have meant that a synthetic prosthesis with good long-term patency has not been developed. A tissue-engineered graft could fulfil the ideal characteristics present in an artery. ECs are of great interest because of their potential in cell therapy for vascular diseases and ischemic tissue, tissue engineering for vascular grafts and vascularized tissue beds, and modeling for pharmaceutical transport across endothelial barriers.
Studying the biology of endothelial cells is a new understanding of the response of endothelial cells to biomaterials and will aid in the design of the next generation of scaffolds for cardiovascular tissue engineering

Aim of thesis:

The aim of this thesis was to understand the behaviour of endothelial cells seeded on the novel nanocomposite for development of small diameter coronary artery bypass grafts.

Ultimately to determine the influence of haemodynamic shear stress responsive genes on endothelial cells seeded on nanocomposite conduits.

2

Molecular aspects of haemodynamics and vascular tissue engineering

2.1 Mechanical forces in the vessel

The haemodynamic forces within blood vessels regulate vascular development, adaptation and pathogenesis of vascular disease. The major stresses affecting the blood vessel wall are shear stress - the longitudinal frictional element that flowing blood directly exerts on EC lining - and circumferential tensile stress, generated by the repetitive pulsatile pressure and translating to a cyclical stretch in the circumferential direction (Figure 2-1).

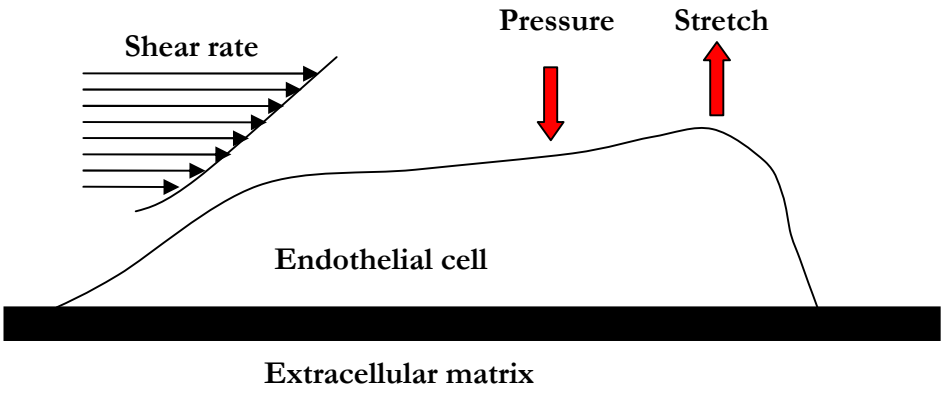

Figure 2-1. Schematic diagram of vessel wall and the mechanical forces.

Stress exerted on the EC can detach them from the graft surface. Circumferential stress stretches individual cells that are anchored. However, due to blood's direct interaction with the inner vessel WSS is the most relevant to thrombosis (238). Shear stress is described as the force per unit area generated by flow of a viscous liquid (238). On the basis of a Newtonian fluid (239), in a tubular chamber having radius r, flow direction z, fluid viscosity μ, and fluid velocity v the following mathematical formula can be used to calculate shear stress τ (see equation 1):

$$\tau = \mu(dv_z/dr) \qquad (1)$$

Poiseuille considered Newtonian fluid behaviour in a vessel. However, the mechanics of blood flow are more complex than Poiseuille fluid dynamics that apply principality to steady flow in a rigid tube of circular cross section. In the arterial circulation, blood flow is pulsatile; it is non-Newtonian and the vessel is a compliant tube of changing cross-sectional shape and area with many side branches and bifurcations. Each of these variables have been considered in flow models in order to achieve accurate assessment of WSS *in vivo* (240-242).

Shear stress and shear rate values are usually given as dynes/cm^2 (or Pa) and 1/s, respectively. Alternatively, wall shear stress can be expressed as N/m^2. According to the international system (SI) of units as the viscosity of whole blood is about 0.035 Pa (243), the normal shear stresses and shear rates in the human aorta are 1.6-12 dynes/cm^2 and 45-305 1/s, respectively. The average shear stress in a venous circulation is 0.2 dynes/cm^2 that is substantially less than the shear stress in a bypass graft inserted into the arterial circulation (3-6 dynes/cm^2) (244). Table 2-1 illustrates the range of normal shear stress gradients experienced at various locations. Of note is that the average shear stress in a venous circulation is substantially less than the shear stress in a bypass graft inserted into the arterial circulation (244).

Table 2-1. As blood flow is pulsatile, the velocity profile varies within the cardiac cycle to produce a range of shear stress gradients and is influenced by curvatures in the vessel wall notably, bifurcations and branches. This table shows the range of calculated mean shear stress in regions of uniform geometry and away from branched vessels. Zamir *et al* calculated wall shear stress at every point in the arterial tree to be at the same constant value of 15 dynes/cm^2 (245).

Blood vessel	Mean shear stress range (dynes/cm^2)
Human aorta	1.6-12
Large artery	20-40
Vein	0.2
Bypass graft inserted into arterial circulation	3-6

Pathology based studies indicate that atherosclerotic lesions are at branches and bends of the arterial tree (246) where there are variations in shear stress. Initially, it was suggested that high shear stress resulted in mechanical damage of the endothelium thereby initiating vessel wall pathology (247). Extremely high shear values, 105-350 dynes/cm^2 have been detected at top of plaques in stenotic atherosclerotic coronary arteries (248). Further work has led to the conclusion that low shear stress also has an important factor in the development of early atherosclerotic lesions (246;249;250), yet it is still not fully understood as to why and no single theory has been suggested that adequately answers this paradox. Atherogenesis due to decreased shear stress is associated with a reduction in several vascular wall functions including endothelial nitric oxide synthase (eNOS) production, vasodilation and EC repair. These are coupled with an increase in leukocyte adhesion, apoptosis, SMC proliferation and collagen deposition (251).

The effects of shear stress have been extensively studied in blood vessels that respond with an active process 'remodelling' that involves the endothelium, vascular SMC, fibroblasts and ECM. Much of the investigation of the effect of haemodynamics has been conducted *in vitro* with precise control of the mechanical environment. The range of shear stresses examined *in vitro* has typically been 0-100 dyn/cm^2 mainly in steady unidirectional laminar flow, but with some attention to the effects of pulsatile flow (252).

2.1.1 The endothelial response to shear stress

Although the entire vessel wall, including ECs, SMCs and the ECM is subjected to stretch as a consequence of pulsatile pressure, shear stress is received principally at the endothelial surface therefore in this thesis we are primarily interested in the EC response to shear stress. To determine the effects of flow on ECs, studies in which flow can be systematically varied are needed. It is difficult to achieve this *in vivo* and it is also difficult to define the characteristics of the haemodynamic environment. Limited studies have been performed using pressure transducers, Doppler ultrasound and *ex vivo* models of the vasculature. As a result, a vast amount of work has been focused on evaluating EC function when they have been exposed to flow *in vitro*. Shear stress has been achieved by flowing fluid across EC monolayer under controlled conditions. Tensile stress is generated by applying a cyclic strain which stretches the EC monolayer.

The tools that have been used to apply flow have been the parallel-plate and the cone-plate apparatus. A parallel plate is a flow chamber with one side consisting of a gelatine-coated glass plate on which the cultured EC rest, the other side is usually a polycarbonate plate and these two flat surfaces are held apart by a Teflon gasket (253). Cone-plate apparatus consists of a stainless steel cone driven by an electric motor and a stage that holds a culture dish with a glass plate inserted at the bottom of the dish. Rotation of the cone forces the fluid concentrically between the cone and glass plate, exposing cells attached to the gelatine-coated glass plate to fluid shear stress (254). Many researchers have used flow circuits as an *in vitro* system to investigate the responses of cultured EC to haemodynamic forces at the cellular and molecular level (255;256).

In response to shear stress EC undergo changes in cell shape, alignment and microfilament network remodelling in the direction of flow (Figure 2-3). Bovine aortic endothelial cells (BAEC) exposed to nonreversing sinusoidal shear stress of 40 ± 20 dynes/cm^2 for 24 hours showed marked elongation compared to static (no flow) conditions (252;257). This response mimics the phenotype of EC observed in its *in vivo* state (258). Reorganisation of the F-actin filaments, a major component of the cytoskeletal structure of EC, was observed prior to the morphological response of the EC; suggesting that it may be related to the sensing mechanism of shear stress (257). Adaptation to flow is believed to contribute to reducing shear gradients along the EC surface (259). When exposed to reversing sinusoidal shear stresses of 20 ± 40 and 10 ±

15 dynes/cm^2, BAEC changed less rapidly in shape and were less elongated than their steady controls. With oscillatory shear stresses of 0 ± 20 and 0 ± 40 dynes/cm^2, BAEC cell shape remained polygonal as in static culture and did not exhibit actin stress fibers, such as those that occurred in all the other flows (252). These results demonstrate that EC can discriminate between different types of pulsatile flow environments.

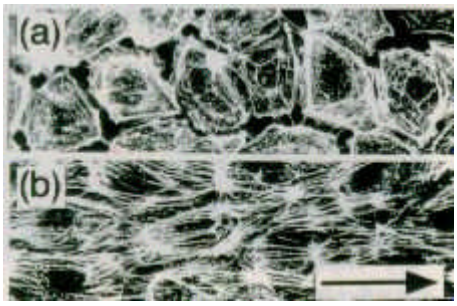

Figure 2-2. Morphology of endothelial cells before (a) and after (b) applying shear stress (252).

2.1.2 Shear stress regulates gene expression

Shear stress regulates EC function by altering the gene expression profile, including growth factors, adhesion molecules, vasoactive substances and cell signalling molecules. Various genes have been shown to be upregulated or downregulated in response to different magnitudes of shear stress (see Table 2-2). Previous *in vitro* and *in vivo* findings have shown that a sudden onset of shear stress activates EC signalling pathways and modulates EC gene expression (260-262).

Laminar shear stress induces gene expression in a time dependant manner. The sudden application of shear stress to EC in static culture showed a transient increase in the expression of a large number of genes, but most of these genes were downregulated during sustained application of shear stress (24 hours) (260). DNA microarray studies have been performed and reveal comprehensive analysis of gene expression profiles in EC under shear stress (263;264). Human aortic endothelial cell (HAEC) monolayer were seeded onto glass slides and placed into a flow system composed of a silicone gasket mounted between the glass slide and an acrylic plate and exposed to laminar shear stress of 12 dynes/cm^2 for 24 hours (263). This level of shear stress is encountered under physiological conditions in the straight part of the aorta and is frequently used to study the effects of shear stress on EC (265). A significance difference ($P < 0.05$) was

observed in 125 genes between the sheared and static samples. Several proinflammatory and prothrombotic genes were significantly downregulated, including an adapter protein myeloid differentiation primary response gene 88 (MYD88, 0.37 ± 0.15) that is essential for signalling.

The EC growth factor, transforming growth factor-β2 (TGF-β2, 0.42 ± 0.05) was also significantly downregulated by 24 hours of shear stress (263). Furthermore, ECM-related genes such as cytokeratin 4 (0.34 ± 0.04) and laminin-α4 (0.54 ± 0.08) were also observed to be significantly downregulated. This was further confirmed by the significant upregulation of matrix metalloproteinase-1 (MMP-1, 2.77 ± 0.35) in response to 24 hours of shear stress. Many signal transduction related-genes in particular those related to endothelium-specific receptor tyrosine kinases such as angiopoeitin-Tie 2 and FlK-1 (266;267) were found to be upregulated. The screening of mRNA from human umbilical vein endothelial cells (HUVEC) identified 52 genes to have significantly altered expression when exposed to shear stress of 25 dynes/cm^2, compared with static conditions (264). The most dramatically up-regulated gene expression was observed in the cytochromes P450 (CYP) gene's (264;268). In particular, the CYP 1A1 and 1B1 were only affected by shear stress in HUVEC. The strong induction of these CYP genes by shear stress is consistent with the suggestion that physiological levels of shear stress are protective for the endothelium.

Turbulent flow patterns including flow separation, flow reversal, and low and fluctuating wall shear stress (< few dyne/cm^2) occurs at branched points and bifurcations in the arterial vasculature where they are prone to atherosclerotic lesions (250;269). Several studies have examined the response of EC to turbulent shear stress. EC produce urokinase-type plasminogen activator (uPA) that has been shown to stimulate the migration and proliferation of SMC and indirectly activate MMP that degrades the ECM (270). Its increased expression has also been observed in SMC during neointimal formation in injured rat arteries (271).

The effects of laminar and turbulent shear stress on the expression of uPA at both protein and mRNA level was investigated in human coronary artery endothelial cells (HCAEC) (272). A parallel plate-type apparatus (253) was used to apply laminar shear stress of 15 dynes/cm^2 and a cone-plate-type apparatus (254) was used to apply turbulent shear stress of 1.5 dynes/cm^2. ELISA and real-time PCR analysis showed laminar flow to downregulate uPA gene expression by HCAEC whilst turbulent shear

stress markedly increased its expression. A nuclear run-on assay demonstrated a decrease in the transcription of uPA gene expression in HCAEC after 3 hours exposure to laminar flow, whereas turbulent shear stress had no effect. This study provides some evidence that turbulent shear stress may contribute to the pathogenesis of atherosclerosis by increasing endothelial uPA production. Laminar shear stress increases the atheroprotective gene NO in HUVEC whereas turbulent shear stress has no effect (273). Recent studies have revealed striking differences in the number of endothelial genes that respond to laminar or turbulent shear stress (274).

Table 2-2. mRNA response to mechanical forces when exposed to cultured cells.
Keys: BAEC – bovine aortic endothelial cells; HAEC – human aortic endothelial cells ; HUVEC – human umbilical endothelial cells; HCAEC – human coronary artery endothelial cells; PCAEC – porcine coronary artery endothelial cells; HUSMC – human umbilical smooth muscle cells; HSVEC - human sapheneous vein endothelial cells; HASMC – human aortic smooth muscle cells; TGF – transforming growth factor; PDGF – platelet derived growth factor; bFGF – basic fibroblast growth factor; MMP – matrix metalloproteinase; TIMP - Tissue inhibitors of metalloproteinases, ICAM- intracellular adhesion molecule; VCAM – vascular adhesion molecule; EGR1-early growth response-1; cfos – transcription factor; Tie2 - angiopoeitin-1; eNOS – endothelial nitric oxide synthase; CYP - cytochrome P450; MCP-1 - monocyte chemoattractant protein-1; tPA – tissue plasminogen activator ; uPA – urokinase-type plasminogen activator; PAR-1 - protease-activated receptor-1.

Gene	Cell type	Shear stress/Cyclic strain	Period	Response	Author
Growth factors					
TGF-β1	BAEC	15 dynes/cm²	24 hrs	Increase	(275)
TGF- β2	HAEC	12 dynes/cm²	24 hrs	Decrease	(263)
PDGF-A	HUVEC	16 dynes/cm²	1.5-2 hrs	Increase	(268)
PDGF-B	HUVEC	31 dynes/cm²	4 hrs	Decrease	(268)
	BAEC	60 cycles/min; 10 % strain	4hrs	Increase	(276)
bFGF	HUVEC	15 dynes/cm²	24 hrs	Increase	(277)
	BAEC	36 dynes/cm²	6 hrs	Increase	(278)
		20 cycles/min; 20 % strain	20 min	No change	(278)
ECM/ECM degradation enzymes					
Collagen VII	HCAEC	15 dynes/cm²	3, 6, 12, 24, and 48 hrs	Increase	(279)
MMP-1	HAEC	12 dynes/cm²	24 hrs	Increase	(263)
MMP-2	BAEC	60 cycles/min; 2.5 % strain	8 hrs	Increase	(280)
TIMP1/2	HAEC	12 dynes/cm²	24 hrs	No change	(263)
Adhesion molecules					
ICAM-1	HUVEC	2-25 dynes/cm²	12 hrs/48 hrs	Increase	(281;282)
	HUVEC	15 dynes/cm²	4 hrs	Increase	(283)
VCAM-1	HUVEC	2-25 dynes/cm²	12 hrs	Decrease	(281)
	HUVEC	15 dynes/cm²	4 hrs	No change	(283)
	HUVEC-HUSMC coculture	12 dynes/cm2	6 hrs	Decrease	(284)
E-selectin	HUVEC-HUSMC coculture	12 dynes/cm2	6 hrs	Decrease	(284)
Cell signalling					
EGR-1	HUVEC	20 dynes/cm²	30 min	Increase	(285)
		3 dynes/cm²	30 min	No change	
c-fos	HUVEC	16 dynes/cm²	30 min	Increase	(286)
	HUVEC	16 dynes/cm²	1 hr	Decrease	(286)
Tie2	HAEC	12 dynes/cm²	24 hrs	Increase	(263)
Vasoactive compounds					
eNOS	BAEC	60 cycles/min; 10 % strain	24 hrs	Increase	(287)
	PCAEC	60 cycles/min; 6 % strain	18-24 hrs	No change	(288)
	HUVEC	8 dynes/cm²	6 hrs	Increase	(273)
Endothelin-1	HUVEC	25 dynes/cm²	6 hrs, 24 hrs	Decrease	(264)
	HUVEC	8 dynes/cm²	6 hrs	Decrease	(273)
CYP 2C	PCAEC	60 cycles/min; 6 % strain	18-24 hrs	Increase	(288)
Others					
MCP-1	HUVEC	16 dynes/cm²	1.5 hrs	Increase	(289)
	EC-SMC coculture	12 dynes/cm²	1.5 and 6 hrs	Decrease	(290)
tPA	HSVEC	60 cycles/min; >7 % strain	1, 3 and 5 days	Increase	(291)
	HUVEC	25 dynes/cm²	24 hrs	Increase	(292)
uPA	HCAEC	1.5 dynes/cm²	I hr 3hrs	Increase Decrease	(272)
PAR-1	HASMC	60 cycles/min; 20 % strain	6 hrs	Increase	(293)
CYP 1A1, CYP 1B1	HUVEC	25 dynes/cm²	24 hrs	Increase	(264)

2.2 Haemodynamics plays a key role in tissue engineering

2.2.1 Neointimal thickening in prosthetic grafts

Following prosthetic arterial grafting, neointimal thickening, prominently at the distal anastomosis, has been implicated as the major cause of restenosis and long term graft failure. Studies have established that non-uniform haemodynamics including disturbed flows in particular at the anastomosis, abnormal WSS, compliance mismatch and mitogen release from platelets, leukocytes and vessel wall cells are the aetiologies of neointimal hyperplasia. The extent of neointimal thickening depends on the rate of blood flow or shear stress. When grafts are allowed to heal under high blood flow or high shear stress, a smaller neointima is formed as compared to those that heal under normal flow or shear stress (294). Subsequently when the high shear stress (~50 dynes/cm^2) exposed grafts are returned to normal shear stress (~10 dynes/cm^2), the neointima begins to expand due to SMC proliferation and ECM production (295). During arterial development there is a balance between cell proliferation and matrix protein synthesis and as well as cell death and matrix degradation (296-298).

Berceli and colleagues examined whether flow-induced neointimal regression in prosthetic grafts occurs through a similar perturbation mechanism. PTFE grafts (5 cm in length and 4 mm in diameter) were placed in male baboons and the haemodynamics were monitored using Duplex ultrasonography (299). The prosthetic graft was able to heal and the growth of neointima was observed in a normal flow environment largely because of subendothelial SMC replication. They demonstrated that the rate at which neointimal hyperplasia develops is dependent on the balance between subendothelial cell replication and cell death in the region adjacent to the graft. By modulating the haemodynamics environment and more specifically through changes in shearing forces, the balance between these processes appears to be altered and results in a change in neointimal thickness within the graft. Regression occurred by day 7 through simultaneous reduction in cell number and loss of surrounding matrix. This agrees with recent findings that reveal an increase in MMP such as MMP-2 and MMP-9 under conditions of high flow (300). These findings are similar to other studies where cell proliferation and death were closely regulated by shear stress (297). To examine ECM changes during neointimal regression, blood flow through PTFE grafts, which had healed for 2 months under normal blood flow (~10 dynes/cm^2), was switched to high

flow (~40-60 dynes/cm^2) for up to 56 days. Under all conditions studied the graft neointima was rich in hyaluronan and verscan and lacked elastin, similar to the intimal ECM produced after angioplasty (301).

2.2.1.1 Genes involved in neointimal thickening

Compliance mismatch between the graft and native artery at the anastomosis leads to excessive stretching of the SMC, leading to enhanced proliferation. Turbulence of blood flow around the anastomosis causes EC damage which in turn leads to expression of growth factors that affect the SMC. This alteration of active genes can change the levels of intracellular proteins and the production of ECM molecules, resulting in the SMC migrating into the neointima then proliferating and so causing deposition of an ECM causing a restenotic anastomotic lesion. While many researchers have identified factors responsible for intimal hyperplasia, the mechanism of action of these factors has yet to be elucidated.

Several genes have been identified with altered expression at the distal anastomosis following prosthetic arterial grafting (302-304). Using microarray technology, gene expression patterns *in vivo* were evaluated at the distal anastomosis of a canine prosthetic arterial grafting model across several time intervals (305). After 7, 14, 30 and 60 day implantation, 1 cm of distal ePTFE grafts at the anastomosis and adjacent native artery was removed for RNA extraction. The screening of selected genes, in particular collagen type I, α-I and α-II and osteopontin, showed an increase in mRNA expression at all time points. Collagen type 1 was also shown to be upregulated by Geary *et al.* in the neointima as compared to normal primate aorta and is a major part of the ECM (306). Subsequently Kalish and colleagues used a similar model and found collagen type I (α-II), III, IV and XI and procollagen type I expression to be upregulated in autologous vein bypass grafting *in vivo* (307). However certain genes which have been associated with IH were shown to be absent, including fibroblast growth factor, PDGF-α, TGF-β, osteopontin and elastin (307). It is suggested that the genes that are associated with vein graft remodelling are not identical to the genes expressed after injury models and prosthetic arterial bypass grafting. As well as collagen expression, osteopontin a phosphoprotein that functions as a cell adhesion and migration molecule has found to be involved in the development of medial thickening and neointima formation (308). Reduced mRNA expression of genes such as

smoothelin-B, a marker of mature contractile VSMC (309) were also observed at the anastomosis (neointima and adjacent) throughout each time point examined in both prosthetic and autologous vein bypass grafting (305;307). Overall the genes that have been found to be expressed at earlier time points were found to be transcription factors (jun-B and c-fos) key for activating growth promoting genes. However, many of the genes that were upregulated at the later time points (30 - 60 days) of implantation, such as allograft inflammatory factor (AIF-I) in which its expression may be due to the prosthetic material present at the anastomosis and matrix –associated genes such as fibronectin and collagen type II (α-I) (301). Further studies are required to localise such gene products to a specific cell type at the anastomosis.

EC that produce, among other substances PDGF-BB and bFGF, have an important role in the development of anastomotic neointimal hyperplasia. PDGF has a major role in promoting migration of SMC from the media to the intima and bFGF is characterised by its affinity for heparin and its ability to stimulate EC and SMC proliferation. ePTFE disks were seeded with HUVEC in serum-free media (310). The release of PDGF-BB and bFGF from EC seeded ePTFE was significantly higher when than that released by EC seeded into TCP. This release of mitogens confirms that EC seeded ePTFE grafts might synthesise and release growth factors that regulate SMC proliferation and the process of intimal thickening (311). Pitsch and colleagues seeded EC on Dacron grafts and implanted them in a canine model (n = 11) for 20 weeks in order to identify the cells in vascular grafts that produce PDGF (312). The EC and SMC were cultured from grafts and adjacent aorta. Increased PDGF was observed in graft SMC as compared with aortic SMC, suggesting that graft SMC may be a contributing factor to the development of intimal hyperplasia. Elsewhere the effect of high blood flow on the expression of eNOS was investigated in femoral arteriovenous shunt (AVS) rats created by inserting U-shaped polyurethane tubes in the left femoral arteries and veins. At the site of the distal anastomosis mRNA expression levels of eNOS were increased whereas inducible nitric oxide synthase (iNOS) was not (313).

2.2.2 Gene expression in prosthetic grafts

Understanding the cellular response to a foreign substance is vital. The investigation of gene expression patterns allows determining if the cells are expressing any detrimental effects in the short and long term. In later chapters, gene expression of

cells seeded on nanocomposite is the prime investigation of this thesis. In particular the cells response to shear stress is examined.

Gene expression associated with cellular proliferation, adhesion and ECM formation have been poorly studied on cylindrical prosthetic grafts. The lack of such studies may have been due to the difficulties in harvesting cells from the graft surface in order to extract mRNA. As reported above, studies to characterise gene expression in response to flow have been determined through applying flow to cultured EC and vascular SMC. Other reports have focused on seeding cells onto flat sheets of polymer and monitoring gene expression (314;315). Zhang and colleagues (314) assessed cell growth *in vitro* on a peptide based poly(urea-urethane) polymer. Rabbit bone marrow stromal cells (RBMSC) were cultured for 7 days on flat sheets of degradable lysine-di-isocyanate-glycerol-urethane (LDI-glycerol) and compared expression for collagen type 1, TGF-β1 and osteocalcin. There was no significant difference between the mRNA expression of these factors in RBMSC grown on LDI-glycerol polymer or on control tissue culture polystyrene. The Menconi group (315) extracted RNA from BAEC after 5 days of culture of flat sheets of two poly(ether)urethanes: Biomer and Tecoflex SG60D respectively. Expression of fibronectin, actin, vimentin, histone and collagen was investigated and it was found that significantly lower levels of fibronectin, actin and vimentin were being produced by day 5, whilst no collagen at all by day 5 and very limited levels of histone in both polymers.

Although the expression of vital genes has been found to alter when present on flat sheets of polymer in response to shear stress, there is still the question whether these genes behave in a similar way when seeded on cylindrical grafts and exposed to flow. In this thesis, one objective was to focus on developing a reliable method for obtaining functional mRNA from cells seeded on vascular prosthetic grafts (see Chapter 4). This would then enable the next major challenge in this work of investigating gene expression in response to shear stress.

Currently only two-dimensional models exist and three-dimensional studies are required to understand the behaviour in particular gene function of vascular cells when seeded onto three-dimensional grafts used for bypass surgery. Three-dimensional models also more accurately represent an *in vivo* environment. Li and colleagues studied the profile genomic remodelling of SMC in three-dimensional collagen matrix and on a

two-dimensional collagen matrix surface and to elucidate the signalling events leading to the differential expression profile (316). HASCMC were cultured on two-dimensional and three-dimensional collagen matrix for 24 hours and then extracted for RNA isolation. DNA microarray revealed changes due to the differences in matrix geometry. Compared to two-dimensional matrix, the expression of p21 (cell cycle regulator) was found to increase compared to three-dimensional matrix. Hence this may suggest the factor responsible for the decreased proliferation in three-dimensional culture. Moreover, three-dimensional matrix yielded higher levels of gene expression for matrix proteins collagen 1 and fibrinogen, indicating that SMC were more synthetic in this matrix. The matrix remodelling gene, MMP-1 did not change with matrix geometry. This study helped to define the molecular mechanisms involved in the phenotypic modulation by matrix geometry, as the results suggest that SMC in three-dimensional matrix are more synthetic, less proliferative and less contractile.

In vitro models of vasculogenesis and angiogenesis have shown EC to sprout, proliferate, migrate or differentiate in a three-dimensional manner (317). Ueda *et al* constructed an *in vitro* three-dimensional model composed of networks of capillary-like structure in order to assess the effects of shear stress on microvessel formation (318). Bovine pulmonary microvascular EC (BPMEC) were seeded onto collagen gels and supplemented with bFGF to promote network formation (319). The collagen gel with three-dimension networks were then placed into a parallel-plate flow chamber and subjected to laminar shear stress. Growth of the network was observed by electron microscopy and measured in terms of length. After 9 hours, applied shear stress did not significantly affect the network formation (length, 1.38 ± 0.14); however after 24 hours the enhancement was significant (length, 3.13 ± 0.46). Previous studies reported that laminar shear stress induced bFGF mRNA expression (320;321), this study shows that in the presence of bFGF, the migration velocity of EC without shear stress only slightly increased, whereas that of EC under shear stress conditions significantly increased.

Few studies have been attempted to understand the molecular response vascular cells have when present on vascular grafts. Ideally further work is still required to understand the interaction of cells present on biomaterials and their ability to adapt and create a functional tissue.

2.2.3 Application of shear stress for development of small diameter grafts

Recent efforts in developing small diameter grafts for CABG have been limited. These efforts range from developing hybrid grafts such as a bypass graft constructed from a synthetic material and lining the lumen with EC, to growing a living tissue (*in vitro*) using EC, SMC and ECM components (as discussed in Chapter 1).

In cell culture, EC rapidly lose their differentiated nature and when seeded onto vascular graft material, they do not sufficiently adhere or differentiate. Furthermore, as with most eukaryotic cell culture preparations, a proportion of the seeded cells will spontaneously lose their initial attachment, become spherical, and float away, caused by either cell death or damage during the culture process (322). Once the graft is exposed to *in vitro* and *in vivo* pulsatile flow, a high proportion of the remaining cells are washed off from the lumen (323). Maximum cell loss from the graft occurs rapidly in the first 30 minutes with up to a mean cell loss of 70.2% of the original number. After that, a slower exponential cell loss occurs from 30 minutes to 24 hours after implantation. In arterial vessels the high shear stress on EC is successfully resisted by a well-developed intracellular cytoskeleton, which guarantees better surface attachment as well as the flattened, longitudinal alignment of spread EC. The differentiation of the cytoskeleton begins only after a confluent monolayer is achieved (324) and therefore cell attachment and then spreading remains a primary principle during the period of preconfluence.

In an effort to improve EC attachment and EC retention rate (retention of EC when the grafts are exposed to flow) techniques have been used which include precoating the graft lumen with EC specific adhesive moieties (325), and shear stress preconditioning (326).

Many researchers have used a variety of precoating substrates that are mostly found in the extracellular basement membrane of blood vessels these range from chemical coating such as collagen type I/III, laminin and poly-1-lysin to preclotting with plasma, blood and fibroblast matrix/fibrin glue (327). In a recent report, Fernandez *et al.* assessed the quality control of precoating 4 mm internal diameter ePTFE grafts for *in vitro* EC seeding (328). The grafts were coated with fibronilitically inhibited fibrin glue which is currently being used in clinical trials (329;330). Histologic cross sections of the graft lumen revealed the inner surface completely covered by a monolayer of flattened

EC, positive for CD31 and CD34. Furthermore the EC monolayer integrity was still maintained after 2 hours of physiological shear stress. In an *in vitro* experiment, EC were seeded to vascular biomaterials which were coated with fibrin. In comparison those that were not coated with fibrin revealed approximately 40 % of cell adhesion whereas the coated grafts presented a confluent monolayer of cells after 48 hours. After 1hour of shear stress of 2.5 dynes/cm^2, coated ePTFE and Dacron grafts showed an undisturbed confluent monolayer whereas few cells were retained on the bare ePTFE and Dacron (331). These studies have shown that surface coating dramatically improves cell adhesion, proliferation and cell retention to resist forces of shear stress on vascular material surfaces. ECM (collagens, proteoglycans elastin etc) secreted from cells contribute to the adherence of cells to the prosthetic graft.

2.2.3.1 Stabilizing the ECM

A further study investigated whether increasing and stabilising the ECM secreted from cells could enhance cell adhesion and therefore improve cell retention on the prosthetic graft (332). As SMC secrete greater amounts of ECM than EC, they hypothesised that seeding SMC could be used to improve cellular adhesion onto prosthetic materials. Seeding of SMC on grafts has been studied by a few groups (333;334) but limited reports have focused on SMC seeding in the context of enhancing EC adhesion and retention. The SMC cellular layer between the seeded EC and the graft surface was used to enhance EC retention on prosthetic grafts (335). Furthermore, a zymogen tPA mutant gene was transduced into the EC. As discussed earlier, tPA is a thrombolytic protease which converts inactive plasminogen into active plasmin, which then degrades fibrin complexes, a major component of a thrombus. Transfecting cells with the wild-type tPA leads to overexpression of tPA which induces non-specific proteolysis of the supporting ECM and so decreasing the retention of seeded EC on prosthetic grafts (336;337). Zymogen tPA has low protease activity once secreted from the cells and should exhibit limited digestion of the ECM while being able to enhance the antithrombogenic activity of seeded cells. After ePTFE grafts were exposed to *in vitro* flow of 6.1 dynes/cm^2 for 60 minutes, approximately 60 % of EC (retention rate of 39 %) were lost when the cells had been seeded an a graft alone. The retention rate of EC seeded on top of SMC (73 %) was significantly higher than that of EC seeded alone. Grafts seeded with cells carrying the gene for the zymogen tPA showed significant improvement in cell retention (54 %) compared to those with wild-type tPA (39 %). In

conclusion to this study, dual seeding with SMC and EC could result in a better adhesion of SMC on the graft surface, or the interaction between EC and SMC increase the cell adhesion respectively.

The dual-cell seeding on the surface of prosthetic grafts will best mimic the natural vessel structure of vessels. In addition, the presence of zymogen tPA was not shown to increase protease activity significantly but played a part in decreasing fibrin on the lesion site thus enhancing antithrombosis and therefore increasing cell retention. Dual seeding of ePTFE grafts was assessed *in vivo* and further confirmed an increased in cell retention after 1 day implantation (335). Further studies are still required to determine whether the overlying EC modulate proliferation of underlying SMC.

2.2.4 Shear stress preconditioning

Shear stress preconditioning of EC seeded grafts has made a major impact in vascular tissue engineering and has been shown to promote EC retention and differentiation on the inner graft surface (326;338-340). The idea has been to subject cells to low shear stress and then to apply the insult that is physiological levels of shear stress. Table 2-3 outlines the preconditioning studies that have been carried out on vascular cell seeded grafts.

Table 2-3. Overview of preconditioning in tissue engineering.
Keys: ePTFE – expanded polytetrafluoroethlene; PU – polyurethane; PCU – poly(carbonate)urethane; RAEC – rat aortic endothelial cells; PASMC – porcine aortic smooth muscle cells; PAEC – porcine aortic endothelial cells; FB – fibroblasts; SMC – smooth muscle cells; EC – endothelial cells; SV – sapheneous vein.

Year pub.	Vascular graft	Application	cells	Test/preconditioning	Outcome
1988 (341)	ePTFE, Dacron	Evaluate conditions to produce EC monolayer	HUVEC	Perfused *in vitro* to confluence then subjected to varying flow to achieve durable EC monolayer on graft	Confluence complete post 2hrs of *in vitro* perfusion (15 ml/min) Confluency maintained after exposure to flow (100 ml/min)
1991 (342)	Fibronectin-coated ePTFE	Flow applied to study effects of cell density and post-seeding incubation time on cell retention	HSVEC	Grafts with different cell densities and incubated at various times were exposed to 90 minutes of pulsatile flow *in vitro*	↑ cell retention when grafts exposed to flow for 90 minutes after seeding compared to later time points
1991 (343)	Porous PTFE	Assessment of cell proliferation	SMC	*In vivo* luminal shear stress	Elevated shear stress inhibited SMC proliferation
1995 (339)	PU	Assessment of cell retention	BAEC	*In vitro* culture for 6 days with/without laminar shear stress (1-2 dyne/cm^2 for 3 days and 25 dyne/cm^2 for 3 days)	↑ cell loss in static grafts compared to grafts preconditioned by shear stress
1998 (208)	ePTFE, PCU	Effect of shear stress on polymer	HUVEC	*In vitro* pulsatile shear stress	Higher % of cells retained on PCU than ePTFE grafts
1999 (338)	PU	Assessment of cell retention	RAEC	*In vitro* shear stress initiated at 1 dyne/cm^2 for 3 days, following 25 dyne/cm^2 for further 3 days. Grafts underwent *in vivo* implantation for 24 hrs and 3 months	Confluent EC monolayer observed lining the graft lumen after shear stress pre-treatment prior to implantation *in vivo*. Grafts pre-treated contained undisrupted EC post implantation
2002 (214)	PCU	Development of tissue engineered bypass graft	HUVEC	*In vitro* pulsatile flow	↑ cell metabolic activity observed on RGD/Hep-bonded graft than native PCU
2003 (344)	Micropatterned PU films	Flow studies to assess cell retention on μ-patterned/non-patterned PU	BAEC	*In vitro* shear stress of ~60 dynes/cm^2 for 1 hr	μ-patterned PU polymer generated reduced stress, leading to notably ↑ in retention of EC under high shear stress
2003 (344)	PU	To reduce thrombogenecity by lining luminal surface with vascular cells	SMC, FB and EC from SV	Grafts perfused under pulsatile flow	Seeding of mix culture of cells resulted in improved EC adherence and resistance to shear stress
2004 (326)	Tissue engineered graft using Dacron scaffold	Assessment of cell retention	PASMC, PAEC	*In vitro* 1-2 dyne/cm^2	Confluent EC lining with ↑ numbers of flattened cells on preconditioned SMC collagen matrix

The application of shear stress to vascular prosthesis was investigated recently. This study aimed to assess whether cells seeded onto vascular grafts or heart valve prosthesis could withstand shear stress immediately or whether they required a period of low flow to adapt (345). In contrast to artificial precoating of the graft surface, the synthesis of ECM proteins by interstitial or other vascular cells could improve the link between EC and the surface. Excellent adhesion of EC was shown on the ECM built with Fb (346;347). The matrix was composed of culturing foetal human Fb on polyurethane sheet. Fb and SMC represent the physiologic substrate on which EC attach. Together with these cells, EC can synthesise their own ECM and form a basement membrane that is proved by the increased synthesis of collagen IV and laminin on grafts preseeded with Fb and SMC compared with EC seeded alone. PCU vascular grafts were seeded with a mixed culture of Fb and SMC followed by EC from SV. The grafts were exposed to recovery phase (0.9 ± 0.3 l/min at 80 pulses per minute resulting in maximum pressure of 50/30 mmHg) and high flow (3.2 ± 0.61 l/min resulting in maximum pressure of 160/0 mmHg). The first group of grafts were exposed to high flow immediately, the second group were exposed to an recovery phase of 15 minutes and the third group were subjected to 30 minutes of recovery phase. A cell loss of approximately 40 % was found after 4 hours perfusion with normal flow (grafts exposed to high flow immediately) from all cell types Fb SMC and EC. After 15 minutes of recovery phase, the remaining confluence coverage of this prosthesis was 82 ± 8 % and the defects were much smaller compared to those seen on the grafts perfused without an recovery phase.

Immunohistochemical staining against CD90 and α-actin revealed a still confluent layer on the luminal surface of the grafts. Staining against collagen IV and laminin proved the basement membrane to be uninterrupted. After 30 minutes of adaptation phase, there was no cell loss observed and EC layer remained confluent. The cells demonstrated a change in shape indicating adaptation to shear stress. An adaptation phase of 30 minutes proved to be sufficient to allow seeded cells to adapt to shear stress and increase their adhesion and resistance. In this study, the cells faced shear stress after static culturing. The intention was to examine whether the cells could adapt to flow within a reasonable time interval. Miyata *et al* also reported improved EC adhesion on PTFE prosthesis after delayed exposure to shear stress (348). There was great cell loss from the grafts when normal flow was applied immediately. The introduction of an adaptation phase with lower flow and resulting pressures, however,

showed that the cells had not lost their ability to react to shear stress after being cultured under static conditions.

In our department the effect of flow on EC and SMC seeded grafts have also been studied (208;326). The objective has been to assess a compliant graft for effective cell attachment and cell retention at physiological levels of pulsatile shear stress over a 6-hour period of physiological pulsatile flow. HUVEC seeded on PCU and ePTFE vascular grafts were exposed to varying shear stress (13.8 ± 0.6 dyne/cm^2) using a pulsatile flow model. Dynamic scintigraphy images showed a higher percentage of cells were shown to be retained on the PCU graft after exposure compared to ePTFE (208). The flow model used in this study provided an effective model for assessing cell retention on graft materials under flow. Other groups have also analysed the effects of shear stress *in vitro* on vascular cell seeded bypass grafts (344;348). Our group employed both tissue engineering and shear-stress preconditioning to generate conduits suitable for the application as vascular grafts (326). Tissue engineered grafts were composed of compliant outer wraps of Dacron used to give physical structure to the constructs, fibronectin together with collagen to form the ECM substratum, porcine aortic EC and a layer of underlying SMC in order to increase EC adherence and differentiation. This study tested the hypothesis that incorporation of such elements into the development of arterial substitutes would result in significantly improved EC retention. A physiological flow circuit was used to precondition the tissue engineered grafts at 10–20 dynes/cm^2. On being subjected to 1 hour of shear stress, the tissue engineered grafts that had been pre-coated with fibronectin prior to EC seeding demonstrated significant enhanced resistance to shear stress compared to static grafts ($p < 0.05$) and the continued viability of the endothelium was indicated by steadily increasing tPA production. Furthermore, environmental scanning electron microscopy revealed an almost confluent EC lining in tissue engineered grafts to compared non-preconditioned groups. We have enhanced EC attachment and resistance to shear stress by incorporating a period of preconditioning at 10–20 dynes/cm^2, as well as by surface modification with fibronectin and collagen to mimic endogenous ECM. Whilst the benefit of seeding EC on to these tissue engineered grafts is not apparent in acute studies, it is hypothesized that the interaction of SMC within the matrix and EC will lead to ultimate basement-membrane formation and subsequently a stable endothelium will be sustainable in the long term. Evidence in the literature supporting this hypothesis is based on co-culture models (349). Seliktar and colleagues (350) investigated the ECM-remodelling capacity of tissue

engineered grafts undergoing mechanical conditioning and concluded that matrix remodelling occurs via the MMP system, and that such remodelling would be highly beneficial in an engineered construct. Stegemann and co-workers (351) have demonstrated that rat SMC in collagen gels, when subjected to mechanical strain, adopt a contractile phenotype and produce dense ECM. Similarly, Gulbins *et al* also seeded human EC, Fb and SMC onto nondegradable polyurethane vascular grafts and preconditioned them with 30 to 40 mL/min at 80 pulses per minute, resulting in a pressure of 50/30 mmHg (344). Flow was then increased to 120 mL/min after 30 mins, resulting in a pressure of 140/80 mmHg. Total shear stress lasted for 2 hours. Seeding of a mixed culture improved EC adhesion and resistance to shear stress. This outcome was caused by an increased synthesis of ECM proteins, collagen IV and laminin. This supports the hypothesis that Fb and SMC are of great importance for the synthesis of the ECM and that intercellular interactions contribute to improved adhesion.

The action of shear stress on the attachment, morphology and adherence of human EC to ePTFE, Dacron and polyurethane has been assessed. These were coated with ECM proteins (collagen type I/III) (352). Fluid shear stresses of 10 and 20 dynes/cm^2 (1 and 2 Pa), equivalent to the mean shear stress that develops at the proximal end of a femoro-popliteal bypass (339;353), was applied by using a cone-and-plate rheometer (354-357) for 1 hour. The number and area of cell coverage and degree of cell spreading was determined by using image analysis techniques. The researchers found that an increase in shear stress from 10 to 20 dynes/cm^2 showed a significant reduction in the number of cells remaining adherent in ePTFE (66 ± 19 % at 10 dynes/cm^2 and 49 ± 20 % at 20 dynes/cm^2) and Dacron (48 ± 24% and 30 ± 2 %) but not on poly(ether)urethane (44 ± 17 % and 40 ± 14 %) respectively. It was evident from this study that after 6 days in culture and 1 exposure to flow enabled the remaining HUVEC to resist shear stress, having spread to a greater extent than on static control samples. These results are consistent with recent reports in that the action of shear stress exposed to growing EC significantly enhances cell adhesion *in vitro* (338;358). They also found that collagen coating improved primary cellular adhesion and coverage significantly, the degree of spreading depended on the application of shear stress. Previous studies have identified that both fibronectin and collagen type I/III results in a higher attachment of HUVEC to prosthetic vascular biomaterials (325;359).

Ott and colleagues seeded poly(ether)urethane vascular grafts (1.5 internal diameters) with BAEC and cultured for 6 days with/without laminar shear stress, first at 1-2 dynes/cm^2 for 3 days and then 25 dynes/cm^2 for 3 days (360). The preconditioned grafts and static grafts were further exposed to shear stress at 25 dynes/cm^2 for 25 seconds. Preconditioned grafts showed less cells being dislodged ($1.05 \times 10^4 \pm 0.16 \times 10^4$) compared to static grafts ($1.35 \times 10^6 \pm 0.44 \times 10^6$). These findings suggest that EC adhesion and retention on vascular grafts *in vitro* is markedly enhanced by preconditioning the seeded EC monolayer with long-term shear stress. This study demonstrated EC to exhibit increased adhesive strength in response to arterial levels of shear stress (360) and therefore it has been suggested that this concept of shear stress pre-treatment could also enhance EC retention on vascular grafts implanted *in vivo*.

As viscosity is an important factor influencing shear stress, blood does not behave like an ideal fluid, thus causing additional forces on the EC layer compared with those caused by a cell-free medium. Therefore grafts will have to prove their resistance to physiological shear stress in animal experiments. Despite a lack of in depth molecular studies in this field of preconditioning using shear stress, research to date indicates that preconditioning promotes cell retention. In addition increase in ECM proteins and cell spreading has been observed.

2.2.5 Genes of potential relevance to shear stress studies on seeded vascular conduits

This chapter has provided an insight of gene expression and signal transduction pathways involved in determining the responses of vascular cells to shear stress and the role of haemodynamic forces in thrombus formation and intimal hyperplasia following bypass surgery. Despite the intensive studies on the effects of shear stress on EC, the interplay between shear stress and vascular grafts in modulating EC gene expression and function has been very limited. In vascular tissue engineering, shear stress has been mimicked in vitro to enhance EC retention and adhesion to biomaterials. A lack of understanding has been the gene response of vascular cells to biomaterials with and without flow. From this literature review a selection of genes are of potential interest in understanding EC behaviour on vascular grafts, in particular in response to shear stress in the development of a small-diameter vascular graft. The genes described below are of potential interest in this thesis.

2.2.5.1 PECAM-1 is more than an endothelial marker

PECAM-1 has been implicated in a number of important biological processes, including vascular development (361;362), leukocyte emigration at sites of inflammation (363;364), T cell activation (365;366), platelet aggregation and homeostasis (367;368) and the maintenance of vascular endothelial barrier function (369). PECAM-1 also plays a role in angiogenesis. In terms of EC, angiogenesis can be viewed as a process in which these cells sever their initial cell-cell contacts, proliferate and migrate into the perivascular matrix where they re-establish their cell-cell associations to form new patent vascular channels (370). Although studies do not support a role for PECAM-1 in EC proliferation (371), a number of reports have implicated PECAM-1 in EC motility (372-374) and in the EC cell-cell associations required for the organisation of EC into tubular networks (371;374-377). The mechanism of PECAM-1's participation in angiogenesis is still unsettled.

The expression of PECAM-1 has been investigated in EC seeded on vascular graft materials (378). Dacron coated with fibronectin was used as circular pieces of 15 mm in diameter and seeded with EC from HUVEC and adipose microvessels (HAMVEC). Cells were cultured for 1-2 days and the expression of PECAM-1 was determined by flow cytometry and immunofluorescence microscopy. The cells were not stimulated. The expression of PECAM-1 was found to be constitutively expressed with similar mean fluorescent intensities suggesting that its expression is dependent neither on the EC origin nor on the underlying polymer surface. This report has been consistent with studies based on the *in vivo* situation, where PECAM-1 is found to be constitutively expressed on the endothelium of all vessel types (379). In contrast Cenni *et al*, reported the downregulation of PECAM-1 expression by HUVEC cultured on knitted Dacron (380). It can be hypothesised that a decrease in the expression of PECAM-1 underlies poor adhesion capability of these cells on knitted Dacron or that the lack of fibronectin coated on this polymer in the latter study, thus resulting in deficient cell spreading and many nonherent cells. Although many researchers have used fibronectin to coat vascular materials in order to improve endothelialisation, in the areas not covered by endothelium an increase in platelet deposition occurs (381).

2.2.5.2 Vascular endothelial growth factor receptor in activation of ECs

VEGF, the prototype member of an expanding family of angiogenic polypeptides (382-384) is an EC specific mitogen that acts through two tyrosine kinase receptors, VEGFR-1 (385) and VEGFR-2 (386), whose expression is restricted almost exclusively to EC (387;388). Expression of VEGF and VEGFRs correlates well with phases of vasculogenesis and angiogenesis, and disruption of either the VEGFR-1 or the VEGFR-2 gene results in lethal hematopoietic and vascular abnormality (389). In addition to its involvement in angiogenesis, VEGF may serve other functions such as the endogenous regulation of vessel permeability, raising the possibility that factors other than VEGF may determine the angiogenic or nonangiogenic status of EC. For example, it has been observed that cytokines such as TGF-β1 are capable of modulating VEGF-induced *in vitro* angiogenesis (390;391). Regulation of VEGFR expression is likely to play a fundamental role in the determination of EC activation status. It has been demonstrated that VEGFRs -1 and -2 is strongly upregulated during phases of capillary growth (387;388). To date, very little is known about the molecular mechanisms that regulate VEGFR expression.

2.2.5.3 Vascular growth factors

The transforming growth factor – beta (TGF-β family of cytokines exert pleiotropic effects upon a wide variety of cell types. Three mammalian isoforms exist; TGF-β1 -β2 and -β3 encoded by separate genes. TGF-β1 isoform has been demonstrated to be of fundamental importance during vascular development, atherogenesis, neointimal proliferation and vessel remodelling (392). It has been found to be a potent regulator of ECM synthesis, cell cycle progression, apoptosis, differentiation and migration.

The predominant effects of TGF-β1 on EC are the inhibition of migration, restriction of cell cycle progression and induction of apoptosis, all of which are dose-dependant (393). TGF-β1 induces increased expression of integrins, fibronectin, collagens types I, IV and V and plasminogen activator inhibitor (394). TGF-β1 also influences SMC proliferation in a dose-dependant manner (395;396). It has been shown to be stimulatory at low concentrations and inhibitory at high concentrations.

In angiogenesis, TGF-β1 has shown to facilitate VEGF and bFGF dependent capillary sprout formation (397) and promotes the stabilisation of the developing vessel by mediating the recruitment of perivascular cells, promoting ECM synthesis and reducing ECM proteolysis (398).

Shear stress is the potent stimulator of TGF-β1 expression. EC have shown to express TGF-β1 in a shear stress-dependent manner (399). Increases of TGF-β1 mRNA were observed from 6 hour to 24 hour points of applied shear stress (15 dynes/cm^2). Different forms of fluid shear stress have shown to influence vascular endothelial TGF-β1 mRNA expression. TGF-β1 mRNA was shown to be up-regulated during steady pulsatile flow (19 dynes/cm^2) than for oscillatory flow (0+/-19 dynes/cm^2) (400). Given the preferential localisation of early atherosclerotic lesions in arterial regions exposed to low and/or oscillatory shear stress and the implication of TGF-β1 as an athero-protective gene, these results are consistent with the notion that regions transiently exposed to oscillatory flow may be particular prone to atherosclerosis. TGF-β1 expression is a key interest in this thesis. Understanding the expressional response in a three-dimensional grafts would more likely represent an *in vivo* environment. It has shown to increase the expression of the major ECM proteins, fibronectin and collagen. This effect is general response to TGF-β1 seen in primary cultures and established lines of cells from various types, normal and transformed.

2.2.5.4 Extracellualr matrix genes

Collagens are the major protein comprising the ECM. There are at least 12 types of collagen. Types I, II and III are the most abundant and form fibrils of similar structure. Type IV collagen forms a two-dimensional reticulum and is a major component of the basal lamina. This review has shown the expression of collagen's involved in particular in neointimal thickening (Section 2.3). Increases in collagen type 1 (COL-1) have been observed at the anastomosis following prosthetic arterial grafting (306). Increased expression of COL-1 suggests its involvement in the development of medial thickening and neointima formation (308). COL-1 importance in this thesis has been demonstrated later.

Another gene of interest is MMPs due to their particular role in cell behaviour such as endothelial cell migration and matrix remodeling. As discussed earlier (see

Section 2.2.3.6.1) its importance its investigation in this thesis would gain an understanding of cell-graft behaviour.

2.2.5.5 Housekeeping gene

Control genes, which are often referred to as housekeeping genes, are frequently used to normalise mRNA levels between different samples. Housekeeping genes are constitutively expressed; however the expression level of these genes may vary among tissues or cells and may change under certain circumstances. Thus, the selection of housekeeping genes is critical for gene expression studies.

Glyceraldehyde-3-phosphate dehydrogenase (GAPDH) an enzyme of glycolysis is one of the most commonly used housekeeping genes used in comparisons of gene expression data. The expression of GAPDH mRNA has been measured in a panel of 72 different pathologically normal human tissue types (401). Comparative levels of expression were observed demonstrating that GAPDH can be used as the internal control to add value to gene expression data. Many researchers have used GAPDH as a control in expressional studies (402-405). The expression of GAPDH has not been effected by shear stress (406-408).

2.3 Conclusion

The study of haemodynamics is a prosperous field that involves characterising the biological responses to mechanical forces. Specific arteries exhibit flow characteristics that are three-dimensional and developing. Diseased arteries can create a high level of turbulence that can cause the tubes to collapse. The normally functioning endothelium maintains patency and haemostasis in the vascular system.

Due to the poor patency rates of prosthetic grafts currently used clinically primarily due to poor compliance and thrombogenicity, seeding and tissue engineering are being used to improve patency in artificial conduits. Upon implantation of EC seeded vascular graft into the arterial circulation, cells are immediately exposed to arterial pressure, shear stress and pulsatile flow. One obstacle of a tissue engineered graft has been the poor retention of cells after exposure to *in vivo* flow (208). Various groups have investigated the effects of shear stress on cell retention (345;409). Shear

stress preconditioning has been employed as a means of increasing the retention of cells to the graft surface prior to implantation (338). However, the great disadvantage of such a conduit is the time necessary for maturation leading to unacceptable delays. This maturation process is essential to produce a graft that can withstand haemodynamics stress. Once implanted, the tissue-engineered graft can contract in response to immediate haemodynamics conditions and remodel in the long term.

The studies in this review demonstrate that the exposure of EC to haemodynamic flow alter the gene expression of these cells. This represents an alteration to the physiology of the cells and heralds the case for preconditioning of grafts before exposure to arterial flow. Results obtained from studies of adhesion molecule expression have been conflicting with VCAM-1 expression has been reported to be decreased (281), unaffected (282) or increased (410). Both shear stress and cyclic strain promote the expression of NOS (273) and subsequently we assume NO. Likewise in experimental set-ups, the application of shear stress to cultured EC induces increases in prostacyclin and tPA release (292;411). Key to the studies of cellular adhesion is the ECM modulation by EC; increases in MMP2/9 (280) and decrease in laminin (263).
The multiple methods and genes used in the studies reviewed here demonstrate many interesting areas of further research but, at present, this field lacks direction. A key point is that, to date, no gene expression studies have been conducted on endothelial cell seeded cylindrical grafts in vitro. In the absence of such studies the interactions between cells, biomaterials and flow can not be adequately elucidated to aid development of future strategies. The future of this research must focus upon such studies if meaningful advances are to be made in this field.

3

Materials and Methods

3.1 Introduction

This chapter discusses the methods and rationale behind the techniques used throughout this thesis.

Early investigators used animal tissue such as bovine, porcine or canine endothelium as their source of EC (412). In order to make the transition from laboratory research to clinical practice it is necessary to obtain a source of cells from the patient themselves. In humans there is increasing evidence to show that cells of the same type from different tissues are morphologically, biochemically and functionally diverse. These findings of endothelial heterogenecity have resulted in debate regarding which type and source of EC are suitable for *in vitro* and *in vivo* studies and it has become accepted that this is a major consideration in tissue engineering. As a result of this numerous sources of cells have been investigated, including non-essential vessels such as the SV or umbilical vein and omentum or subcutaneous adipose tissue (212;413;414). EC from a suitable piece of SV allows approximately 1 x 10^4 cells to be extracted (195;415). This amount of cells would only provide a sparse coating of cells in a single stage procedure, requiring an extensive cell proliferation post-seeding to achieve a

monolayer. In addition blood-flow induced shear stress could also result in the loss of a large number of seeded cells (323).

Two techniques that have been developed in order to harvest EC from autologous vein are mechanical scraping (416) and enzymatic digestion using collagenase or trypsin (417). Mechanical scraping uses an abrasive action to remove EC from the vascular wall which leads to significant EC damage, the possibility of contamination with SMC and provides a poor harvest of EC (417). Enzymatic digestion using collagenase or trypsin to remove the endothelium avoids the problem of mechanical damage to the cells and provides much improved EC recovery. This technique can be used to extract EC from tissue samples however contamination with other cell types has been a significant problem (418). From solid tissues, extraction is more difficult. Usually the tissue is minced, and then digested with the enzymes trypsin or collagenase to remove the extracellular matrix that holds the cells. After that, the cells are free floating, and extracted using centrifugation or aspheresis. Digestion with trypsin is very dependent on temperature. Higher temperatures digest the matrix faster, but create more damage. Collagenase is less temperature dependent, and damages fewer cells. Cells are often categorized by their source.

Some groups have claimed that no EC could be extracted from subcutaneous fat using conventional collagenase digestion whereas others have claimed that up to 80 % of cells extracted are EC using the same technique (419-421). Many authors have suggested that the only way to obtain a pure culture of EC from subcutaneous fat would be to use purification techniques such as a Percoll gradient, filtration or magnetic beads (200). This is because it is thought that collagenase digestion of fat leads to the extraction of EC, FB and SMC. The problem with the Percoll and filtration techniques is that they reduce the number of EC that can be extracted whereas Percoll is also thought to be detrimental to the subsequent proliferation of the extracted EC (200). Magnetic beads, including platelet endothelial cell-adhesion molecule ('PECAM'; CD31) and Ulex Europaeus I-coated Dynabeads, have been used for extraction of EC for culture and cell characterization but have never been used for seeding.

A further potential source of cells for seeding are those extracted from omentum. These have been characterized as mesothelial cells (MC) (422). Both EC and

MC have a similar function producing substances such as tPA and urokinase plasminogen activator (423;424). In animal experiments, most trials involving the seeding of grafts using cells derived from omentum have shown good results (417;425-428), except those reported by Verhagen and co-workers (429). Based on this work another potential source of MC may be from peritoneal lavage, which has not been previously evaluated for vascular seeding. Ivarsson and co-workers proposed that it was possible to extract between 3 x 10^6 and 8 $\times 10^6$ cells from about 500 ml of lavage fluid (430). A convenient source of EC has been the human umbilical vein. The extracted cells can be cultured and propagated for at least 16 population doublings. In all cell experiments throughout the work in this thesis, human umbilical vein endothelial cells (HUVEC) were extracted from human umbilical vein cords using the collagenase enzymatic digestion technique.

Various approaches to the assessment of EC proliferation and viability have been undertaken. Foremost are methodologies looking for known morphological factors, including ultrastructural studies that require substantial effort, skilled personnel, and often expensive equipment but during the extensive processing required do not yield quantifiable results and destroy the sample (431). The assessments of EC membrane integrity with dye uptake and vital stains have been used as an indirect measure of viability, but they are terminal assays that destroy the cell or interfere with its function (432-434).

Continuous monitoring of EC viability is achievable by the measurement of glucose uptake and lactic acid release into an incubation medium, but such methodologies are labour intensive and relatively insensitive (435). The reduction of colourless tetrazolium salts by mitochondrial succinate dehydrogenase activity into an intensively coloured formazan product uses hazardous reagents and requires washing, fixing and extraction steps that destroy the cell (436-438). Furthermore, the insoluble intracellular crystals that disrupt the cellular membrane result in an extracellular precipitates attached to the polymeric substrate that on polyurethanes remains bound to the substrate even after extraction by detergent, thus affecting the outcome of this particular assay (439). Other methods of assessing cell viability are measurement of Trypan Blue exclusion or propidium iodide exclusion and measurement of crystal violet

inclusion or Neutral Red inclusion. ^{3}H-thymidine incorporation has been used as a measure of viability and cell proliferation in EC (440) but radioisotopes have many disadvantages, including the terminal nature of the measurement, labour-intensive handling and disposal (along with expense), and excessive processing time with ^{3}H-thymidine incorporation. Quantification of DNA synthesis by measuring bromodeoxyuridine (BrdU) uptake is a method of assessing cell proliferation. The use of BrdU requires extensive processing of samples at predetermined time points; therefore, no continuous monitoring of a single sample can be performed with this method (441).

The evaluation of seeded cell viability is hindered by the current lack of a reproducible method that is non-toxic to EC, allows continuous or repeated measurements, has a range of sensitivity that allows the measurement of degrees of viability, is not dependent on cell division, and is convenient and safe to use. Direct cell counting, cell dislodging, dye uptake, ^{3}H-thymidine uptake, or DNA or protein staining either requires a transparent scaffold or leads to termination of culturing before measurement (442;443). Furthermore, the dyes and solubilisers used in spectroscopic assays such as the end-product formazan of the calorimetric MTT (3-(4,5-dimethyl thiazoloyl-2-yl)-2,5-5diphenyl tetrazolium bromide) assay (MTT assay) chemically interact with the polymer itself and/or any surface coatings present, particularly for polyurethane formulations (436;437). In this study, it is essential that the EC remain viable after being seeded onto the prosthetic graft and those samples can be monitored at several time points. Thus the requirement was to use a suitable technique to monitor viability of EC seeded on prosthetic grafts. The Alamar blue™ redox assay has been applied as a technique to monitor the viability of EC seeded on prosthetic grafts (444). The validity of the test was assessed with sodium azide and mitomycin C, known physiological perturbators. The Alamar blue™ redox assay demonstrated that EC were viable and functional postseeding on the prosthetic grafts. The technique allows the continuous assessment of the metabolism and viability of seeded cells, is simple to perform, and does not destroy the cells or graft materials. As well as viability, proliferation may also be measured by this assay. As with tetrazolium salts, Alamar blue monitors the reducing environment of the proliferating cell. Alamar blue™ is soluble, stable in culture medium and is non-toxic. The continuous monitoring of cells in culture

is therefore possible. Specifically, Alamar blue™ does not alter the viability of cells cultured for various times as monitored by Trypan Blue exclusion (445).
The techniques used in this thesis have been validated (as described below) and demonstrate a reproducible technique that can be used to measure viability, proliferation and cytotoxicity of cells.

In order to assess shear stress on cell function, a flow circuit mimicking physiological shear stress was developed (214) and used for all flow studies. Chapter 2 provides a review of the techniques used for applying *in vitro* shear stress to cultured cells using cone and plate apparatus or flow circuits.
The flow circuit used in the study is capable of stimulating *in vitro* the pulsatile flow waveform, pressures and degrees of oxygenation of physiological arterial circulation *in vivo*. This system has been validated extensively for physiological parameters (214) and has been used in previous studies (36). This model was used to investigate the shear stress response to EC seeded on nanocomposite conduits. The model stimulates specifically a given artery situation such as coronary flow waveforms (see caption of Figure 3.3 for further details).

3.2 Cell Culture

3.2.1 Extraction of endothelial cells from human umbilical cord

HUVEC were harvested from human umbilical cord vein as described by Jaffe (444). All procedures were carried out using aseptic techniques in a tissue culture flow hood. Human umbilical cords were obtained from the labour ward of the Royal Free Hospital, Hampstead and stored in 40 ml of collecting medium consisting of 29.8 ml basic medium, 10 ml foetal bovine serum (Invitrogen, Paisley, U.K.) and 0.2 ml of 50 mg/ml gentomycin (Sigma Chemical Company, Dorset, U.K.). The basic medium was obtained from a stock solution made from 500 ml M199 medium (Invitrogen, Paisley, U.K.), 15 ml of 7.5 % sodium bicarbonate solution and 5 ml of penicillin/streptomycin solution consisting of penicillin 10,000 U/ml and streptomycin 10 mg/ml (Invitrogen, Paisley, U.K.).

Cords approximately 15 cm in length were collected within 24 hours of delivery and used if free of clamp marks or needle holes. Each end of the umbilical vein was cannulated with 4 cm lengths of nasogastric tubing and then secured with sterile silk ties. The cord was flushed several times with warm sterile phosphate buffered saline (PBS) to remove all clotted blood prior to instillation of 25 ml of warm, filtered collagenase solution consisting of 12.5 mg collagenase A suspended in 25 ml of basic medium. Both ends of the vein were clamped and the cord incubated at 37 °C for 10 minutes. The cord was massaged gently in order to loosen the EC and the collagenase/cell suspension was then collected into a 50 ml centrifuge tube. The vein was further washed with PBS to collect any loose cells. The collagenase/cell suspension was then neutralised by adding an equal volume of warm complete medium obtained from stock made up of 157 ml basic medium, 40 ml Foetal bovine serum and 3.6 ml of 200 mM L-glutamine solution (Invitrogen, Paisley, U.K.). The cell suspension was centrifuged at 300 g for 7 minutes, the supernatant medium was removed and the cell pellet was resuspended in 5 ml of complete medium. The cell suspension was then transferred to a 25 cm^2 tissue culture flask and incubated at 37 °C/5 %CO_2. After 24 hours, the flasks were gently washed with 8 ml of warm PBS to remove red blood cells and fed with 5 ml of complete medium. The flasks were viewed daily under high power transilluminated microscopy and the presence of EC verified by confirmation of their characteristic cobblestone morphology and staining for vWF (von willebrand factor).

Once a confluent monolayer was achieved cultures were passaged by removing the cell culture medium, washing with 8 ml of PBS and then adding 3 ml of 10 % trypsin-EDTA solution (Invitrogen, Paisley, U.K.). The flasks were then incubated for 3 minutes prior to gentle tapping in order to loosen all the cells. The trypsin was then neutralised by the addition of 10 mls of complete medium. The cell suspension was spun at 300 g for 7 minutes, supernatant discarded and cell pellet resuspended in 10 ml of complete medium. The cell suspension was then placed in gelatine coated 75 cm^2 tissue culture flask. Cultures were passaged every 2-3 days at a ratio of 1:2 and fed every 48 hours.

3.3 Polymer synthesis

The Department has developed and patented (446); a new nanocomposite polymer based on POSS-PCU. Details of the synthesis of the nanocomposite have been previously described (70). In brief to synthesise the nanocomposite, dry poly-hexamethylene carbonate diol was mixed with trans-cyclohexanediolisobutylsilsesquioxane (Sigma-Aldrich) – the POSS, in a 500ml reaction flask equipped with a nitrogen inlet and mechanical stirrer. The mixture was heated to dissolve the POSS in the polyol and then gradually by removal of the heat source. Methylene diisocyanate (MDI) was added to the polyol blend and then reacted, under nitrogen, at 75 °C to form a pre-polymer. This consists of POSS moieties with MDI attached at each of its hydroxyl groups, and polycarbonate with MDI reacted to the diol groups on either end. Dimethylacetamide (DMAC) was slowly added to the pre-polymer to form a solution, which is then cooled to 40 °C. Chain elongation was carried out by drop-wise addition of a mixture of ethylenediamine and diethyamine in DMAC. Finally a mixture of 1-butanol and DMAC was added slowly to the polymer solution. All the chemicals, reagents, glassware and associated relevant equipment were purchased from Aldrich Co. Ltd. (New Road, Gillingham, U.K.).

3.4 Assessment of cell metabolism and survival

3.4.1 Cell viability

Alamar blue™ (AB; Serotec, Ltd., Kidlington, U.K) is an assay designed to measure quantitatively cell metabolism and viability by incorporating resazurin and resarufin as colorimetric oxidation reduction indicators that change in colour in response to chemical reduction resulting from cell metabolism. The data may be collected with either fluorescence based or absorbance-based instruments. In this study absorbance was measured at 570 nm and background at 630 nm subtracted. Resazurin has a much higher electrochemical potential than the carriers on the cell membrane, and on contact with the membrane, it is reduced to resarufin. Resazurin acts as an intermediate electron acceptor in the electron-transport chain between the final reduction of O_2 and cytochrome oxidase by substituting for molecular oxygen as an electron acceptor. The rate of bio-reduction is related to the level of redox potential on

the cell membrane that in turn characterises the constitutive part of the metabolic activity of a given cell type. AB has certain properties that make this assay attractive. It is soluble in media, stable in solution, and minimally toxic to cells and produces changes that are easy to measure. AB has been used as a measure of cell viability in tumor neurosis factor hyper-sensitive cell lines (447), studies of apoptotic neuronal death (448), and studies of lymphocyte proliferation (445).

AB is not a new assay because it was first developed to determine how susceptible microorganisms are to various growth-inhibition products and has been used to examine bacterial antibiotic susceptibility (449) and yeast antifungal receptivity (450) and to analyse the *in vitro* cytotoxicity of drugs and chemotherapeutic agents in mouse fibroblasts, macrophages and human tumour cells (451). AB allows a continuous assessment of the metabolism and viability of seeded cells, is simple to perform, and does not destroy the cells (444). Limitations of AB are few. If prolonged incubation times are used (> 24 hours), reversal of the reduction process occurs via a secondary index step, resulting in a colourless solution, particularly when very high cell concentrations are used. Microbial contamination would also reduce AB, thus yielding erroneous results, but this would affect any other assay of EC as well and can be estimated by use of a suitable blank.

All procedures with AB were performed under aseptic conditions because microbial contaminants are also able to reduce AB. AB were added to cell culture medium at a concentration of 10 %. At each AB assay time point, well/grafts were washed with 1 ml PBS and 1 ml of the 10 % AB/medium mixture added to each sample. Blanks were also included with 1 ml of the 10 % AB/medium added to samples with no cells. After 4 hours a 100 μl sample of AB/medium mixture was removed and the absorbance at 570 nm and 630 nm measured in a 96-well plate (Helena Biosciences, Sunderland, U.K.) using a Multiscan MS UV visible spectrophotometer (Labsystems, Somewhere, U.K). The absorbance at 630 nm (background) was subtracted from that at 570 nm and results expressed as a percentage of the control (blank value). Duplicate wells per treatment at each time point were measured and each experiment repeated four times.

3.4.2 Cell proliferation

The Quant-iT™ PicoGreen® assay (Molecular Probes Europe BV, Leiden, The Netherlands) quantifies double-stranded DNA in solution using an ultrasensitive fluorescent nucleic acid stain. Detecting and quantifying small amounts of DNA is important in a wide range of biological applications. The most commonly used technique for measuring nucleic acid concentration is the determination of absorbance at 260 nm. The Hoechst (bisbenzimide) dyes are sensitive fluorescent acid stains that are selective for double stranded DNA (dsDNA), does not show significant fluorescent enhancement in the presence of proteins, and allows the detection and quantification of DNA concentrations as low as 10 ng/ml DNA. The PicoGreen dsDNA reagent enables researchers to quantitate as little as 25 pg/ml of dsDNA with a standard spectrofluorometer and fluorescein excitation and emission wavelengths. The sensitivity exceeds that achieved with the Hoechst 33258-based assay by 400-fold. The PicoGreen method is also simpler than that of previous methods (452) because a single concentration of the PicoGreen reagent allows detection over the full dynamic range of the assay. This assay has been extensively used in biocompatibility tests to evaluate the viability and proliferation of cells cultured on polymers (453).

Stock standard DNA solution (100 μg/ml) was diluted in Tris-EDTA (TE) assay buffer to provide a standard curve of 0 – 1000 ng/ml DNA (see Figure 3-1) for full layout of preparation of the standard curve). Figure 3-1 demonstrates an example of a typical standard curve prepared from these dilutions.

Cell samples were trypsinised as above and the cells frozen and thawed then further disrupted by being passed through a small-bore needle three times. 100 μl of standard/sample was added to a 96-well plate and 100 μl of diluted PicoGreen (PicoGreen dimethylsulfoxide (DMSO) stock solution diluted ×200 in TE assay buffer) was added to each standard/sample well. Plates were then incubated for 5 min in the dark. Standards/samples were then excited at 480 nm and the fluorescence emission intensity measured at 520 nm using a Fluroskan Ascent FL spectrofluorometer (Thermo Life Sciences, Basingstoke, U.K.).

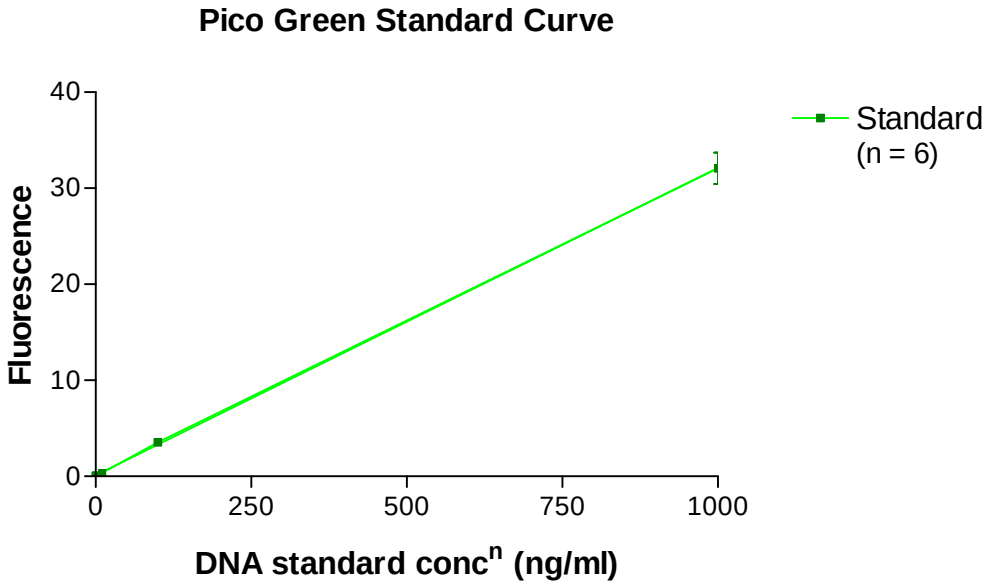

Figure 3-1. Validation of a typical standard curve between 0 – 1000 ng/ml calf thymus DNA in TE. The calf thymus DNA standard, provided at 100 μg/ml in the PicoGreen Kit, was diluted 50-fold in TE to make the 2 μg/ml working solution. To serve as an effective control, the dsDNA solution used to prepare the standard curve was treated the same way as the experimental samples and should contain similar levels of such compounds. If the absorbance measurement in the samples were high, the samples were then diluted and the assay repeated.

3.4.3 Cell toxicity

Lactate dehydrogenase (LDH) is a stable cytosolic enzyme. The normal plasma membrane is impermeable to LDH, but damage to the cell membrane results in a change in the membrane permeability and subsequent leakage of LDH into the extracellular fluid (454). *In vitro* release of LDH from cells provides an accurate measure of cell integrity and cell viability. As a result, measuring the release of LDH has proved to be a method used in various tests for cytotoxicity in both immunological studies and in biocompatibility studies, where it has now become an important *in vitro* screening test (455).

To determine the amount of LDH released, LDH in cell culture medium is measured by a spectrophotomeric enzyme assay. The amount of LDH released is quantified using a 30 minute coupled enzymatic assay based on the conversion of a tetrazolium salt INT (2-*p*-iodophenyl-3-*p*-nitrophenyl-5-phenyl tetrazolium chloride)

into a red formazin product, with the amount of colour formed being proportional to the number of lysed cells.

LDH was measured using a CytoTox 96® non-radioactive cytotoxicty assay kit (Promega, Southampton, U.K.). 50 µl CCM from each sample was transferred to a 96-well plate (Helena Biosciences, Sunderland, U.K.). 50 µl of substrate mix (1 vial substrate plus 12 mls assay buffer) was added to each well and the plate covered in foil to prevent light access. Samples were then incubated at room temperature for 30 min after which the reaction was stopped by the addition of 50 µl stop solution (1 M acetic acid). Absorbance was then read at 492 nm using a Multiscan MS UV visible spectrophotometer (Labsystems, Ashford, U.K.).

3.5 Application of physiological shear stress

Flow circuits consist of a pump, tubing and medium flowing through it. They have a heater and pH-buffering system and have the capacity to exchange gases and, depending on the culture period, nutrients for wastes. Furthermore they usually have monitoring system to measure parameters like pressure and flow. They can be used for developing tissues, assessing tissues both in biological and mechanical terms.

Traditional pumps – as for example used clinically for heart bypass and dialysis machines - can be either centrifugal or roller. Centrifugal pumps consist of a fanned impeller or a nest of smooth plastic cones that sit inside a plastic housing. The impellers or cones are magnetically coupled with an electric motor and, when rotated rapidly, generate a pressure differential that causes the movement of fluid. On the other hand a roller pump includes a length of tubing, located inside a curved raceway. The raceway lies at the outer perimeter of rollers mounted on the ends of rotating arms (usually two, 180 degrees apart). The system is arranged so that one roller is compressing the tubing at all times. Flow of blood is induced by compressing the tubing, thereby pushing the blood ahead of the moving roller. Flow rate depends upon the size of the tubing, length of the track, and rotation rate of the rollers (revolutions per minute). For a given pump and type and size of tubing, flow is proportional to pump speed (in revolutions per minute) (456). An alternative pumping system has been described using a mechanical ventilator to drive air into a fluid-filled circuit creating pulsatile laminar flow with

physiological variables of flow, blood and pulse pressure (456-459). It has been used to successfully tissue engineer myofibroblasts and EC on bio absorbable scaffolds into vascular grafts in a 'biomimetic' environment (460). This innovative design has however been confined to a limited number of researchers and is relatively complex compared to more traditional systems.

The advantage of centrifugal pumps is that when the fluid is blood, there is less cell destruction. The model employed (Figure 3-2) in this thesis has been developed and validated in the department. The flow system has been extensively used in previous cell-graft studies (36) and is capable of stimulating *in vitro* the pulsatile flow waveform, pressures and degree of oxygenation of physiological arterial circulation *in vivo* (214). The model consisted of a variable-speed electro-magnetic centrifugal pump (Bio Medicus Inc., Minnetonka, U.S.A.); flexible plastic tubing and reservoir; flow waveform conditioner (FWC); Maxima hollow fibre oxygenator (Johnson & Johnson Cardiovascular, McNeilab Inc., Anaheim, CA, U.S.A.) supplied with 95 % O_2/ 5 % CO_2; an outflow resistance; a 6 mm calibre tubular flow probe and Transonic Medical Flowmeter (TMF) system (HT207, Transonic Medical System Inc., U.S.A.) and a Miller Mikro-tip catheter transducer (Miller Instruments, Inc., Houstan, Texas, U.S.A.). The flow circuit was primed with cell-culture medium adjusted for viscosity: M199; 10 % Foetal Bovine Serum; 7.5 % sodium bicarbonate; 200 mM L-glutamine penicillin 10,000 U/ml, streptomycin 10 mg/ml and 8 % low molecular weight Dextran (77,000 Dalton, purchased from Sigma, Poole, Dorset, U.K.) buffered at pH 7.2. The whole circuit was kept under sterile conditions.

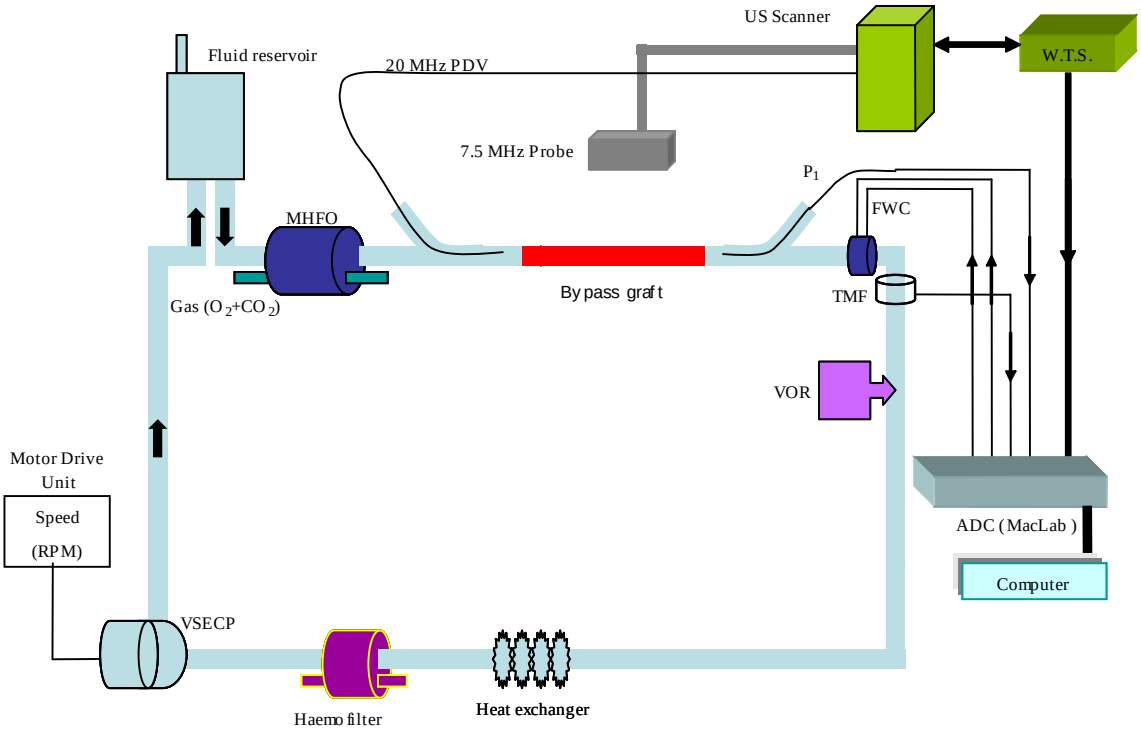

Figure 3-2. The flow circuit comprising a variable-speed electromagnetic centrifugal pump, flexible plastic tubing, fluid reservoir and circulating solution oxygenated through a Maxima hollow fibre oxygenator with 95% air and 5% CO_2. Automatic pH, pO_2 and pCO_2 controller. A flow waveform conditioner (FWC) sited in series with the circuit is used to generate arterial flow waveforms. This was constructed in-house and consisted of a solenoid connected to an electronic control box from which the frequency and duration of solenoid occlusion could be governed. Instantaneous flow rate is measured using Transonic Medical Flowmeter (TMF) system. Serial intra luminal pressure measurements can be made at discrete sites along the graft using a Millar Mikro-tip catheter transducer introduced via a Y-connection port. Graft radius, flow rate and shear stress are determined using an ultrasound duplex (US) scanner with a wall tracking system (WTS). All outputs are fed into a computer using an analogue-to-digital data acquisition recording system (ADC). Flow circuit also consists of a Variable Speed Electromagnetic pump (VSECP) and Variable Outflow Resistance (VOR).

3.6 Total RNA extraction

An RNeasy kit was used to isolate total RNA (Qiagen Ltd, Crawley, U.K). The RNeasy procedure represents a novel technology for RNA isolation. It combines the selective binding properties of a silica-gel-based membrane with the speed of microspin technology. A specialised high-salt buffer system allows up to 100 μg of RNA longer than 200 bases to bind the silica-gel membrane. Biological samples are first lysed and homogenised in the presence of a highly denaturing guanidine isothiocyanate (GITC)-containing buffer that immediately inactivates RNases to ensure isolation of intact RNA. Ethanol is added to provide appropriate binding conditions, and the sample is then applied to an RNeasy mini column where the total RNA binds to the membrane and contaminants are efficiently washed away. High-quality RNA is then eluted in 30 μl or more, of water. This kit was used as it provides a fast and simple method for the preparation of up to 100 μg total RNA from eukaryotic cells and tissues. A wide range of biological samples can be simultaneously processed in less than 30 minutes. Time-consuming and tedious methods, such as CsCl step-gradient ultracentrifugation and alcohol precipitation steps, or methods involving the use of toxic substances such as phenol and/or chloroform, are replaced by this procedure. The purified RNA was ready to use in standard downstream applications such as reverse transcriptase polymerase chain reaction.

The cell pellet was loosened by gentle tapping and 350 μl of buffer RLT (lysis buffer containing guanidine isothiocyanate and 10 μl of β-mercaptoethanol (β-ME) per 1ml of buffer RLT) was added to the cell pellet. The resulting lysate was homogenised by vortexing (with cell numbers ≤ 1 x 10^5). 350 μl of 70 % ethanol was added to the homogenised lysate and mixed by pipetting. 700 μl of the sample, including any precipitates that were formed was added to an RNeasy mini column placed in a 2 ml collection tube and centrifuged for 15 seconds at ≥ 8000 x g (≥ 10,000 rpm). The flow-through was discarded.

To wash the column 700 μl of buffer RW1 (containing guanidine salt) was added to the column and centrifuged for 15 seconds at ≥ 8000 x g (≥ 10,000 rpm). The flow-through and collection tube was then discarded. The column was transferred to a new 2 ml collection tube and 500 μl of diluted RPE buffer (Buffer RPE is a concentrate and

100 % of ethanol was added before use) was pipetted onto the column. The column was centrifuged for 15 seconds at ≥ 8000 x g (≥ 10,000 rpm) and the flow-through discarded. Another 500 µl of buffer RPE was added to the column and centrifuged for 2 minutes at ≥ 8000 x g (≥ 10,000 rpm) to dry the silica-gel membrane. To eliminate any chances of possible buffer RPE carryover (this can interfere with downstream reactions), the column was placed in a new 2 ml collection tube and centrifuged for 1 minute at full speed.

To elute, the column was placed in a new 1.5 ml collection tube. 50 µl of RNase-free water was directly added onto the silica-gel membrane and centrifuged for 1 minute at ≥ 8000 x g (≥ 10,000 rpm). The elution step was repeated with a second volume of RNase-free water into the same collection tube. Total RNA concentration was measured and used for PCR. To avoid contamination or degradation of RNA, PCR was conducted immediately post RNA extraction in all experiments. The extraction of RNA is shown in Figure 3-3.

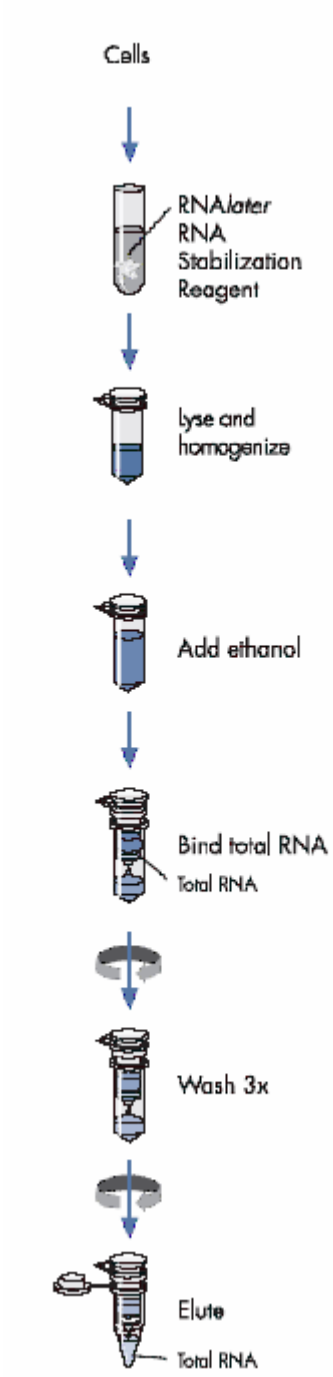

(1) Sample disrupted and lysed with GITC-containing buffer (Buffer RLT)

(2) Sample homogenised to shear genomic DNA and reduce viscosity of lysate

(3) Ethanol added to adjust binding conditions

(4) Sample applied to spin column for adsorption of RNA to membrane

(5) Contaminants removed with wash spins (Buffer RW1 and RPE)

(6) RNA eluted ready-to-use in water

Figure 3-3. Protocol demonstrating stages of RNA extraction. Adapted from RNeasy mini handbook 04/2006.

3.7 Analysis of gene expression

3.7.1 Polymerase chain reaction (PCR)

The original purpose of a PCR (Polymerase Chain Reaction) was to make a huge number of copies of a gene. Reverse Transcription (RT reaction) is a process in which single-stranded RNA is reverse transcribed into complementary DNA (cDNA) by using a reverse transcriptase enzyme, primer, dNTPs, RNase inhibitor. The resulting cDNA can be used in RT-PCR (reverse transcription-polymerase chain reaction) reaction. RT-PCR is a sensitive technique for mRNA detection and semi-quantification. Compared to the two other commonly used techniques for quantifying mRNA levels, Northern blot analysis and RNase protection assay, RT-PCR can be used to quantify mRNA levels from much smaller samples. This technique is sensitive enough to enable semi-quantification of RNA from a single cell.

There are three major steps in a PCR (see Figure 3-4) process, which are repeated for between 25 to 40 cycles (see Figure 3-5). This process is carried out on an automated cycler, which can heat and cool the tubes with the reaction mixture in a very short time. The three steps can be summarised as follows:-

Step 1 Denaturation at 94°C: During the denaturation, the double strand DNA melts open to single stranded DNA and all enzymatic reactions are stopped (for example: the extension from a previous cycle).

Step 2 Annealing: The primers move within the mixture by Brownian motion. Ionic bonds are constantly formed and broken between the single stranded primer and the single stranded template. Some more stable bonds form and last a little bit longer (where primers match exactly). On those small pieces of double stranded DNA (template and primer), polymerase can attach and begin to copy the template DNA. Once there are a few bases built in, the ionic bond is so strong between the template and the primer that it does not break down anymore.

Step 3 Extension at 72°C: This is the ideal working temperature for the polymerase. The primers, where there are a few bases built in, have a stronger ionic attraction to the

template than the forces attempting to break these attractions. The bases (complementary to the template) are coupled to the primer on the 3' side (the polymerase adds dNTP's from 5' to 3', reading the template from 3' to 5' side; bases are added complementary to the template). Primers that are on positions with no exact match become loose again (due to the increased temperature) and do not result in an extension of the fragment.

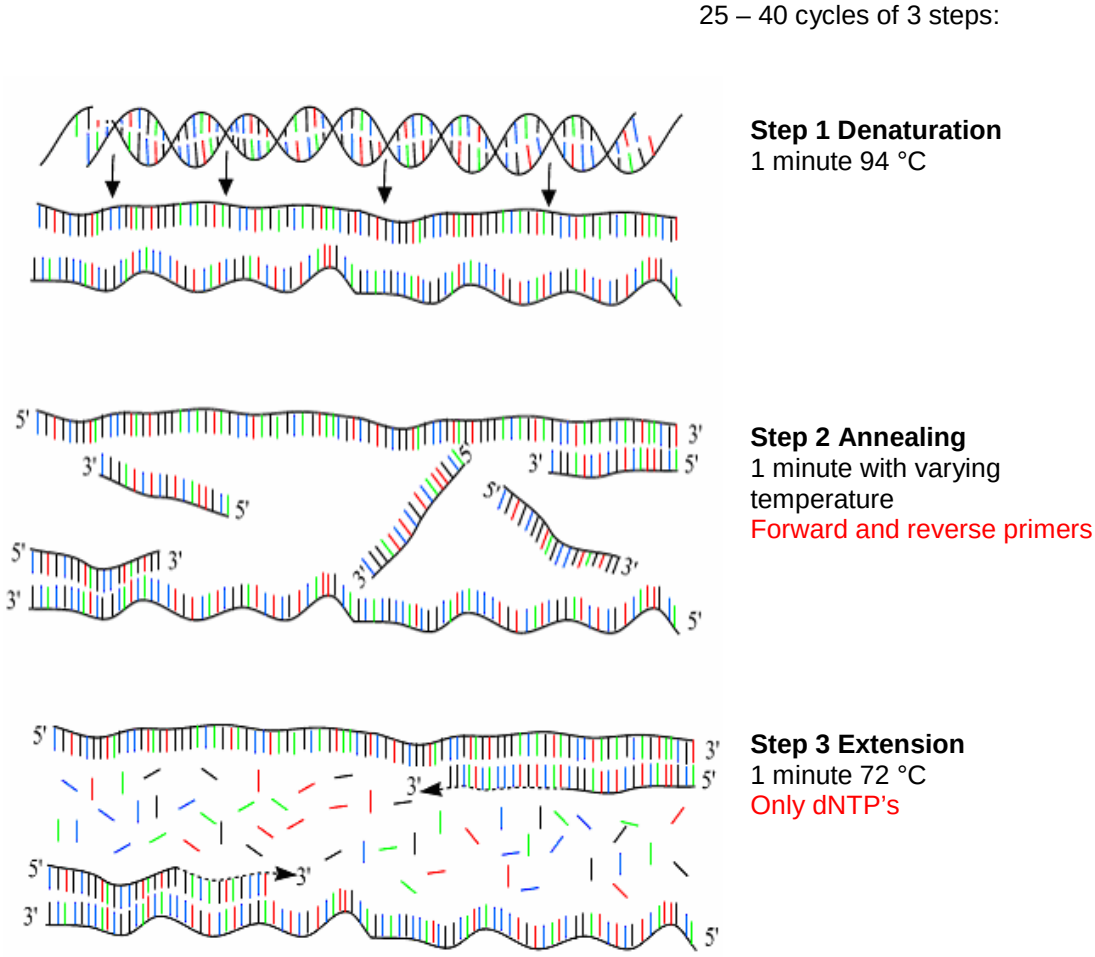

Figure 3-4. The different steps in PCR. Because both strands are copied during PCR, there is an exponential increase of the number of copies of the gene. If there is only one copy of the wanted gene before the cycling starts, after one cycle, there will be 2 copies; two cycles will result in 4 copies and so on.

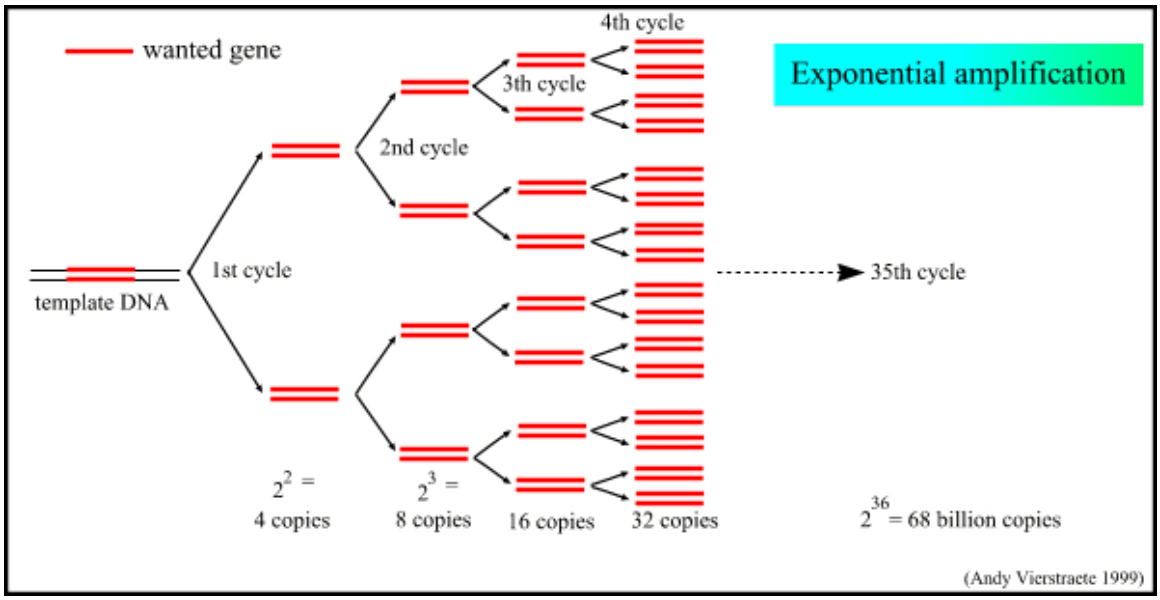

Figure 3-5. The exponential amplification of the gene in PCR.

3.7.1.1 One-step reverse transcriptase polymerase chain reaction (RT-PCR)

The Qiagen one-step RT-PCR kit (Qiagen Ltd, Crawley, U.K.) was used in all PCR experiments. This provided a convenient method for highly efficient and specific RT-PCR using any RNA. The components in this method are optimised to allow both reverse transcription (RT) and PCR amplification to take place as a "one-step" reaction. The general method of conducting RT-PCR for the PCR experiments in the subsequent chapters is summarised below.

The Qiagen one-step RT-PCR kit contains:

- RT-PCR enzyme mix (contains Omniscript™ reverse transcriptase, Sensiscript™ reverse transcriptase and HotStartTaq® DNA polymerase).
  The Sensiscript™ reverse transcriptase was optimised for use with very small amounts of RNA (< 50 ng) ideal in these experiments where a low yield of RNA was obtained. The HotStartTaq® DNA polymerase provided highly specific amplification. During the reverse transcription process the polymerase is completely inactive and does not interfere with the reverse-transcriptase reaction. After reverse

transcription (by Omniscript™ and Sensiscript™) the reactions were heated at 95°C to activate the DNA polymerase which eliminates extension from non-specifically annealed primers and primer-dimers in the first cycle ensuring highly specific reproducible PCR.

- RT-PCR buffer 5x (contains 12.5 mM $MgCl_2$)
  The buffer was designed to enable both efficient reverse transcription and specific amplification. It was particularly important for one-step RT-PCR performed with limiting RNA amounts.

- Q-solution 5x
  This facilitates amplification of difficult templates by modifying the melting behaviour of nucleic acids.

- dNTP mix contains 10mM each of dATP, dCTP, dGTP and dTTP

- RNase-free water

Total RNA concentration and purity was calculated by measuring the absorbance at 260 and 280 nm using an Eppendorf Biophotometer (Eppendorf^{AG}, Hamburg, Germany). These absorbance measurements cannot discriminate between DNA and RNA, therefore to determine the RNA concentration the ratio between the absorbance at 260 and 280 nm provides a workable estimate. Pure RNA has an A_{260}/A_{280} ratio of 1.8 - 2.3 in RNA free water.

A master mixture containing 10 µl of 5× Qiagen One-Step RT–PCR buffer, 10 µl of 5× Q-Solution, 400 µM of each of the deoxynucleoside triphosphates, 2 µl of Qiagen One-Step RT–PCR enzyme mixture and 0.5 µM of each of the primers was added. The master mix contains all the components required for RT-PCR except the template RNA. The template RNA was added at a concentration of 1 pg – 2 µg/ reaction. A negative control (without template RNA) was included in all experiments. RNase free water was added to give a total volume of 50 µl. Samples were centrifuged and placed in a thermal cycler, a MasterCycler Gradient PCR machine (Eppendorf^{AG}, Hamburg,

Germany) with a heated lid. For maximum yield and specificity, temperatures and cycling conditions were optimised for each gene studied (see Table 3-1).

Table 3-1. Determining thermal cycle conditions for PCR.
* The PCR conditions for the primers used in this study are: GAPDH: 40 cycles (94, 50, 72 °C); PECAM-1: 35 cycles (94, 50, 72 °C); TGF-β1: 35 cycles (94, 55, 72 °C); COL-1: VEGFR-1 and VEGFR-2 35 cycles (94°, 59° and 72°). Primers were supplied by Sigma-Genosys (Sigma-Genosys, Haverhill, U.K.).

STEP	TIME	TEMPERATURE	ADDITIONAL COMMENTS
Reverse transcription	30 min	50 °C	
Initial PCR activation step	15 min	95 °C	
3-step cycling Denaturation Annealing Extension	 1 min 1 min 1 min	 94 °C 50 - 68 °C***** 72 °C	 ~5 °C below T_m of primers
Number of cycles	25 - 40		Dependant on the amount of template RNA and the abundance of the target transcript
Final extension	10 min	72 °C	

3.7.1.2 PCR product analysis

PCR products were analysed by 2% agarose gel electrophoresis prepared with 100 mls 10 x TAE (Tris Acetate EDTA-buffer) and 2 g of agarose (Sigma-Aldritch, Gillingham, Dorset U.K.). The solution was boiled in a microwave for 2 minutes to dissolve the agarose. Once heated, the solution was left to cool down to about 60 °C at room temperature. 2 µl ethidium bromide was added to the gel solution. This was then poured into the gel rack with a comb at one side of the gel. Once the gel had solidified, 10 x TAE was added to fill the gel tank and the combs of the gel were slowly removed. PCR samples (20 µl of PCR product and 5 µl loading dye) were loaded onto the gel and run with a 100 base pair marker at 80 V for 1 hour. The products were semi-quantified using a GeneGenius darkroom with 'GeneSnap' version 6.02. (Syngene, Cambridge, U.K.).

Figure 3-6 demonstrates examples of amplification of PCR products on a gel. It is important to determine if the product is of the right size. If there is a product, for example a band of 500 bases, but the expected gene should be 1800 bases long. In this case, one of the primers probably fits on a part of the gene closer to the other primer. It is also possible that both primers fit on a totally different gene or that the primers fit on the desired locations, and also on other locations. In this case, different bands are present in one lane on a gel (see Figure 3-6).

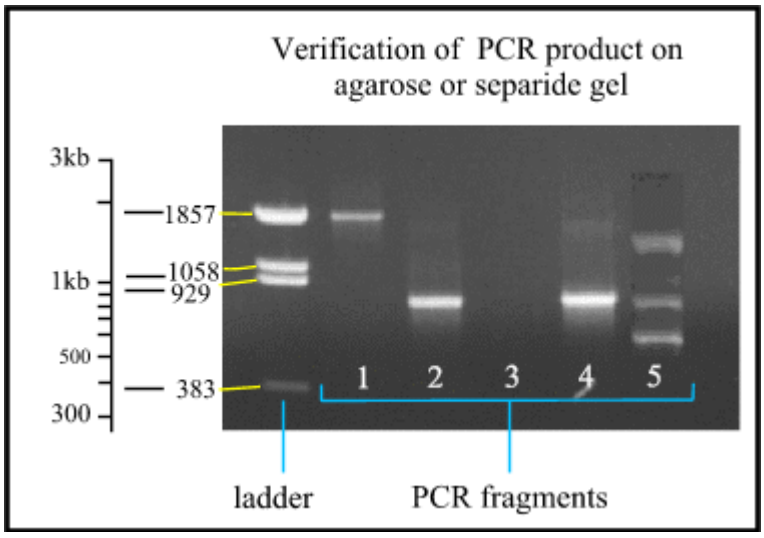

Figure 3-6. Verification of a PCR product on a 2 % agarose gel.
The ladder is a mixture of fragments with known size to compare with the PCR fragments. The distance between the different fragments of the ladder is logarithmic. Lane 1: PCR fragment is approximately 1850 bases long. Lane 2 and 4: the fragments are approximately 800 bases long. Lane 3: no product is formed, so the PCR failed. Lane 5: multiple bands are formed because one of the primers fits on different places.

3.8 Cell visualisation

Examination of cells on synthetic polymers can only be performed by few staining methods. Immunoflourescent staining using antibodies was found to stain the polymer as well as the cells making it difficult to visualise the presence of cells on the polymer. To overcome this, two techniques were used toluidine blue staining and scanning electron microscopy (ScEM). Toluidine blue is a metachromatic dye. It is a blue nuclear counterstain and can be used to demonstrate Nissl substance. It has been

used as a surface stain or on paraffin sections. The Toluidine blue method has been used as a successful stain in determining viability of cells on biomaterials (461).

ScEM is a type of capable of producing high-resolution images of a sample surface. Due to the manner in which the image is created, ScEM images have a characteristic three-dimensional appearance and are useful for judging the surface structure of the sample. ScEM allows visualising the topography, morphology, composition and crystallographic information of a sample.

3.8.1 Toluidine blue staining

Cells were washed with PBS and then fixed in formaldehyde for 10 minutes at room temperature. Five hundred microlitre of a 0.1% solution of Toluidine blue (Sigma Chemical Company, Poole, Dorset, UK) was then added to each well and incubated for 30 minutes at room temperature. Cells were then destained in water and photographed.

3.8.2 Scanning electron microscopy (ScEM)

All ScEM images in this thesis were conducted at the Electron Microscopy Unit, Royal Free hospital. Samples were fixed in 1.5% glutaraldehyde for a minimum of 2 hours. The tissue was then washed with several changes of phosphate buffered saline (Oxoid, Merck Ltd, Hunter Boulevard, Magna Park, Lutterworth, U.K.) and postfixed using 1% osmium tetroxide/1.5% potassium ferricyanide for 12 hours. The grafts were washed with distilled water and dehydrated through graded acetone (30%, 50%, 70%, 90% and 100% HPLC grade 2 x 15 minutes each). After dehydration the grafts were transferred to Tetramethylsilane for 10 minutes and then allowed to air dry. The grafts were attached to aluminium stubs with double sided sticky tabs (TAAB Laboratories Equipment Ltd, Unit 3 Minerva house, Calleva Ind. Park, Aldermaston, Reading, Berks.) and then coated with gold using an SC500 (EMScope) sputter coater. The stubs were examined and photographed using a Philips 501 scanning electron microscope.

3.9 Data analysis and statistical methods

In this thesis results were analysed using the statistical software package GraphPad Prism. Student's t-test or one way ANOVA were used during the data analysis. Data are presented as mean ± SD or mean ± SEM.

4

Development of an RNA isolation procedure for the characterisation of human endothelial cell interactions with cardiovascular bypass grafts

4.1 Introduction

Insofar as can be established from the literature review in Chapter 2, little work has been performed on gene expression studies of the effects of shear stress in a cylindrical graft. Gene expression has been well characterised *in vitro* on monolayer's of EC seeded on glass and subjected to shear stress (462). There have been reports that growth factors such as TGF-β have been shown to up-regulate and cause a decrease in certain adhesion molecules such as VCAM-1 under physiological shear stress. An important question is would the genotype be the same if physiological shear stress was applied in cylindrical conduits rather than flat sheets of polymer? Cells interacting with novel biomaterials may exhibit distinct patterns of gene expression depending on the molecular nature of the surface they are contacting. It is well-documented that many cell types grown in three-dimensional culture exhibit drastically different phenotypes than their plate-grown counterparts (463;464). Studies of individual genes have demonstrated that transcript levels can change as a function of biomaterial contact (465-468). Recently, Gerritson *et al.* demonstrated differential gene expression of cells growing in various human endothelial tube models (469).

Research to date on seeding vascular grafts has focused on evaluating EC attachment, adhesion and proliferation in cylindrical conduits by various methodologies such as radiolabeling, immunostaining and the Alamar blue™ assay (444). There are limited reports on evaluating the effect of polymers on gene expression for cell proliferation, cell adhesion, cytoskeleton and ECM (314;315). Investigating gene expression in a cylindrical graft would enable the understanding of the molecular effects of cell adhesion and proliferation on the vascular substitute as well as potentially evaluating the mechanisms responsible for prosthetic graft failure.

The lack of studies may be due to the difficulties in extracting cells present on the graft surface in order to obtain functional messenger RNA (mRNA). This is because the extraction of RNA from cells seeded on polymer presents many obstacles. Firstly, RNA stabilisation is an absolute prerequisite for reliable gene-expression analysis. In general, the extraction of RNA from cells or tissue must be performed quickly. The greater the time it takes to extract the RNA; the higher the risk of RNA degradation thus compromising RNA quality and yield. Changes in gene expression pattern can occur due to specific and non-specific RNA degradation as well as transcriptional induction. Such changes in gene expression pattern need to be avoided for a reliable quantitative gene-expression analysis. In addition to RNA stability issues, cells present on the graft are supplemented with cell culture medium and incomplete removal can inhibit lysis as well as interfere with PCR. Finally and most importantly, the surface of a prosthetic graft has a more complex chemistry than tissue culture plates making isolating cells much more difficult and may result in a reduced RNA yield. As a result of this the production of high quality RNA in a sufficient amount for further analysis from EC seeded onto cylindrical prosthetic graft is a challenge.

In tissue culture studies, cell removal is usually achieved by trypsinising. Cells that are grown in a monolayer in cell culture flask, or on slides, are usually trypsinised and collected as a cell pellet for RNA extraction, in accordance with RNeasy kit instructions. However, removing cells using trypsin from the surface of a seeded or tissue engineered vascular graft is much more challenging. Zhang and colleagues (314) have used a scraping technique in order to extract RNA from rabbit bone marrow stromal cells cultured for 7 days on flat sheets of degradable lysine-di-isocyanate-glycerol-urethane and compared expression for collagen type I, TGF-β1 and osteocalcin. The group of Menconi (315) again used a scraping technique in order to

isolate RNA but from bovine EC after 5 days culture on flat sheets of two poly(ether)urethanes Biomer and Tecoflex SG60D respectively. Expression of fibronectin, actin, vimentin, histone and collagen was investigated.

The study carried out in this chapter aimed to develop a highly reliable and quantitative technique for the isolation of RNA from human EC grown on a vascular graft that will allow accurate representation of the entire cell population, a key factor for studies in cell/material interaction. As well as RNA purity and cell viability the expression of two genes, TGF-β1 and GAPDH was assessed. GAPDH is a housekeeper gene that has been shown to be expressed in constant amounts across cell lines (401). TGF-β1 is involved in diverse biological processes, such as cell proliferation, migration, differentiation, survival, and cell–cell and cell–matrix interaction and has been demonstrated to be key to the formation of extracellular matrix (ECM) by EC under flow (392;399;470).

4.2 Materials and methods

4.2.1 Material chemistry

The conduit used in this study was a vascular graft based on polyurethane, PCU with an internal diameter of 5 mm and length of 50 mm that exhibits arterial viscoelasticity (422;471).

4.2.2 Cell culture and graft seeding

HUVEC were cultured as described in Chapter 3. Cell numbers were amplified in tissue culture at 37 °C and 5% CO_2/95% air. Confluent cultures at third passage were used in all experiments. Following trypsinisation and resuspension in complete tissue culture medium, a cell count was obtained. Fifty millimetre tubular lengths of PCU graft were seeded with HUVEC at 3×10^5 cells/cm^2. Cells were added as a suspension to each graft segment, the ends of the graft plugged, and the graft segments rotated 90° every 15 minutes for 2 hours to achieve an even covering of HUVEC on each graft. Grafts were then left overnight for efficient cell adhesion and used the next day. As a

comparison and to ensure each technique was carried out accurately an equal number of cells were seeded onto 6-well polystyrene tissue culture plates (TCP) as above.

Viability of seeded cells was assessed using an Alamar blue™ assay following the protocol described in Chapter 3. Following overnight seeding graft samples and controls were washed with PBS and the washings collected for cell counting to assess seeding efficiency. One millilitre of Alamar blue™ (10%) v/v in complete medium was added to each graft/well and incubated for 4 hours. Duplicate 100 µl samples were then removed and the absorbance's read spectroscopically at wavelengths of 570 nm and 630 nm.

4.2.3 RNA extraction

Prior to the extraction of the RNA using a "Qiagen RNeasy™" kit (method outlined in Chapter 3, Section 3.6) cells were removed from the graft and wells of polystyrene plate in one of the three ways detailed below:

(I) *Trypsinisation*: graft segments/wells were washed with PBS and 1 millilitre trypsin-EDTA (0.25%) was added for 5 min.
(II) *Cell scraping*: graft segments/wells were washed with PBS and the graft segments were then split lengthwise to expose the inner graft surface. One millilitre PBS was then added and the graft segments/wells were scraped using a cell scraper.
(III) *Direct lysis*: graft segments/wells were washed with PBS and the graft segments were then split lengthwise to expose the inner surface of the graft. One millilitre cell lysis buffer was then applied directly to the cells on the graft and using a cell scraper the lysates were collected.

4.2.4 Analysis of total RNA and mRNA

The RNA concentration and purity was calculated by measuring the absorbance at 260 and 280 nm. The quality of the RNA was assessed by agarose gel electrophoresis and the mRNA was used for PCR (see Chapter 3) of the housekeeping gene GAPDH and the growth factor gene TGF-β1. For amplification this was carried out by a MasterCycler Gradient PCR machine, RT-PCR was performed using a one-step PCR kit. A master mix containing 10 µl 5× Qiagen one-step RTPCR buffer, 10 µl 5× Q-

Solution, 400 μM from each of the deoxynucleoside triphosphate, 2 μl Qiagen One-Step RTPCR enzyme mix and 0.5 μM from each of the primers was added. For each sample, 0.5 μg of template RNA and RNase free water was added to make a total volume of 50 μl. Cycle conditions for GAPDH were 40 cycles (94, 50, 72 °C) and for TGF-β1 were 35 cycles (95, 55, 72 °C).

4.2.5 Scanning electron microscopy

Complete removal of cells from the polymer was difficult to assess visually therefore trypsinising, scraping and direct lysing of cells from the polystyrene plates allowed microscopic assessment that each technique applied was fully removing the cells from the surface. Following removal of cells from the graft by the various methods, representative graft samples were analysed with ScEM. This enabled the visualisation of how efficient each isolation method was and enabled any damage to the graft by the removal of cells to be monitored.

4.2.6 Data analysis and statistical methods

The experiments were repeated six times. Data are presented in mean ± SD. Comparison between groups was made by one-way ANOVA (Kruskal–Wallis) test with post comparison using Dunn's comparison test.

4.3 Results

4.3.1 Cell viability

The Alamar blue™ results demonstrated that viable HUVEC were present on all the graft segments seeded as well as in the wells of the polystyrene plates (Figure 4-1). There was no significant difference between the three groups within either the seeded graft samples or the seeded plates. Significantly higher ($P < 0.01$) Alamar blue™ activity was found where cells were seeded in the wells of the plate compared to the seeded graft in all cases.

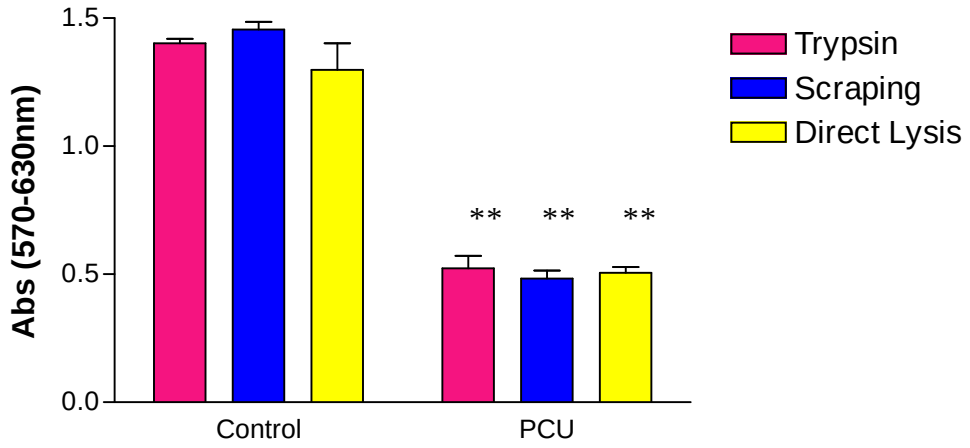

Figure 4-1. Alamar blue™ viability assay test. Absorbance was measured in arbitrary units (AU) at 570 and 630 nm wavelengths. The control groups represent cells seeded on polystyrene wells and the PCU group are cells present on the graft. **P < 0.01 compared to control, Student's t-test.

4.3.2 RNA quantity, purity and quality

The amount of RNA extracted by the three different isolation methods is shown in Figure 4-2. In the case of RNA extracted from HUVEC seeded in the wells of the plate, the trypsinisation method produced a significantly higher yield of RNA (0.728 µg/µl) compared to cell scraping (0.445 µg/µl; $P < 0.05$) and directly lysing (0.308 µg/µl; $P < 0.01$).

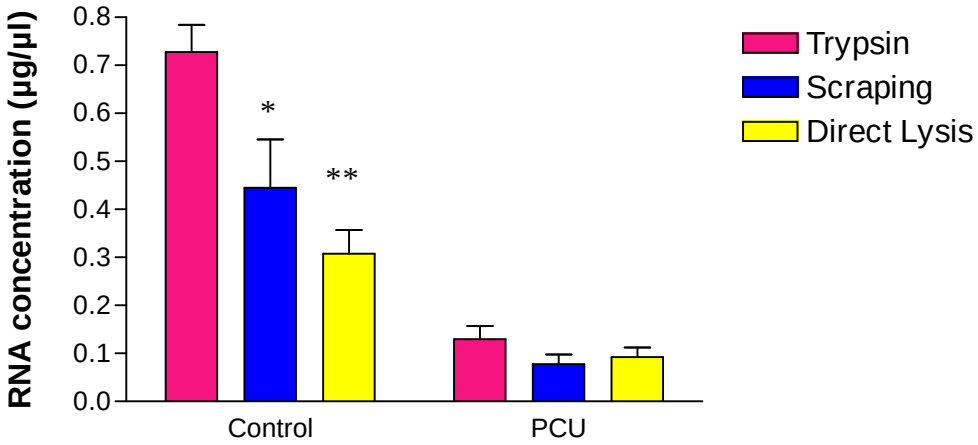

Figure 4-2. Comparison of RNA yields in µg/µl isolated by different methods between the control and PCU group. *P < 0.05, **P < 0.01 compared to trypsin, Student's t-test.

When extracting RNA from HUVEC seeded onto the graft segments again trypsinising the cells produced the highest yield (0.13 µg/µl) of RNA compared to scraping the cells (0.078 µg/µl) and directly lysing the cells (0.093 µg/µl) from the graft surface. In this case, there was no significant difference in the yield of RNA obtained between any of the three isolation methods from the graft material. In all cases purity was greater than 95% (Figure 4-3).

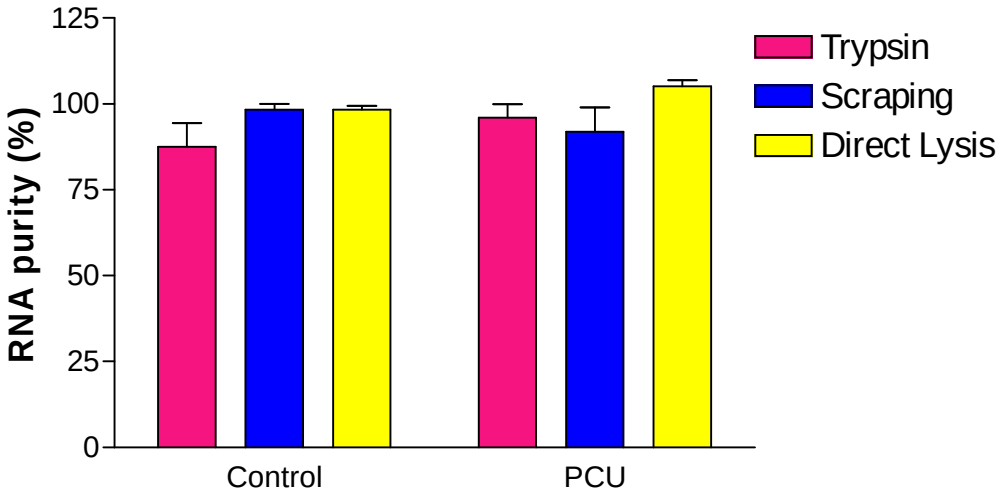

Figure 4-3. Comparison of RNA purity expressed as percentage for each sample. No significant difference was observed in purity between any of the three isolation methods from the control and graft material.

Figure 4-4 is a standard 2% agarose gel of the total RNA. This illustrates the quality of total RNA obtained from each isolation method. In all cases the ribosomal RNA can be clearly seen, demonstrating that there is little or no RNA degradation prior to extraction. PCR conducted on all samples demonstrated equal levels/µg of RNA of the housekeeping gene GAPDH (Figure 4-5). It can be seen that all isolation methods produced mRNA suitable for further investigation by PCR and all samples were comparable to those obtained from the control wells. Further studies of the RNA isolated from each sample showed similar levels of expression of TGF-β1 (Figure 4-6).

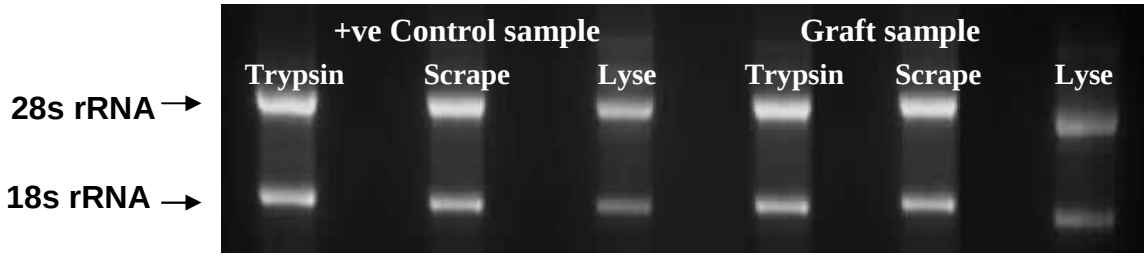

Figure 4-4. Total RNA of HUVEC from the control and PCU using the three isolation methods. Two distinct 28S and 18S ribosomal RNA bands are shown on 2% agarose gel. Intensity of 28S is two times as that of 18S band with no degrading. Total RNA integrity showed no difference between the extraction methods.

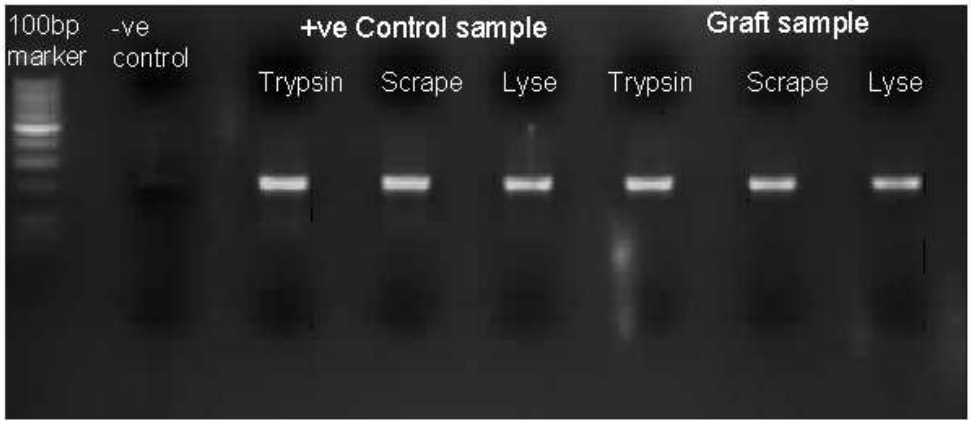

Figure 4-5. Two percent agarose gel shows amplification of the house-keeping gene GAPDH which was observed in all the RNA samples obtained from each sample. This indicates functional mRNA was extracted.

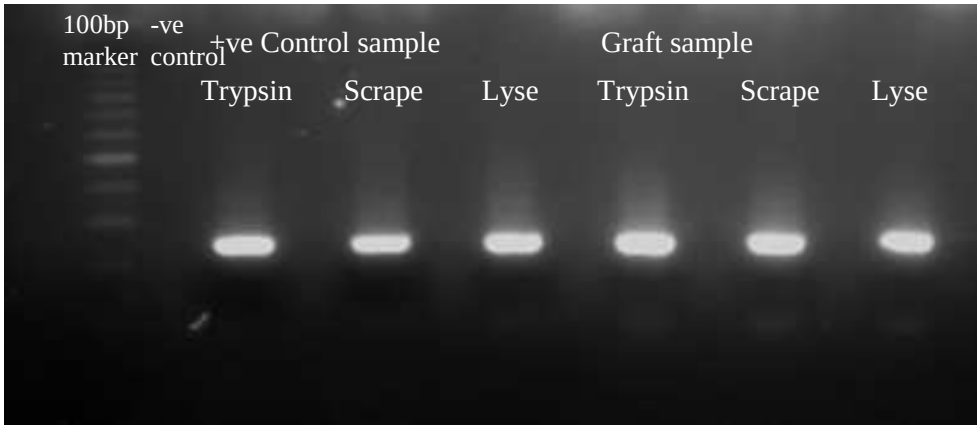

Figure 4-6. Two percent agarose gel demonstrating the expression of TGF-β1 amplicon from HUVEC isolated from the extraction methods applied in the control and PCU group.

4.3.3 Efficiency of cell removal

From the assessment of representative graft sections prior to and after isolation it was observed that in some cases cell removal from the graft was less complete than in others. Figure 4-7 shows the graft segments post cell isolation. Figure 4-7 (A) and (B) shows native PCU with honeycomb surface and seeded with HUVEC respectively. Trypsinisation resulted in the majority of cells being removed from the graft surface (Figure 4-7 C) and showed no apparent damage to the graft surface (Figure 4-7 D). Mechanically scraping the cells from the graft did not result in the removal of all the cells from the surface (Figure 4-7 E) and also caused damage to the graft surface (Figure 4-7 F). Furthermore, directly lysing the cells from the graft surface again showed visible cells present after isolation (Figure 4-7 G) and also resulted in some damage to the surface of the graft (Figure 4-7 H)

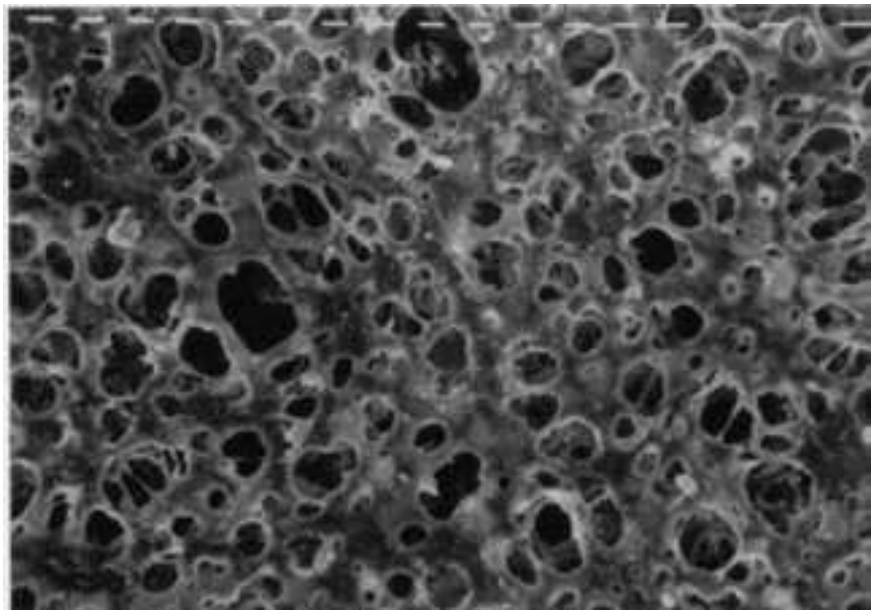

A)

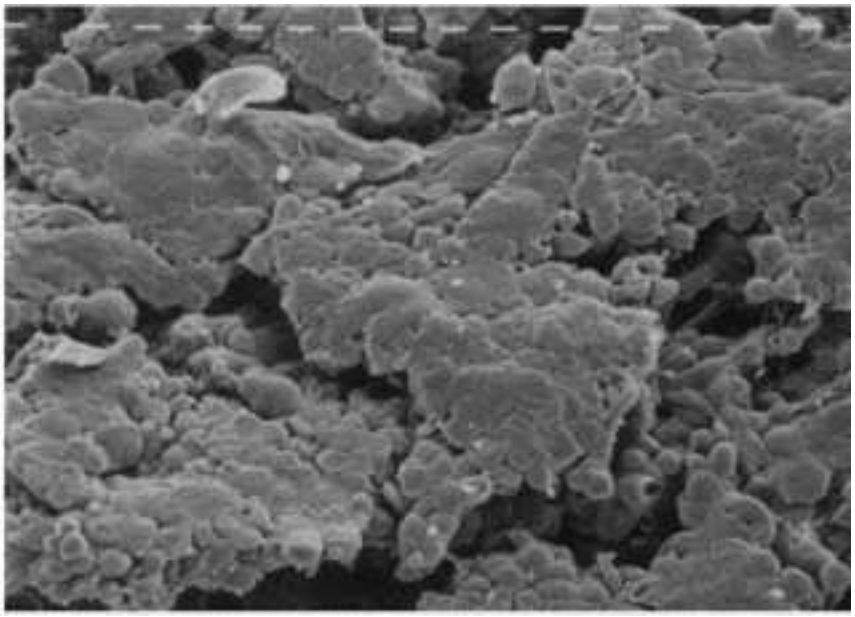

B)

Figure 4-7. Typical ScEMs show native PCU with honeycomb surface (A) and seeded with HUVEC (B).

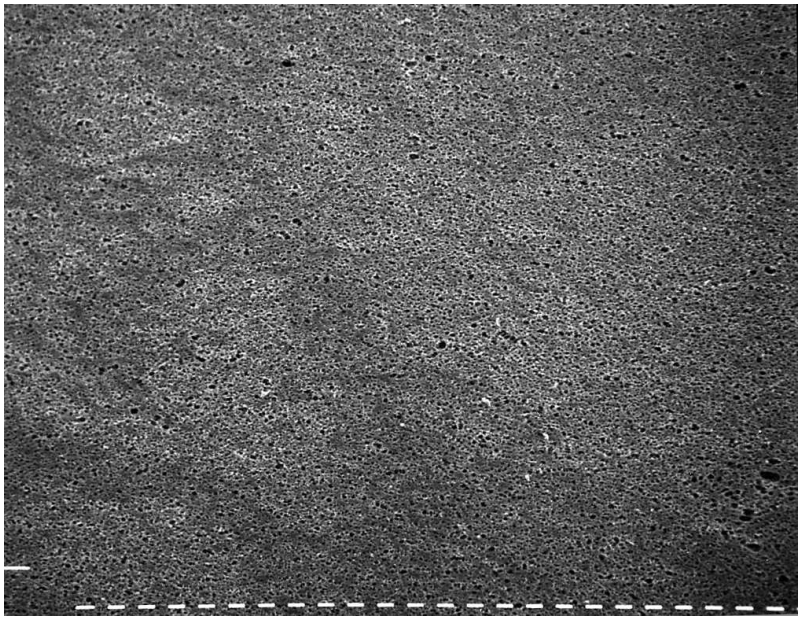

C)

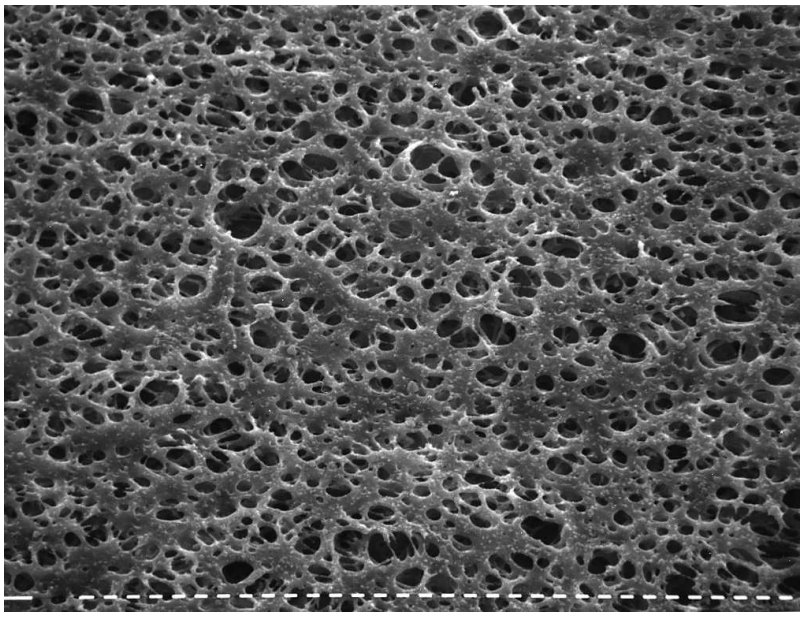

D)

Figure 4-7. ScEMs show high magnification of surface of PCU after trypsinisation (C) and low magnification of PCU showing post trypsinisation (D).

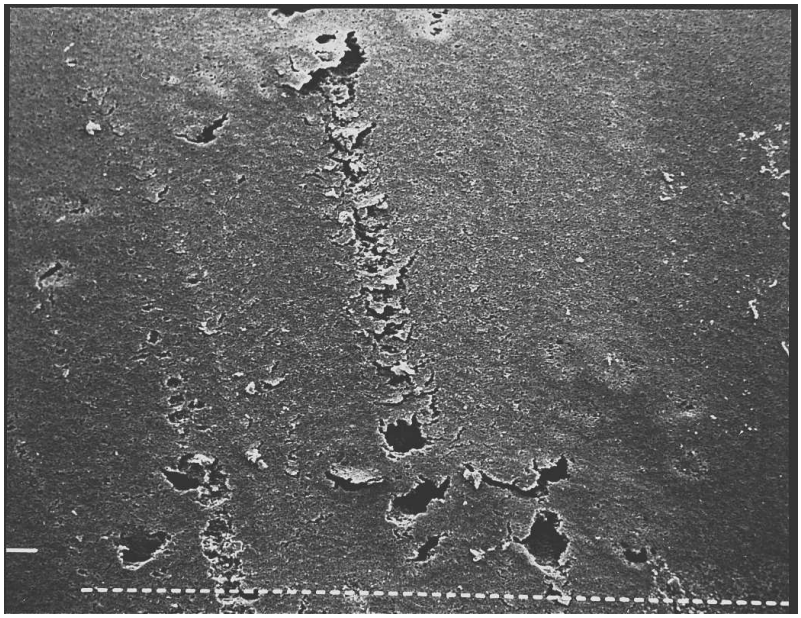

E)

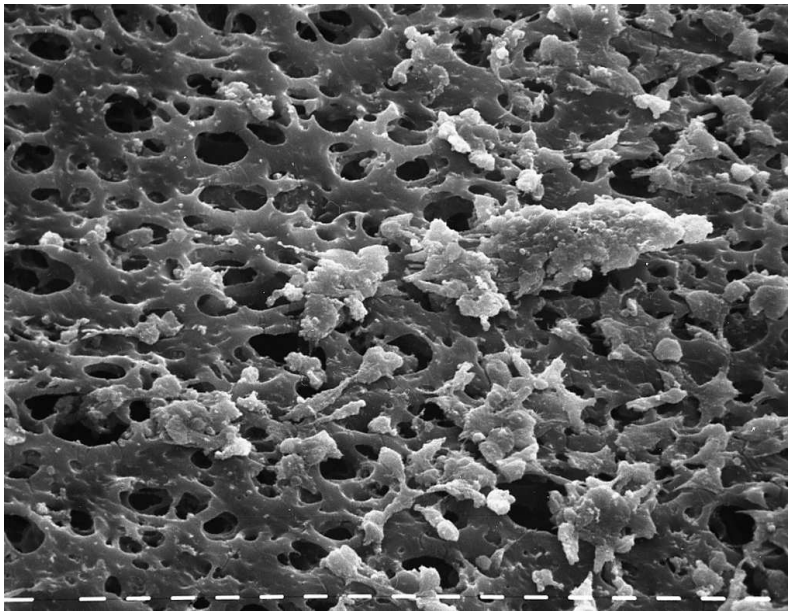

F)

Figure 4-7. ScEMs show high magnification of PCU post-scraping (E) and low magnification of PCU post-scraping (F).

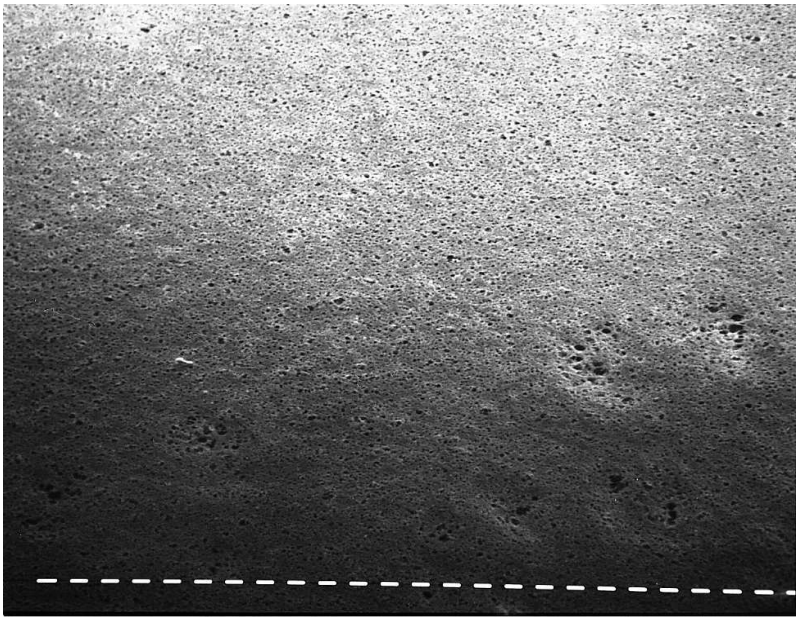

G)

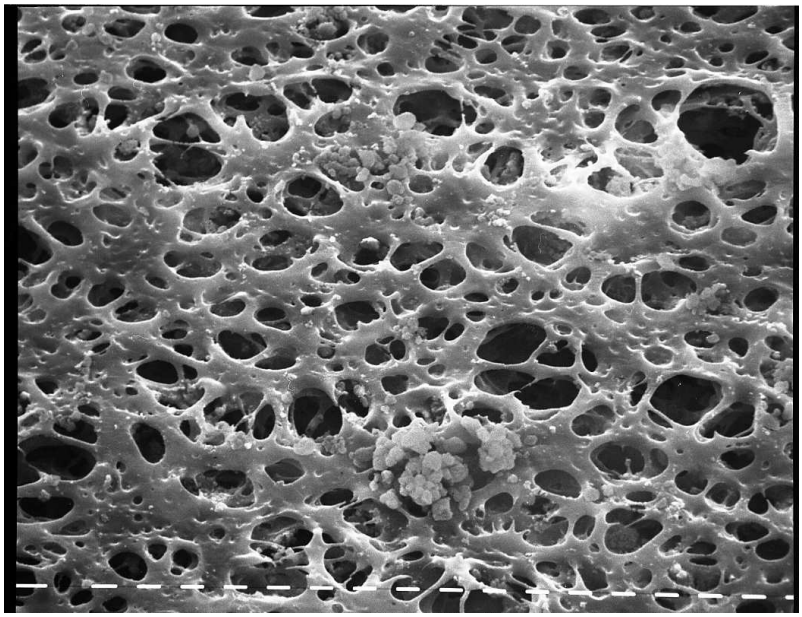

H)

Figure 4-7. ScEMs show high magnification of PCU after directly lysing (G) and low magnification of PCU post-lysing (H).

4.4 Discussion

No work has been conducted in order to develop quantifiable RNA extraction methodology in the context of cardiovascular prostheses. The methodology of RNA extraction that has been used to date from *in vivo* samples of seeded prosthetic grafts is based on scraping cells from the inner surface (302;313). Despite other groups demonstrating changes in gene expression they have not reported what efforts they have made to ensure that the RNA extracted is a reliable indication of all the cells extracted from the graft. Studies have investigated flat sheets of poly(ether)urethane used in vascular grafts and a peptide based degradable urethane seeded with cells (314;315).

Gene expression in cylindrical vascular prosthesis is of interest as to date it has not been possible to study the effects of shear stress on cellular/material interaction and EC remodelling. Removing cells from a graft surface is more challenging than tissue culture plastic. As an example, in Dacron grafts the surface consists of a complex woven, knitted textile or mesh form. In ePTFE grafts the drawing and sintering process used to extrude grafts produces a cylindrical tube with a highly porous wall consisting of fibrils and nodules of different pore sizes. Extrusion of polyurethanes leads to solid walls or if coagulating, into porous walled structures. PCU based vascular grafts have spongy middles and a single skin structure that allows it to maintain compliance and pulsatile flow *in vivo* (208;214) resulting in a significant proportion of the cells becoming trapped in the spongy middle. This honeycombed surface structure is ideal for cell seeding (199;214;314;422;444) but further complicates cell retrieval.

The tubular nature of the grafts makes application of trypsin in an aseptic manner more difficult than in a culture flask. Direct lysis of the cells with the RNeasy lysis buffer (containing guanidine isothiocynate) was included in this study as this buffer stabilises the RNA and thus reduces degradation. Scraping is a physical method of removing cells from the surface commonly used for routine tissue culture; it was used here in case the chemical means of cell collection were effected by, or affected, the graft material.

RNA isolation was examined from PCU vascular grafts using three methodologies to assess how effective they were for extracting RNA from PCU vascular grafts. The cellular metabolism was significantly greater in the control group (polystyrene tissue

culture plates) compared to the PCU group. This suggests that fewer cells adhered to the graft than the wells of the polystyrene plates. This was due to a leakage of cells through the PCU graft pores during seeding, which resulted in a lower number of cells on the graft. Fewer cells may also explain, in part, why there was a significant difference in the RNA yield between PCU and control groups for each isolation method.

There was not a significantly greater amount of RNA extracted in the PCU group using trypsin although this method did produce more RNA than either scraping or direct lysis. We have found that trypsinisation is the best methodology for investigating gene expression on cells grown on polymers, despite not showing a significantly higher yield. The lysis and scraping methodologies used on the PCU graft presented many obstacles which we postulated made them less suitable for obtaining reliable RNA from seeded grafts for PCR.

Stable RNA is a prerequisite for reliable gene-expression analysis and the extraction of RNA from cells or tissue must be performed rapidly. The greater the time it takes to extract the RNA the higher the risk of RNA degradation, thus compromising RNA quality and yield. Changes in the pattern of gene expression can occur due to specific and non-specific RNA degradation. It was found that the lysis and scraping procedures were more time consuming and technically more difficult than trypsinisation and therefore more likely to result in changes of gene expression pattern during isolation. Applying lysis buffer directly to the graft can also inhibit cell lysis due to the potential presence of culture medium in the pores of the graft resulting in the entire cell population not being obtained.

The ScEM images also provided evidence that there were cells still present on the graft after lysing and scraping showing that most of the cell population was not extracted, especially those cells that were embedded in the graft pores which are more likely to undergo alterations in gene expression. Trypsinisation is significantly better on polystyrene culture plates; resulting in higher total RNA from PCU graft and did not damage the graft. The current *in vitro* model studying gene expression after shear stress has been carried out on two dimensional cultures where the characteristics of the flow and the interactions of the cells with the material are different from the clinical scenario. The use of microarrays would be more complex given the reduced yield of RNA from cylindrical grafts although PCR would be possible on carefully selected genes. Amplification schemes are available to prepare small quantities of DNA for use on

microarrays, these will allow the amounts of RNA isolated here to be suitable for these studies (263;472).

In this experiment two genes were examined for potential use in future studies. GAPDH is frequently used as the housekeeping gene of choice and was used as a positive control for RNA quality. Similar levels of expression in each group suggested that the RNA would be of good quality for subsequent genes expression investigation. In addition, TGF-β1 has been demonstrated to be important in the production of ECM (473) and is thought to be essential in remodelling of EC under shear flow (400). Similar levels of expression of TGF-β1 were observed in all samples demonstrating that there was no difference between the methods of isolation used on the graft and in the culture plates. This indicates that the method applied on the graft in order to isolate RNA has no effect on the RNA function. It was also important at this stage, as no flow was applied, that we consider a gene demonstrated to be up-regulated by HUVEC prior to flow. The use of genes such as collagen have been reported by some groups not to be up-regulated until some time after the cells have been exposed to shear flow.

In addition to the studies of shear flow and EC, which have already been carried out extensively it is fundamental that the interaction of cells and materials should be studied using gene expression. The understanding of how cells interact with the graft would open an array of possibilities to modify cellular behaviour by genetic modification of these cells when used for tissue engineering; the use of haemodynamics may be better adapted to promote cell adhesion, differentiation and proliferation. This study demonstrates that the study of gene expression in tubular conduits of PCU is possible and that the RNA extracted is reliable and reproducible.

4.5 Conclusion

This study demonstrates for the first time a quantitative methodology for the isolation of RNA from PCU vascular grafts. Before embarking upon this project it was very important to establish whether it was possible to extract RNA successfully from cells seeded onto conduits. The final plan for this project was to study a novel nanocomposite polymer which was being developed. When the project began this

nanocomposite polymer was still undergoing further development (particulars of conduit design can be found in Chapter 6) and thus was not available in conduit form to study RNA extraction from cells seeded on it. In order to study a similar system and progress the project whilst polymer development was taking place it was decided to employ another porous polymer conduit previously investigated our group (PCU) to study RNA extraction from cells seeded on a porous cylindrical conduit. As a result of this the conclusions reached in this chapter are based on previously published data on PCU seeding whereas the rest of the thesis is based on the employment of nanocomposite.

Three methods of cell/RNA isolation from the graft were analysed and showed that there were no significant differences between cell scraping, direct cellular lysis on the graft and trypsinising the cells from the graft prior to RNA extraction with a commercial RNA extraction kit. Despite this trypsinisation alone showed cell removal without damage to the graft and provided higher levels of RNA. It can be concluded, therefore, that RNA isolation from cells seeded onto PCU graft is best achieved by the removal of cells from the graft by trypsin prior to RNA extraction.

5

In vitro cytotoxicity analysis of nanocomposite

5.1 Introduction

All natural and synthetic materials used as implantable devices ("biomaterials") must be screened for adverse effects on cells and tissues. Biocompatibility is the ability of a material to perform with an appropriate host response in a specific application (1). It is not possible to make a single test that determines whether a material is biocompatible or not. This usually requires *in vitro*, animal and clinical testing.
The biocompatibility of a scaffold or matrix for a tissue-engineering products refers to the ability to perform as a substrate that will support the appropriate cellular activity, including the facilitation of molecular and mechanical signalling systems, in order to optimise tissue regeneration, without eliciting any undesirable effects in those cells, or inducing any undesirable local or systemic responses in the eventual host. Although animal studies are ultimately required before a new material can be licensed for clinical use, all potential materials are screened first in tissue culture systems.

While current prosthetic materials are not suitable for CABG, we believe that the answer lies with a new generation of nanocomposite incorporating silicon in the form of POSS molecules. The nanocomposite polymer used in this thesis has been extensively

characterised including the synthesis, mechanical and physical properties of the polymer by researchers in our department (70;474). Given the importance of endothelialisation in vascular grafts, this investigation sought to study the ability of this nanocomposite to sustain endothelialisation. The properties engendered in the polymer were to achieve both anti-platelet and protein inhibitory qualities coupled with the ability to demonstrate cytocompatibility allowing cells to grow on its surface. The silsesquioxane being present on the polymer surface permits the anti-platelet and anti-coagulant function but prevents the cytotoxic effects associated with materials containing silicon. This allows EC to grow on its surface as required in tissue-engineered of CABG. Apart from indicating its safety as a biomaterial at the cellular level, such information would also serve as a measure of its potential for developing bio-hybrid vascular grafts.

Current *in vitro* biocompatibility assays are based upon the exposure of cultured cells to test materials, either as a solid sample or as particles. Previous studies into the cytocompatibility of similar materials have investigated the effect on cells of either direct contact with the material or indirect contact by utilising cell culture medium exposed to material for a time prior to use. Techniques used to evaluate cytocompatibility include examining cell morphology by light microscopy and ScEM, [3-(4,5-dimethylthiazol-2-yl)-2,5-diphenyltetrazolium bromide] (MTT) metabolic activity assays, neutral red viability staining and cell counting by using Tryphan blue (2;3;5;18). In this study, both the direct and indirect effects of the nanocomposite on HUVEC have been explored by looking at the total amount of DNA present in the cells using a Pico green assay system, examining cell metabolism using an Alamar blue™ metabolic assay and looking at cell damage by measuring LDH release. Cell morphology was studied by staining with Toluidine blue in the case of indirect contact and carrying out ScEM studies in the case of direct contact.

5.2 Material and Methods

5.2.1 Polymer production

The synthesis of nanocomposite has been described in Chapter 3. The nanocomposite was cast by pouring 3 ml of the polymer solution into a 10 cm diameter

glass dish and was left for 18 hours in a circulating air oven at 55 - 65 °C. Following casting, the graft material was thoroughly washed with PBS. The polymer coated glass dishes were sterilised by autoclaving prior to use.

5.2.2 Endothelial cell culture

HUVEC were isolated from human umbilical cord vein as described earlier. In brief, cell numbers were amplified by tissue culture in cell culture medium (CCM). At confluence, cells were removed using 0.25% trypsin-EDTA and split in a 1:2 ratio. Confluent cultures at passage three were used in all experiments.

5.2.3 Assessment of cytocompatibility

5.2.3.1 Indirect effect of nanocomposite on HUVEC

A sample of the graft was powdered using a Mikro Dismembartor U (B. Braun Biotech International, Melsungen, Germany). Following powdering, graft samples were sterilised by autoclaving. Powdered graft was then added at concentrations of 1, 10 and 100 mg/ml to CCM and shaken for seven days at 37 °C in a shaker. Following exposure to powdered nanocomposite the treated CCM samples were centrifuged to remove the powdered nanocomposite.

Twenty-four-well plates were seeded with 1 ml HUVEC at a concentration of 2×10^5 cells/ml for 24 hours. Cells were then exposed to the following treatments: untreated CCM (CCM_0), 1 mg/ml treated CCM (CCM_1), 10 mg/ml treated CCM (CCM_{10}), 100 mg/ml treated CCM (CCM_{100}) and, in order to show the efficiency of the assays used, 1 μM staurosporine (CCM_{ST}) which is a potent inhibitor of phospholipids/calcium-dependant protein kinase and causes cell death. LDH, AB and Pico green assays were carried out 24 and 96 hours post-exposure.

5.2.3.2 Direct effect of nanocomposite on HUVEC

Sections of graft material were cut into 16 mm diameter discs and autoclaved to sterilise them. The discs were then placed into a 24-well plate. Twelve graft discs were

seeded with 1 ml HUVEC at a concentration of 2×10^5 cells/ml for 24 hours (nanocomposite-seeded). Twelve wells containing discs of graft were left unseeded with only CCM in them as a control (nanocomposite-unseeded). LDH, Alamar Blue and Pico green assays were carried out 24 and 96 hours post-seeding and samples of graft sent for ScEM studies.

5.2.3.3 Assessment of cell proliferation on nanocomposite

Thin films of the nanocomposite were cast in 60 mm × 120 mm glass Petri dishes and sterilised by autoclaving. 2×10^5 HUVEC were then seeded in six dishes with a further six being left unseeded as a control. As a comparison, uncoated dishes were seeded with the same number of cells. At 1, 3, 6, 10, 13 and 16 days post-seeding a 4 hours Alamar Blue and Pico green assay were carried out on all samples.

5.2.4 Lactate dehydrogenase assay to assess cell damage on nanocomposite

LDH was measured using a CytoTox 96® non-radioactive cytotoxicty assay kit. The amount of LDH released was measured using a 30 minutes coupled enzymatic assay based on the conversion of a tetrazolium salt INT (2-*p*-iodophenyl-3-*p*-nitrophenyl-5-phenyl tetrazolium chloride) into a red formazin product, with the amount of colour formed being proportional to the number of lysed cells (refer to Chapter 3).

Fifty microlitre CCM from each sample was transferred to a 96-well plate. Fifty microlitre substrate mix (1 vial substrate plus 12 mls assay buffer) was added to each well and the plate covered in foil to prevent light access. Samples were then incubated at room temperature for 30 min after which the reaction was stopped by the addition of 50 µl stop solution (1 M acetic acid). Absorbance was then read at 450 nm using a Multiscan MS UV visible spectrophotometer.

5.2.5 Alamar blue™ assay to assess cell viability and metabolism on nanocomposite

Alamar blue™ as described earlier responds to chemical reduction resulting from cell metabolism by changing colour. The advantages of this assay are that it is soluble in media, stable in solution, minimally toxic to cells and produces changes that are easily monitored (444). Alamar blue™ was added to CCM at a concentration of 10% (v/v). At each AB assay time point grafts/wells were washed with 1 ml PBS and 1 ml of the AB/CCM mixture added to each graft/well. One millilitre AB/CCM mixture was placed into each of six empty wells as a negative control. After 4 hours, a 100 µl sample of the AB/CCM mixture was removed and the absorbance at 570 and 630 nm measured in a 96-well plate using a Multiscan MS UV visible spectrophotometer. The absorbance at 630 nm (background) was subtracted from that at 570 nm.

5.2.6 Pico green assay to assess cell quantity on nanocomposite

The Pico green assay quantifies double-stranded DNA in solution using an ultrasensitive fluorescent nucleic acid stain. Briefly, stock standard DNA solution (100 µg/ml) was diluted in TE assay buffer to provide a standard curve of 0–1000 ng/ml DNA. Cell samples were trypsinised as above and the cells disrupted by being passed through a small-bore needle three times. Hundred microlitre of standard/sample was added to a 96-well plate and 100 µl of diluted Pico green (Pico green dimethylsulfoxide stock solution diluted ×200 in TE assay buffer) was added to each standard/sample well. Plates were then incubated for 5 minutes in the dark. Standards/samples were then excited at 480 nm and the fluorescence emission intensity measured at 520 nm using a Fluroskan Ascent FL spectrofluorometer.

5.2.7 Assessment of cell morphology on nanocomposite

5.2.7.1 Toluidine blue staining

Cells were washed with PBS and then fixed in formaldehyde for 10 min at room temperature. Five hundred microlitre of a 0.1% solution of Toluidine blue (see Section

3.8.1) was then added to each well and incubated for 30 min at room temperature. Cells were then destained in water and photographed.

5.2.7.2 Scanning electron microscopy

Sections of unseeded nanocomposite and nanocomposite seeded with HUVEC were washed three times with PBS and prepared for ScEM. The specimens were then attached to aluminium stubs and an SC500 (EM Scope) sputter coater used to coat them with gold. The stubs were then examined and photographed using a Phillips 501 scanning electron microscope.

5.2.8 Data analysis and statistical methods

Data are presented in mean ± SD. Comparison between groups was made by one way ANOVA (Kruskal-Wallis) test with post-comparison using Bonferroni's Multiple Comparison test. *indicates $p < 0.05$ and *** that $p < 0.001$.

5.3 Results

5.3.1 Indirect effect of nanocomposite on HUVEC

5.3.1.1 Lactate dehydrogenase assay

After 24 hours indirect exposure there was no significant difference ($p > 0.05$) between the CCM_0 group and any of the nanocomposite-treated CCM groups. Cells treated with CCM_{ST} had a higher level of LDH activity compared to the CCM_0 group ($p < 0.001$) (Figure 5-1 a.).

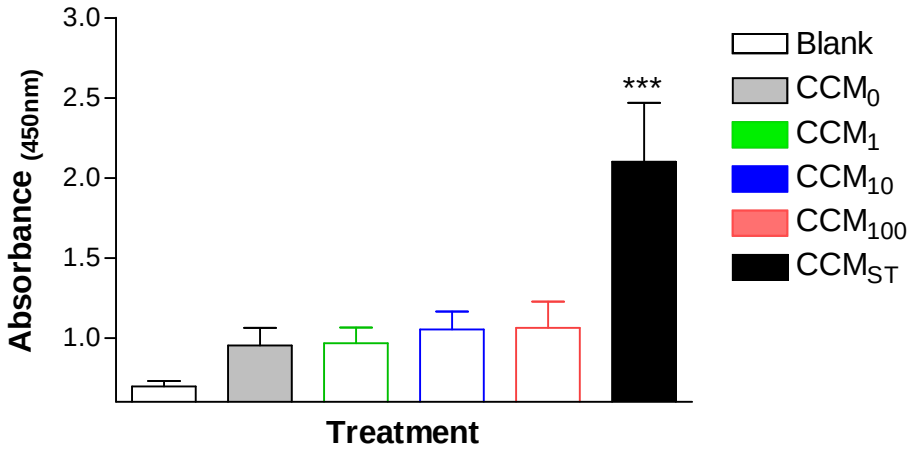

Figure 5-1 a. LDH assay test on HUVEC exposed to nanocomposite-treated CCM for 24 hours. Absorbance was measured in arbitrary units at 450 nm wavelength. Data are mean ± SD (n = 6).

5.3.1.2 Alamar blue™ assay

Indirect exposure to nanocomposite for 24 hours showed no significant difference between the CCM_0 group and the three nanocomposite-treated CCM groups. The cells treated with CCM_{ST} showed significantly less AB activity than the CCM_0 group ($p < 0.001$) (Figure 5-1 b.). In the case of the indirectly exposed 96 hours cells there was no significant difference in AB activity between the CCM_0 cells and the CCM_1 or CCM_{10} groups; however, there was a significant reduction in AB activity in the case of the CCM_{100} sample ($p < 0.05$). After 96 hours exposure to CCM_{ST} no viable cells were present (Figure 5-1 c.).

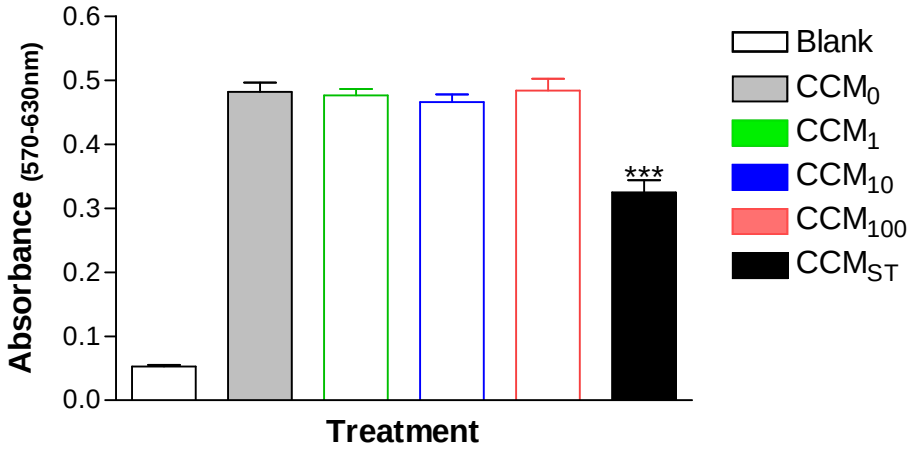

Figure 5-1 b. Alamar blue™ viability assay test on HUVEC exposed to nanocomposite-treated CCM for 24 hours. Absorbance was measured in arbitrary units at 570 nm wavelength and background at 630 nm subtracted. Data are mean ± SD (n = 6).

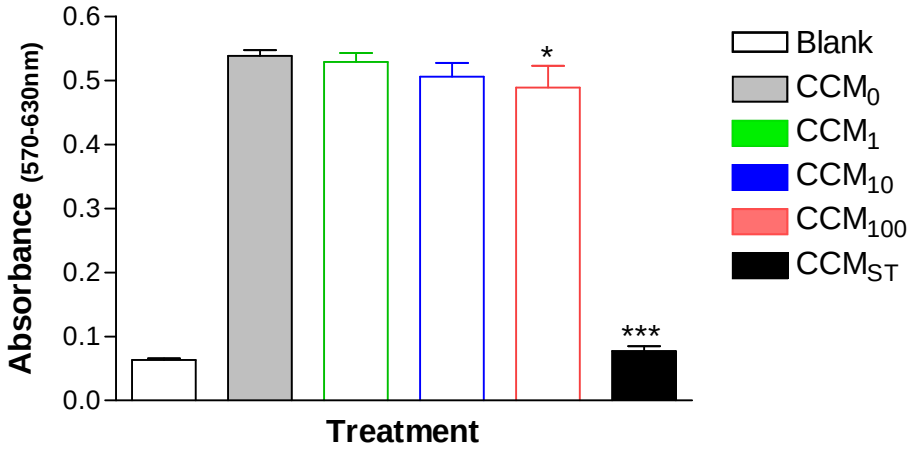

Figure 5-1 c. Alamar blue™ viability assay test on HUVEC exposed to nanocomposite-treated CCM for 96hours. Absorbance was measured in arbitrary units at 570 nm wavelength and background at 630 nm subtracted. Data are mean ± SD (n = 6).

5.3.1.3 Pico green assay

After 24 hours indirect exposure to nanocomposite-treated CCM between 780.1 ± 55.3 and 916.9 ± 38.0 µg/ml DNA was extracted, with no significant difference being observed between the CCM_0 cells and any of the test groups (Figure 5-1 d.). In the case of the 96 hours indirect exposure experiment again there was no significant difference

between the CCM_0 cells and the three different concentrations of nanocomposite-treated medium exposed cells. However, there was significantly less DNA in the staurosporine exposed group (Figure 5-1 e.).

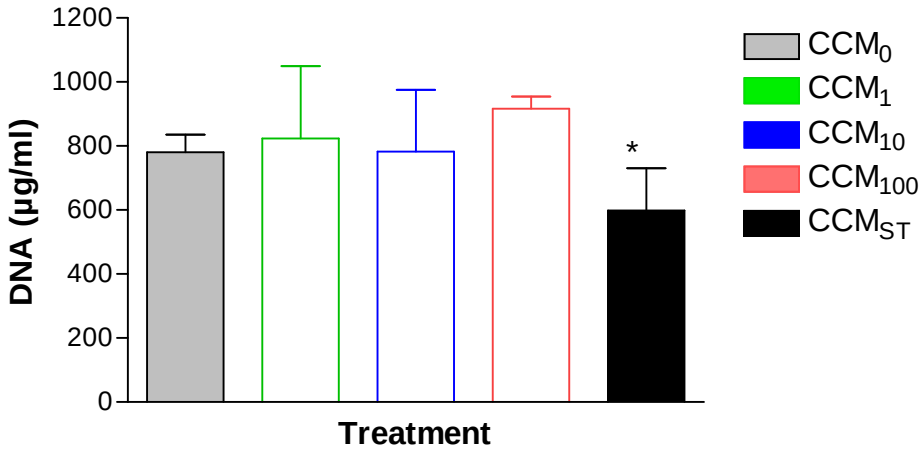

Figure 5-1 d. Pico Green assay test on HUVEC exposed to nanocomposite-treated CCM for 24 hours. Data is presented as DNA amount in µg/ml. Data are mean ± SD (n = 5).

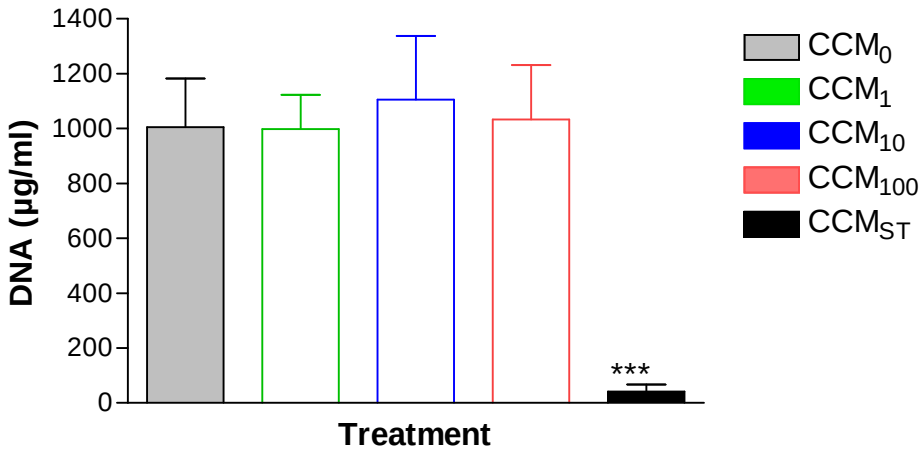

Figure 5-1 e. Pico Green assay test on HUVEC exposed to nanocomposite-treated CCM for 96 hours. Data is presented as DNA amount in µg/ml. Data are mean ± SD (n = 5).

5.3.1.4 Toluidine blue staining

The results from the Toluidine blue staining can be seen in Figure 5-2. It can be seen that at both 24 and 96 hours post-exposure to CCM_{100} cell appearance and

numbers are comparable to cells exposed to untreated CCM (Figure 5-2 a, b, d and e.). However, exposure to CCM_{ST} clearly results in cell damage at both time points (Figure 5-2 c and f.).

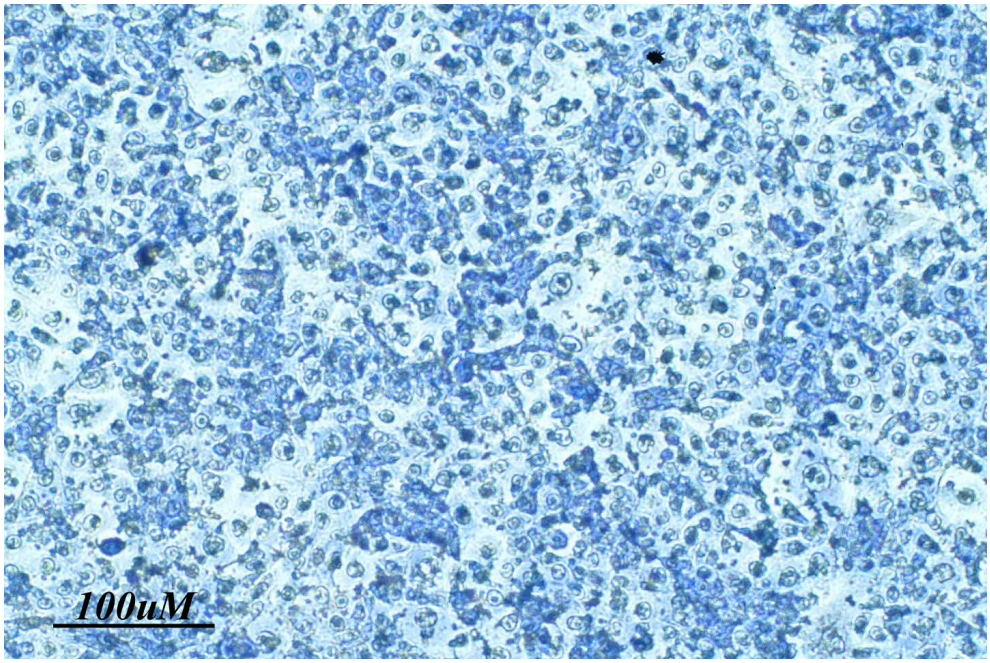

a) 24 hours CCM_0

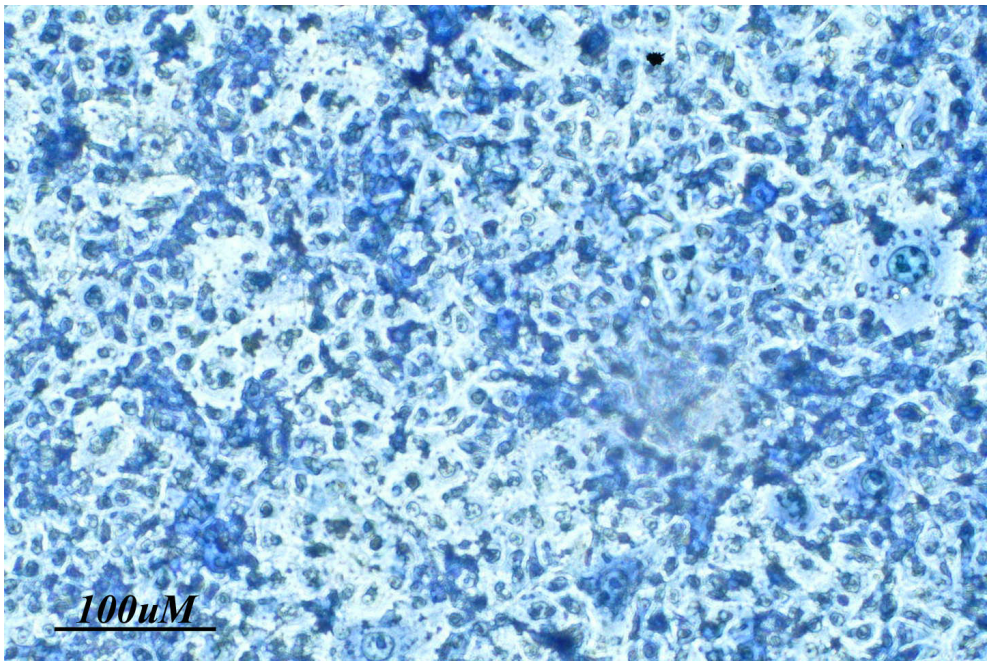

b) 24 hours CCM_{100}

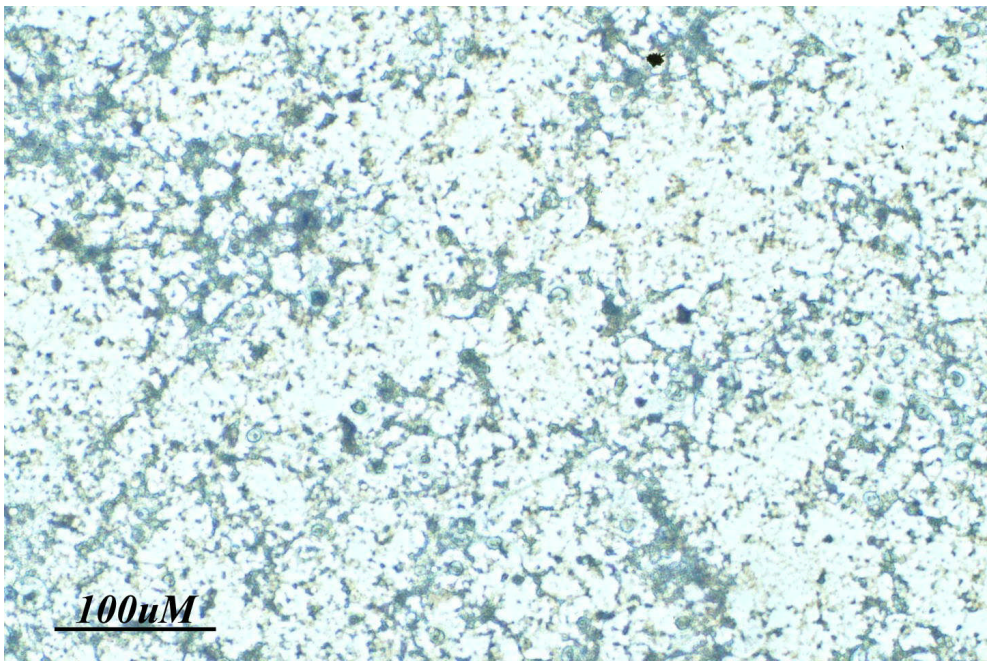

c) 24 hours CCM_{ST}

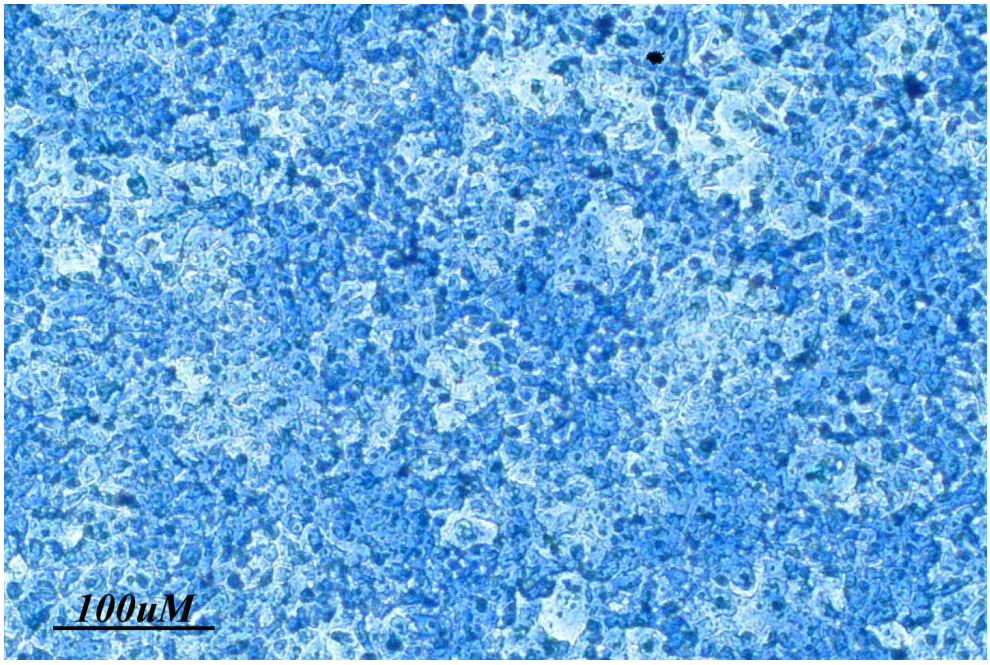

d) 96 hours CCM_0

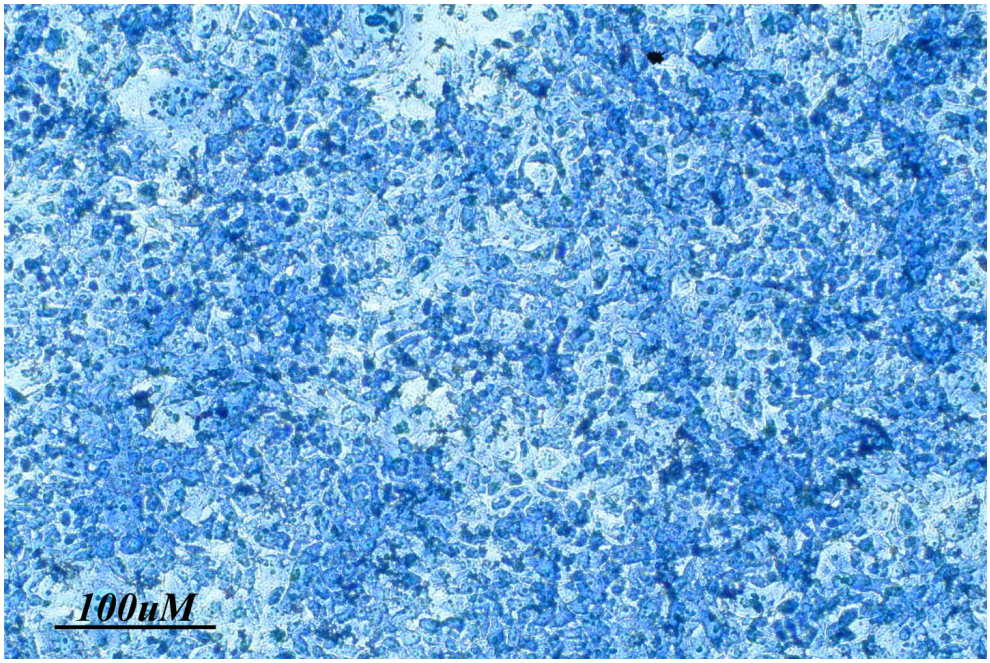

e) 96 hours CCM_{100}

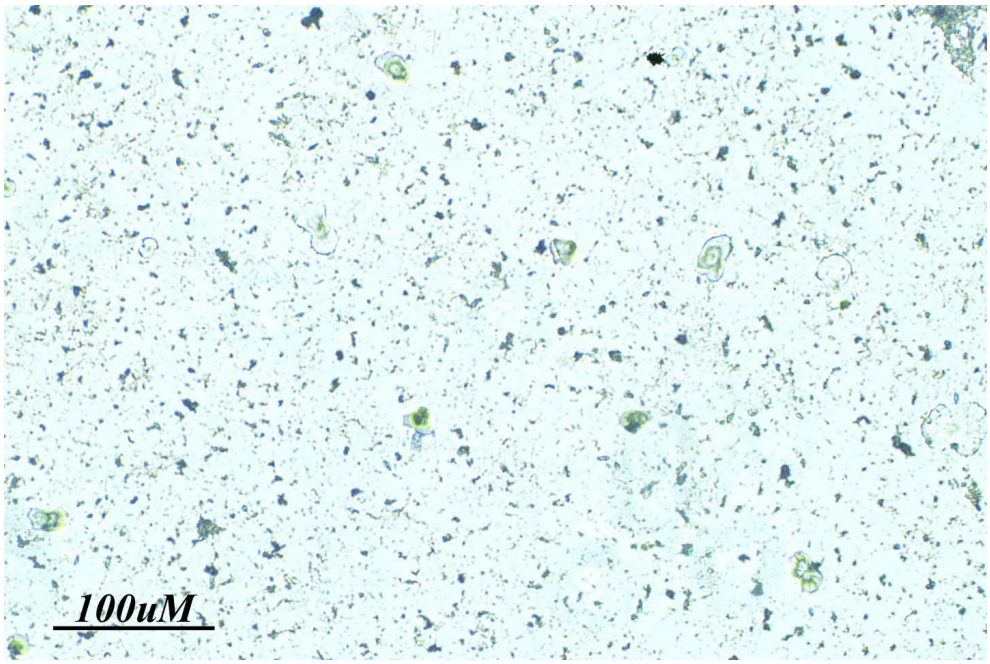

f) 96 hours CCM_{ST}

Figure 5-2. Toluidine blue staining of HUVEC exposed to nanocomposite-treated CCM for 24 hours (a, b and c). Toluidine blue staining of HUVEC exposed to nanocomposite-treated CCM for 96 hours (d, e and f).

5.3.2 Direct effect of nanocomposite on HUVEC

5.3.2.1 Lactate dehydrogenase assay

After 24 hours direct exposure a significantly higher level ($p < 0.001$) of LDH activity was found from the nanocomposite-seeded group compared to the CCM_0 group (Figure 5-3 a.).

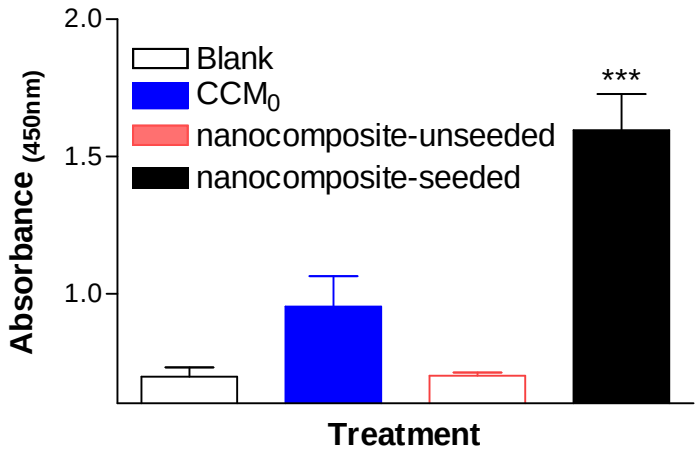

Figure 5-3 a. LDH assay test on HUVEC seeded directly onto nanocomposite for 24 hours. Absorbance was measured in arbitrary units at 450 nm wavelength. Data are mean ± SD (n = 6).

5.3.2.2 Alamar blue™ assay

Direct exposure to nanocomposite for 24 hours showed viable cells present, though at a lower level of Alamar Blue activity compared to the CCM_0 group ($p < 0.001$) (Figure 5-3 b.). After 96 hours direct exposure viable cells were still present on the nanocomposite-seeded, again at a lower level compared to the CCM_0 cells ($p < 0.001$) (Figure 5.3 c.).

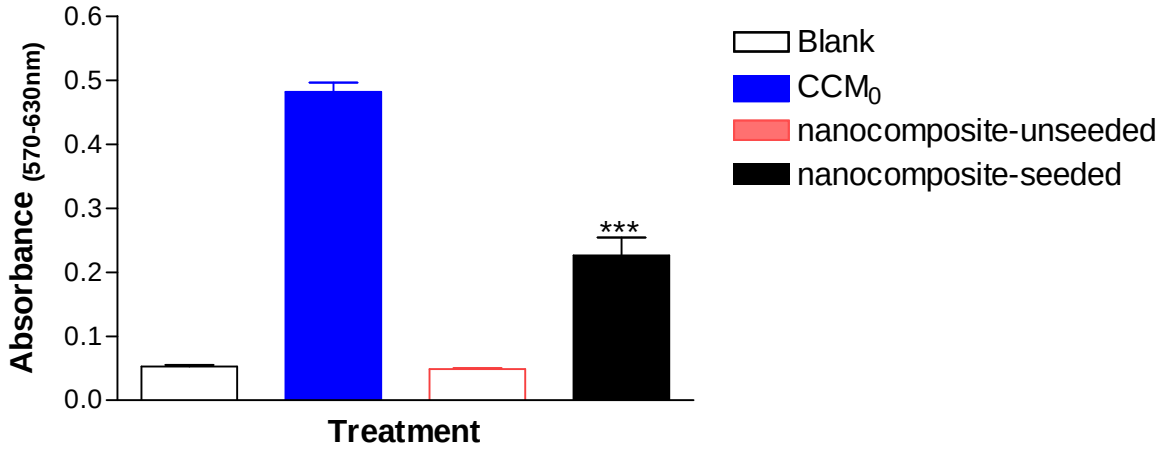

Figure 5-3 b. Alamar blue™ viability assay test on HUVEC seeded directly onto nanocomposite for 24 hours. Absorbance was measured in arbitrary units at 570 nm wavelength and background at 630 nm subtracted. Data are mean ± SD (n = 6).

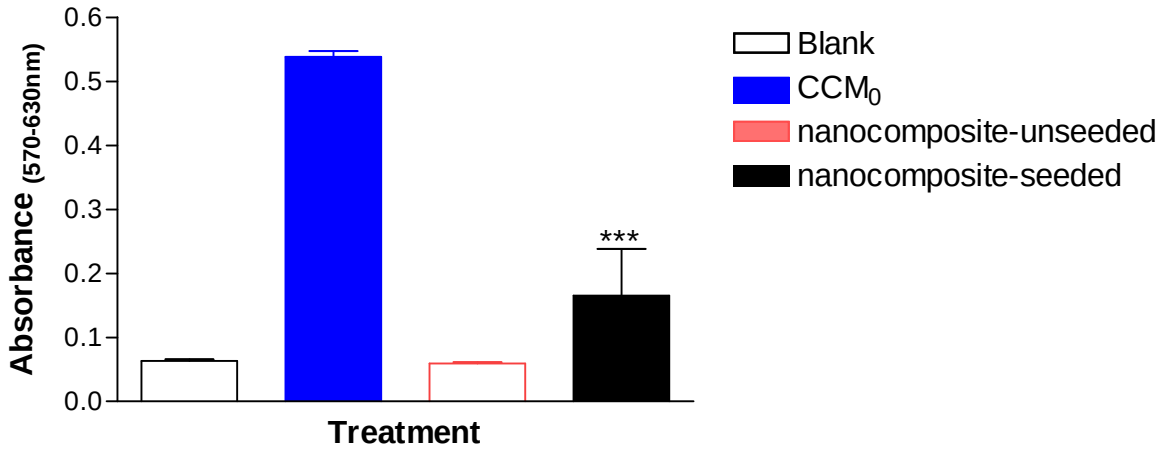

Figure 5-3 c. Alamar blue™ viability assay test on HUVEC seeded directly onto nanocomposite for 96 hours. Absorbance was measured in arbitrary units at 570 nm wavelength and background at 630 nm subtracted. Data are mean ± SD (n = 6).

5.3.2.3 Pico green assay

Direct exposure for 24 hours to nanocomposite resulted in the presence of 417.3 ± 50.4 μg/ml DNA. After 96 hours direct exposure 323.6 ± 232.9 μg/ml of DNA was extracted from the graft samples.

5.3.2.4 ScEM studies

ScEM studies showed that the surface of the nanocomposite graft material was uniform and demonstrated that EC were present on the graft material at both 24 and 96 hours post-seeding (Figure 5-4).

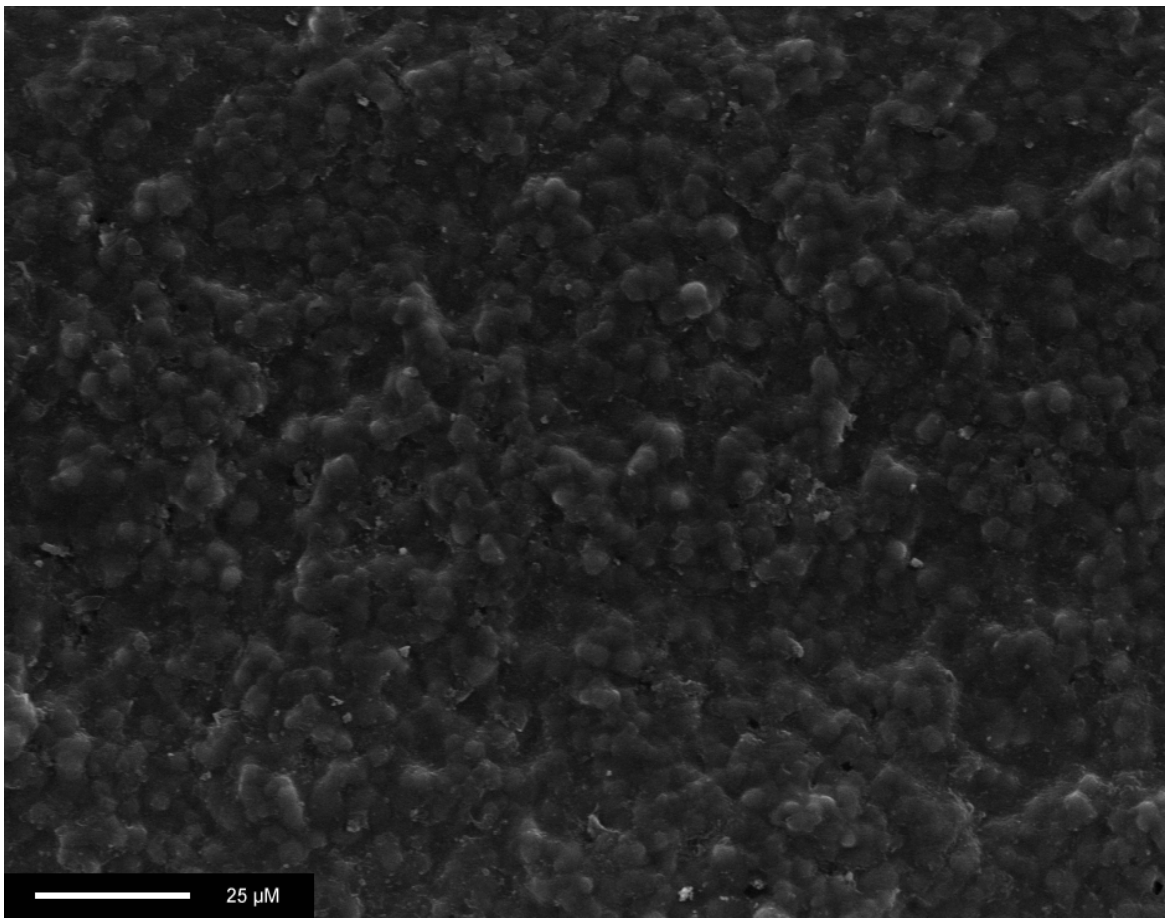

Unseeded Graft

Figure 5-4 a. ScEM of surface of nanocomposite graft (×640).

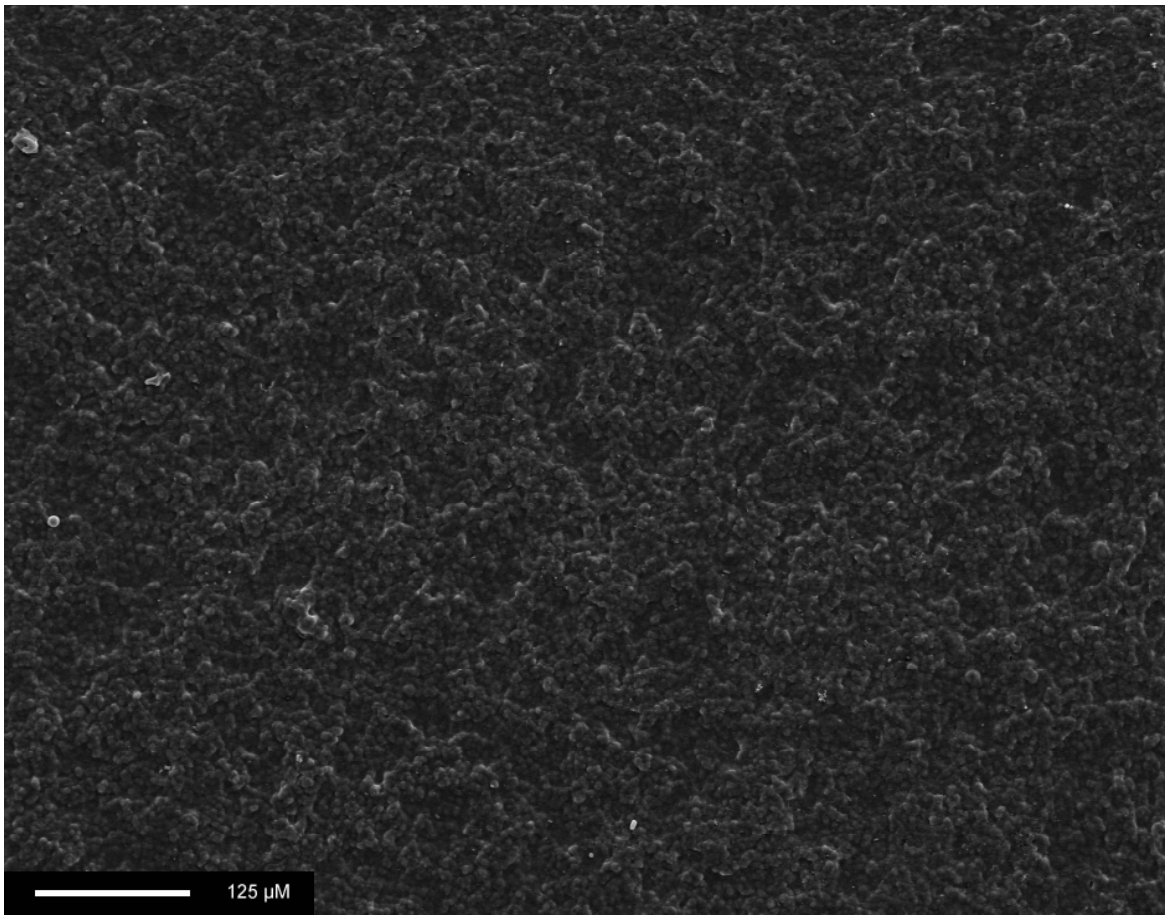

Unseeded Graft

Figure 5-4 b. ScEM of surface of nanocomposite graft (×160).

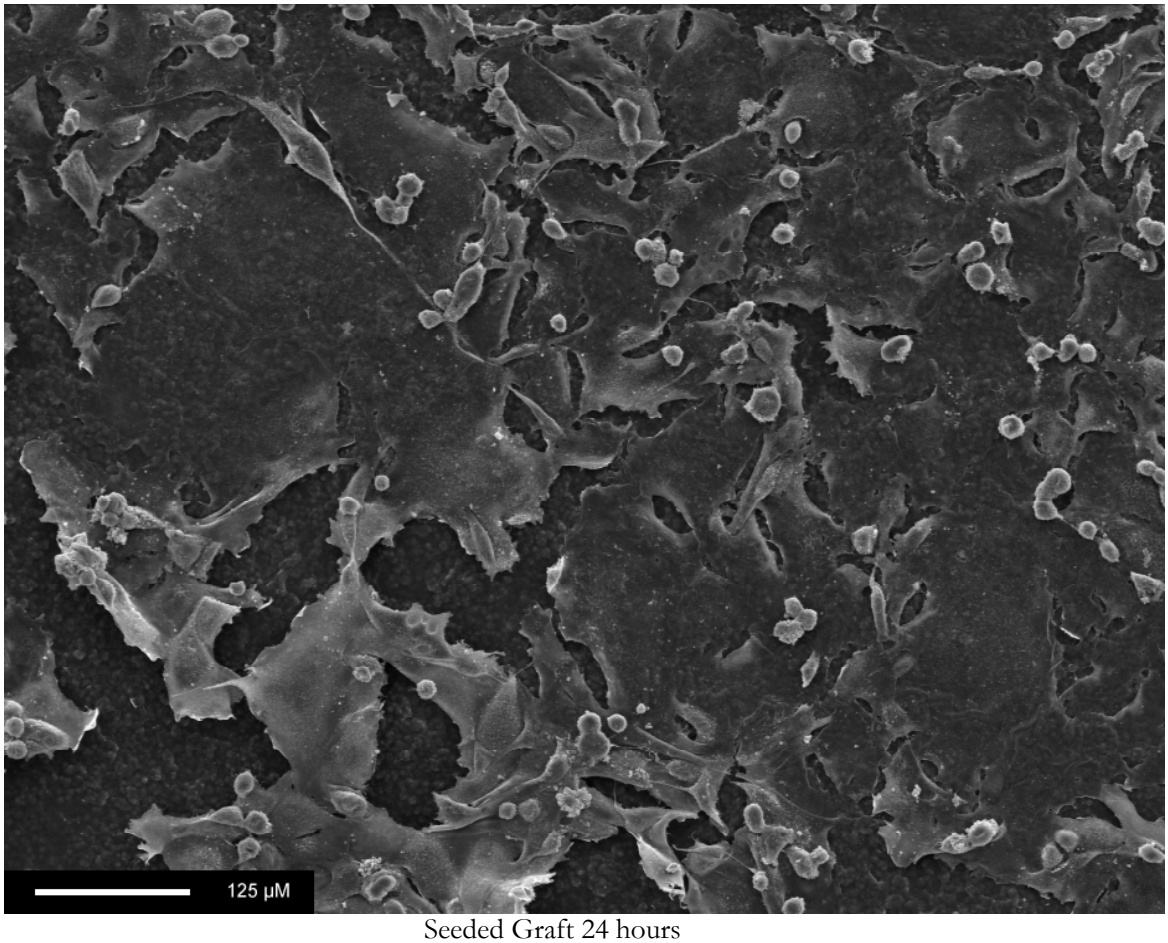

Seeded Graft 24 hours

Figure 5-4 c. ScEM of HUVEC seeded directly onto nanocomposite after 24 hours (×160).

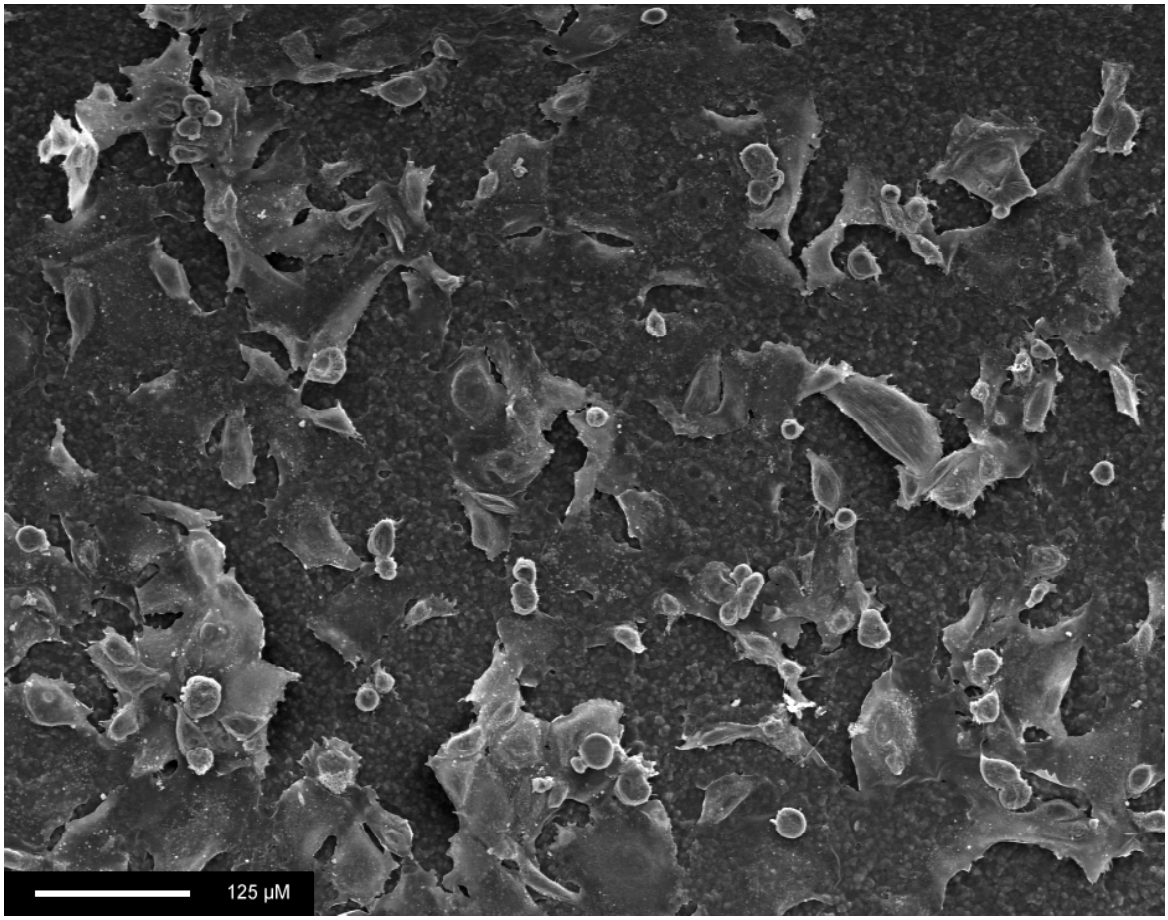

Seeded Graft 96 hours

Figure 5-4. **d.** ScEM of HUVEC seeded directly onto nanocomposite after 96 hours (×160).

5.3.3 Assessment of cell proliferation on nanocomposite

Figure 5-5 and 5-6 shows the results from the proliferation study. It can be seen that the HUVEC exhibit a typical growth curve on both nanocomposite and glass, with confluence being reached at day 10. Again the AB results are lower for the cells seeded on nanocomposite compared to those seeded on glass.

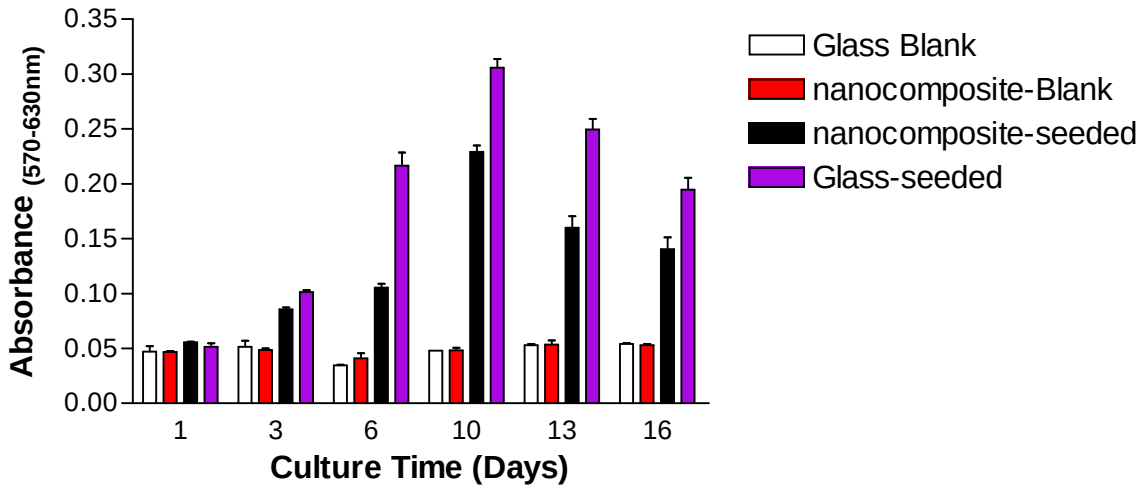

Figure 5-5 Alamar blue™ viability assay test on HUVEC seeded directly onto nanocomposite for 16 days. Absorbance was measured in arbitrary units at 570 nm wavelength and background at 630 nm subtracted. Data are mean ± SD (n = 6).

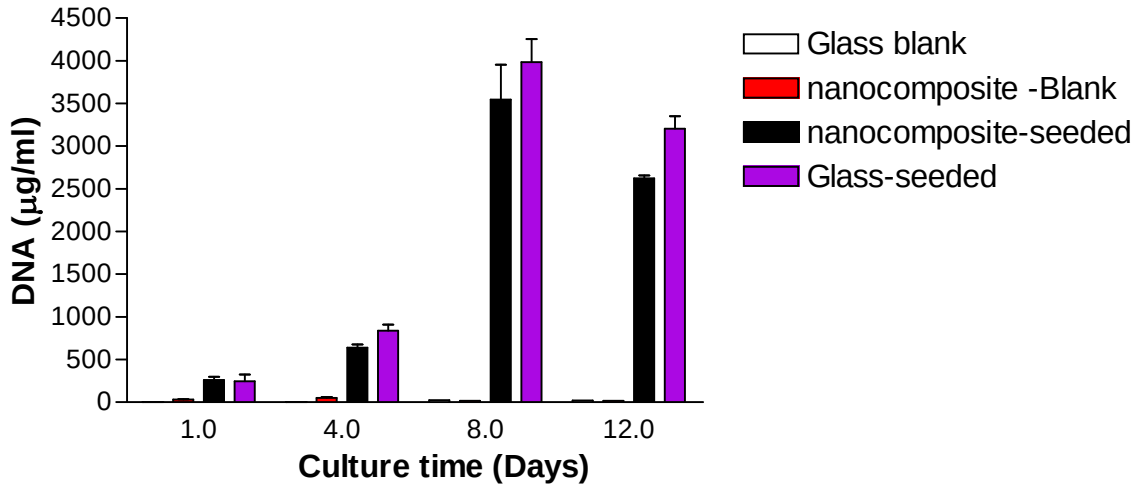

Figure 5-6. Pico Green assay on HUVEC seeded directly onto nanocomposite for 12 days. Data is presented as DNA amount in µg/ml (n = 6).

5.4 Discussion

The improvement and understanding of surface thrombogenicity has become an important field of research. In tissue engineering it has been found that silicon and its analogues, such as oxides, dramatically reduce protein adsorption and platelet adhesion (6). The mechanism has been hypothesised to be related to the surface charge (7);(8) causing structural changes to the blood proteins (9);(14) such as fibrinogen (59). Silicon itself is very un-reactive and therefore research has been focused on moieties such as siloxane, in particular PDMS especially when combined with polyurethanes, rubbers or on its own (190-192). PDMS on its own or with rubbers is mechanically very weak and therefore cannot be used in bio-medical devices. As a result various methodologies have been attempted in order to combine it with polyurethane. To date the results *in vivo* have been very poor due to dramatic losses in bio-stability caused by the non-reaction of PDMS with either the soft or hard segments resulting in two separate polymers (193;194). Until now silicon and siloxane-based materials possessed poor growth characteristics for human cells such as EC (209) making them unsuitable for tissue engineering.

It was therefore felt that a need still existed for a polyurethane containing silicon that is mechanically strong and so bio-stable, but in addition possesses the advantageous qualities of reduced protein and platelet adsorption and most importantly would still allow the growth of cells such as EC without causing related cytotoxic effects. The original hypothesis was that the synthesis of a polyurethane containing silsesquioxane would result in a class of inorganic-polymers (nanocomposite) that would possess all the desirable attributes described above (210).

In the clinical scenario the choice of a material to be used for CABG prostheses must incorporate cytocompatibility to EC in two areas; indirect and direct contact of EC with the material. In this study in the case of indirect contact an initial exposure for 24 hours to CCM treated with powdered nanocomposite produced no significant effect on either cell metabolism or cell numbers compared to the CCM_0 as shown by the results of the AB and PG assays. The use of Staurosporine as a positive control proves the principle that these assays are capable of demonstrating cell damage and further suggests that the toxicity of nanocomposite is low. A longer 96 hours exposure again produced no significant change in cell numbers though metabolism was reduced

significantly in the case of the CCM_{100} group. In contrast by 96 hours post-exposure the CCM_{ST} group showed no cell metabolism and extremely low cell numbers. This indicated that toxicity by nanocomposite on EC was not apparent other than mildly at CCM_{100}.

Twenty four hours of post-seeding, of EC onto nanocomposite showed the presence of viable EC from the PG results and ScEM analysis and that the cells were metabolising (as shown in Figure 5-4). Whilst both the cell numbers and metabolism were significantly less than for the CCM_0 cell group this may be due to improved seeding and attachment on TCP (which is optimal for cell attachment and growth) compared to nanocomposite and is similar to the results obtained in previous studies on ePTFE and compliant PCU (444). There was a significantly increased level of LDH activity compared to the CCM_0 cells suggesting that seeding efficiency on nanocomposite was lower than on TCP or glass or that initial cell damage had occurred. Extended 96 hours direct exposure showed similar results to the 24 hour period and again demonstrated the presence of viable cells on the material. The cell proliferation study showed that HUVEC can be maintained on nanocomposite for an extended period (16 days) and that the growth pattern is similar to that for HUVEC grown on a glass surface.

5.5 Conclusion

In conclusion it can be said that the results obtained in this study demonstrate that indirect exposure to nanocomposite does not result in serious damage to EC at concentrations likely to be encountered in a clinical situation. Furthermore, the nanocomposite can be successfully seeded with EC and indicates that, once seeded, the EC remain viable and proliferate for a period of days. This combined with its other advantages suggests that nanocomposite is suitable for further development in the development of a coronary bypass graft.

6

Fabrications of a small diameter compliant nanocomposite coronary artery bypass graft

6.1 Introduction

Advanced novel fabrication methods are needed to build three-dimensional scaffolds that incorporate multiple functionally graded biomaterials with a porous internal architecture that will enable the simultaneous growth of multiple tissues, tissue interfaces and blood vessels. Various methods have been utilised to manufacture porous grafts for vascular bypasses. These include electrospinning (475), electrospraying, dip-coating (476) and extrusion (477).

Electrospinning of polymer is an approach for the production of much smaller diameter fibers which are of interest for tissue engineering. While electrospinning has been known for some time and attempts have been made to produce vascular grafts by this technique, only recently has interest in electrospinning for polymer biomaterial processing been revived (475). In electrospinning highly viscous polymers are able to 'spin' into a flowing fibre from the 'Taylor Cone'. This cone is generated by an electric field applied to a metal capillary through which the polymer extrudes. The electrostatic repulsion effect due to the electric field allows the spun fibres to be whipped and thinned simultaneously to be collected on a surface (see Figure 6-1). The degree of thinning can thus be accurately controlled. If a low viscosity polymer is subjected to the

same electric field, a spray effect is generated as the electrostatic repulsion forces the droplets to disperse in an aerosol - this is known as electrospraying (476).
The basic elements of a laboratory electrospraying system are simply a high voltage supply, collector (ground) electrode/mold, source electrode, and a solution or melt to be sprayed or spun. The sample is confined in any material formed into a nozzle with various tip bore diameters (such as a disposable pipette tip) with a thin source electrode immersed in it. The collector can be a flat plate wire mesh or, in more sophisticated modifications, a rotating metal drum or mandrel on which the polymer is wound.

Dip-coating refers to the immersion of a scaffold into polymer solution in order to coat it. An additional process is required to solidify the result. This may be by casting (i.e. heating the polymer so that the solvent evaporates) or phase inversion by swapping the solvent for a non-solvent (477). Freehand dip-coating can cause great variability between grafts produced, and for adequate control, a mechanised dipping process is necessary. Kannan *et al* has produced microvessels from the nanocomposite using a semi-mechanised dip-coating followed by phase inversion (478). His work involved dipping needles via a mechanical arm into polymer solution, then allowing a capillary action to act and distribute thin coating of polymer uniformly before dropping into a coagulant. Using this technique gave good results in terms of wall uniformity and mechanical properties. One of the techniques assessed in this chapter used for manufacture of small diameter vascular grafts was essentially a modification of this method called extrusion-phase inversion.
The extrusion technique refers to the pressured drawing of a material (usually a polymer) through a template to form a three dimensional model with a cross section mirroring the template. This requires a highly viscous polymer which will hold its shape after drawing out. The pressure is usually provided by a screw system pump. The technique used here depends on a layer of polymer coating a mandrel as it passes through it, with shape being given by the exit aperture; this method is extrusion. However, the viscosity of the polymer is much lower than that used in typical extrusion. Therefore, phase inversion must be commenced immediately to prevent the polymer flowing off the mandrel. A vertical dip-coating coagulative extruder has been used to manufacture uniform walled porous 5 mm internal diameter conduits. The porosity imparts compliance which would ideally match that of a native artery.

The concept of phase inversion can be explained by consideration of the nanocomposite as a pure polymer with a variable amount of solvent in which it is dissolved. The higher the amount of solvent, the higher the viscosity (i.e. the more solid). Phase inversion relates to the controlled removal of solvent by swapping it for a non-solvent. Previous studies have proven that polyurethanes may be made porous by placing the polymer solution in a non-solvent solution such as water which leach into it and forms porous materials as a result of the release of DMAC from the polymer solution into the water. This technique depends upon the homogeneity, viscosity and concentration of the coating polymer as well as the type of mandrel used (479). When using this method, achieving a uniform coating on the mandrel depends upon consistent polymer flow patterns on the mandrel. Extruding these polymers solutions have proved successful in vessels of above 3 mm in internal diameter and dip-coating remains the primary method of fabricating smaller vessels (479).

The objective of this study was to determine the ideal method of fabricating small diameter nanocomposite vascular grafts with similar compliance characteristics to native arteries using phase inversion. The parameters assessed were method of polymer deposition namely electrospraying or extrusion. In this study basic compliance and burst pressure was measured in order to determine a suitable conduit for progression to *in vitro* shear stress work.

6.2 Materials and Methods

6.2.1 Nanocomposite synthesis

The synthesis of nanocomposite polymer solution has been described in Chapter 3.

6.2.2 Nanocomposite deposition onto mandrels and formation of porous nanocomposite vascular grafts

6.2.2.1 Electrospraying-phase inversion

Using a 10^{-5} m^3 syringe on an infusion system; Semat A99FMZ syringe pump (Semat International Ltd., St. Albans, Hertfordshire, UK) with a silicone rubber tube,

the polymer was made to flow at a rate (FR) of 1.338 x 10-9 m^3/s through a point needle (1070 μm diameter) held in an epoxy resin. The polymer solution was passed through an electric field of 6.2 kV to form a stable cone jet (Figure 6-1) with the ground electrode being placed at a distance of 10 mm from the needle tip. The electrical field was supplied by a high voltage supply (Glassman Europe Ltd., Tadley, Hampshire, U.K.) while illumination was provided by a LED and a signal generator. The polymer droplets were deposited onto cylindrical 5 mm diameter stainless steel rotated mandrels (Venflon BD systems, U.S.A) so as to form a thin film on its surface. The polymer/mandrel was set in deionised water at 0 °C for the phase inversion step.

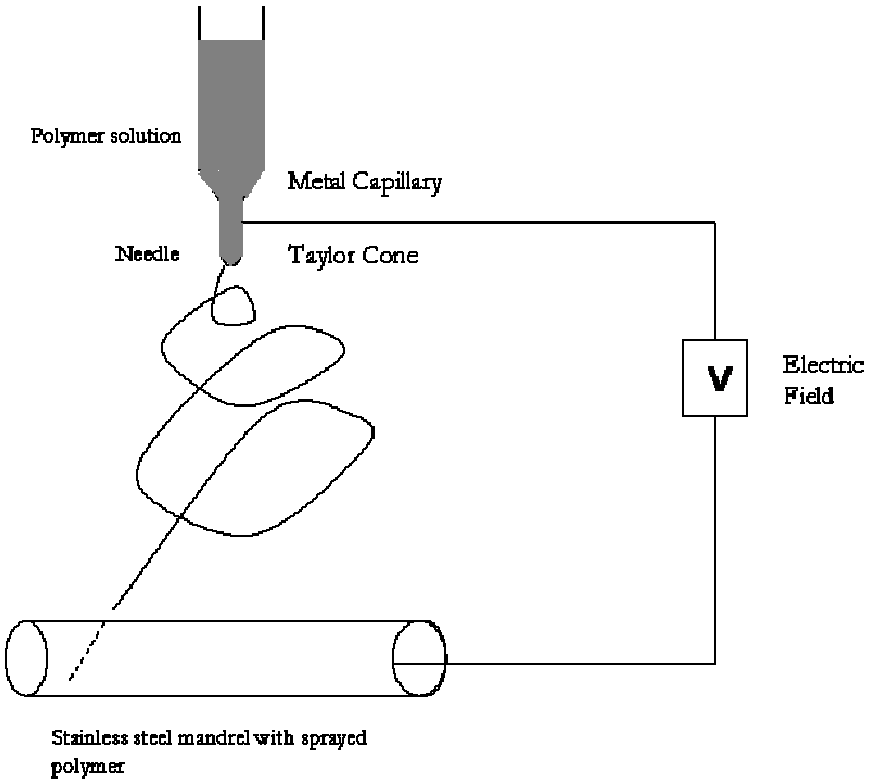

Figure 6-1. Using electrospinning as a method of producing a porous graft from a liquid polymer.

6.2.2.2 Extrusion-phase inversion

The extrusion device (referred to as an automated bio-processor) contains a mechanical arm, polymer chamber and coagulant reservoir (Figure 6-2). A mechanical arm capable of descending vertically downwards at 10 mm/sec was positioned such that it held a 5 mm diameter stainless steel cylindrical mandrel within the exit aperture of a polymer chamber (Figure 6-2 A). This latter structure, encased within a perpex block, was also made from stainless steel, comprising of a circular 5 mm entry aperture superiorly; a luer-lock syringe compatible polymer introduction channel laterally (Figure 6-2 B); a 6 mm circular exit aperture inferiorly which could be surplanted by other aperture adapter (Figure 6-2 C); and a PTFE sliding cover for the exit aperture (Figure 6-2 D and E). The Perspex block was held in a bracket such that the mandrel cross-section was aligned perfectly concentric with respect to the exit aperture.

With the mandrel's base centrally placed and level with the exit aperture, the PTFE sliding cover was closed before 3.0 ml of nanocomposite polymer solution was injected slowly into the polymer chamber. For the first step it was very important that the syringe contained no air bubbles. This was allowed to settle for 15 minutes to ensure that any small air bubbles that were present could rise to the nanocomposite surface.

A vertical column of coagulant solution was placed directly below the sliding cover leaving a 5 mm gap between the two. The coagulant solution was deionised water at 0 °C. This coagulation step has been investigated in our laboratory to be the condition for extruding porous nanocomposite conduits. The relative importance of porosity of grafts have been extensively explored with groups investigating pore sizes of 10 to 45 microns that is required for spontaneous endothelialisation (480).

The cover was opened and the mandrel driven downwards vertically into the coagulant at 10 mm/sec immediately afterwards (Figure 6-2 F). A pressure switch on the mechanical arm ensured it stopped descending when it reached the polymer chamber. The alignment was checked during this extrusion by visually comparing the layers of nanocomposite coating either side of the mandrel within the coagulant solution in the moments before coagulation occurred. This was undertaken in two planes perpendicular to each other about the longitudinal axis of the mandrel, and was facilitated by viewing against a natural light background.

The column was undisturbed for 20 minutes after which time the mandrel was disconnected from the mechanical arm and placed in coagulant solution and left at 5 ^{0}C for a minimum of 12 hours. Thereafter, the mandrel was removed from the coagulant and dried with paper towels, before transferring to an absolute ethanol bath for degassing over 10 minutes, thereby facilitating removal of the formed tube from the mandrel. This latter step was carried out by gently loosening the conduit from the rod along its whole length with small circular and longitudinal stresses after which the whole tube easily slid off without excessive strain. Each extruded tubes was produced with an overall length of 18 cm.

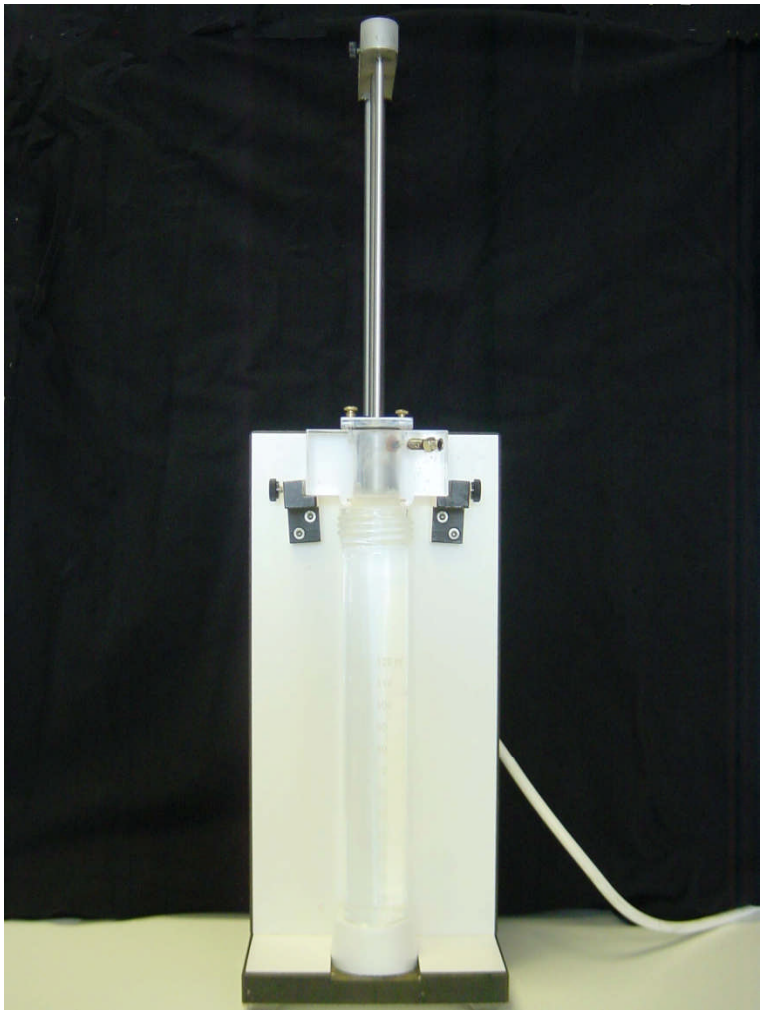

A

Figure 6-2. An automated bio-processor used to extrude polymer into conduits. A) The device consists of a mechanical arm that travels vertically at 10 mm/s, polymer chamber and coagulant reservoir containing 0 °C deionised water.

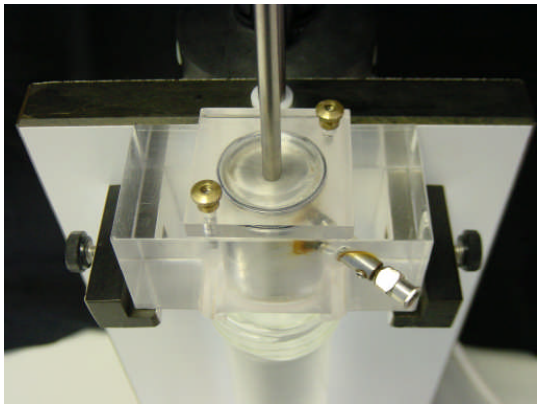

B

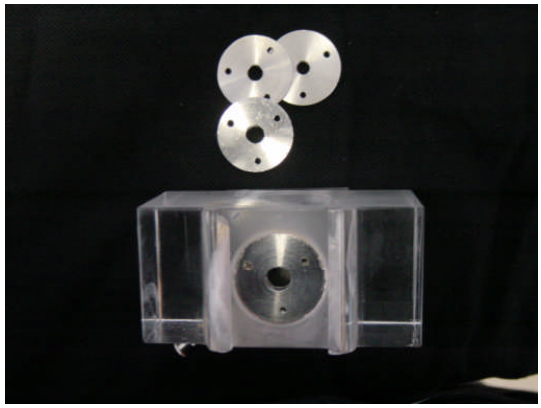

C

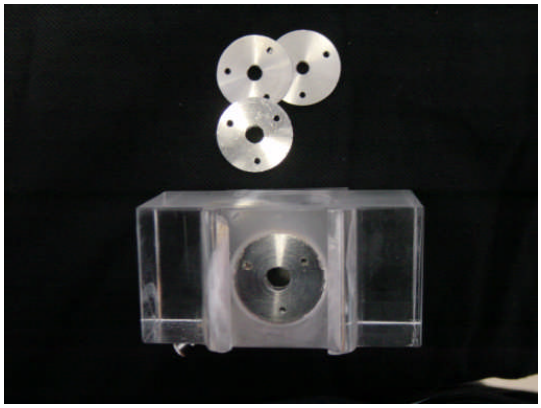

D

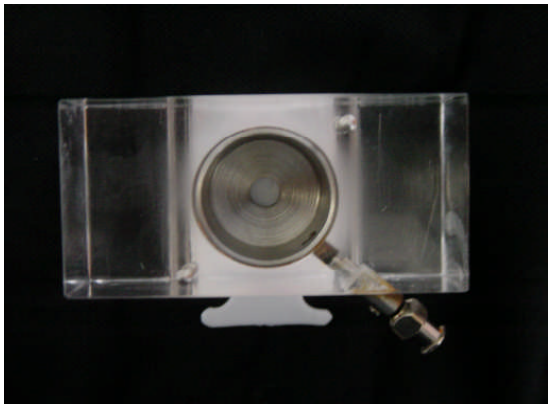

E

Figure 6-2. B) Shows polymer chamber with mandrel entering superiorly and polymer introduction channel laterally, C) Under surface of polymer chamber showing adaptors enabling control of exit aperture size, D) Exit aperture cover closed and E) Exit aperture cover open.

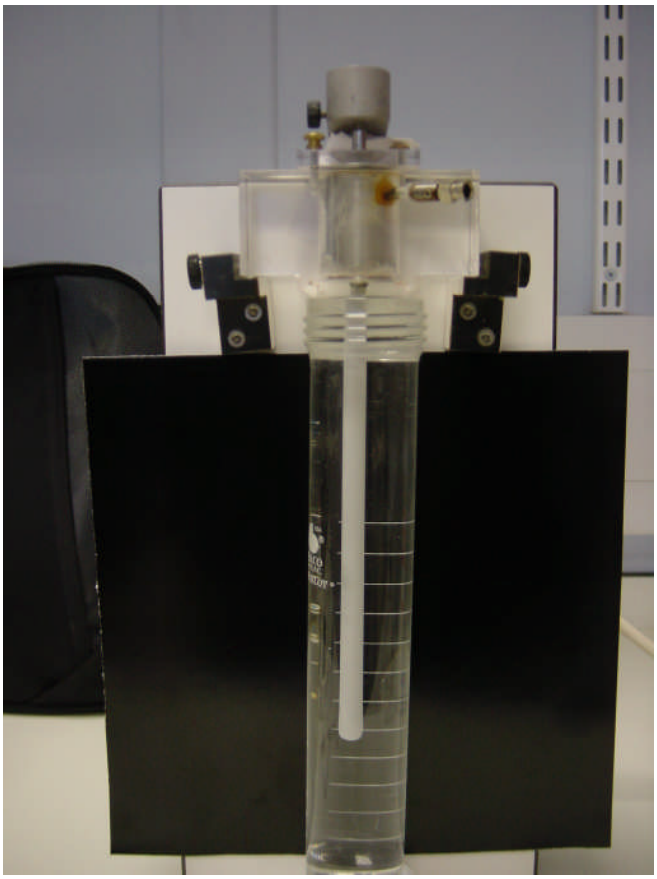

E

Figure 6-2. E) Extrusion performed by driving mandrel through polymer chamber and then into coagulant.

6.2.3 Reproducibility of conduit

Six conduits were fabricated with no selection of 'best specimen'. The image analysis software was used to measure the uniformity of wall thickness at 72 points distributed equally around the circumference, so assessing the reproducibility of the electrospraying and extrusion process.

6.2.4 Compliance

Fifty millimetre lengths were taken from the midsection of the extruded and electrosprayed tubes, so as to harvest the most uniform part, leaving the bulbous ends. The grafts remained in deionised water, rather than dry storage to ensure no shrinkage or changes to the mechanical properties due to graft dehydration. Intraluminal pressures were measured in mmHg. The segments of the conduits were then longitudinally stretched by 10 %, so as to mimic conformational changes expected within an *in vivo* system, before being connected to the flow circuit using commercially available 21G intravenous cannulae (Venflon BD Ltd, UK) and placed in a water bath. The flow circuit was then filled with clinical-grade native citrated blood (0.40 haematocrit) at 37 ºC maintained using a heat exchanger (Portex, Hythe, UK) taking care to evacuate any air within the system which could cause damping. On initiating pulsatile flow at a frequency of 1 Hz, physiological mean pressures of 30 to 70 mmHg were achieved whilst maintaining the pulse pressure at 39.633 (± 3.952) mmHg throughout the tests. Both anterior and posterior vessel wall motion with each pulse was assessed using a 7.5 MHz linear array Duplex probe and an echo-locked wall tracking system (Walltrack; Pie Medical Systems). The data was then interpreted using analogue-to-digital data acquisition recording system (ADC/Maclab; AD Instruments, Hastings, UK).

As the control, freshly harvested human iliac arteries and femoral vein from cadaveric rats were used in comparison to these nanocomposite conduits. These grafts were obtained in accordance with human and animal research guidelines. Also as a comparison the compliance of ePTFE was measured. All experiments were repeated 6 times for each pressure range using different sets of vessels (n = 6). Unlike previous experiments with the PCU vascular grafts (57;481), there was no need to pre-clot these nanocomposite conduits as there was no significant leakage of blood through their walls. This may be explained by the microporous nature of the conduits walls.

6.2.5 Burst strength

To measure burst pressure of the conduits high pressure syringe pump (Harvard Apparatus PHD 2000 Programmable) containing freshly deionised water (pH 7.0) was connected via a transducer (Honeywell Component No. 22PCCFB6G) to unused fifty millimetre lengths of conduits fabricated in the same manner as those used for compliance study (Figure 6-3). This was vertically suspended with distal clamping and weighted to ensure 10 % longitudinal stretch. The transducer was precalibrated by connecting it to a standard clinical sphygmomanometer and a voltmeter to record voltage readings at 0 mmHg, 100 mmHg and 200 mmHg from which offset and gain Figures were calculated and entered into a personal computer with bespoke software for recording the pressure at a sample rate of 10 Hz.

The transducer was connected via a 10 v power source to the personal computer. Water was expelled from the pump with the graft unclamped to allow the apparatus to be filled completely, whilst ensuring all air was eliminated from the apparatus. The clamp and weight was applied and an initial infusion rate of 0.2 ml/min was commenced, and this was gradually increased to take account of the percolation of water through the wall at high pressure and ensure an increasing intraluminal pressure. The infusion was continued until the graft material burst, and the burst pressure recorded. Six graft conduits were subjected to assess burst pressure.

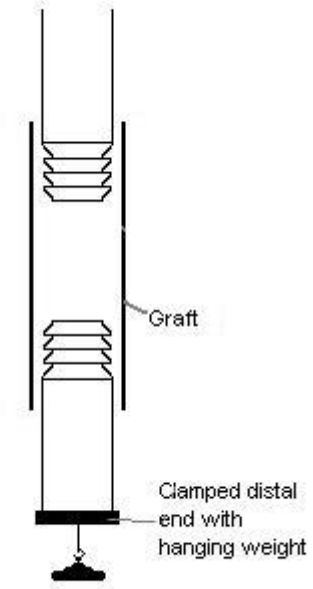

Figure 6-3. High pressure syringe pump used to measure burst pressure.

6.2.6 Scanning electron microscopy

The fabricated conduits were assessed by ScEM to visualise the detail of the wall cross section and pores.

6.3 Results

6.3.1 Electrospraying-phase inversion

6.3.1.1 Assessment of reproducibility of electrosprayed conduits

Table 6-1 shows the measurements of wall thickness of the six independent conduits fabricated using the electrospraying-phase inversion technique. The wall thickness of each conduit measured was found to widely vary where the lowest mean pressure was 0.002 mm and the highest being 0.31 mm. A high variation in mean wall thickness can be seen in Figure 6-4.

Table 6-1. Measurement of wall thickness in mm from conduits fabricated by electrospraying-phase inversion. The image analysis software was used to measure the uniformity of wall thickness at 72 points distributed equally around the circumference, so assessing the reproducibility of the cylindrical graft conduits.

Graft	Mean wall thickness (mm)	Minimum (mm)	Maximum (mm)	Standard Deviation
1	0.23	0.11	0.45	0.0574
2	0.05	0.006	0.35	0.0141
3	0.11	0.02	0.29	0.0054
4	0.31	0.22	0.63	0.0214
5	0.008	0.001	0.20	0.0132
6	0.002	0.0009	0.007	0.0356

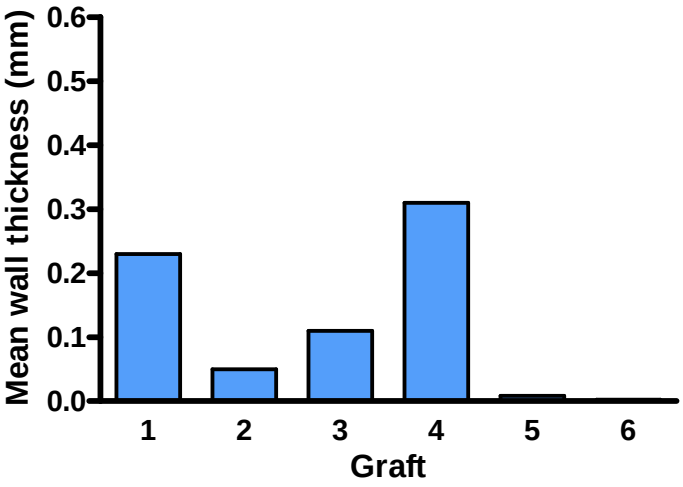

Figure 6-4. Mean wall thickness in mm of six independent fabrications of cylindrical graft conduits using electrospraying-phase inversion.

6.3.1.2 Measurement of compliance

The compliance of conduits produced by electrospraying was unsuccessful. This is because all the grafts placed in the flow circuit were found to burst when pulsatile flow was applied. As a control, the compliance of artery, vein and ePTFE can be found in Figure 6-8. This demonstrates that compliance measurements were carried out successfully even though no data were obtained for electrosprayed conduits.

6.3.1.3 Measurement of burst pressure

Conduits that were produced by electrospraying-phase inversion burst within the initial flow rate were applied at an infusion rate of 0.2 ml/min. The conduit measured with a mean wall thickness of 0.31 mm (see Table 6-1, graft 4) was the only conduit found to burst at 100 mmHg.

6.3.1.4 Scanning electron microscopic observations of electrosprayed grafts

Figure 6-5 shows ScEM of a typical conduit that has been fabricated using the electrospraying-phase inversion technique. As can be seen, although there is a uniform layer of polymer around the conduit, the nanocomposite conduit seems to be relatively

weak, indicating its pore activity when physiological flow was applied. There are also large gaps within the conduit, making them leak.

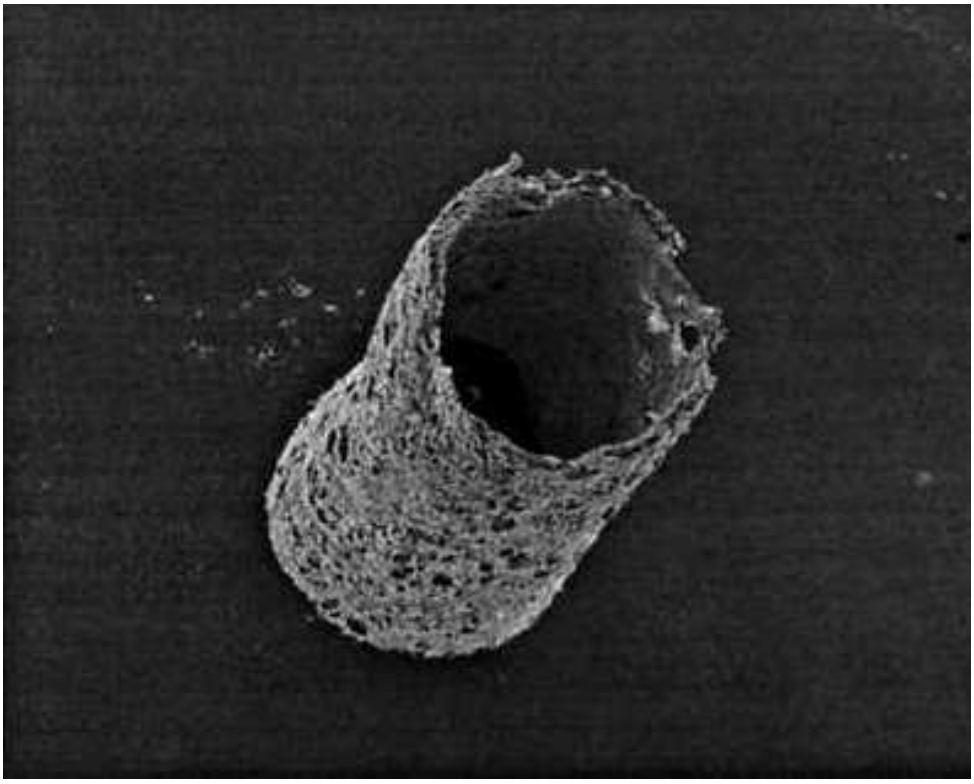

Figure 6-5. ScEM of the electrosprayed conduit on 5 mm internal diameter mandrels. The sprayed conduit was then immersed into a coagulant solution to form a porous graft.

6.3.2 Extrusion-phase inversion

6.3.2.1 Assessment of reproducibility of extruded conduits

Figure 6-6 shows the nanocomposite polymer extruded using the automated bio-processor (as shown in Figure 6-2) with phase inversion into small diameter nanocomposite conduit. The wall thickness for conduits produced by extrusion-phase inversion is shown in Table 6-2. The mean wall thickness was obtained by measuring the wall thickness over 72 points around the circumference of the graft. The mean lowest wall thickness was 0.47 mm and the highest was 0.56 mm. In Figure 6-7 the

mean wall thickness is plotted *vs.* graft. The average mean wall thickness of the six extruded grafts was 0.507 mm.

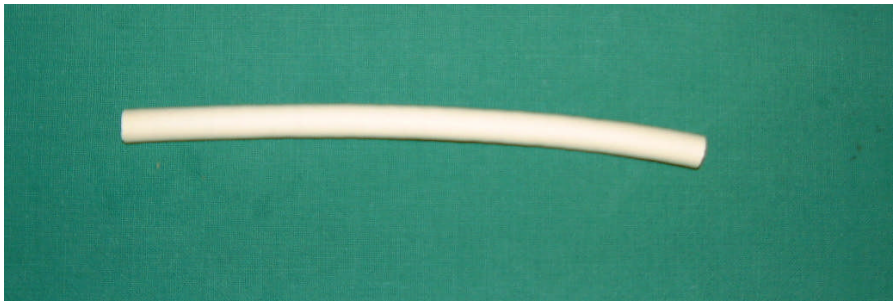

Figure 6-6. Photograph of five millimeter internal diameter nanocomposite conduit using extrusion-phase inversion.

Table 6-2. Wall thickness measurements for each extruded conduit based on image analysis software at 72 points distributed equally around the circumference, so assessing the reproducibility of the cylindrical graft conduits.

Graft	Mean wall thickness (mm)	Minimum (mm)	Maximum (mm)	Standard Deviation
1	0.47	0.37	0.65	0.06541
2	0.56	0.39	0.77	0.03212
3	0.50	0.44	0.61	0.01323
4	0.51	0.32	0.71	0.12154
5	0.48	0.43	0.66	0.12145
6	0.52	0.44	0.68	0.01436

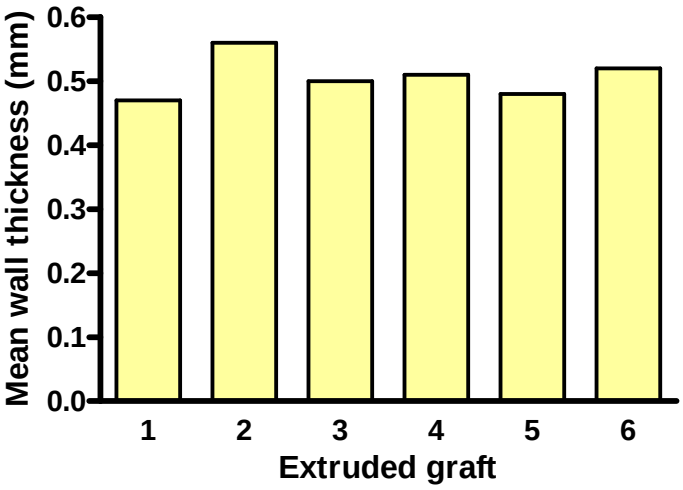

Figure 6-7. Mean wall thickness in mm of six independent fabrications of cylindrical graft conduits using extrusion-phase inversion.

6.3.2.2 Measurement of compliance

The compliance as well as the pressure ranges over which they are determined is shown in Figure 6-8 for nanocomposite conduits, artery, vein and ePTFE grafts.

The compliance of human external iliac artery was found to range from 30 %/mmHg x 10^{-2} at a mean pressure of 40 mmHg to less than 5 %/mmHg x 10^{-2} at 120 mmHg mean pressure. The compliance of ePTFE was found to be in the region of 1 %/mmHg x 10^{-2}. A compliance of 7 – 10 %/mmHg x 10^{-2} was measured for the nanocomposite graft.

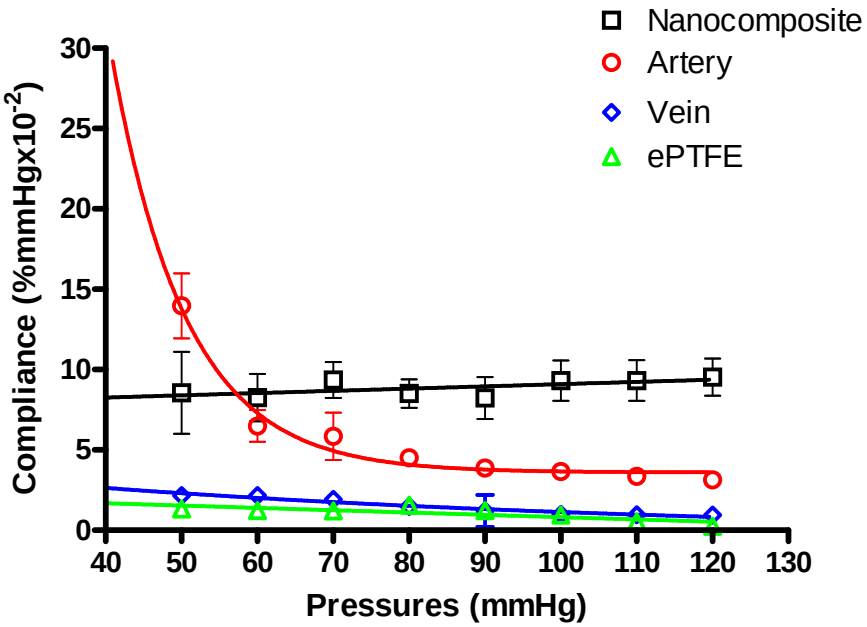

Figure 6-8. Measure of compliance *vs.* mean pressure for different conduits. The compliance characteristics on human external iliac artery, femoral vein, ePTFE and extruded nanocomposite conduits. The pulse pressure was 60 mmHg. Nanocomposite conduit is compliant unlike ePTFE.

6.3.2.3 Measurement of burst pressure

The burst pressure of extruded conduits can be found in Table 6-3. The lowest burst pressure was shown to be 420 mmHg and the highest at 475 mmHg. The average burst pressure of the nanocomposite conduits was 450 mmHg.

Table 6.3. Shows the burst pressures in mmHg for nanocomposite conduits fabricated by extrusion-phase inversion.

Tube	Burst pressure mmHg
1	450
2	475
3	460
4	445
5	420
6	450

6.3.2.4 Scanning electron microscopic observations of extruded grafts

Figure 6-9 shows ScEMs of extruded-phase inversion nanocomposite conduits. The conduits extruded demonstrated uniformity as well as a microporous structure ideal for seeding.

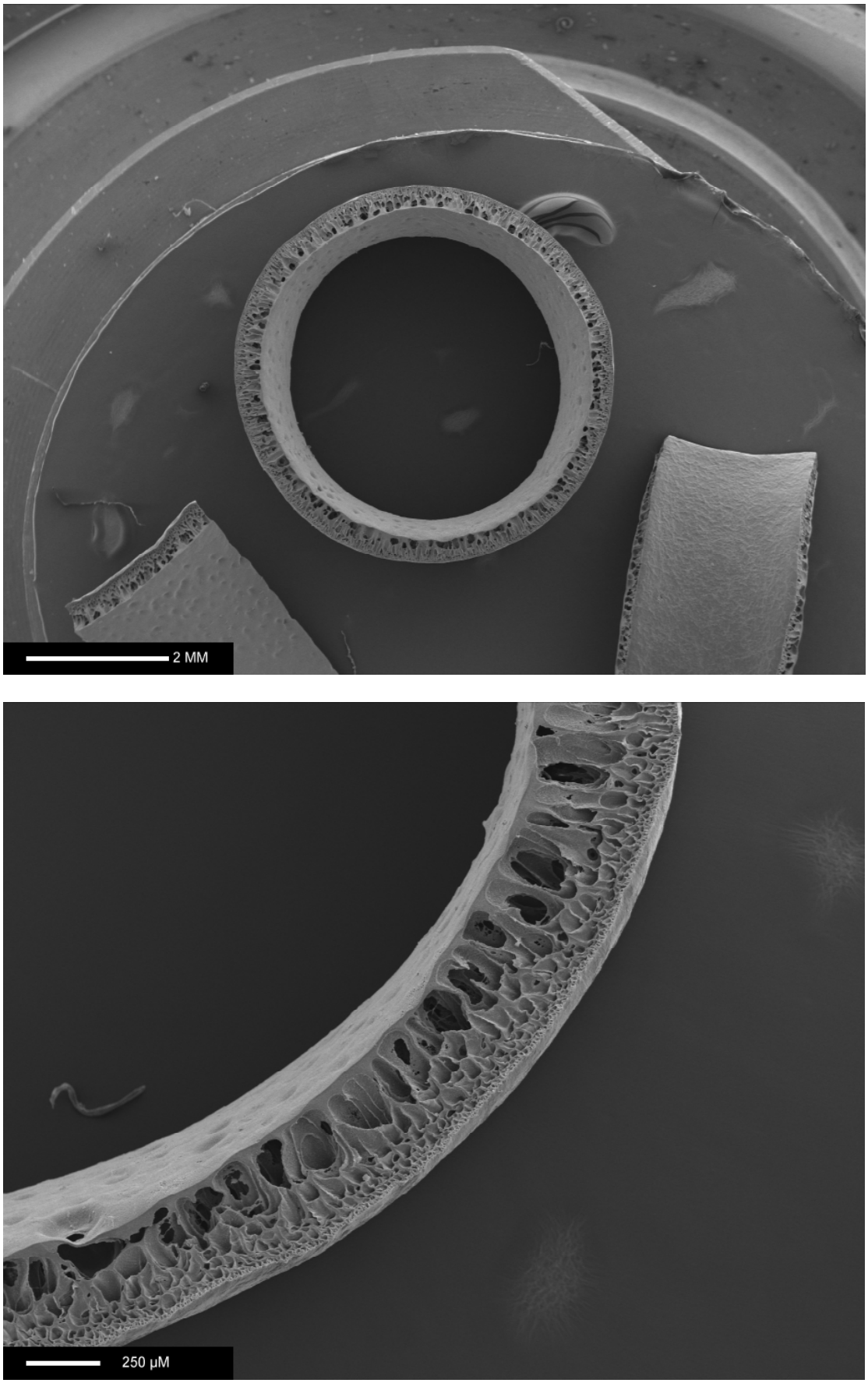

Figure 6-9. ScEM images of conduits produced using the extrusion-phase inversion technique where a) internal view and b) microporous layers.

6.4 Discussion

The objective of this chapter was aimed at developing compliant small diameter conduits for use as a coronary bypass grafts with similar compliance characteristics to native small diameter arteries using the techniques, electrospraying and extrusion (based on the dip coating method), both with the phase inversion step.

Electrospraying has been represented previously as an attractive means to achieving small diameter conduits (476). In electrospraying charged droplets are generated at the tip of a metal needle with a several kV dc field, and are subsequently delivered to a grounded target. The droplets are derived by charging a liquid to 5-20 kV, which leads to charge injection into the liquid from the electrode. Attempts at electrospraying the nanocomposite onto mandrels as a technique proved futile as polymer deposition was uneven. After phase-inversion the conduit was relatively weak. The conduits showed to burst when initial pressure was applied. When tested for compliance all the conduits failed within the initial application of physiological flow. In this study, it was proved that the electrospinning application did not produce compliant conduits with sufficient strength for future flow studies.

The drawback with freehand dip coating is that it can cause great variability between grafts produced, and for adequate quality control, a method based on the mechanised dipping process was assessed. This technique of extrusion combined with phase inversion is not novel-it is used to manufacture of the Chronoflex graft which is commercially available as a vascular access graft, utilising the patented method of Charlesworth (482). However, this is a horizontal extruding system that requires a constant rotational torque during phase inversion to ensure evenness of the graft walls. The idea of using a vertical extruding system relying on gravity for a uniform graft wall thickness, lead to the development of a novel bench-top extruding device. The extrusion technique used in this thesis was devised by a fellow Ph.D. student, Dr. Sandip Sarkar in order to achieve tubular conduits with sufficient integrity for subsequent *in vitro* research.

The compliance and burst pressure was measured for each fabricated conduit in order to determine a suitable model. The compliance for an artery is used to describe its

distention in response to applied pressure. Compliance is expressed in % per mmHg x 10^{-2}. A vessel's compliance is a measure of how easily it dilates in response to internal pressure increases (483). Physiological flow in a healthy human achieves a typical mean pressure of 80 to 100 mmHg with a pulsatile pressure of 40 mmHg, suggesting that matching arterial compliance would require a value nearer 3-5 % mmHg x 10-2. In human femoral arteries a compliance value of 5.3 %/mmHg x 10^{-2} has been reported (484). Another documented value for arterial compliance is 8.1 ± 5.9 %/mmHg x 10^{-2} over the pressure range 30 to 100 mmHg, but the position of the artery is not documented (481). The compliance of the human vein is shown as 4.4 ± 0.8 %/mmHg x 10-2 in the SV over an unknown pressure range (484) and 5.0 ± 6.7 %/mmHg x 10-2 over passage range 30 to 100 mmHg at an unknown position (481). As veins consist of the same material as arteries they will undergo a similar response. Veins however consist of different proportions of the material (more collagen, less elastin) because they have to operate at different pressures *in vivo*. The collagens properties will be recruited at much lower pressures.

Compliance test was measured by an *in vitro* flow circuit to show the strength, endurance and viscoelasticity of the conduits. In addition, it also demonstrates the reproducibility of graft performance between the various conduits, thereby serving a quality control function. Although the compliance of nanocomposite conduits fabricated by electrospraying was unsuccessful, those that were fabricated by extrusion showed superb results. The compliance of extruded nanocomposite conduit was measured at 7 – 10 %/mmHg x 10^{-2}. As the compliance of the iliac artery measured was 5 %/mmHg x 10^{-2} at 120 mmHg, this suggests that the extrusion based nanocomposite conduit would match the arterial compliance *in vivo*. In comparison, the compliance of ePTFE was shown to be very low. The graft would not be able to successfully dilate during pulsatile flow with consequences on both blood flow profile as well as wall stress. Firstly the flow of blood from the artery into the relatively stiff graft would cause a calibre mismatch, concentrating stress at the anastomosis.

The burst pressure for the internal carotid artery is approximately 5000 mmHg (485). PTFE as a vascular prosthesis has a burst pressure of 600 mmHg (485). One way to strengthen the conduits is to increase their wall thickness. However, in this study the concept of measuring the burst pressure of these conduits was to assess whether they could withstand physiological stress.

The ideal graft would conform to arterial compliance at all physiological pressures, not just for reasons of compliance matching but also to prevent over-distention. The bypass prosthesis in current use does not have the problem of over-distention due to their inelastic status. However, development of elastic alternatives requires incorporation of the composite model demonstrated in arteries by way of the complementary systems of elastin and collagen.

6.5 Conclusion

This study has demonstrated the development of compliant nanocomposite conduits using extrusion-phase inversion technique, with a burst pressure able to withstand physiological flow. As mentioned in Chapter 4 extrusion of polyurethanes leads to solid walls or if coagulating, into porous walled structures. PCU based vascular grafts have spongy middles and a single skin structure that allows it to maintain compliance and pulsatile flow *in vivo* (208;214). The mechanical characterisation described in this chapter affords a description of how the nanocomposite material behaves under stress. Although this information is essential for a baseline in developing any new material the results do not immediately translate to an indication of EC-graft behaviour under the physiological stresses of pulsatile flow. In order to undertake this translation, understanding of the stresses acting on the graft wall is desirable, and this has been reviewed in Chapter 2. However, analysis of EC interaction with the compliant graft would be required to quantify the action of stress. Each of these is in itself a complex field requiring sophisticated theoretical models and models have been sought. One way is by stimulating the potential stress on the wall by mimicking pulsatile flow. The flow circuit described in Chapter 3 and used in measuring graft compliance in this Chapter does this.

7

EC & nanocomposite hybrid grafts: seeding and culture

7.1 Introduction

An important aspect of the development of a successful synthetic CABG is to investigate the possibility of carrying out EC seeding of an artificial conduit. Evidence for the requirement of a luminal EC lining is provided by the poor patency observed when unseeded synthetic grafts with diameters less then 6 mm are employed (486). These grafts exhibit extremely poor, clinically unacceptable long term patency when compared to the 'gold standard' use of autologous grafts. The predominant reason for this is that blood contact with the artificial graft surface results in the potential formation of blood clots which cause a loss of patency (197). Thus an ideal clinically acceptable artificial bypass graft would be to develop a conduit that allows seeding with an achievable density of cells and be able to stimulate these cells under physiological flow to proliferate, support and develop a stable and functional graft reducing the likelihood of blood clots forming. Previous studies have demonstrated that many of these problems can be overcome if the graft is seeded with EC prior to implantation but take-up of this process has, to date, been limited due to the technical expertise required to extract and seed the graft and the additional expense incurred in the process (230;329;487).

As discussed in Chapter 4, polymers can differ greatly in their interactions with cells seeded on them. This can affect factors such as the time required for cells to adhere to the material, the number of cells required to obtain a confluent cell layer, the ability of cells to withstand physiological flow when exposed to blood flow and the ability of the cells to survive and proliferate on the material. The PCU graft employed in this study to investigate the optimal method for isolating RNA from EC seeded on an artificial graft has been shown to have a honeycomb structure (199;422;444) which results in a greater potential surface area available for cell attachment when compared to materials such as ePTFE which do not have a honeycomb structure and therefore leads to the possibility of higher seeding densities being employed (199). When developing an EC seeded nanocomposite hybrid graft an important initial stage is to determine the optimal seeding efficiency of the graft. Seeding a high density of EC onto a graft surface not only requires a large amount of initial tissue to isolate the cells from but also extensive cell culture to generate the large number of cells required. At very high seeding densities many of the cells seeded may be wasted as the excess cells do not adhere to the surface resulting in cell death. Alternately utilising a seeding density which is too low will not result in a confluent layer of EC on the graft and may increase the chance of cells being washed away when exposed to flow. Previous work on lining PCU and ePTFE vascular grafts with EC have established the optimal seeding conditions (197;199) under various conditions for these materials. The optimal cell density required is determined by a variety of factors such as the availability of cells, the type of graft being seeded and the seeding time employed. To determine the optimal seeding density a broad range of cell concentrations are assessed and then narrowed down to the optimal cell number for the graft of choice and the seeding time employed. For example in the case of PCU initial seeding density saturation occurred at 16×10^5 cells/cm^2 when seeded for 4 hours and these conditions resulted in a confluent EC layer (199). This was therefore determined as the optimal conditions for seeding PCU graft conduits.

In order to determine if there were any significant differences between the optimal seeding density for PCU and the nanocomposite conduits employed for the flow studies this study was repeated to determine the optimal seeding conditions for the nanocomposite. In addition to examining cell confluence and metabolism at each seeding density two further important factors were investigated, RNA yield from cell extraction (vital to later gene expression studies) and cytotoxicity. To assess cell seeding

concentrations, HUVEC were seeded on nanocomposite conduits at achievable cell densities; 6.3 x 10^3 cells/cm^2, 1.2 x 10^4 cells/cm^2 and 2.5 x 10^4 cells/cm^2. To assess the optimal seeding time, after 4, 8, 12 and 24 hours of incubation at 37°C cell seeding efficiency and viability was assessed using Alamar blue™. An LDH assay was used to monitor cell death. For each seeding density and incubation time the total RNA was extracted and the purity measured.

Secondly the question of the stability of gene expression of the HUVEC employed for cell seeding was addressed. There is phenotypic variation between ECs in different portions of the vascular tree, and between arterial and venous cells. Cells from different locations within an individual not only express different markers but can also generate different responses to the same stimilus. Cells from different individuals can vary in the responses to stilmuli, even when obtained from the same portion of the vasculature. Due to the high numbers of cells required for successful seeding of the nanocomposite conduits and the large numbers of conduits required for the exposure to flow experiments it was recognised that there would be a necessity to utilise cells from several different HUVEC isolations and, perhaps, different passage numbers in the course of the study envisaged. In order to investigate the effects of passage number (and time) on gene expression HUVEC were investigated from the initial cell isolation to passage 11 by extracting RNA at each passage, examining the quality of RNA extracted and carrying out RT-PCR analysis for GAPDH, TGF-β1, COL-1 and PECAM-1 at each stage.

The aim of this part of the study was to validate the proposed model employed for the shear stress studies by analysing the most suitable cell density and conditions for EC seeding to obtain a sufficient amount of RNA for further studies and to ensure that the ideal culture passage number was employed in order to investigate changes in gene expression.

7.2 Materials and Methods

7.2.1 Assessment of seeding efficiency and seeding time

7.2.1.1 Conduit seeding

HUVEC were cultured to passage three and seeded in 5 cm length with 5 mm internal diameter tubular nanocomposite conduits prepared using the extrusion-phase inversion method as described in Chapter 6. All conduits were autoclaved prior to use.
Following trypsinisation, and resuspension in complete tissue culture medium, a cell count was obtained and diluted in 1ml of complete medium to three cell seeding concentrations; 6.3 x 10^3 cells/cm^2, 1.2 x 10^4 cells/cm^2 and 2.5 x 10^4 cells/cm^2.
For conduit seeding the cells were added as a suspension to each graft segment. The ends of the graft were plugged, and the graft segments rotated 90° every 15 minutes for the first two hours to achieve an even covering of HUVEC on each graft.
To assess the efficiency of cell adhesion on the nanocomposite, grafts were incubated for 4, 8, 12 and 24 hours at 37 °C. Unseeded grafts were placed with complete medium and incubated at 37°C. As a comparison and to ensure each technique was carried out accurately the same densities of cells were seeded onto 6-well polystyrene tissue culture plates (TCP) as above.

7.2.1.2 Cell viability

Grafts and control tissue culture plates were washed twice with PBS and the viability of seeded cells was assessed using an Alamar blue™ assay. One millilitre of Alamar blue™ (10%) in complete medium was added to each graft/well and incubated for 4 hours. Duplicate 100 µl samples were then removed and the absorbance's read spectroscopically at wavelengths of 570 nm and 630 nm.

7.2.1.3 Cell damage

To assess cell damage over seeding conditions, LDH assay was measured as previously described. Fifty microlitres cell culture medium from each sample was transferred to a 96-well plate. Fifty microlitres substrate mixes (1 vial substrate plus

12 mls assay buffer) was added to each well and the plate covered in foil to prevent light access. Samples were then incubated at room temperature for 30 minutes after which the reaction was stopped by the addition of 50 µl stop solution (1 M acetic acid). Absorbance was then read at 450 nm using a Multiscan MS UV visible spectrophotometer.

7.2.1.4 RNA extraction

Total RNA from each graft and 6-well plate was extracted using the method described in Chapter 3. Cells were trypsinised to remove them from the surface and centrifuged to obtain a cell pellet. Cells were lysed with RLT lysis buffer and RNA extracted as previously described. The yield and purity for each sample was measured at 260 and 280 nm using GeneSpec.

7.2.1.5 Cell staining

Cells seeded in grafts were stained using the Toluidine blue method. Following seeding at 6.3 x 10^3 cells/cm^2, 1.2 x 10^4 cells/cm^2 and 2.5 x 10^4 cells/cm^2 per conduit for 24 hours, nanocomposite conduits were washed in sterile PBS and stained using the method outlined in Chapter 3, Section 3.8.1.

7.2.2 Assessment of genotype stability

7.2.2.1 Cell culture and RNA extraction

HUVEC were isolated from human umbilical cord vein as described earlier. The initial cell isolation was called P0 for RNA extraction purposes and was taken as a control. HUVEC were cultured in 75 cm^2 tissue culture flasks from passage 1 to 11. Cultures were passaged every one to two weeks at a ratio of 1:2 and fed every 48 hours as described in Chapter 3. Once a confluent monolayer was achieved cells were removed by washing with 8 ml of PBS and then adding 3 ml of 10 % trypsin-EDTA solution. The flasks were incubated for 3 minutes prior to gentle tapping in order to loosen all the cells. The trypsin was then neutralised by the addition of 10 mls of complete medium. The cell suspension was spun at 300 g for 7 minutes, supernatant

discarded and cell pellet collected. At each passage split, confluent cells from one flask were isolated for RNA extraction and the rest were resuspended in 10 ml of complete medium to continue culturing.

7.2.2.2 Analysis of gene expression at each passage

RT-PCR was conducted for the expression of GAPDH, TGF-β1, COL-1 and PECAM-1. 0.5μM from each of the primers was added to the PCR mix. For each sample, 0.5μg of template RNA was employed with RNase free water added to make a total volume of 50μl. Cycle conditions for all PCR reactions are described in Chapter 3. All PCR products were run on a 2 % agarose gel and the intensity was measured for each band.

7.2.3 Data analysis and statistical methods

Assessment of genotype stability study was repeated four times for each passage number. Concentrations of RNA obtained are presented in mean ± SD. Comparisons of gene intensity between groups were made by one-way ANOVA (Kruskal–Wallis) test with post comparison using Dunn's comparison test.
The assessment of seeding efficiency and seeding time was repeated six times for each cell density/seeding time measured. Statistical analysis used one-way ANOVA with Tukey's multiple comparison tests.

7.3 Results

7.3.1 Assessment of seeding and seeding time

7.3.1.1 Cell viability

Figure 7-1-1 shows Alamar blue™ cell viability assay post HUVEC seeded on TCP and nanocomposite conduits at cell densities of 6.3 x 10^3 cells/cm^2, 1.2 x 10^4 cells/cm^2 and 2.5 x 10^4 cells/cm^2 per conduit after a) 4 hours, b) 8 hours, c) 12 hours and d) 24 hours of seeding time.

Significant differences ($p < 0.001$) in cell viability were observed between the TCP and nanocomposite groups at all seeding time points. There were no significant differences in cell viability between any of the cell densities seeded in nanocomposite conduits that were seeded for 4, 8 or 12 hours (Figure 7-1-1 a, b and c respectively). Significant increases in viability were only seen at 24 hours in nanocomposite conduits seeded with 1.2 x 10^4 cells/cm^2 ($p < 0.01$) and 2.5 x10^4 cells/cm^2 ($p < 0.001$) compared to 6.3 x 10^3 cells/cm^2. At 24 hours post seeding, no differences were observed in cell viability in nanocomposite conduits seeded with 1.2 x 10^4 cells/cm^2 compared to 2.5 x 10^4 cells/cm^2.

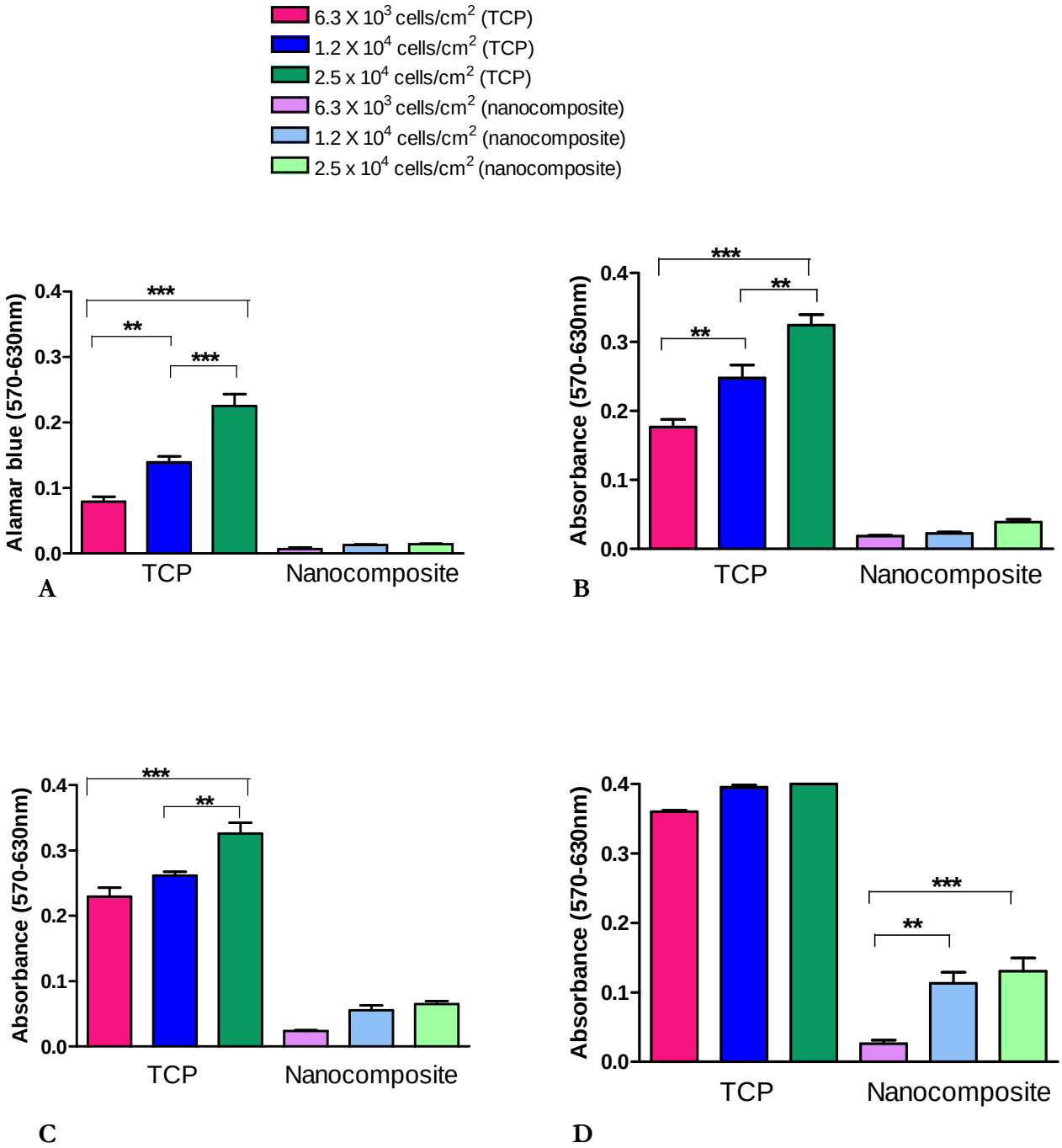

Figure 7-1-1. Alamar blue™ cell viability of HUVEC at 6.3 x 10^3 cells/cm^2, 1.2 x 10^4 cells/cm^2 and 2.5 x 10^4 cells/cm^2 seeded on tissue culture plates (TCP) and nanocomposite conduits post a) 4 hours, b) 8 hours, c) 12 hours and d) 24 hours incubation time.
Absorbance was measured in arbitrary units at 570nm wavelength and background at 630 nm subtracted. Data are n = 6. *P < 0.05, **P < 0.01 and ***P < 0.001. All statistical analysis utilised one way ANOVA with Tukey's multiple comparison test.

Figure 7-1-2 shows Alamar blue™ cell viability results of nanocomposite conduits seeded at three cell densities of a) 6.3 x 10^3 cells/cm^2, b) 1.2 x 10^4 cells/cm^2 and c) 2.5 x 10^4 cells/cm^2 comparing against 4, 8, 12 an 24 hours seeding time. Conduits seeded with 6.3 x 10^3 cell/cm^2 (Figure 7-1-2 a) showed significant increases ($p < 0.05$) in cell viability at 12 and 24 hours only compared to 4 hours seeding time. There was no significant difference between any other seeding time points at this seeding density. At 1.2 x 10^4 cells/cm^2 (Figure 7-1-2 b) and 2.5 x 10^4 cell/cm^2 (Figure 7-1-2 c), nanocomposite conduits showed a significant increase in cell viability post 12 ($p < 0.05$) and 24 hours ($p < 0.001$) of seeding compared to 4 hours. Increases were also observed after 24 hours ($p < 0.001$) seeding compared to 8 hours. At 1.2 x 10^4 cells/cm^2 (Figure 7-1-2 b) and 2.5 x 10^4 cell/cm^2 (Figure 7-1-2 c) a significant difference ($p < 0.01$) in cell viability was seen at 24 hours compared to 12 hours.

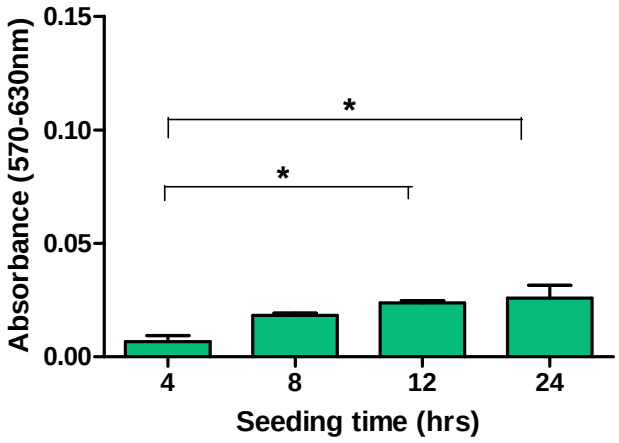

Figure 7.1.2 a. Alamar blue™ cell viability of HUVEC seeded at 6.3 x 10^3 cells/cm^2 on nanocomposite conduits for 4, 8, 12 and 24 hours. Absorbance was measured in arbitrary units at 570 nm wavelength and background at 630 nm subtracted. Data are n=6. *P < 0.05, all statistical analysis utilised one way ANOVA with Tukey's multiple comparison test.

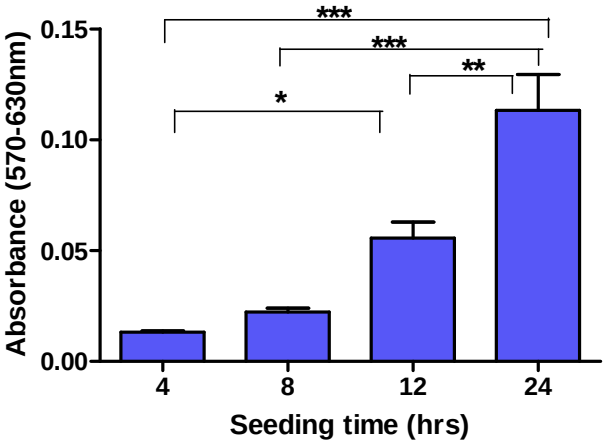

Figure 7-1-2 b. Alamar blue™ cell viability of HUVEC seeded at 1.2 x 10^4 cells/cm^2 on nanocomposite conduits for 4, 8, 12 and 24 hours. Absorbance was measured in arbitrary units at 570 nm wavelength and background at 630 nm subtracted. Data are n=6. *P < 0.05, **P < 0.01 and ***P < 0.001, all statistical analysis utilised one way ANOVA with Tukey's multiple comparison test.

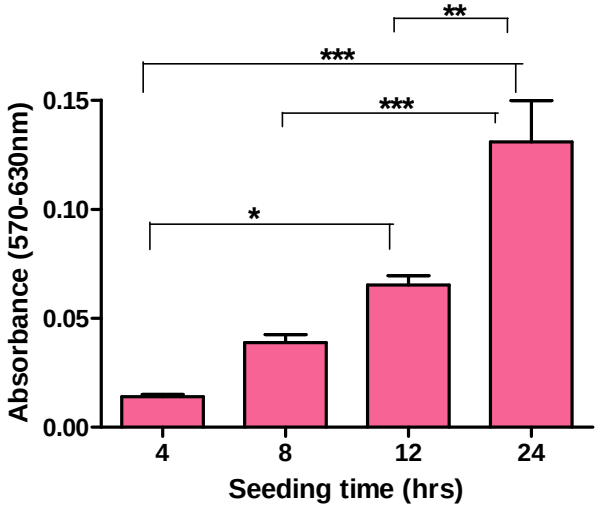

Figure 7-1-2 c. Alamar blue™ cell viability of HUVEC seeded at 2.5 x 10^4 cells/cm^2 on nanocomposite conduits for 4, 8, 12 and 24 hours. Absorbance was measured in arbitrary units at 570 nm wavelength and background at 630 nm subtracted. Data are n=6. *P < 0.05, **P < 0.01 and ***P < 0.001, all statistical analysis utilised one way ANOVA with Tukey's multiple comparison test.

7.3.1.2 Cell damage

Figure 7-2-1 shows the LDH assay for cells seeded on nanocomposite conduits and TCP at 6.3 x 10^3, 1.2 x 10^4 and 2.5 x 10^4 cells/cm^2 for a) 4 hours; b) 8 hours; c) 16 hours and d) 24 hours of seeding time.

HUVEC seeded on TCP was used as a control. Differences in LDH activity were observed in all cell densities seeded in TCP compared to those seeded in nanocomposite conduits at 4, 8, 12 and 24 hours of seeding.

There was a significant difference between 6.3 x 10^3 and 1.2 x 10^4 cells/cm^2 post 4 hours ($p < 0.001$), 8 hours ($p < 0.01$), 12 hours ($p < 0.01$) and 24 hours ($p < 0.001$) seeding time on the nanocomposite conduits. After 4 hours of seeding time there was no significant difference between 1.2 x 10^4 cells/cm^2 and 2.5 x 10^4 cells/cm^2 seeded on nanocomposite conduits. This was significant post 8, 12 hours ($p < 0.01$) and 24 hours ($p < 0.001$).

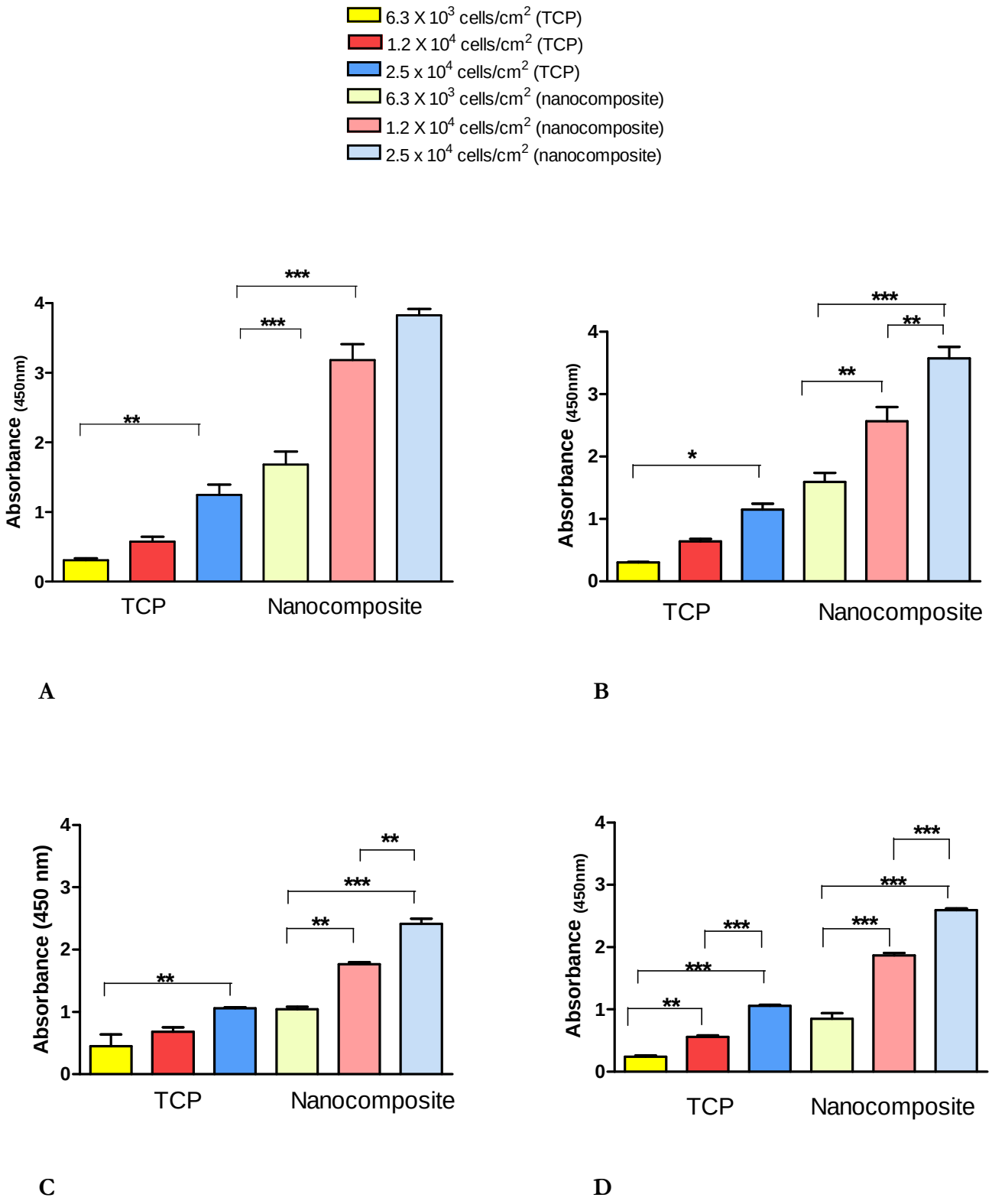

Figure 7-2-1. LDH assay test measuring cell toxicity on HUVEC seeded on TCP and nanocomposite conduits at 6.3 x 10^3, 1.2 x 10^4 and 2.5 x 10^4 cells/cm^2 for a) 4 hours, b) 8 hours, c) 12 hours and d) 24 hours of seeding time. *P < 0.05, **P < 0.01 and ***P < 0.001 using one-way ANOVA with Tukeys's multiple comparison test.

Figure 7-2-2 shows the LDH assay for cells seeded on nanocomposite conduits at a) 6.3 x 10^3 cells/cm^2; b) 1.2 x 10^4 cells/cm^2 and c) 2.5 x 10^4 cells/cm^2 for 4, 8, 12 and 24 hours.

Cells seeded on nanocomposite conduits at a density of 6.3 x 10^3 cells/cm^2 (Figure 7-2-2 a) showed a significant difference between 4 and 24 hours ($p < 0.01$); 4 and 12 and 8 and 24 hours ($p < 0.05$) of seeding time. There was no significant difference in seeding time between 12 and 24 hours of incubation at this cell density.

Nanocomposite conduits seeded with HUVEC at 1.2 x 10^4 cells/cm^2 (Figure 7-2-2 b) showed a higher level of LDH activity at 4 hours compared to 12 and 24 hours ($p < 0.01$). This was also significant for 8 hours compared to 12 hours ($p < 0.05$) of seeding incubation time on the nanocomposite conduits.

HUVEC seeded at 2.5 x 10^4 cells/cm^2 (Figure 7-2-2 c) on nanocomposite conduits showed a significant higher ($p < 0.001$) LDH activity at 4 hours compared to 12 and 24 hours of seeding. Significant differences were also observed at 8 hours of seeding compared to 12 ($p < 0.001$) and 24 hours ($p < 0.01$) seeding time on the conduits.

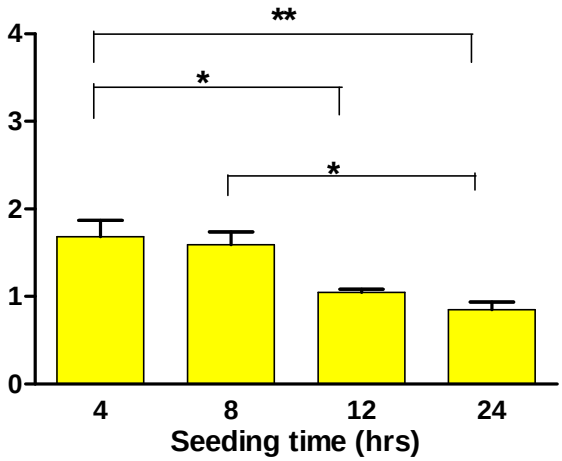

Figure 7-2-2 a. LDH assay test on HUVEC seeded onto nanocomposite conduits at 6.3 x 10^3 cells/cm^2 for 4, 8, 12 and 24hours. Absorbance was measured in arbitrary units at 450 nm wavelength. *P < 0.05 and **P < 0.01 using one-way ANOVA with Tukey's multiple comparison test.

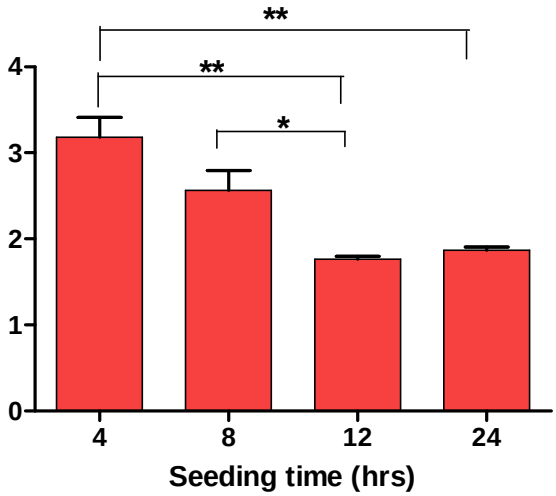

Figure 7-2-2 b. LDH assay test on HUVEC seeded onto nanocomposite conduits at 1.2 x 10^4 cells/cm^2 for 4, 8, 12 and 24hours. Absorbance was measured in arbitrary units at 450 nm wavelength. *P < 0.05 and **P < 0.01 using one-way ANOVA with Tukey's multiple comparison test.

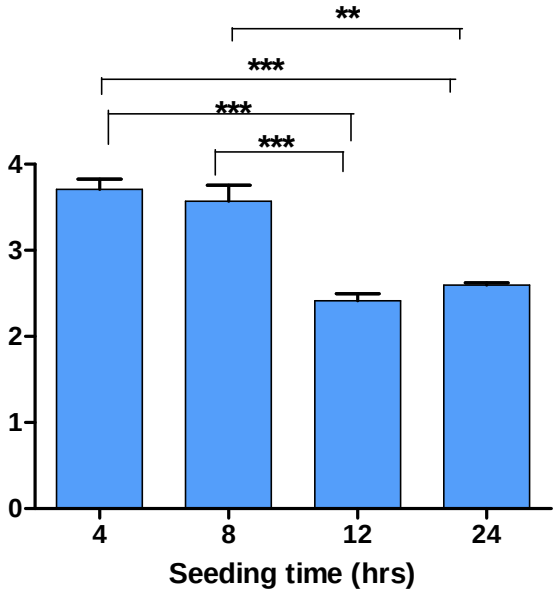

Figure 7-2-2 c. LDH assay test on HUVEC seeded onto nanocomposite conduits at 2.5 x 10^4 cells/cm^2 for 4, 8, 12 and 24hours. Absorbance was measured in arbitrary units at 450 nm wavelength. **P < 0.01 and ***P < 0.001 using one-way ANOVA with Tukey's multiple comparison test.

7.3.1.3 RNA yield

Figure 7-3-1 shows the RNA yield obtained from HUVEC seeded in TCP and nanocomposite conduits at 6.3 x 10^3 cells/cm^2, 1.2 x 10^4 cells/cm^2 and 2.5 x 10^4 cells/cm^2 for a) 4 hours; b) 8 hours; c) 12 hours and d) 24 hours of seeding time.
A significant difference ($p < 0.001$) in RNA yield was observed in all the control groups (TCP) and nanocomposite conduits. After 4 and 8 hours (Figure 7-3-1 a and b respectively) of seeding time, there was no significant difference in RNA yield between all seeding densities. A significant difference was observed at 12 hours ($p < 0.01$) and 24 hours ($p < 0.001$) (Figure 7-3-1 c and d respectively), where an increase in RNA yield was obtained with a cell density of 1.2 x 10^4 cells/cm^2 and 2.5 x 10^4 cells/cm^2 compared to 0.5 x 10^6 cells/cm^2 seeded on nanocomposite conduits. There was no significant difference in RNA yield at 12 hours or 24 hours (Figure 7-3-1 c and d respectively) of seeding time between 1.2 x 10^4 cells/cm^2 and 2.5 x 10^4 cell/cm^2 seeded on nanocomposite conduits.

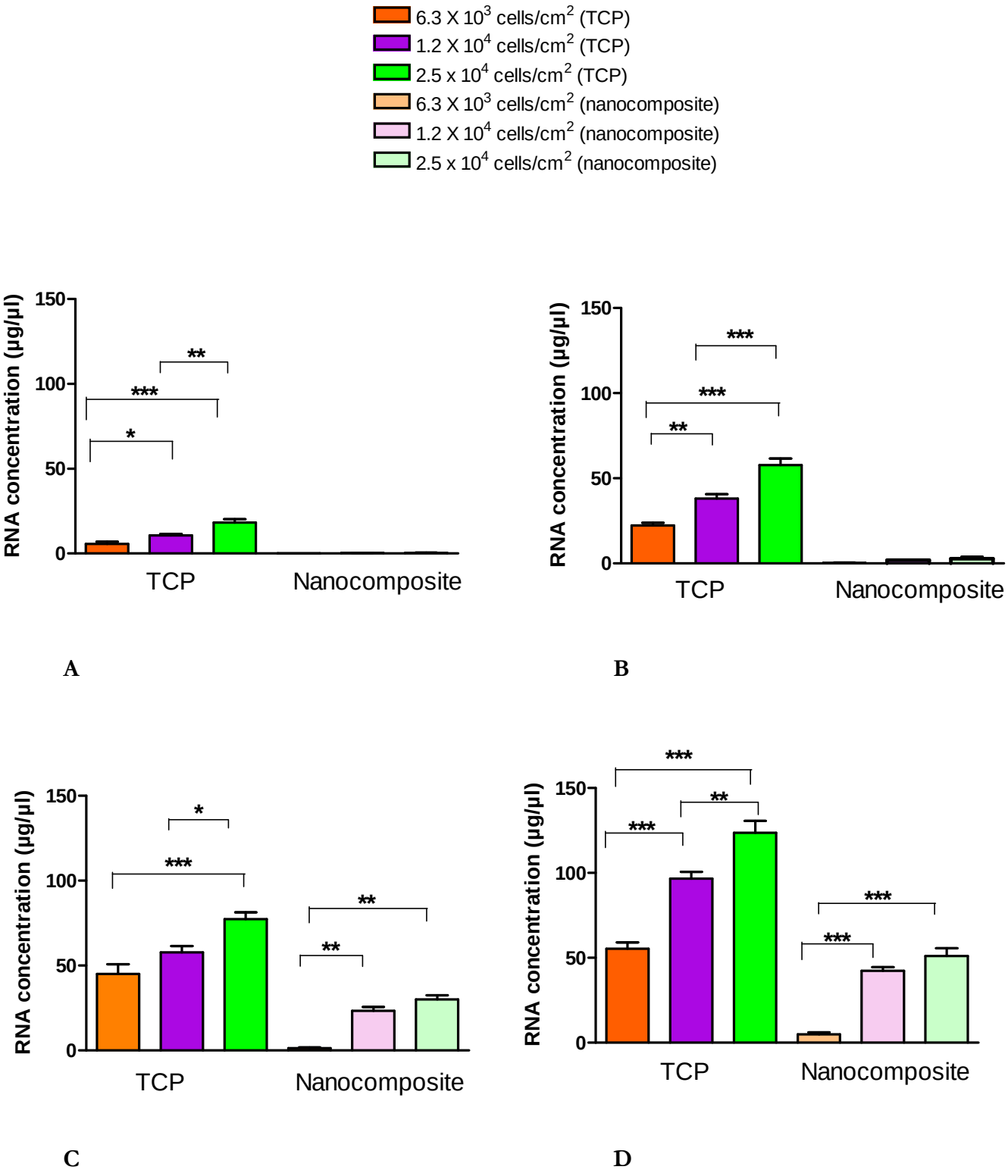

Figure 7-3-1. shows comparison of RNA yield measured at absorbance of 260 nm and 280 nm obtained from conduits seeded at 6.3 x 10^3 cells/cm^2, 1.2 x 10^4 cells/cm^2 and 2.5 x 10^4 cells/cm^2 on TCP and nanocomposite conduits for a) 4 hours, b) 8 hours, c) 12 hours and d) 24 hours of seeding time. *P < 0.05, **P < 0.01 and ***P < 0.001 using one-way ANOVA with Tukey's multiple comparison test.

Figure 7-3-2 represents RNA yield obtained from conduits over seeding time (hours) for a) 6.3 x 10^3 cells/cm^2; b) 1.2 x 10^4 cell/cm^2 and c) 2.5 x 10^4 cells/cm^2 seeded on nanocomposite conduits.

Conduits that were seeded with 6.3 x 10^3 cells/cm^2 (Figure 7-3-2 a) showed a significant increase in RNA yield at 24 hours of seeding time compared to 4, 8 ($p < 0.01$) and 12 hours ($p < 0.05$). A significant difference ($p < 0.001$) in RNA yield was observed in all seeding time points (except at 4 hours when compared to 8 hours) in nanocomposite seeded with 1.2 x 10^4 cells/cm^2 (Figure 7-3-2 b).

Nanocomposite conduits seeded with 2.5 x 10^4 cells/cm^2 (Figure 7-3-2 c) showed a significant increase in RNA yield post 24 hours ($p < 0.001$) of seeding time compared to all time points but was less significant ($p < 0.01$) compared to 12 hours of seeding time on the nanocomposite conduits.

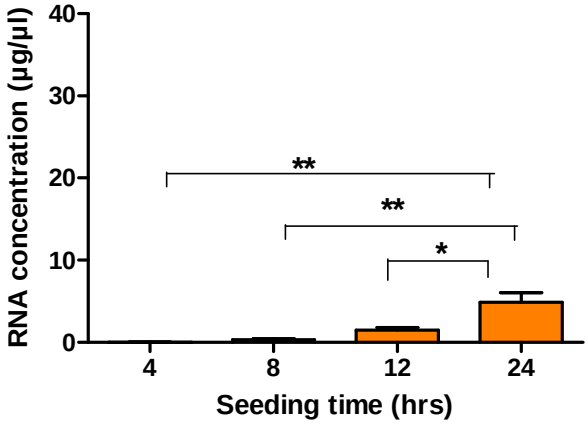

Figure 7-3-2 a. shows RNA yield measured at absorbance of 260 nm and 280 nm obtained from nanocomposite conduits seeded at 6.3 x 10^3 cells for 4, 8, 12 and 24 hours of seeding time. *P < 0.05 and **P < 0.01. Statistical analysis utilised one-way ANOVA with Tukey's multiple comparison test.

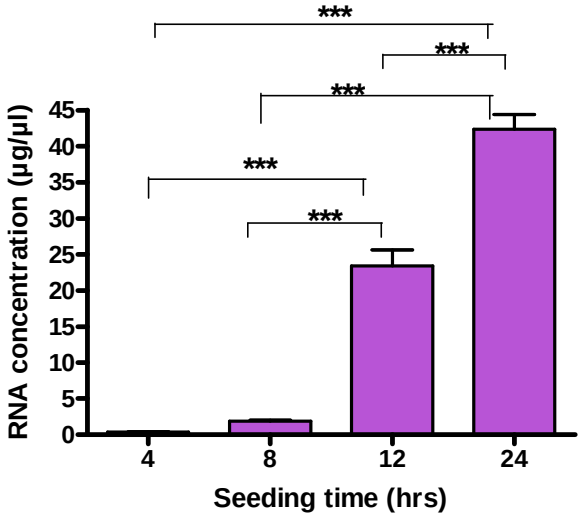

Figure 7-3-2 b. shows RNA yield measured at absorbance of 260 nm and 280 nm obtained from nanocomposite conduits seeded at 1.2 x 10^4 cells for 4, 8, 12 and 24 hours of seeding time. ***P < 0.001 using one-way ANOVA with Tukey's multiple comparison tests.

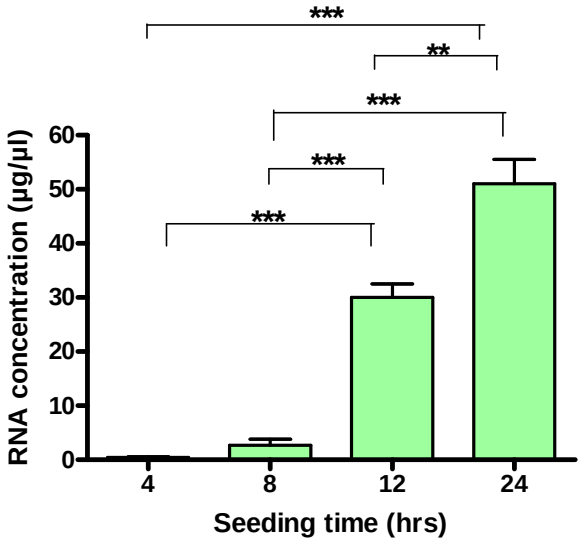

Figure 7-3-2 c. shows RNA yield measured at absorbance of 260 nm and 280 nm obtained from nanocomposite conduits seeded at 2.5 x 10^4 cells for 4, 8, 12 and 24 hours of seeding time. **P < 0.01 and ***P < 0.001 using one-way ANOVA with Tukey's multiple comparison test.

7.3.1.4 RNA purity

The purity of RNA was obtained for each cell density and seeding time. Figure 7-4 shows the RNA purity measured for HUVEC seeded on TCP and nanocomposite conduits at three cell seeding densities of 6.3 $x10^3$ cells/cm^2, 1.2 x 10^4 cells/cm^2 and 2.5 x 10^4 cell/cm^2 incubated at a) 4 hours; b) 8 hours; c) 12 hours and d) 24 hours.
No significant difference in RNA purity was observed in any of the groups (TCP and nanocomposite conduits).

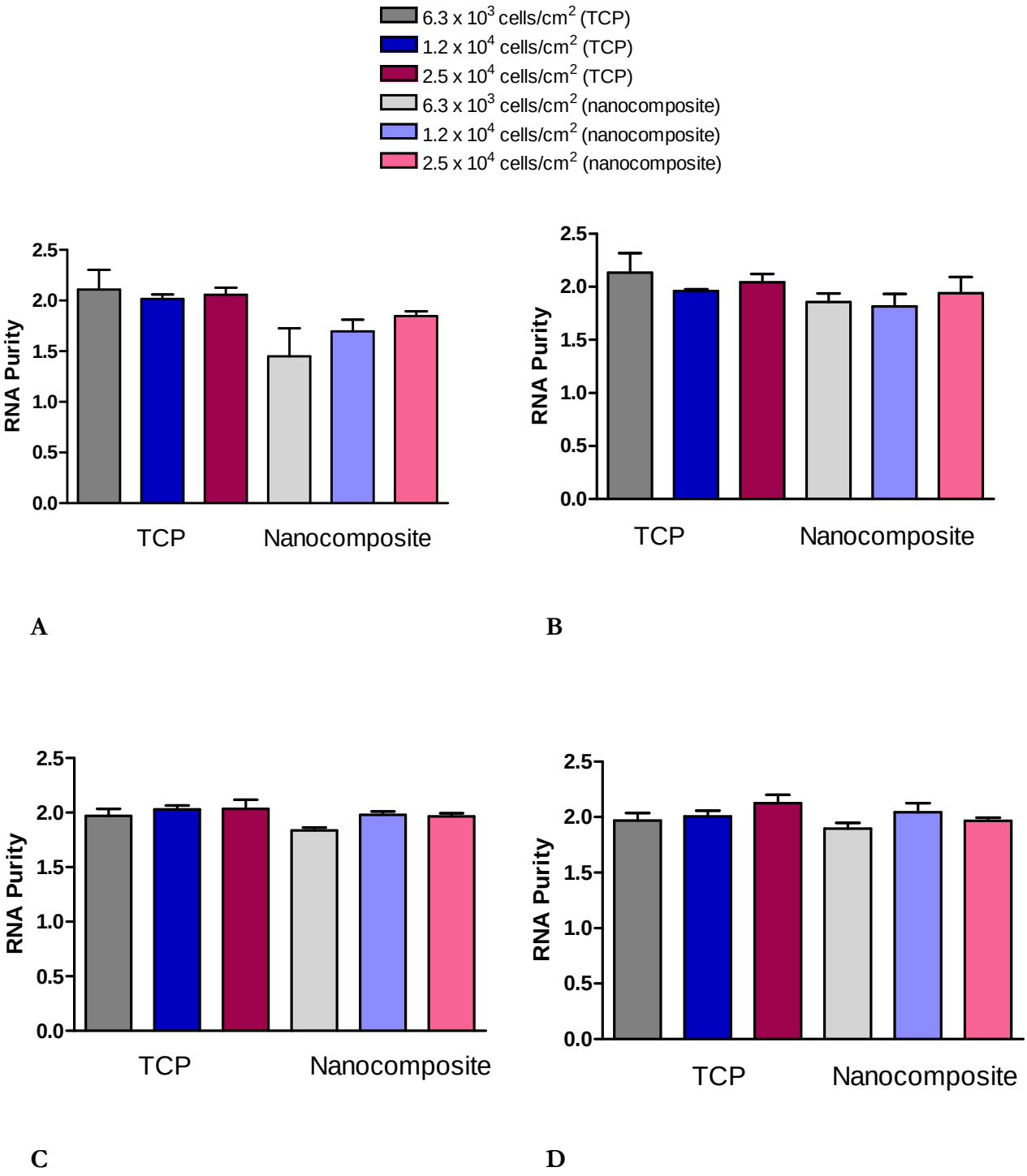

Figure 7-4. Comparison of RNA purity obtained from TCP and nanocomposite conduits seeded at 6.3 x 10^3, 1.2 x 10^4 and 2.5 x 10^4 cells/cm^2 for a) 4 hours; b) 8 hours; c) 12 hours and d) 24 hours seeding time. There was no significant difference in RNA purity between any of the seeding densities and seeding times.

7.3.1.5 Cell staining

The Toluidine blue images below (Figure 7-5) show HUVEC staining on nanocomposite conduits seeded at a) 6.3 x 10^3 cells/cm^2, b) 1.2 x 10^4 cells/cm^2 and c) 2.5 x 10^4 cells/cm^2 for 24 hours. As can be seen differences were observed at cell densities. Greater numbers of cells seem to be present in conduits seeded at 1.2 x 10^4 cells/cm^2 and 2.5 x 10^4 cells/cm^2 compared to 6.3 x 10^3 cells/cm^2 over 24 hours seeding time.

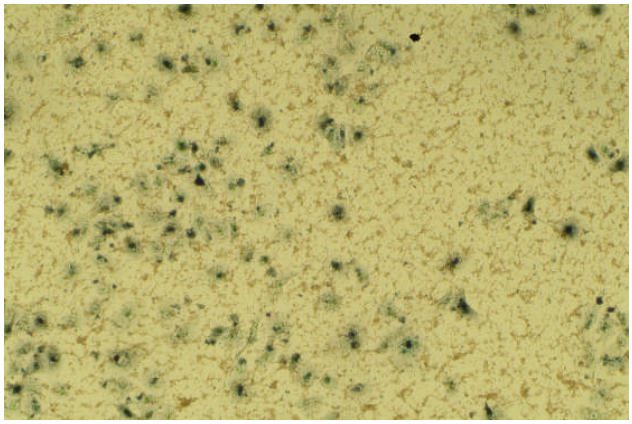

A

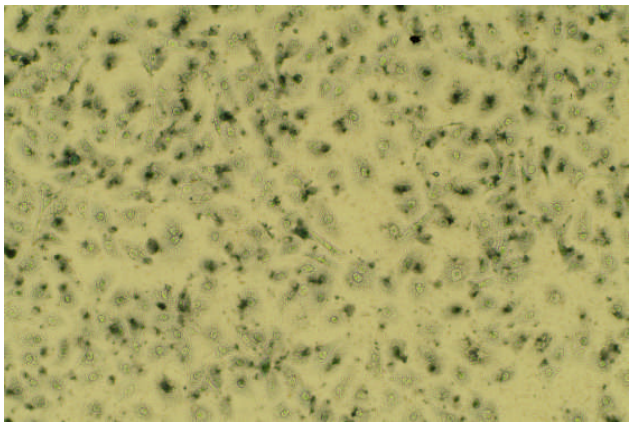

B

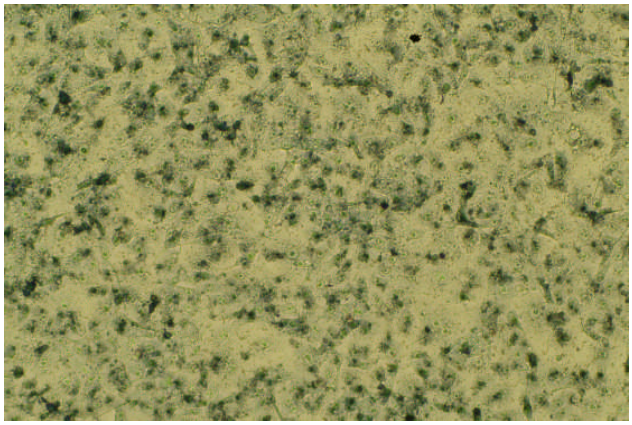

C

Figure 7-5. Toluidine blue staining represents HUVEC seeded on nanocomposite conduits at a) 6.3 x 10^3 cells/cm^2, b) 1.2 x 10^4 cells/cm^2 and c) 2.5 x 10^4 cells/cm^2 for 24 hours.

7.3.2 Assessment of genotype stability

7.3.2.1 RNA quantity and purity

The quantity and purity of the RNA isolated at each passage is shown in Table 7-1. The amount of RNA isolated varied between 254 and 575 ng/μl and the ratio A_{260}/A_{280} between 1.90 and 2.20. The purity of total RNA achieved was good in all cultured passages.

Table 7-1. RNA quantity and purity measured at absorbance of 260 nm and 280 nm.

Passage	P0	P1	P2	P3	P4	P5	P6	P7	P8	P9	P10	P11
Conc^{n}(ng/μl) (mean ± SEM)	547 ± 2.8	479 ± 2.6	575 ± 1.1	421 ± 3.9	382 ± 4.0	426 ± 1.8	495 ±4.4	274 ± 5.0	277 ±1.3	343 ± 2.8	484 ± 4.6	254 ± 3.2
Ratio (260nm/280 nm	1.92	1.97	1.98	1.93	1.90	1.96	1.92	2.20	2.12	1.90	1.92	1.95

7.3.2.2 Analysis of GAPDH, TGF-β1, COL-1 and PECAM-1 PCR products

All PCR products from each passage were loaded on a 2 % agarose gel. Figure 7-6 shows 2 % agarose gels of PCR products for GAPDH, TGF-β1, COL-1 and PECAM-1 expression over passage 0 to 11.

The mRNA levels of GAPDH remained relatively constant in the passage study however slight changes were observed for the expression at passages 8, 9 and 10 (Figure 7-6 e & f).

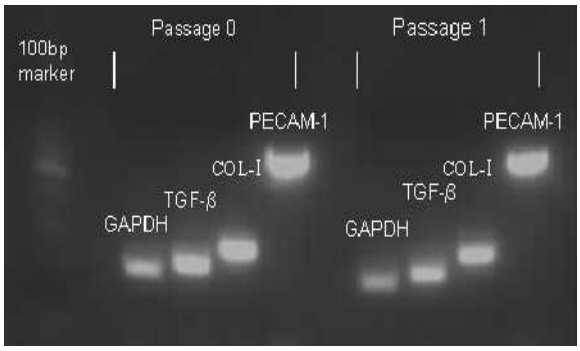

A

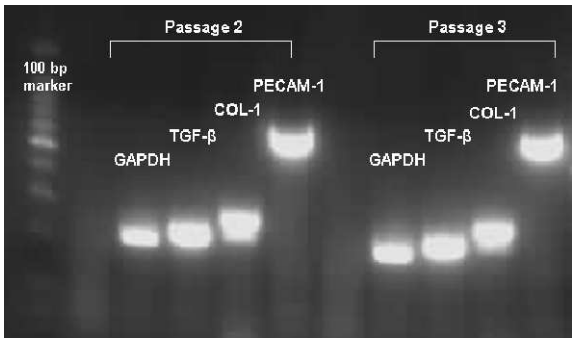

B

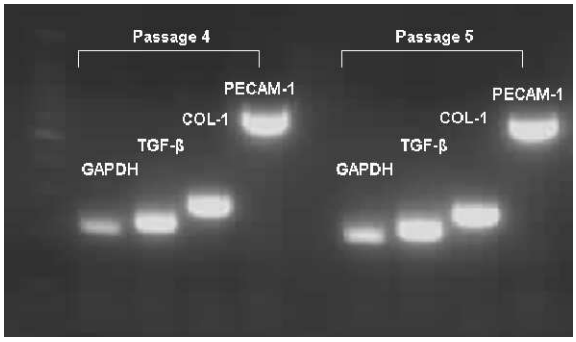

C

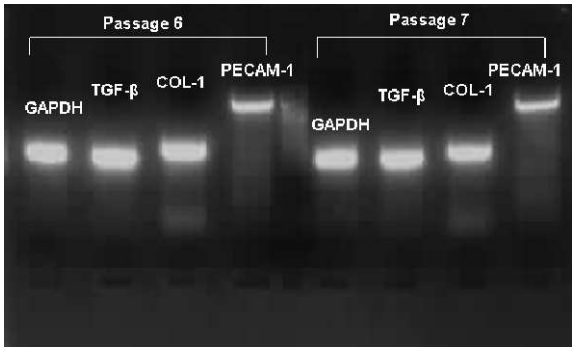

D

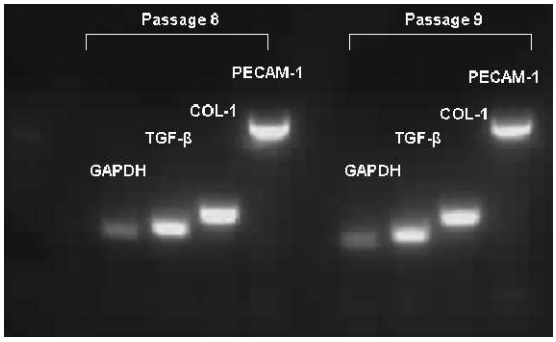

E

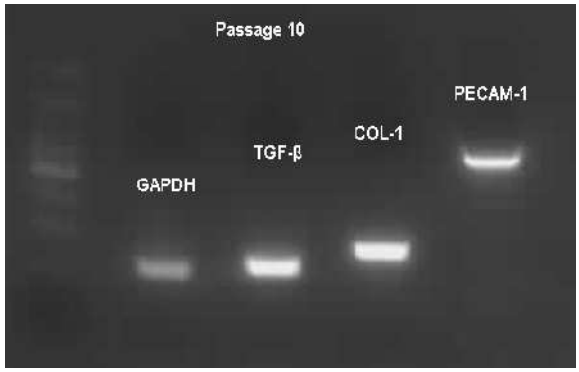

F

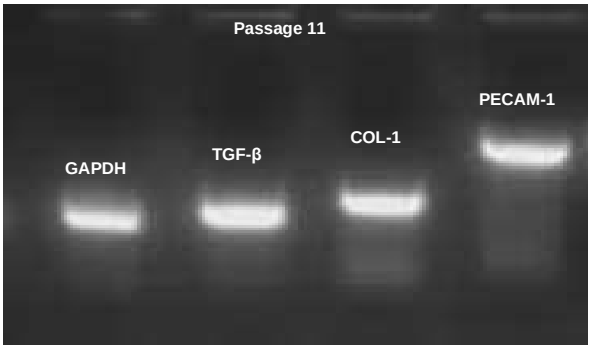

G

Figure 7-6. PCR products of GAPDH, TGF-β1, COL-1 and PECAM-1 mRNA expression on a 2 % agarose gel. The gel images show gene expression for HUVEC cultured where (a) P0 and P1, (b) P2 and P3 (c) P4 and P5, (d) P6 and P7, (e) P8 and P9 (f) P10 and (g) P11.

7.3.2.3 Analysis of gene intensity

Relative levels of GAPDH, TGF-β1, COL-1 and PECAM-1 over culture passages 0 to 11 were determined using Syngene. The intensity of GAPDH was determined for each band. As the products were loaded on different gels the intensity of TGF-β1, COL-1 and PECAM-1 mRNA levels were normalized by GAPDH mRNA level measured from the equivalent gel.

Figure 7-7 shows the intensity of gene expression from HUVEC at passage 0 to 11, for a) GAPDH, b) TGF-β1, c) COL-1 and d) PECAM-1. Statistical analysis was assessed for TGF-β1, COL-1 and PECAM-1 using the Kruskal-Wallis test. There was no significant difference in any of the genes between the initial extractions, P0 to HUVEC cultured to passage 11.

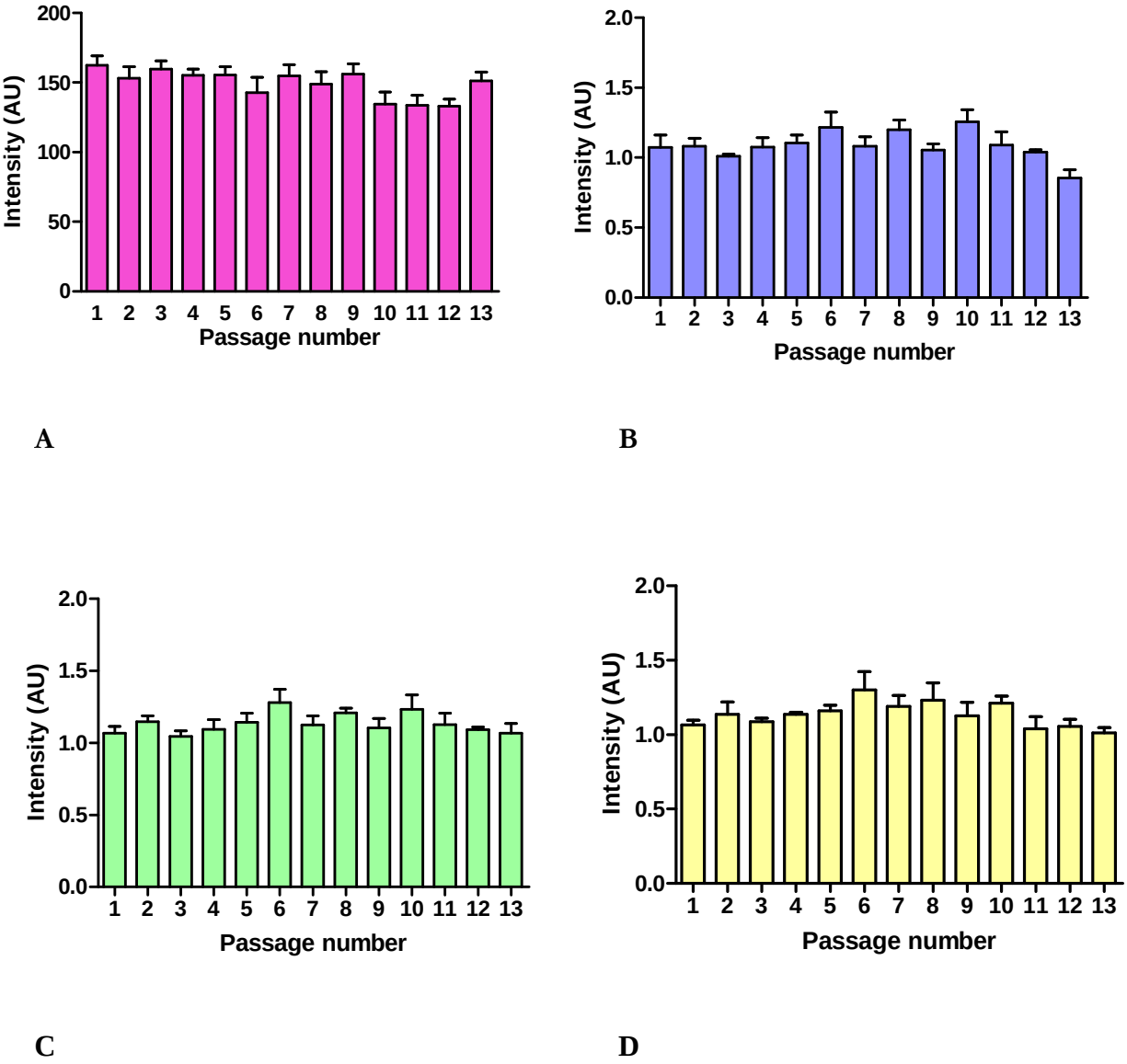

Figure 7-7. Intensities of gene expression in arbitrary unit (AU) from RNA obtained from passage 0 to 11 for a) GAPDH, b) TGF-β1, c) COL-1 and d) PECAM-1.
GAPDH gene intensity was measured for each band. TGF-β1, COL-1 and PECAM-1 mRNA levels were normalized by GAPDH mRNA level. No significant increases in expression were observed in any of the genes comparing between passages 0 to 11. Statistical analysis was performed for TGF-β1, COL-1 and PECAM-1 using Kruskal-Wallis test. (n = 6).

7.4 Discussion

Before embarking on shear stress and gene expression studies it was felt that this investigation was a prerequisite in the stages of development of a model for studying gene expression in EC-seeded conduits for small diameter coronary bypass graft. The purpose of this chapter was to determine the cell concentration/seeding time combination that produced the maximum number of adhered EC, maximum viable graft surface coverage, and minimal cell number needed in terms for culture time whilst at the same time producing sufficient RNA following extraction to permit gene expression studies to be carried out. This is a fundamental requirement prior to flow studies.

Nanocomposite conduits with an internal diameter of five millimetres and fifty millimetres in lengths were fabricated and the seeding conditions were assessed. Using a model previously utilised for lining vascular grafts with EC as a basis, cells were seeded at 6.3 x 10^3 cells/cm^2, 1.2 x 10^4 cells/cm^2 and 2.5 x 10^4 cells/cm^2 per conduits. Equal numbers were also seeded in TCP as a control. Grafts and TCP were incubated for 4, 8, 12 and 24 hours to assess seeding time. Examining seeding time first, both TCP and nanocomposite demonstrated a time-dependent seeding efficiency. In the case of nanocomposite in all cases (apart from 4 and 8 hours at the lowest seeding density) an increase in seeding time resulted in an improved seeding density reflected in significant increases in cell metabolism when measured by Alamar blue™. As regards initial seeding density in general 6.3 x 10^3 cells/cm^2 resulted in significantly lower seeding compared to the two higher cell densities for the cells seeded on nanocomposite. As a result of this investigation it was decided to employ an initial seeding density of 1.2 x 10^4 cells/cm^2 with a 24 hour seeding time as the conditions for cell seeding in the following flow studies. Whilst there was a slight increase in seeding efficiency using the higher initial seeding density of 2.5 x 10^4 cells/cm^2 it was not felt that the increase in efficiency was sufficient to overcome the difficulty of requiring twice as many cells for the studies. Examination of the RNA yield at each time point confirmed the results obtained in the cell metabolism studies and the advisability of using 1.2 x 10^4 cells/cm^2 with a 24 hour seeding time which resulted in an adequate yield of RNA from the nanocomposite. The RNA purity was unaffected by either the initial seeding density or the seeding time.

The large number of cells needed to seed such grafts meant that alterations in phenotype were a concern in this study. Primary cells in particular have a tendency to change in phenotype in a number of ways with an increasing number of passages. Gene expression is one of the factors that may be affected by changes over time in culture and can be further influenced by the conditions under which the cells are maintained. Stable gene expression under controlled conditions allows changes to be monitored. The results obtained from the RNA extraction from HUVEC over 11 passages demonstrate that levels of expression for GAPDH, TGF-β1, COL-1 and PECAM-1 remained stable indicating that it would be possible to employ cells from different passages in the cell seeding of nanocomposite conduits without compromising the results obtained from later investigations into gene expression

7.5 Conclusion

The results obtained in this part of the study determined that the nanocomposite could be successfully seeded with HUVEC using an achievable cell density and a 24 hour seeding period. Furthermore the use of different passage numbers of HUVEC to achieve adequate numbers of cells should not result in a problem when investigating gene expression as the expression was demonstrated to be stable over a wide passage number. These studies validated the proposed model for seeding nanocomposite conduits and provided a base from which to carry out the investigations into the effect of flow to be carried out.

8

The effect of shear stress on human endothelial cells seeded on cylindrical conduits: An investigation of gene expression

8.1 Introduction

Steady progress in tissue engineering has produced a range of materials that are capable of sustaining tissue ingrowth and limited regeneration. Artificial skin for the healing of chronic wounds or burns is the most marked success (488-490). The engineering of more complicated three-dimensional tissues and organs has been a greater challenge (491;492). Many of the materials aimed for these applications are well characterized chemically and mechanically (493;494). Modulus, strength and fatigue properties can be modelled and predicted for numerous polymers (493;495-497). Degradation rates and corrosion resistance can be tailored by alterations in composition. Little is known, however, about the physiological impact of these materials on the cells they contact in the body. Cells interacting with novel biomaterials may exhibit distinct patterns of gene expression depending on the molecular nature of the surface they are contacting. Little is known about how cells respond on a molecular level to tissue engineering materials.

At present, attempts to seed EC on vascular prosthesis materials are problematic with the major concern being the low number of EC that remain on the graft surface after exposure to *in vivo* shear stress. As reviewed in Chapter 2, conditioning of seeded EC by applying *in vitro* shear stress prior to implantation has been demonstrated to improve cell retention (214) and decrease cell loss post implantation (338). Laminar shear stress maintains normal endothelial structure and function. Turbulent flow and local shear gradients activate endothelial cells and induce a pro-atherogenic state. This reduces expression of eNOS and causes increased expression of vasoconstrictor and pro-inflammatory factors. The pulsatile pattern of shear stress also affects the endothelium. Thus, rapidly changing flow and oscillatory flow with flow reversal and low net flow tends to induce a more pathologic state compared with laminar flow or oscillatory flow that remains unidirectional. The precise molecular mechanisms that mediate the shear stress response are unknown. Many *in vitro* studies of gene expression have been carried out on monolayer's of EC cultured on flat glass or polystyrene and exposed to shear stress (263;498;499). These studies are two-dimensional models where the characteristics of the flow and the interactions of the cells with the material are likely to be very different from the clinical scenario in which a cylindrical graft is employed.

As evaluated previously, the major reason for the lack of such studies has been due to the difficulty in extracting mRNA from EC seeded on a cylindrical graft surface. In Chapter 5, this problem was examined and a suitable method of extracting functional and viable mRNA from cell seeded cylindrical vascular grafts was identified (500). So far, this thesis has also gone through evaluating the biocompatibility of the nanocomposite as well as the design of compliant cylindrical nanocomposite grafts and determining hybrid-grafts. Using these established systems, this chapter progressed onto assessing, the effects of physiological flow on seeded cylindrical grafts. There are no other reports in the literature of this being investigated apart from this study (501).

The aim of this study was to first time assess the effects of physiological shear stress on the gene expression of human EC seeded in a cylindrical vascular graft. Gene expression was investigated in HUVEC seeded onto nanocomposite conduits following the application of physiological shear stress for one and four hours. In a further investigation conduits exposed to flow were allowed to remain static for four hours to

determine if expression returned to pre-flow levels. To validate the methods employed identically sized and seeded glass conduits were also examined.

The genes chosen for study were GAPDH, TGF-β1, COL-1 and PECAM-1. As reviewed in Chapter 2, GAPDH is a constitutively expressed house keeping gene that has been well characterised has been shown to be expressed in constant amounts across cell lines. TGF-β1 is involved in diverse biological processes, such as cell proliferation, migration, differentiation, survival, and cell-cell and cell-matrix interaction and has been demonstrated to be key to the formation of ECM by EC under flow (399;502). The endothelial marker, PECAM-1 is expressed on EC and functions as an adhesion and signalling molecule between adjacent endothelial cells and between endothelial cells and circulating blood elements (503;504). The expression of COL-1 was studied as collagens play a role in cell adhesion that is important for maintaining normal tissue architecture and function (505).

8.2 Materials and Methods

8.2.1 Preparation of nanocomposite polymer conduits

The synthesis of nanocomposite has been described in Chapter 3 (70). The nanocomposite was extruded into tubes of 5 mm internal diameter and 5 cm in length using the extrusion-phase inversion protocol described in Chapter 6.

8.2.1.2 Glass conduits

Glass conduits of 5 cm length and 5 mm internal diameter were manufactured to order (Scientific Laboratory Supplies, Wilford, U.K.). Conduits were sterilised by autoclaving prior to use.

8.2.2 Human umbilical vein cell culture

HUVEC at passage three were used in this experiment as described in Chapter 3 (444).

8.2.3 Conduit seeding

Glass and nanocomposite conduits were seeded with HUVEC at 1.2 x 10^4 cells/cm^2, as assessed in Chapter 7. Cells were added as a suspension to each conduit, the ends of the conduit plugged, and the conduits rotated 90° every 15 minutes for 2 hours to achieve an even covering of HUVEC on each conduit. Conduits were then left overnight at 37 ° C and 5 % CO_2/95 %O_2 for efficient cell adhesion and used the next day.

8.2.4 Assessment of seeding efficiency and cell viability

Viability of seeded cells was assessed using an Alamar blue™ assay as described previously. Following overnight seeding conduits were washed with PBS and the washings collected for cell counting to assess seeding efficiency. 1 ml of Alamar blue™ (10 %) in complete medium was added to each conduit and incubated for four hours at 37° C and 5 % CO_2/95 %O_2. Duplicate 100 µl samples were then removed and the absorbance's read spectroscopically. Cell viability on glass and nanocomposite was also assessed following exposure to one or four hours of physiological shear stress or static conditions.

8.2.5 Application of physiological pulsatile shear stress on cell

To test the flow shear stress on the EC, a physiological pulsatile flow circuit was used to simulate the cardiovascular system (as described in Chapter 3). The system has been validated extensively for physiological parameters (214) and has been described in used in previous studies of flow (36). In brief the model simulates specifically a given artery such as coronary or lower limb flow waveforms (See caption of Figure 3-2 in Chapter 3 for further details). The flow circuit was primed with cell culture medium adjusted for viscosity. The whole circuit was kept in sterile conditions. The experimental protocol carried out is summarised in Figure 8-1. Seeded conduits were randomly split into two groups, static and flow exposed. Static conduits were placed in fresh medium and incubated at 37°C for either one or four hours. Flow exposed conduits were placed in the flow system and a set flow rate of shear stress was applied for either one or four hours. In a further study following one and four hours of flow or static exposure, a

subset of conduits were washed with PBS and placed in fresh medium and incubated under static conditions for a further four hours. This group was labelled as the recovery period group.

Figure 8-2 shows a typical distension and pressure waveform generated from measuring distension and pressure versus time using an ultrasound artery wall tracking system (Wall Track, Pie Medical Systems, Maastricht, Netherlands) and Millar catheter (Millar Instruments, Houston, TX, USA). Examples of previously generated plots of the velocity profile inside the artery and shear rate on the wall is shown in Figure 8-3. The haemodynamic data including peak and mean shear stresses are computed and recorded in Table 8-1.

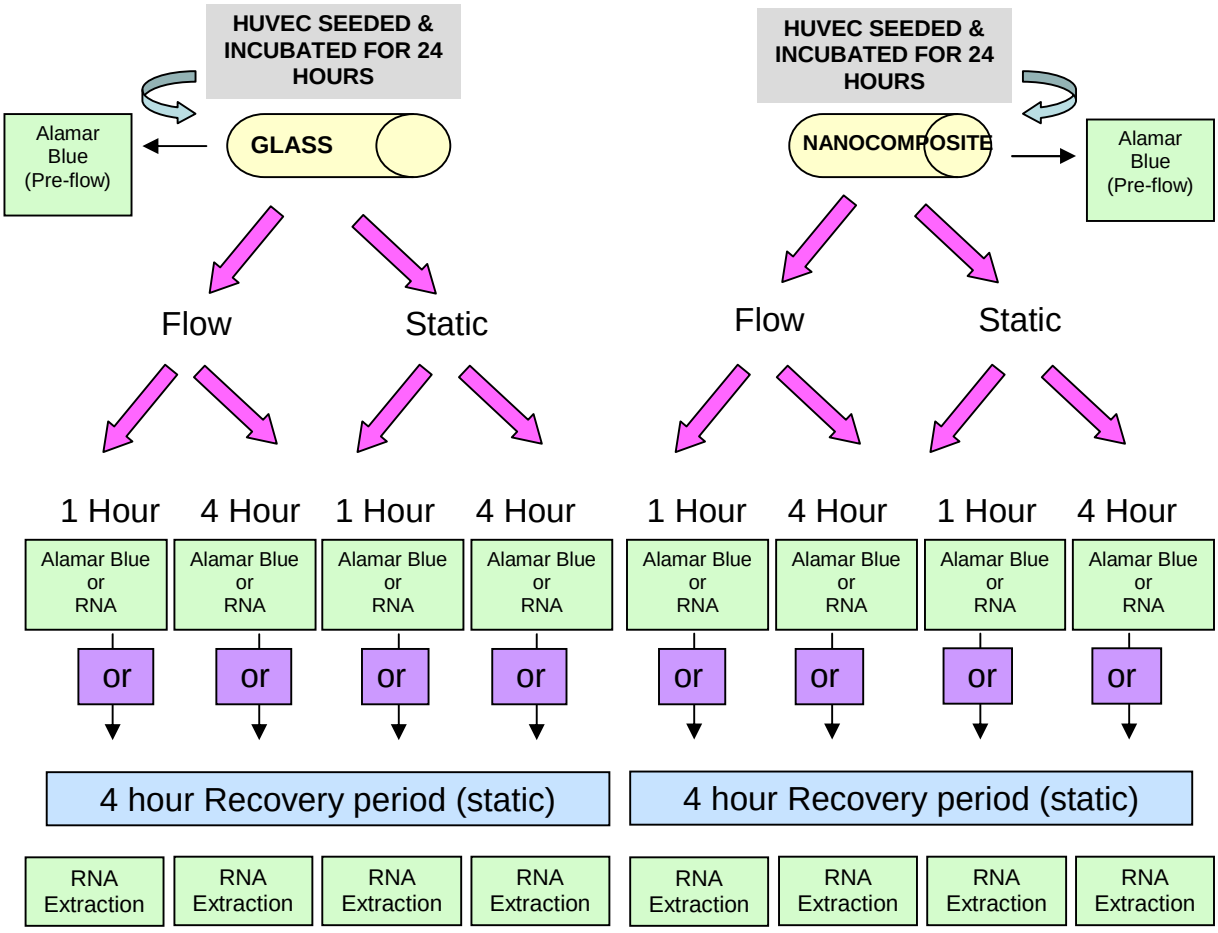

Figure 8-1. Flow chart representing the experimental protocol carried out. Glass and nanocomposite conduits were exposed to 1 or 4 hour of static or physiological flow exposure. A further subset to this experiment includes a recovery period of 4 hour static of conduits prior to 1 or 4 hour static or flow.

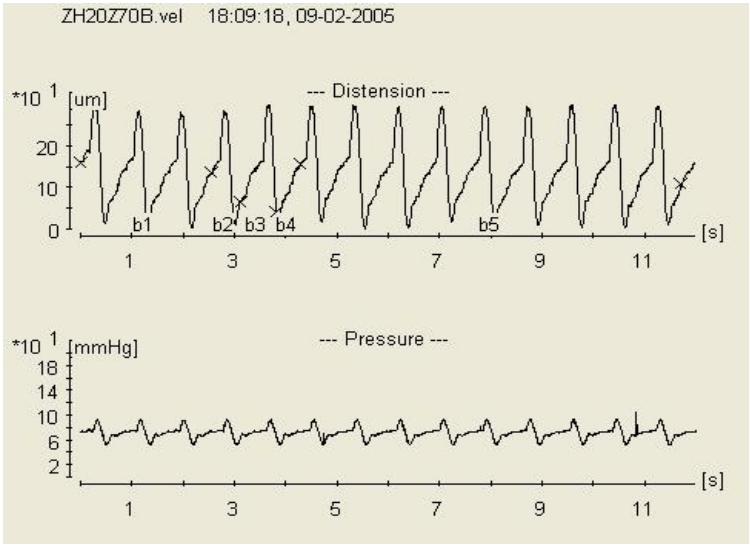

Figure 8-2. Vessel distension detected using an ultrasound wall tracking system and pressure determined using a Millar Mikro-tip catheter transducer from circuit in Figure 3-2 (see Chapter 3).

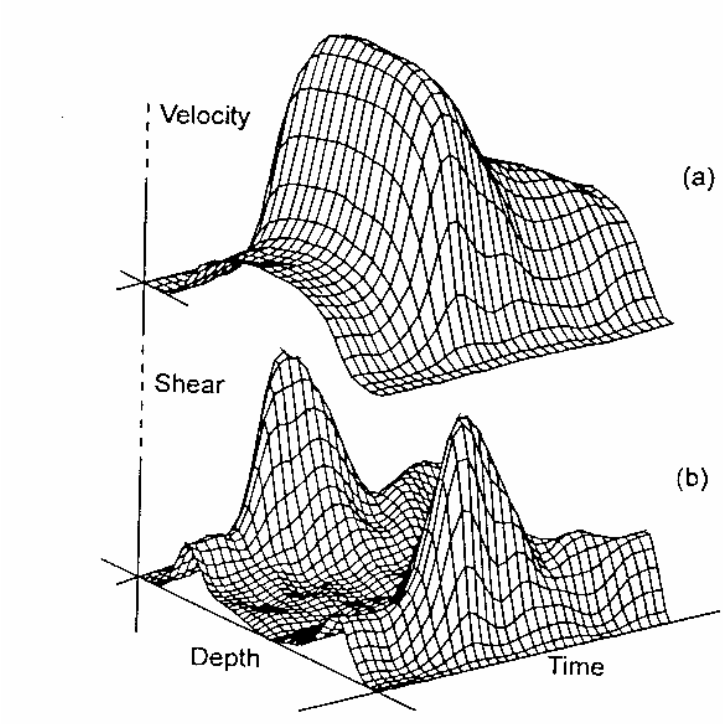

Figure 8-3. A typical time dependent velocity (a) and shear rate distribution (b) acquired by the duplex ultrasound coupled with on-line vessel wall tracking system.

Table 8-1. Summary of haemodynamic parameters measured.

Input parameters	Value	Computed parameters	Value
Frequency of pulsatile cycle	1 Hz	Inlet length (mm)	60
Internal diameter of conduit	5 mm	Peak Reynolds number	512
Temperature	37 ± 1.4	Mean shear stress (dyn/cm^2)	14.0 ± 3.2
Seeded graft length (mm)	50	Systolic shear stress (dyn/cm^2)	30.4 ± 5.8
Seeded density (cells/cm^2)	1.2 x 10^4	Diastolic shear stress (dyn/cm^2)	62.7 ± 9.7
Pressure systolic (mmHg)	120 ± 5	Mean velocity (mm/sec)	436 ± 20
Pressure diastolic (mmHg)	70 ± 6		
pH	7.3 ± 0.1		
pO2 (kPa)	21 ± 2		
pCO2 of solution (kPa)	4.2 ± 0.2		
Viscosity of solution (poise)	0.035 ± 0.2		

8.2.6 RNA extraction and PCR

Following exposure to experimental conditions cells were removed from conduits by washing with sterile PBS and then trypsinising using 1ml of trypsin-EDTA (0.25 %) which was added for 5 minutes incubation at 37°C as described in Chapter 4. RNA was then extracted by using a "Qiagen RNeasy™" kit.

The RNA concentration and purity was calculated by measuring the absorbance at 260 nm and 280 nm using. The quality of the RNA was assessed by 2 % agarose gel electrophoresis and the mRNA obtained was used for PCR of GAPDH, TGF-β1, COL-1 and PECAM-1 genes (Table 8-2). RT-PCR was performed using a one-step PCR kit. For sample obtained from the glass conduits and nanocomposite conduits, 0.5 μg and 0.1 μg of template RNA was used respectively. RNase free water was added to give a total volume of 50 μl. Cycle conditions for GAPDH, 40 cycles (94°C, 50°C, 72°C); TGF-β1, 35 cycles (95, 55, 60 °C); PECAM-1, 35 cycles (94°C, 50°C, 72°C) and COL-1, 35 cycles (94°, 59° and 72°). Amplification was carried using a MasterCycler Gradient PCR machine. PCR products were analysed by 2% agarose gel electrophoresis and semi-quantified using a GeneGenius darkroom with 'GeneSnap' version 6.02. GAPDH band

served as the internal standard to normalise TGF-β1, COL-1 and PECAM-1 signals, since GAPDH is constitutively expressed in HUVEC.

Table 8-2. GAPDH, TGF-β1, PECAM-1 and COL-1 primer sequences.

Locus	Sense (5'-'3)	Antisense (5'-'3)
GAPDH	GAAGGTGAAGGTCGGAGT	GAAGATGGTGATGGGATTTC
TGF-β1	CACCTGCAAGACTATCGACAT	TCGGAGCTCTGATGTGTTGAA
PECAM-1	GCTGTTGGTGGAAGGAGT	GAAGTTGGCTGGAGGTGCTC
COL-1	AACGGCAAGGTGTTGTGCGATG	AGCTGGGGAGCAAAGTTTCCTC

8.2.7 Scanning electron microscopy

Seeded nanocomposite conduits were examined by ScEM pre- and post-flow to visualise whether cells were present on the grafts surface. ScEM images were also taken after trypsinisation of the cells from the conduit in order to determine that complete cell removal was obtained for RNA extraction. Due to the material nature of the glass tubes, ScEM was not performed for these samples.

8.2.8 Data analysis and statistical methods

The experiments were repeated four times. RNA quantity is presented in mean ± SEM. All statistical analysis utilised the Student's t-test comparing flow to static conditions.

8.3 Results

8.3.1 Assessment of seeding efficiency and viability

An Alamar blue™ assay pre-flow following overnight seeding showed no significant difference in seeding efficiency. Viable cells were present on both the glass conduit group and the nanocomposite conduit group following exposure to flow or

static conditions (Figure 8-4, A (Glass) & B (nanocomposite)). A significant decrease (Student's t-test; $P<0.05$) in cell viability was observed in nanocomposite post four hours of flow.

ScEM images showed viable cells present on nanocomposite prior to flow (Figure 8-5, A & B). The efficiency of removal of the cells from nanocomposite is shown in Figure 8-5 C; no cells were left on the graft following trypsinisation.

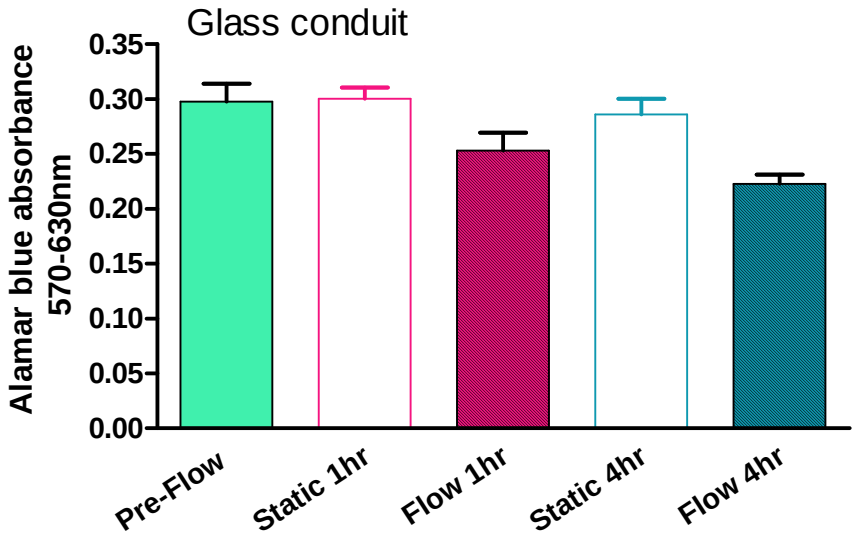

A

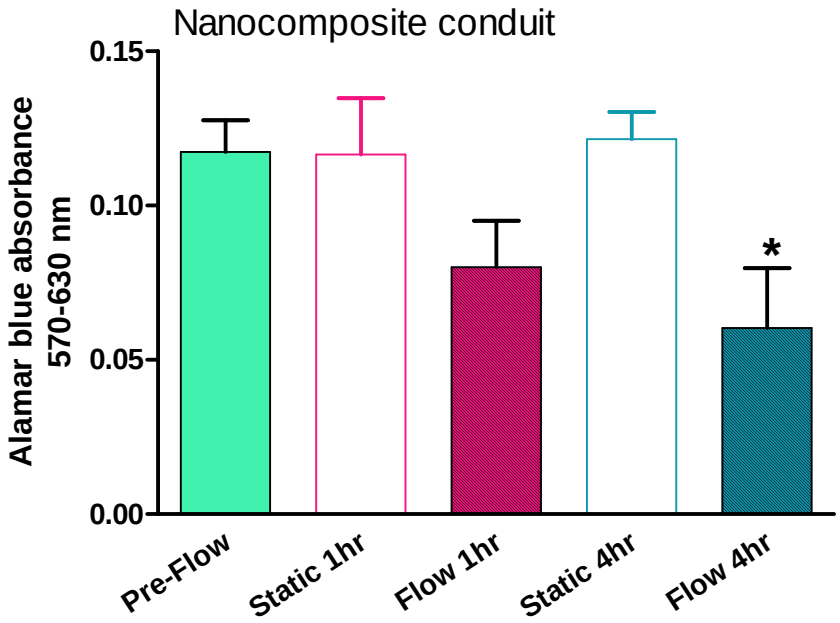

B

Figure 8-4. Cell seeding efficiency and viability post 1 and 4 hour static and flow exposed on A) glass and B) nanocomposite conduits. *P < 0.05 flow were comparison to static using Student's t-test.

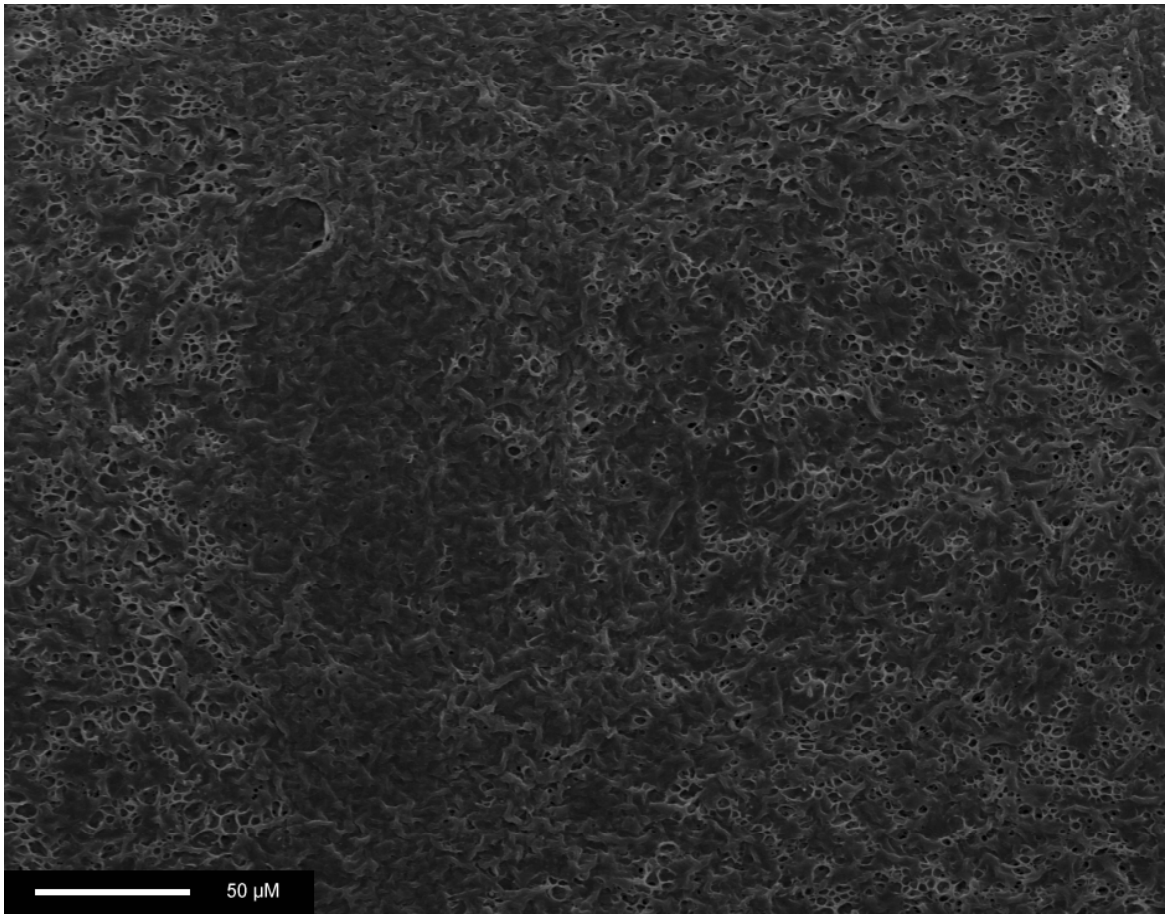

A

Figure 8-5 A. ScEM of a nanocomposite conduit: unseeded.

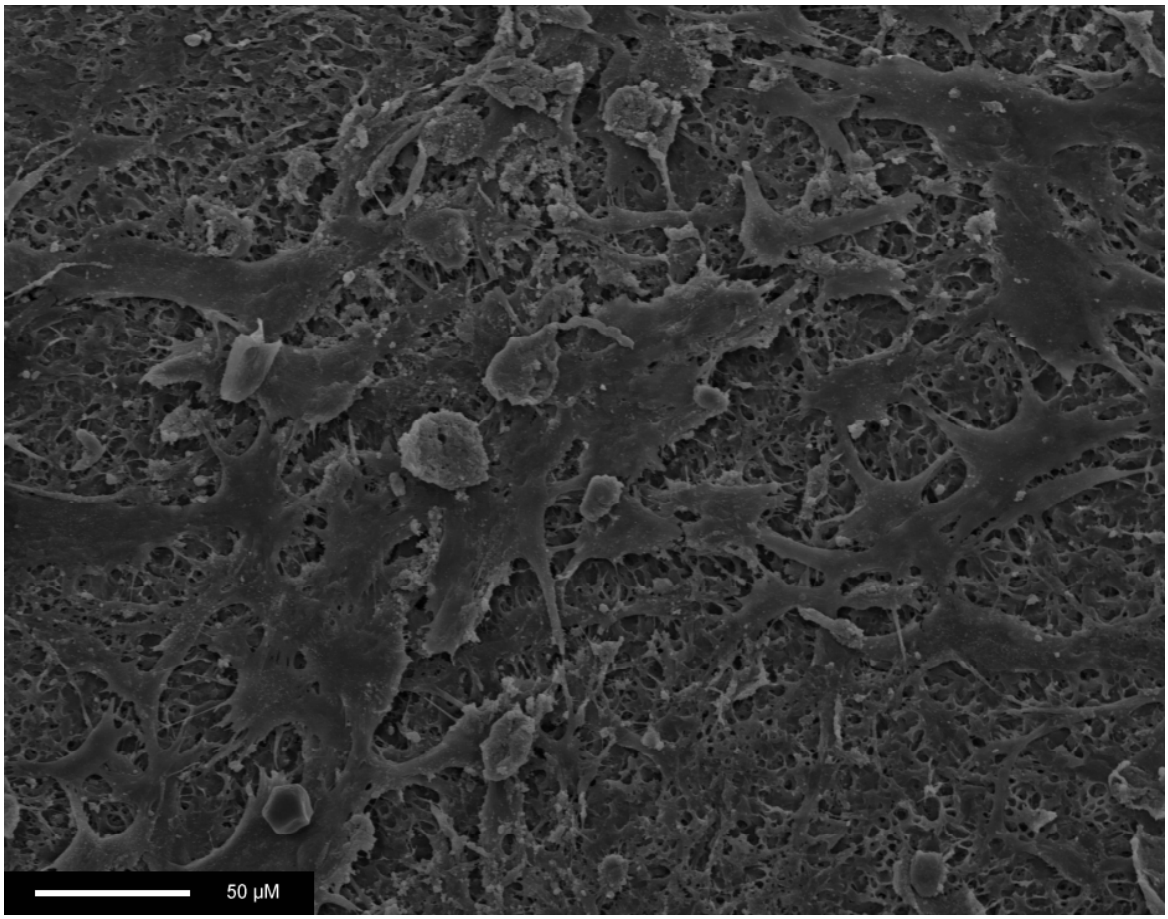

B

Figure 8-5 B. ScEM of a nanocomposite conduit: seeded with HUVEC at 1.2×10^4 cells/cm^2 overnight.

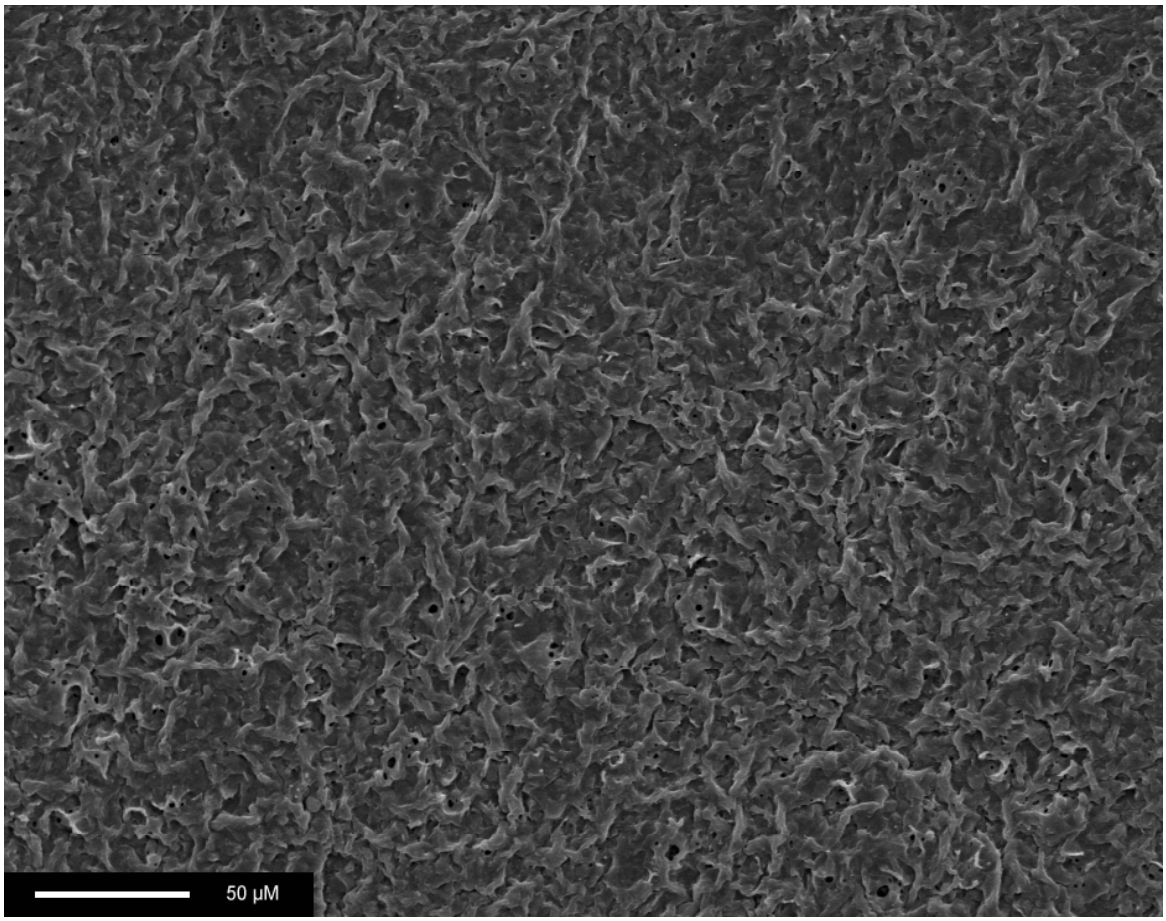

C

Figure 8-5 C. ScEM of a nanocomposite conduit after trypsinisation to remove HUVEC.

8.3.2 Assessment of quantity and quality of RNA extracted

The purity and amount of RNA extracted from HUVEC are shown in Table 8-3. The purity was high in all samples and in all cases purity was greater than 95%. Levels of isolated RNA were lower after flow in both glass and nanocomposite conduits. Nanocomposite conduits showed a significant reduction (Student's t-test; $P<0.05$) in RNA levels after flow and recovery period suggesting that cell loss was greater on the nanocomposite; the reduction on glass was not significant.

8.3.3 Analysis of GAPDH, TGF-β1, COL-1 and PECAM-1 PCR products

Figures 8-6 A & B show 2% agarose gels of the PCR products resulting from a one hour and four hour exposure respectively to either static conditions or flow for HUVEC seeded on the glass conduits.

Figures 8-6 C & D show PCR products resulting from a one hour and four hour static or flow exposure followed by a four hour static recovery period on the glass conduits.

Similarly, Figures 8-6 E & F show 2% agarose gels of the PCR products amplified from one hour and four hour exposure respectively to either static conditions or flow for HUVEC seeded on nanocomposite conduits. Figures 8-6 G & H show the PCR products resulting from a one hour and four hour static or flow followed by a four hour static recovery period on the nanocomposite conduits.

The mRNA levels of GAPDH remained relatively constant in static and flow samples, and slight changes were observed in the other genes (see below). Whilst not fully quantified this allows an idea of increase and decrease of gene expression.

Table 8-3. RNA purity and yield was measured at absorbance of 260 nm and 280 nm. *P<0.05 compared to static, Student's t-test.

(a) Post exposure to pulsatile flow		
Conduit and treatment	RNA Quantity (ng/μl) (mean ± SEM)	RNA Purity (260 nm/280 nm Absorbance)
Glass Conduit		
1 hour static	42.7 ± 4.6	1.813
1 hour physiological flow	34.3 ± 1.4	1.800
4 hours static	39.0 ± 3.4	1.903
4 hours physiological flow	44.7 ± 6.4	1.876
Nanocomposite conduit		
1 hour static	25.2 ± 4.5	1.960
1 hour physiological flow	6.7 ± 2.2*	1.953
4 hours static	28.4 ± 5.3	1.957
4 hours physiological flow	6.6 ± 0.8*	1.877

(b) Post Recovery Period (Static)		
Conduit and treatment	RNA Quantity (ng/μl) (mean ± SEM)	RNA Purity (260 nm/280 nm Absorbance)
Glass Conduit		
1 hour static	35.6 ± 4.9	1.956
1 hour physiological flow	40.0 ± 1.1	1.970
4 hours static	34.9 ± 2.8	1.913
4 hours physiological flow	44.1 ± 4.5	1.967
Nanocomposite conduit		
1 hour static	24.4 ± 2.6	1.946
1 hour physiological flow	10.2 ± 1.8*	1.903
4 hours static	25.0 ± 3.9	1.900
4 hours physiological flow	8.6 ± 2.2*	1.967

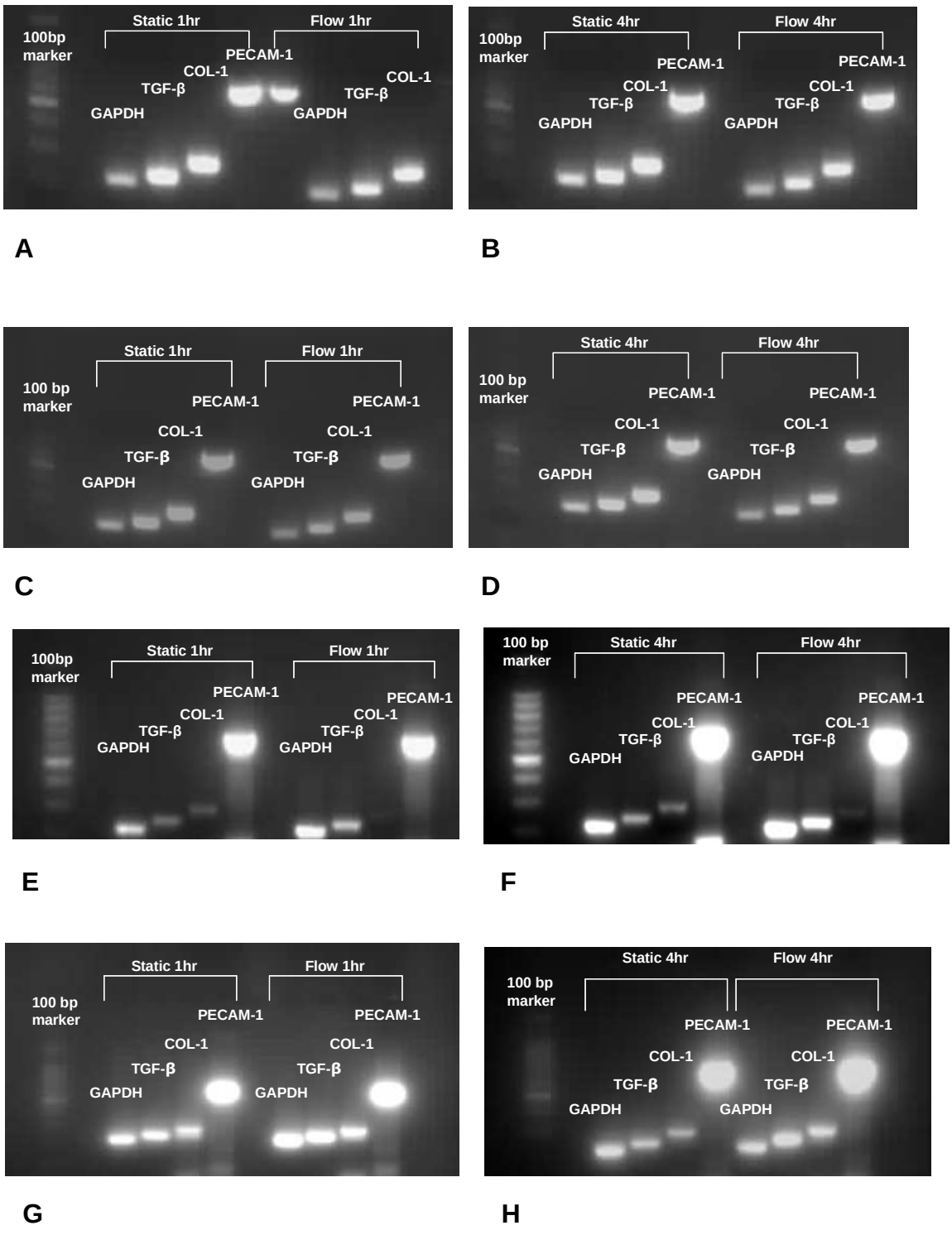

Figure 8-6. Agarose gel (2 %) of PCR analysis from RNA obtained from HUVEC seeded A) on glass conduits following 1 hour static or physiological flow exposure; B) on glass conduits following 4 hour static or flow; C) on glass conduits post recovery period prior to 1 hour static or flow; D) on glass conduits post recovery period prior to 4 hour static or flow; E) on nanocomposite conduits following 1 hour static or flow, F) on nanocomposite conduits following 4 hour static or flow; G) on nanocomposite conduits post recovery period prior to 1 hour static or flow; and H) on nanocomposite conduits post recovery period prior to 4 hour static or flow.

8.3.4 Intensity of gene expression

Relative levels of TGF-β1, COL-1 and PECAM-1 were determined using Syngene. After normalisation by the intensity of GAPDH mRNA bands obtained from static and flow, the levels of gene expression was examined.

Figure 8-7 A & B show the intensity of gene expression resulting from a one hour and four hour exposure respectively, to either static conditions or flow for HUVEC seeded on the glass conduits. Significant increase in TGF-β1 ($P < 0.05$) and COL-1 ($P < 0.05$) mRNA levels was observed after one hour of flow compared to static one hour. There was no significant increase in PECAM-1 mRNA level after one hour of flow. A further significant increase in expression for all genes ($P < 0.01$) was observed after four hours of flow. After four hours recovery, gene expression following one hours flow (Figure 8-7 C) showed increased differences in expression between static and flow conditions. Significant ($p < 0.01$) differences were seen for all genes. This was not the case when four hour flow was allowed a period of recovery (Figure 8-7 D) where all significance was lost after recovery.

Figure 8-7 E & F shows the intensity of gene expression from static and flow one and four hour exposure respectively, for HUVEC seeded on nanocomposite conduits. Gene expression was increased in the flow groups on nanocomposite. Significant ($P < 0.01$) increases under flow were observed in TGF-β1 and COL-1 at four hours. PECAM-1 also showed a significant ($P < 0.05$) increase post four hours of flow. After recovery no significant differences in gene expression were observed for either one or four hours flow (Figures 8-7 G and H respectively).

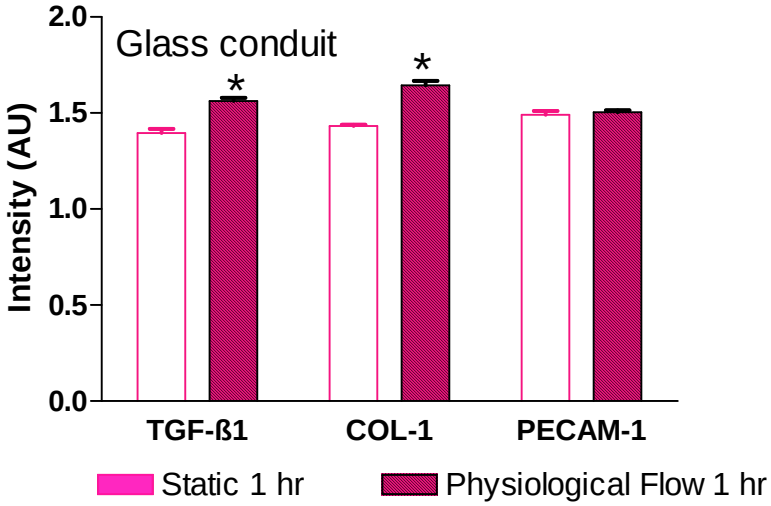
Glass conduit
Intensity (AU)
2.0
1.5
1.0
0.5
0.0
*
*
TGF-ß1
COL-1
PECAM-1
Static 1 hr
Physiological Flow 1 hr

A

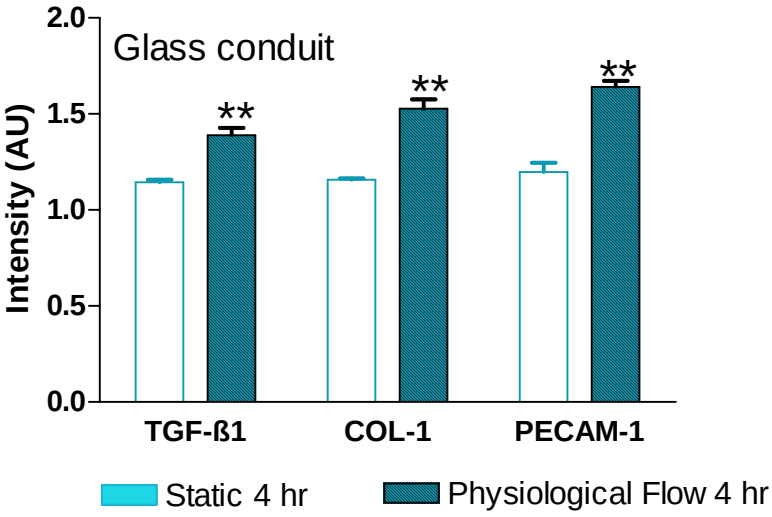
Glass conduit
Intensity (AU)
2.0
1.5
1.0
0.5
0.0
**
**
**
TGF-ß1
COL-1
PECAM-1
Static 4 hr
Physiological Flow 4 hr

B

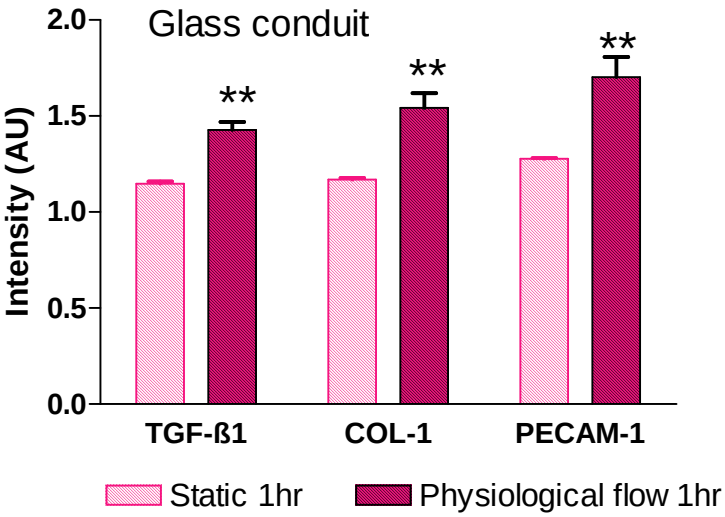
Glass conduit
Intensity (AU)
2.0
1.5
1.0
0.5
0.0
**
**
**
TGF-ß1
COL-1
PECAM-1
Static 1hr
Physiological flow 1hr

C

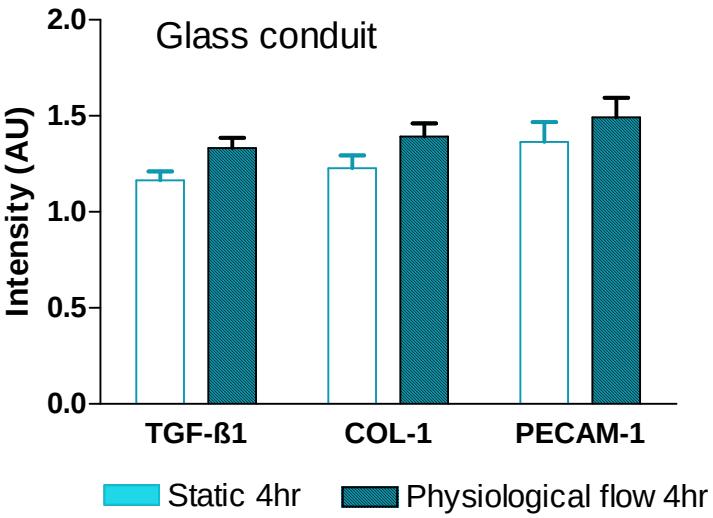
Glass conduit
Intensity (AU)
2.0
1.5
1.0
0.5
0.0
TGF-ß1
COL-1
PECAM-1
Static 4hr
Physiological flow 4hr

D

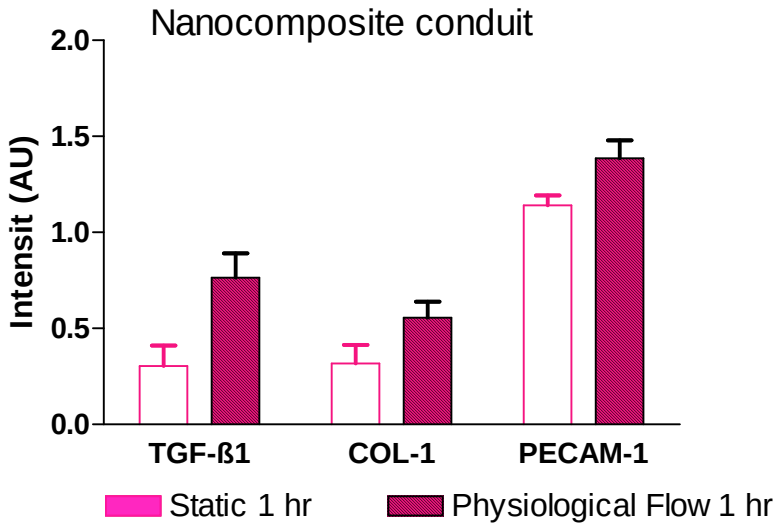
Nanocomposite conduit
Intensit (AU)
2.0
1.5
1.0
0.5
0.0
TGF-ß1
COL-1
PECAM-1
Static 1 hr
Physiological Flow 1 hr

E

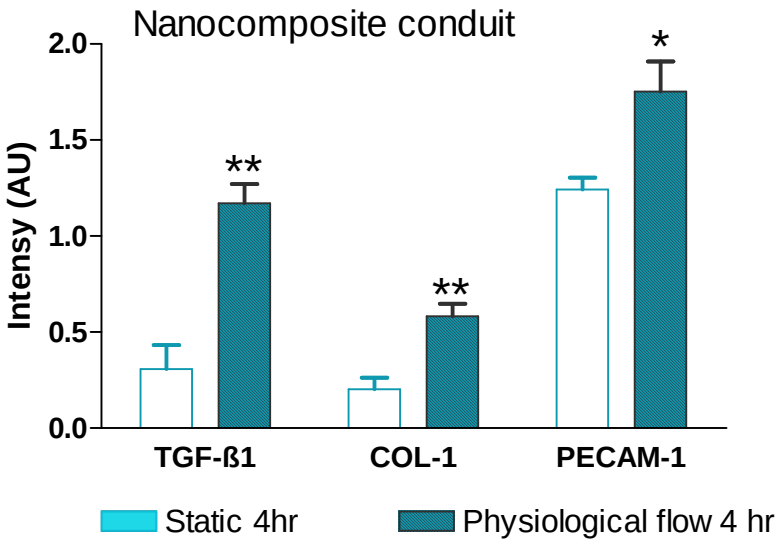
Nanocomposite conduit
Intensy (AU)
2.0
1.5
1.0
0.5
0.0
**
**
*
TGF-ß1
COL-1
PECAM-1
Static 4hr
Physiological flow 4 hr

F

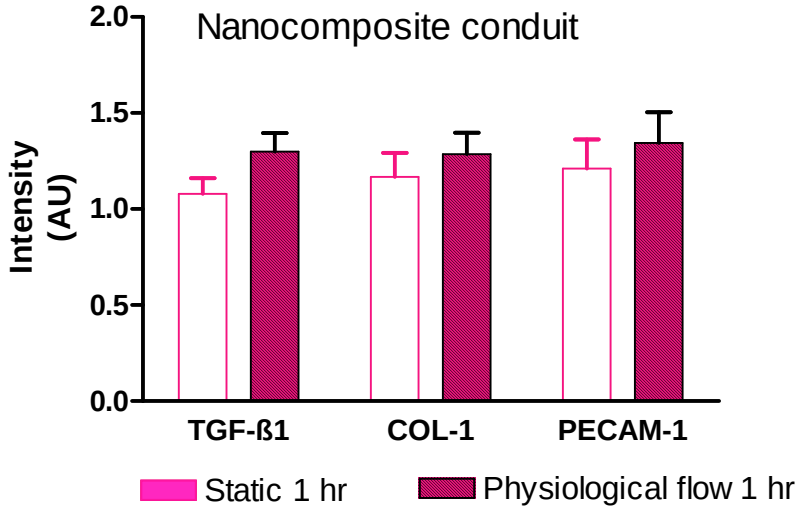

G

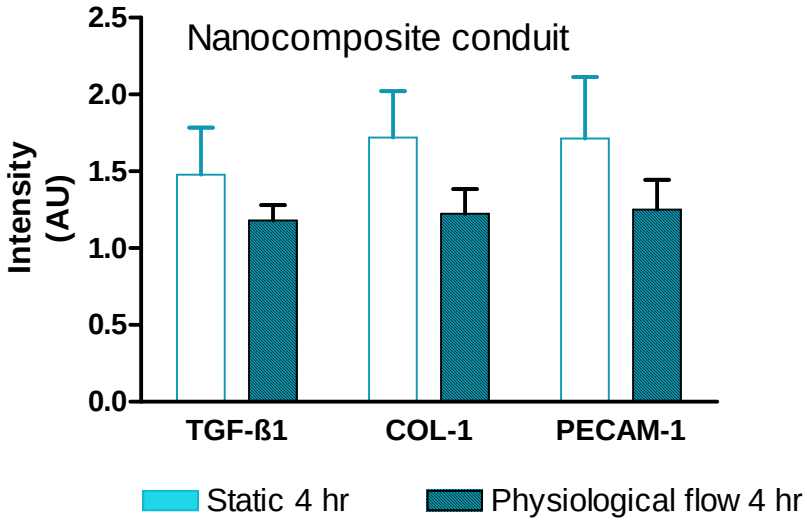

H

Figure 8-7. Intensities of gene expression from RNA obtained from various sources. The Figure shows the intensities of gene expression in arbitrary unit (AU) from RNA obtained from (A) glass conduits following 1 h static or physiological flow exposure; (B) glass conduits following 4 h static or flow; (C) glass conduits post recovery period prior to 1 h static or flow; (D) glass conduits post recovery period prior to 4 h static or flow; (E) nanocomposite conduits following 1 h static or flow; (F) nanocomposite conduits following 4 h static or flow; (G) nanocomposite conduits post recovery period prior to 1 h static or flow; and (H) nanocomposite conduits post recovery period prior to 4 h static or flow. TGF-β1, COL-1 and PECAM-1 mRNA levels were normalized by GAPDH mRNA level. A significant increase in gene expression comparing static with flow conditions for each gene at the same time period is indicated by either '*' ($P<0.05$ using Student's t test) or '**' ($P<0.01$ using Student's t test).

8.4 Discussion

Here described is a study of cell–biomaterial interactions at the level of gene expression. This work is a step toward the use of mRNA analyses to get information for the biological performance of a tissue engineering biomaterial. Although valuable information can be obtained from animal studies, animal studies are often not directly applicable to human cell/biomaterial interactions.

In order to define how EC respond to shear stress in a tubular model, nanocomposite conduits were produced as demonstrated earlier in this thesis. Nanocomposite conduits were successfully seeded with HUVEC then exposed to flow. The markers of gene expression employed in the present study were chosen to maximise the amount of information obtained from the amount of RNA isolated in these initial experiments and investigate two key aspects of EC response to flow: namely ECM production and adhesion molecule expression. As a validation of the techniques employed glass conduits of the same length and diameter were seeded with HUVEC and treated in the same way as the nanocomposite conduits as a positive control as flat glass surfaces have been used in many studies (504;506).

The initial Alamar blue™ results demonstrate that both nanocomposite and glass conduits were successfully seeded with viable HUVEC and those cells remained viable over the course of the exposure to flow. As might be expected, more cells adhered to the glass surface than the nanocomposite as glass has been proven to be a successful surface for cell growth. In the case of the nanocomposite conduits, the successful seeding was confirmed by ScEM studies that showed cells present on the conduit material. The fact that a confluent layer of cells was not observed on the conduit prior to flow may be due to the relatively short seeding time (24 hours), which is a more clinically realistic seeding time compared with allowing the cells to grow for a period of days or weeks on the conduit which would result in a confluent cell coverage.
The culture of HUVEC on flat sheets of tissue culture plastic or glass under conditions of physiological flow results in the cells becoming aligned to flow in a similar manner to that seen *in vivo* (252). However, when exposed to static culture a well documented change in phenotype occurred with a characteristic cobble stone appearance developing.

It was hypothesised that such an alteration in growth characteristics would also result in a more *in vivo* EC like gene expression. In the present study, this was tested by examining the expression of the EC surface protein PECAM-1. PECAM-1 (also known as CD31) is a highly abundant cell-surface glycoprotein expressed on EC that is involved in EC tube formation (refer to review Chapter 2). PECAM-1 may act as a docking molecule, promoting cell-cell adhesion thereby allowing other proteins, such as integrins, to further stabilise the assembly of vascular structures (507). TGF-β1 is a known stimulant of ECM production that is localised in the intima of arteries (392) and COL-I is a fibrous, ECM protein with high tensile strength (263). After one hour exposure to flow, no significant difference in gene expression was observed for any of these genes for the cells present on the nanocomposite. A four hour static recovery period following exposure to one hour flow similarly resulted in no significant change in gene expression. Exposure to flow for a longer four hour period demonstrated significant increases in gene expression for all genes investigated compared with cells maintained under static conditions. Following a four hour recovery period however, there was no significant increase in gene expression levels compared with cells maintained under static conditions. HUVEC seeded on glass conduits showed similar results although there was a significant increase in TGF-β1 and COL-1 expression after 1 hour of flow which was maintained after a static recovery period.

The increased expression of the COL-1, PECAM-1 and TGF-β1 genes after four hours exposure to flow may be related to the cells strengthening their attachment to the nanocomposite substrate under physiological levels of shear stress. The up-regulation of matrix production under flow has already been defined in flat sheets of cultured cells and *ex vivo* EC (508;509). Gene expression one hour post flow was relatively unaltered in the case of the nanocomposite conduits, suggesting that the change in gene expression when exposed to flow is not immediate and is dependent on the time of exposure to flow. This change may also be transitory as after a four hour static recovery period following exposure to flow, there was no significant difference in gene expression. Studies on laminar shear stress have been reported to demonstrate that gene expression is induced in a time-dependant manner (504). The application of shear stress to EC in static culture has been shown to cause a transient increase in the expression of a large number of genes with most of the genes investigated down-regulated during sustained

application of shear stress (24 hours) (260). In Chapter 2, the expression of the genes under study were reviewed

Several groups have looked at gene expression in a comparable way to this thesis. Comparing such studies is complicated by the differences in conditions used by different groups. Flow conditions and timings are not consistent so direct comparison is not possible. To summarise these findings; one study looked at HUVEC without flow and failed to find any expression of TGF-β1, the isoform studied was not give (314). A second study looked at TGF-β1 under shear stress of 15dynes and found that expression was increased over 24 hours.

Looking at the specific isoforms of TGF-β1 reveals that expression TGF-β1 is seen to rise under conditions of shear stress. Like our study where expressions were increased under shear stress conditions two other studies demonstrate increased expression under shear stress. The first looked at expression after 24 hours under an unspecified stress (510) while the used cyclic stress between 6 and 24 hours (399). Both demonstrated an increase in TGF-β1 as demonstrated by our studies. TGF-β2 was studied by one group who studied it in addition to TGF-β1 (510). They demonstrated a reduced expression under similar flow conditions.
Findings such as this demonstrate the role of TGF-β1 in the production of ECM is important under flow conditions. This appears to be a response to flow that corresponds to a need for increased attachment under flow. The evidence that preconditioning increases TGF-β1 further demonstrates that this may be useful in graft development.

The expression of PECAM-1 has been investigated in EC seeded on vascular graft materials, Dacron coated with fibronectin. In one study (378) HUVEC and adipose microvessels (HAMVEC) were cultured for 1-2 days and the expression of PECAM-1 were determined by flow cytometry and immunofluorescence microscopy. The cells were not stimulated. The expression of PECAM-1 was found to be constitutively expressed with similar mean fluorescent intensities suggesting that its expression is dependent neither on the EC origin nor on the underlying polymer surface. In i*n vivo* studies PECAM-1 has been found to be constitutively expressed on the endothelium of all vessel types (378). In contrast Cenni *et al*, reported the

downregulation of PECAM-1 expression by HUVEC cultured on knitted Dacron (380). It can be hypothesised that a decrease in the expression of PECAM-1 underlies poor adhesion capability of these cells on knitted Dacron and that the lack of fibronectin coating provides no stimulation to the cells to increase attachment molecules.

The data presented in this thesis confirms that PECAM may be affected by the stimulus of cells. We show that on polymer alone and in initial cells taken from tissue culture plastic levels of PECAM expression are not as great as is seen under conditions of shear stress. This evidence further indicates that not only is our nanocomposite better for cell attachment than knitted Dacron but that it promotes EC growth that more closely resembles the *in vivo* situation.

The gene expression changes brought about by exposure to shear stress and stretch are complex in nature. This suggests that a pathway of events may be necessary to trigger the expression of the genes studied here and that the results obtained will be dependant on the time of exposure to flow and the type of flow employed.

Relatively accurate methods to quantify gene expression have been developed, such as Northern blotting or real-time PCR based on the use of fluorogenic probes. Northern blot methods usually require additional time consuming selective chromatography to isolate poly(A)+ (polyadenylated) mRNA and radioactive labelled probes to generate a measurable signal to quantify. Real-time PCR is a quantitative method that is based on the concept of monitoring the PCR reaction in the thermal cycle as it progresses (511;512). Although this technique has a number of advantages, especially in terms of comparative accuracy, it is not widely available at present. In this study, a semi-quantitative approach was successively used to determine RNA expression levels by RT-PCR. This method is based on the use of an internal control, which is a housekeeping gene (GAPDH) (513). This method was chosen due to feasibility in the laboratory, the necessity to study different markers in the same sample and the low yield of RNA.

This study indicates that whilst it is difficult to monitor gene expression when small amounts of RNA are extracted from cells seeded on to artificial conduits and exposed to flow, it is, nonetheless, possible to investigate gene expression under these conditions and obtain useful data. Future studies would benefit from protein analysis to

determine whether changes in gene expression were related to changes in protein levels. The range of gene expression investigated could also be expanded with genes such as the MMP, caspase and growth factors being of great potential interest perhaps by using RNA amplification techniques.

8.5 Conclusion

This study represents an initial investigation that, for the first time, demonstrates that changes in the gene expression of cultured EC on a tubular vascular prosthesis when exposed to shear stress *in vitro* can be determined under more clinically relevant realistic conditions than previously. This is of great importance to the understanding of how cells will react when seeded on such conduits and the mechanism by which exposure to flow affects them and has great potential for future development and further investigation.

9

Shear stress preconditioning of human endothelial cell seeded on compliant nanocomposite conduits: A study of gene expression

9.1 Introduction

The previous chapter shows the effect of physiological (haemodynamics) shear stress on EC gene expression. There it was clear that EC seeded on tubular nanocomposite compliant conduit were viable with appropriate nuclear processes. However it does not address the question of how to optimise EC behaviour on the graft. Some of the observed gene expression and in particular increased PECAM-1 is a reflection of the (often frustrated) attempts of EC to remain adherent in the face of blood flow. There is now a large body of evidence showing extra-corporeal preconditioning as a reliable way of potentiating EC adherence and subsequent function in preparation for the living environment.

Researchers have examined the effect of shear stress preconditioning on vascular grafts but these are lacking in gene expression studies. Preconditioning has been shown to positively influence the development of tissue-engineered grafts. Preconditioning with physiological shear stress using a flow circuit developed in-house can significantly enhance EC retention, viability and morphology. EC seeded onto polymer grafts have specific problems with regard to cell attachment and retention (340). Significantly

studies showed the development of a functional and stable endothelium on the prosthetic vascular graft in response to low shear stress (1-2 dyne/cm^2) (326). The mechanism underlying this improvement is suggested to be regulated by the expression of several factors including growth factors and matrix enhancing factors (514). However, these assumptions have been made upon numerous flow experiments applied to cultured monolayer of cells. As reviewed in Chapter 2, cultured cells seeded on flat surfaces have been exposed to preconditioning flow and the cells molecular response assessed. Preconditioning of EC seeded on vascular grafts with shear stress *in vitro* could be used to improve EC retention and differentiation for subsequent *in vivo* use. Unfortunately there has been a lack of studies on understanding the molecular response of cells to preconditioning when seeded on a tubular graft. In this final chapter, all the studies were combined to investigate the overall aim in the process of developing a small diameter coronary bypass graft. This study develops the previous work further by examining the impact of preconditioning on the gene expression of seeded EC on cylindrical nanocomposite, and exposed to physiological flow rates and pressures. This has been shown to enhance cell proliferation, tissue formation and mechanical properties (326). Conduits were preconditioned by exposure to a low shear stress of 1-2 dynes/cm^2 with or without a 24 hour recovery period and then subjected to physiological shear stress of 15 dynes/cm^2. As assessed earlier the genes analysed were GAPDH, TGF-β1, and PECAM-1. Further to this study the expression of VEGFR-1 and VEGFR-2 was studied.

9.2 Materials and Methods

9.2.1 Preparation of nanocomposite polymer conduits

The synthesis of nanocomposite has been described in detail in Chapter 3. An automated bio-processor employed in Chapter 6 was used to extrude the polymer into conduits with an internal diameter of 5mm and length of 5cm. Conduits were sterilised by autoclaving prior to use.

9.2.2 Human umbilical vein cell culture

HUVEC were isolated from human umbilical cord vein following method described in Chapter 3. Cell numbers were amplified by tissue culture in complete medium. At confluence cells were removed using 0.25% Trypsin-EDTA and split in a 1:2 ratio. Confluent cultures at passage three were used in all experiments.

9.2.3 Conduit seeding

Nanocomposite conduits were seeded with HUVEC at 1.2 x 10^4 cells/cm^2. Cells were added as a suspension to each conduit. The ends of the conduit were plugged and the conduits rotated 90° every 15 minutes for 2 hours to achieve an even covering of HUVEC on each conduit. Conduits were left overnight at 37° C and 5 % CO_2/95 %O_2 and used the following day.

9.2.4 Assessment of seeding efficiency and cell viability

Viability of seeded cells on nanocomposite conduits was assessed using an Alamar blue™ assay as described previously (see Chapter 3). Following overnight seeding conduits were washed with PBS and the washings collected for cell counting to assess seeding efficiency. 1 ml of Alamar blue™ (10 %) in complete medium was added to each conduit and incubated for four hours at 37° C and 5 % CO_2/95 %O_2. Duplicate 100 µl samples were removed and the absorbance's read spectroscopically at wavelengths of 570 nm and 630 nm using a Labsystems Multiscan MS UV visible spectrophotometer. All conduits were washed with PBS prior to exposure to flow. Cell viability on nanocomposite conduits was also assessed following exposure to flow.

9.2.5 Application of preconditioning shear stress on EC seeded nanocomposite conduits

To test preconditioning shear stress on the EC, a physiological pulsatile flow circuit was used to simulate the cardiovascular system (as used in Chapter 8). The system is described in detail in Chapter 3. The model was primed with cell culture medium that was adjusted for viscosity and the whole circuit was maintained under

sterile conditions. The experimental protocol is summarised in Figure 9-1. Seeded conduits were randomly split into two groups (A & B) where preconditioning was tested with or without a static recovery period (see below). Conduits were placed in the flow system and preconditioned at low shear stress rates of 1-2 dynes/cm^2 (low flow) and then subjected to pulsatile physiological shear stress of 15 dynes/cm^2 (physiological flow). The haemodynamic data including peak and mean shear stresses are computed and recorded in Table 9-1.

9.2.5.1 Preconditioning without a 24 hour recovery period

To test the effect of preconditioning shear stress on EC function without a static recovery period, group A conduits were preconditioned with 1 hour low flow (P_1) or 4 hours of low flow (P_4). Control conduits were also included where conduits were placed with fresh culture medium and incubated under static conditions at 37° C and 5 % CO_2/95 %O_2 for 1 hour (S_1) or 4 hours (S_4). All conduits were then subsequently exposed to 4 hours of physiological flow.

9.2.5.2 Preconditioning with a 24 hour recovery period

The effect of preconditioning with a 24 hour static recovery period prior to physiological flow was investigated. After 24 hours of seeding, group B conduits were either preconditioned with 1 hour low flow (PR_1) or 4 hours of low flow (PR_4). Control conduits were incubated under static for 1 hour (SR_1) or 4 hours (SR_4). After static or exposure all conduits were then washed with sterile PBS, placed in fresh culture medium and incubated under static conditions for 24 hours. Post recovery period, all conduits were exposed to 4 hours of physiological flow.

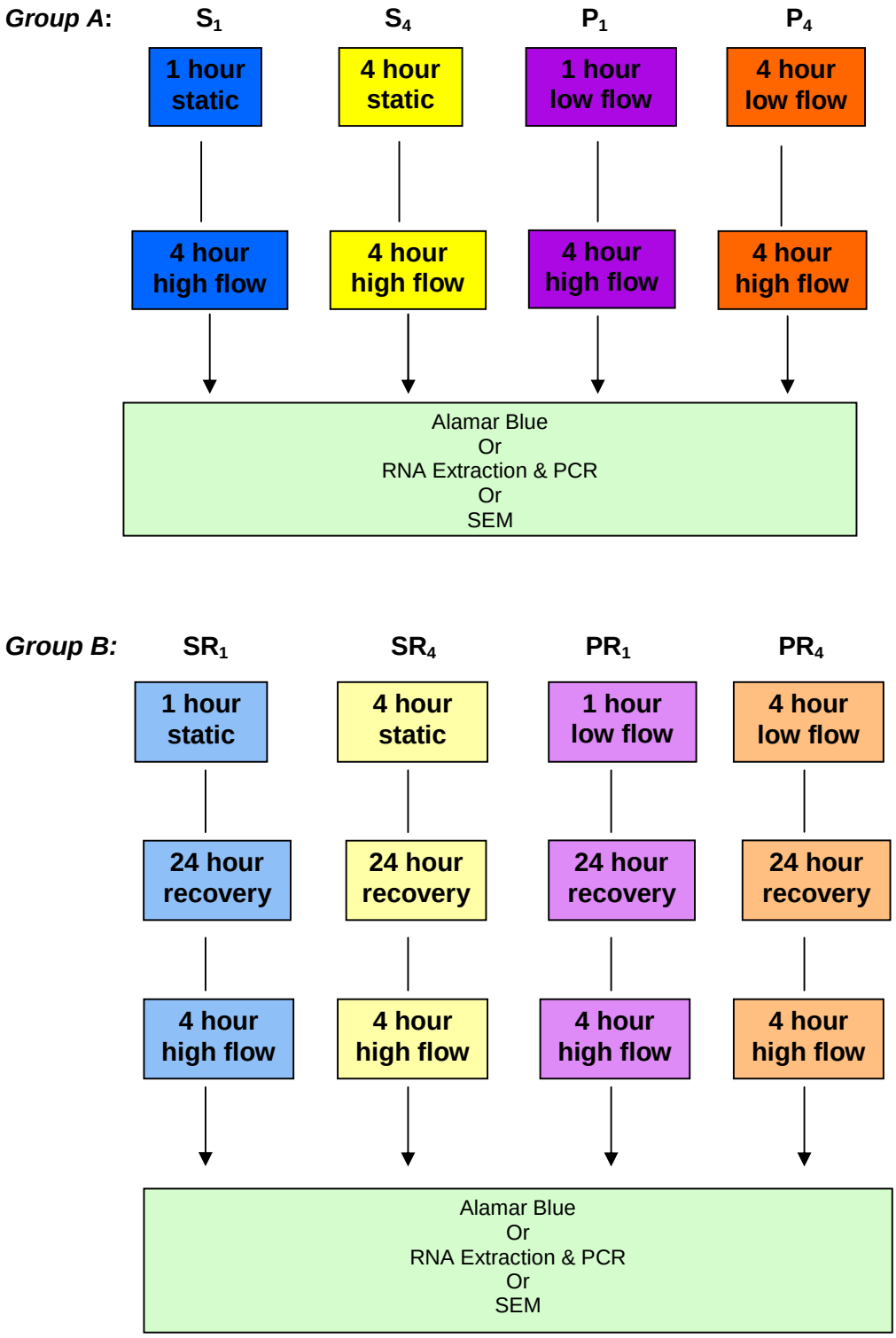

Figure 9-1. Schematic representation of the experimental procedure illustrating a summary of the treatment carried out to each set of conduits. Group A conduits were exposed to either 1 or 4 hours static (S_1 or S_4) or preconditioning (P_1 or P_4) prior to exposure to 4 hours physiological flow while Group B conduits were exposed to either 1 or 4 hours static (SR_1 or SR_4) or preconditioning (PR_1 or PR_4) followed by a 24 hour static recovery period prior to exposure to 4 hours physiological flow.

Table 9-1. Summary of haemodynamic parameters employed in the study.

Input parameters		**Computed parameters**	
Frequency of pulsatile cycle	1 Hz	Inlet length (mm)	60
Internal diameter of conduit	5 mm	Peak Reynolds number	512
Temperature	37 ± 1.4	Mean shear stress (dynes/cm^2)	14.0 ± 3.2
Seeded graft length (mm)	50	Systolic shear stress (dynes/cm^2)	30.4 ± 5.8
Seeded density (cells/cm^2)	1.2 x 10^4	Diastolic shear stress (dynes/cm^2)	62.7 ± 9.7
Pressure systolic (mmHg)	120 ± 5	Mean velocity (mm/sec)	436 ± 20
Pressure diastolic (mmHg)	70 ± 6	Preconditioning shear stress (dynes/cm^2)	1-2 ± 2.9
pH	7.3 ± 0.1		
pO2 (kPa)	21 ± 2		
pCO2 of solution (kPa)	4.2 ± 0.2		
Viscosity of solution (poise)	0.035 ± 0.2		

9.2.6 RNA Extraction and PCR

Following exposure to experimental conditions cells were removed from conduits by washing with sterile PBS and then trypsinising using 1ml of trypsin-EDTA (0.25 %) which was added for 5 minutes incubation at 37^{o}C. RNA was then extracted by using a "Qiagen RNeasy™" kit following the method described in Chapter 3.

The RNA concentration and purity was calculated by measuring the absorbance at 260nm and 280nm and the quality of the RNA was assessed by 2% agarose gel electrophoresis. RT-PCR was performed using a one-step PCR kit for GAPDH, TGF-β1, VEGFR-1, PECAM-1 and VEGFR-2 genes (Table 9-2). A master mix containing 10 µl 5x Qiagen One-Step RT-PCR buffer, 10 µl 5x Q-Solution, 400 µM from each of

the deoxynucleoside triphosphate, 2 µl Qiagen One-Step RT-PCR enzyme mix and 0.5 µM from each of the primers was added. 0.1 µg of template RNA and RNase free water was added to give a total volume of 50 µl.

Cycle conditions for GAPDH and TGF-β1 were 40 cycles (94°, 50° and 72°). For PECAM-1 cycle conditions were 35 cycles (94°, 50° and 72°). Finally for VEGFR-1 and VEGFR-2 cycle conditions were 35 cycles (94°, 59° and 72°). Amplification was carried out using a MasterCycler Gradient PCR machine. PCR products were analysed by 2% agarose gel electrophoresis and semi-quantified using a GeneGenius darkroom with 'GeneSnap' version 6.02. The GAPDH band was used as the internal standard to normalise TGF-β1, VEGFR-1, PECAM-1 and VEGFR-2 signals.

Table 9-2. GAPDH, TGF-β1, PECAM-1, VEGFR-1and VEGFR-2 Primer Sequences.

Locus	Sense (5'-'3)	Antisense (5'-'3)
GAPDH	GAAGGTGAAGGTCGGAGT	GAAGATGGTGATGGGATTTC
TGF-β1	CACCTGCAAGACTATCGACAT	TCGGAGCTCTGATGTGTTGAA
PECAM-1	GCTGTTGGTGGAAGGAGT	GAAGTTGGCTGGAGGTGCTC
VEGFR-1	ATTTGTGATTTTGGCCTTGC	CAGGCTCATGAACTTGAAAGC
VEGFR-2	GTGACCAACATGGAGTCGTG	CCAGAGATTCCATGCCACTT

9.2.7 Scanning electron microscopy

Seeded nanocomposite conduits were examined by ScEM post preconditioning and physiological shear stress to visualise whether cells were present on the graft surface.

9.2.8 Data Analysis and Statistical Methods

The experiments were repeated four times. RNA quantities are presented in mean ± SEM. All statistical analysis utilised one way ANOVA with post-hoc Tukey's test.

9.3 Results

9.3.1 Assessment of Seeding Efficiency and Viability

The Alamar blue™ assays performed pre-flow (following overnight seeding) showed no significant difference in seeding efficiency. Viable cells were present on all seeded nanocomposite conduits.

Figure 9-2 A shows EC viability post 1 and 4 hour static or low flow without a 24 hour recovery period followed by physiological flow. Conduits preconditioned with 1 or 4 hour low flow (P_1 & P_4 respectively) showed no significance difference in cell viability compared to pre-flow. Conduits incubated under static conditions for 4 hours prior to physiological flow (S_4) showed a significant decrease in cell viability ($P < 0.01$) compared to pre-flow, whereas no significant decrease was observed after one hour static incubation (S_1). Despite a noticeable decrease in viability between S_1 and S_4 this was not significant. Comparing P_1 to its static control S_1 also showed no significant difference in cell viability. After four hours of preconditioning P_4, had a significantly higher viability ($P < 0.001$) compared to time matched control S_4.

Pre-conditioning followed by a 24 hour recovery period (Figure 9-2 B) showed significant changes in cell viability in all groups apart from pre-conditioning for one hour (PR_1) to pre-flow. Control conduits not exposed to preconditioning (SR_1 & SR_4) showed significant decreases ($P < 0.01$) in cell viability compared with pre-flow conduits. An increase in cell viability was observed for conduits preconditioned for 1 hour (PR_1) but this was not significant, whereas preconditioning for 4 hours (PR_4) showed a significant increase ($P < 0.01$). Very significant differences ($P < 0.001$) were observed between conduits SR_1 and PR_1 and SR_4 and PR_4.

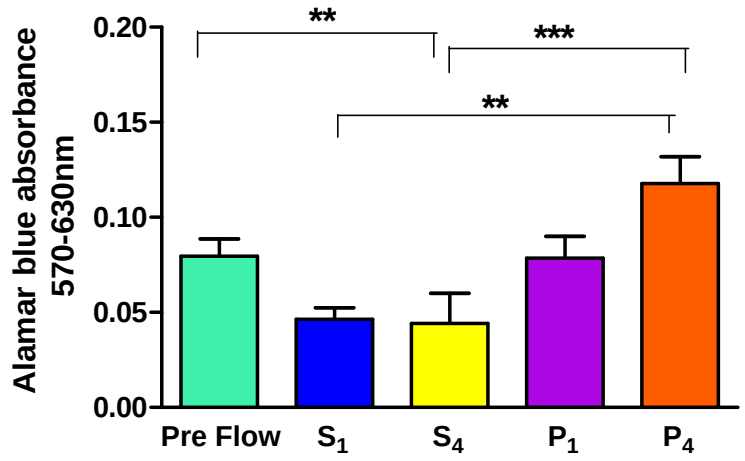

A

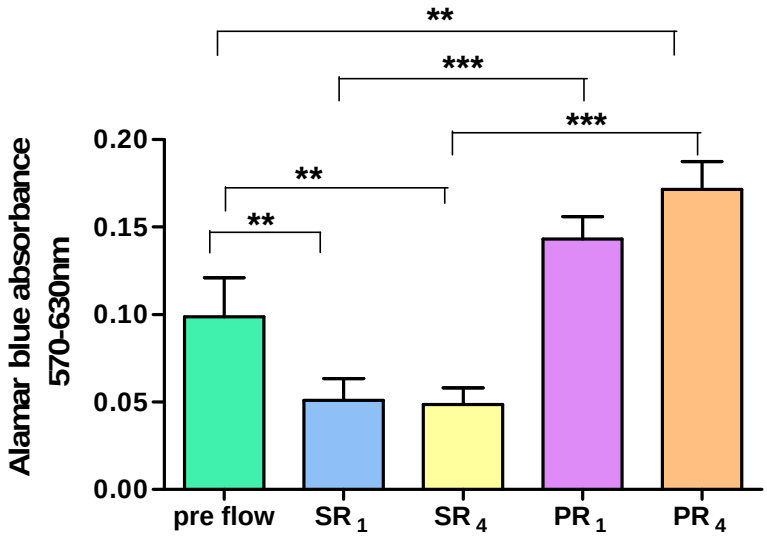

B

Figure 9-2. Assessment of cell viability by an Alamar blue™ metabolic assay: A) shows Pre-flow, S_1, S_4, P_1 and P_4 groups and B) shows Pre-flow, SR_1, SR_4, PR_1 and PR_4 groups. Statistical analysis was carried out by one-way ANOVA (n = 4) with ** $P < 0.01$ and *** $P < 0.001$

9.3.2 Assessment of Quantity and Quality of RNA Extracted

The amount of RNA extracted from HUVEC is shown in Table 9-3. The purity was high in all samples and in all cases purity was greater than 95%.

Table 9-3. RNA yield was measured at absorbance of 260 nm and 280 nm and quantity determined as ng/μl. Group A shows S_1, S_4, P_1 and P_4 samples. Group B shows SR_1, SR_4, PR_1 and PR_4 samples.

Conduit and treatment	RNA Quantity (ng/μl) (mean ± SEM)
Group A	
S_1	4.2 ± 1.2
S_4	2.4 ± 0.7
P_1	12.4 ± 1.3
P_4	18.4 ± 1.5
Group B	
SR_1	3.7 ± 0.6
SR_4	3.0 ± 0.3
PR_1	28.7 ± 3.5
PR_4	36.0 ± 4.9

9.3.3 Analysis of GAPDH, TGF-β1, VEGFR-1, PECAM-1 and VEGFR-2 PCR products

Figure 9-3 A shows a 2% agarose gel of the PCR products for group A, resulting from 1 and 4 hour exposures respectively to either static conditions (S_1& S_4) or low flow preconditioning (P_1 & P_4); following four hours of physiological flow on all conduits. Figure 9-3 B shows a 2 % agarose gel of the PCR products for group B, resulting from 1 and 4 hour exposure respectively to either static conditions (SR_1 & SR_4) or low flow preconditioning (PR_1 & PR_4); following a 24 hour recovery period on all conduits prior to four hour exposure to high flow for HUVEC seeded on the nanocomposite conduits.

The mRNA levels of GAPDH remained relatively constant in static and preconditioned samples, and changes were observed in the other genes (see below).

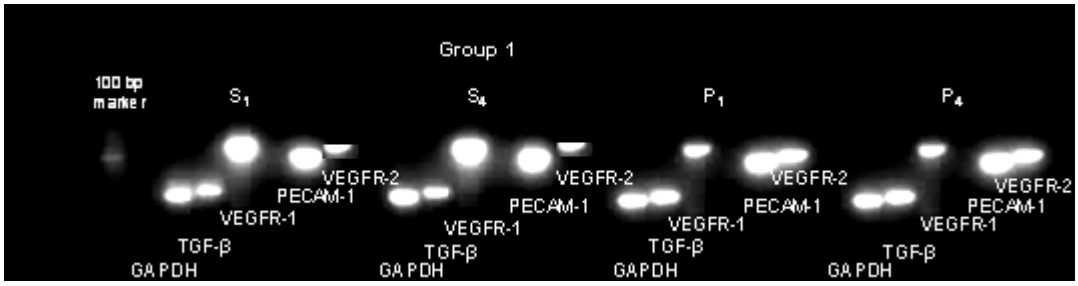

A

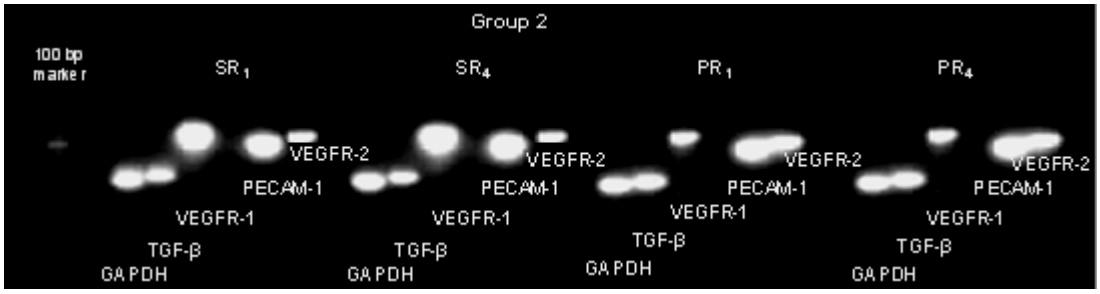

B

Figure 9-3. Typical 2% agarose gels of PCR products with a 100 bp marker. Each sample was analysed for GAPDH, TGF-β1, VEGFR-1, PECAM-1 and VEGFR-2 expression: A) shows S_1, S_4, P_1 and P_4 samples and B) shows SR_1, SR_4, PR_1 and PR_4 samples.

9.3.4 Intensity of Gene Expression

Relative levels of GAPDH, TGF-β1, VEGFR-1, PECAM-1 and VEGFR-2 were determined using Syngene. After normalisation by the intensity of GAPDH mRNA bands obtained from preconditioning, the levels of gene expression were examined.

Figure 9.4 A shows the intensity of gene expression post 4 hours physiological flow after either 1 or 4 hours of preconditioning (P_1 & P_4) compared to time matched controls (S_1 & S_4). Differences in gene expression were observed only in the expression

of VEGFR-1 and VEGFR-2. Significant decreases (S_1-P_1, $P < 0.01$ & S_4-P_4, $p < 0.001$) in VEGFR-1 and significant increases ($p < 0.001$) in VEGFR-2 were seen after 1 and 4 hour preconditioning compared to time-matched controls. All other genes remained essentially unaltered under these conditions.

Figure 9-4 B shows the intensity of gene expression post 4 hours physiological flow after either 1 or 4 hours of preconditioning (PR_1 & PR_4) compared to time matched controls (SR_1 & SR_4) with the addition of a 24 hour recovery period after preconditioning. PECAM-1 expression remained relatively unaltered. TGF-β1 expression was shown to be significantly higher ($P < 0.01$) after 4 hours of preconditioning (PR_4) compared to controls (SR_4). The expression of VEGFR-1 showed a significant decrease after 1 hour only (SR_1-PR_1, $P < 0.05$). Significant increases in VEGFR-2 expression were observed at both time points (SR_1-PR_1, $P < 0.001$ and SR_2-PR_2, $P < 0.001$).

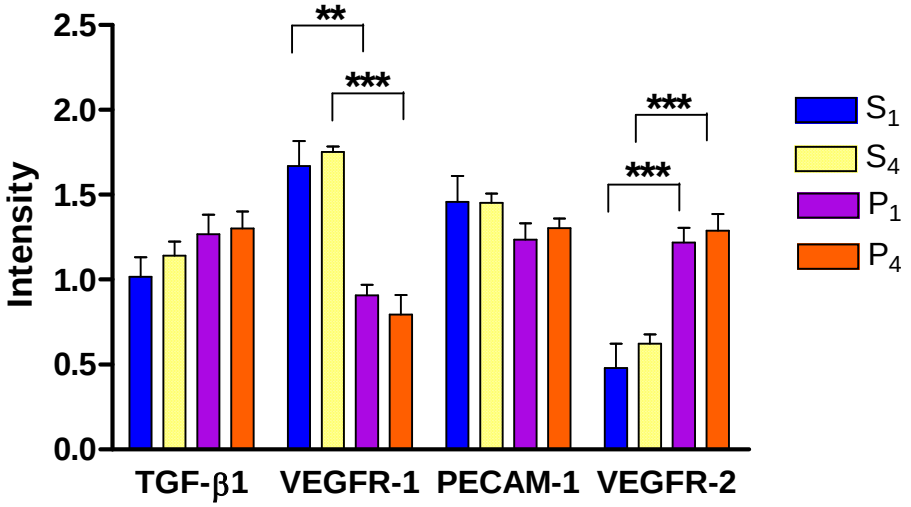

A

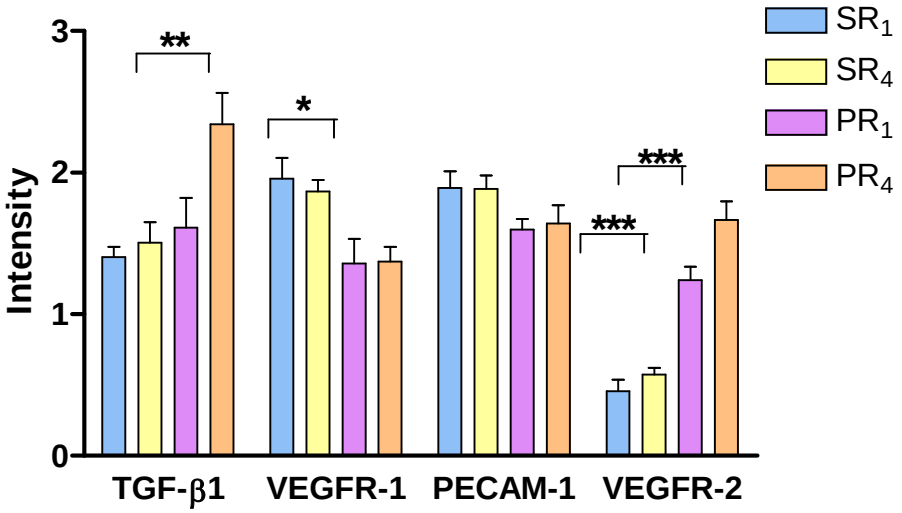

B

Figure 9-4. Intensity analyses of PCR products to determine gene expression levels following normalisation for GAPDH: A) shows S_1, S_4, P_1 and P_4 samples for TGF-β1, VEGFR-1, PECAM-1 and VEGFR-2 and B) shows SR_1, SR_4, PR_1 and PR_4 samples for TGF-β1, VEGFR-1, PECAM-1 and VEGFR-2. Statistical analysis was carried out by one-way ANOVA (n = 4) where * $P<0.05$, ** $P < 0.01$ and *** $P < 0.001$.

9.3.5 Scanning electron microscopy

ScEM was employed to further elucidate cell retention following exposure to flow. Figure 9-5 A shows nanocomposite prior to seeding. Figure 9-5 B shows pre-flow seeded nanocomposite. Figures 9-5 C to F show seeded nanocomposite for treatments S_1, S_4, P_1 and P_4 respectively. Similarly Figures 9-5 G to J show seeded nanocomposite for treatments SR_1, SR_4, PR_1 and PR_4 respectively. All seeded nanocomposites show cells present on the conduit post-treatment in line with the Alamar blue™ results earlier. In the latter chapter ScEM demonstrated no cells were left behind following mRNA extraction from the conduits.

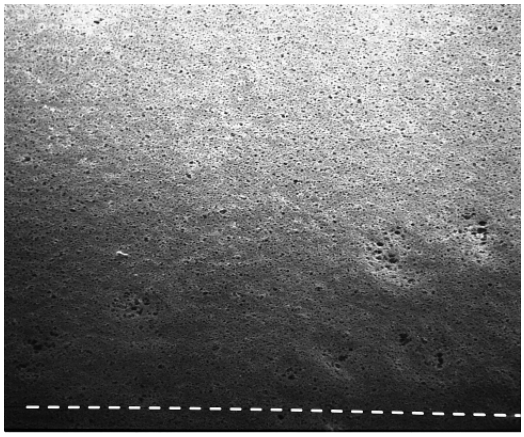

A

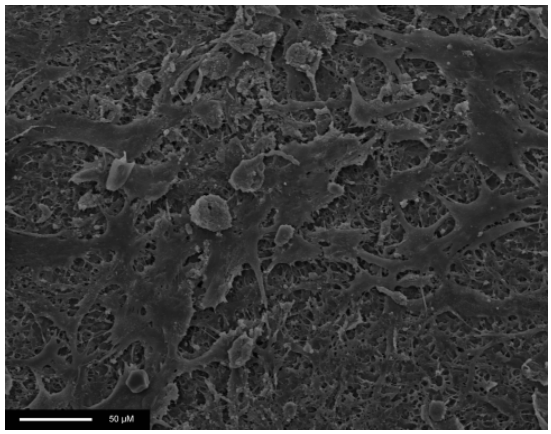

B

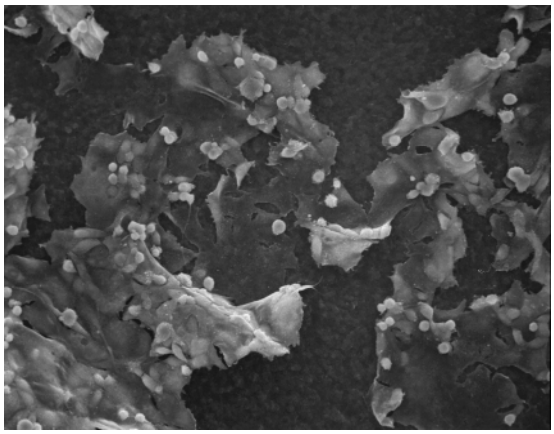

C

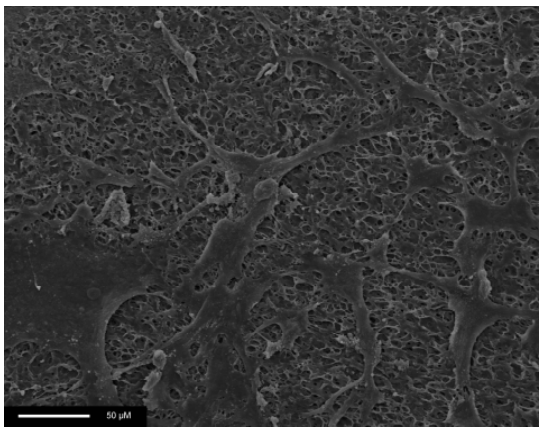

D

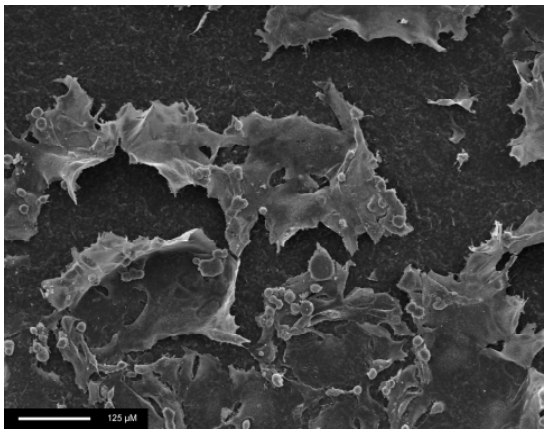

E

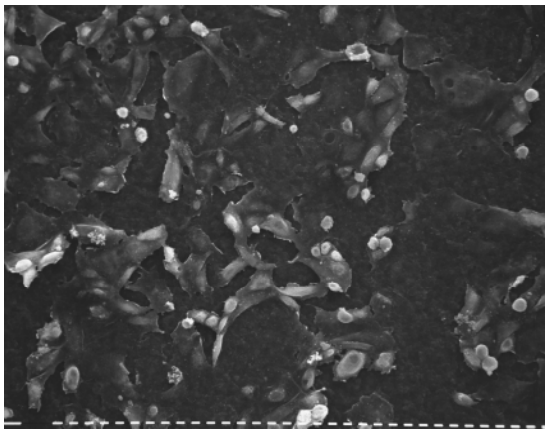

F

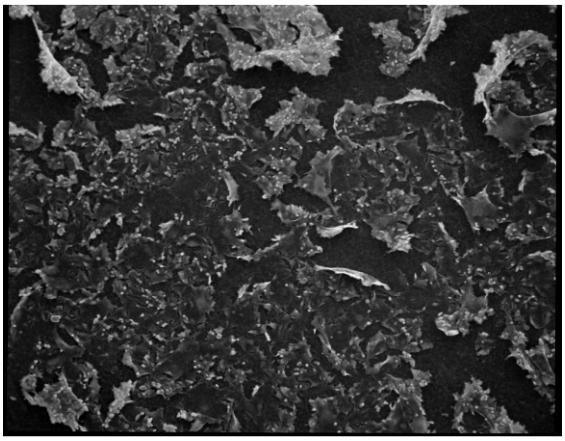

G

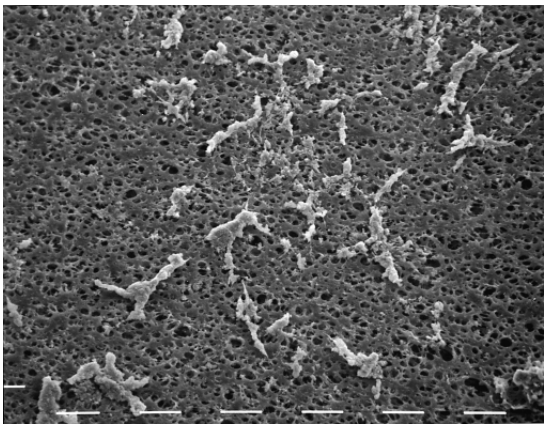

H

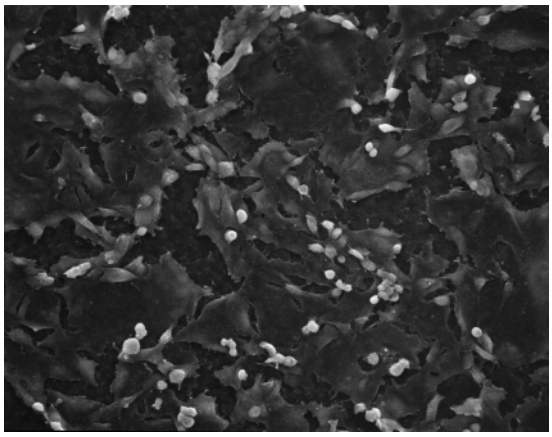

I

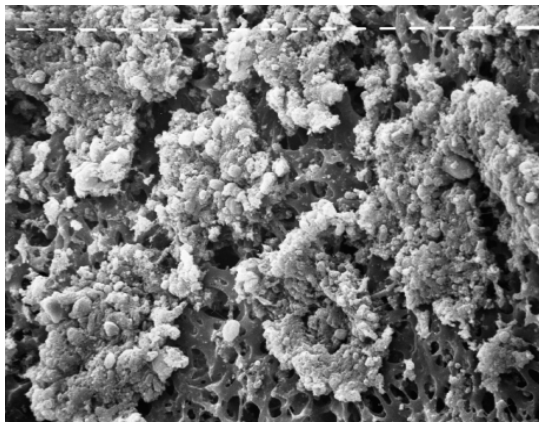

J

Figure 9-5. Typical ScEM of nanocomposite conduits: A (unseeded conduit), B (Pre-flow conduit), C (S_1 conduit), D (S_4 conduit), E (P_1 conduit), F (P_4 conduit), G (SR_1 conduit), H (SR_4 conduit), I (PR_1 conduit) and J (PR_4 conduit).

9.4 Discussion

In the previous chapter, the effect of physiological shear stress on EC seeded nanocomposite conduits was investigated. Significant changes in gene expression were observed. Pulsatile physiological shear stress (~14 dynes/cm^2) was shown to increase gene expression in EC seeded nanocomposite conduits in a time dependant manner (501). Increases in COL-1, PECAM-1 and TGF-β1 genes were seen. It also demonstrated a significant decrease in cell viability for cells seeded on nanocomposite after exposure to four hours of physiological flow. This suggested that physiological

levels of shear stress strips EC seeded on prosthetic materials as has been demonstrated in several studies previously (340). The study also for the first time, demonstrated that gene expression shear stress studies can be successfully carried out on tubular conduits.

Previous work has however suggested that cell loss under physiological flow conditions can be reduced by exposing the cells to a lower preconditioning flow prior to physiological shear stress and that such prior exposure is beneficial in promoting cell adherence (339). Chapter 2 has reviewed these studies where investigations have examined the effects of preconditioning with shear stress on EC function *in vitro*. EC that are exposed to shear stress *in vitro*, applied in a stepwise fashion over days, are induced to become tightly adherent to the substratum and exhibit more differentiated features (214;326;515). Therefore this study tested the hypothesis that exposure of EC seeded on cylindrical nanocomposite conduits to preconditioning shear stress would induce changes in gene expression and that preconditioning could allow the cells to adapt to the material in an improved manner and enhance cell growth and adhesion. EC seeded nanocomposite conduits were exposed to preconditioning shear stress and compared with conduits that were exposed to physiological shear stress. Conduits were preconditioned with a low flow of 1-2 dynes/cm^2 followed by physiological flow. Further conduits were also preconditioned with a 24 hour recovery period prior to physiological flow.

The Alamar blue^{TM} results prior to flow (pre-flow conduits) demonstrated that the nanocomposite conduits employed in the study were successfully seeded with viable HUVEC in a uniform manner. Pre flow conduits were taken as a baseline, and the decrease seen after physiological flow was applied without preconditioning suggests that a significant number of cells are lost under these conditions. This matches to the effect seen in the previous chapter when physiological shear stress was applied to EC seeded nanocomposite conduits. Conversely the application of preconditioning prior to exposure to physiological flow demonstrated that the seeded nanocomposite retained cells under this regime and suggests an improvement in cell adherence and an increase in cell numbers or metabolism following preconditioning when compared to the cells not exposed to preconditioning prior to exposure to physiological flow. The changes are more marked after 4 hours suggesting that this effect may be time dependent and that a longer period of preconditioning before the application of physiological flow results in

greater protection for the cells. The ScEM studies support these conclusions regarding the relative numbers of cells remaining following exposure to physiological flow.
The investigation of expression levels for a variety of genes was carried out in an attempt to elucidate the potential mechanisms behind the changes observed in the study of cell metabolism and numbers. In the case of TGF-β1 whilst there was a general increase in expression in the preconditioned groups this increase was only significant in the case of the 4 hour preconditioning followed by a 24 hour recovery period prior to exposure to physiological flow indicating that while TGF-β1 may be involved in the longer term changes observed in this study it's short term effect is limited (508;509).

PECAM-1 expression remains relatively stable under all treatments suggesting that the remaining HUVEC following exposure to flow retain their EC phenotype regardless of the application of preconditioning. A significant decrease in VEGFR-1 expression was observed in both one and four hour preconditioned cells when followed by immediate exposure to physiological flow and after a 24 hour recovery period. This situation was reversed in the case of VEGFR-2 where a significant increase of gene expression was observed in the preconditioned groups. Both VEGFR-1 and VEGFR-2 are known to bind vascular endothelial growth factor (504) with high affinity and previous studies have shown that VEGFR-2 mediated signalling can result in significant changes in morphology together with alterations in actin organisation in EC with high expression levels of this receptor (387). Significantly other studies have shown that the expression of VEGFR-2 is induced by the application of shear stress associated with a reduction in VEGFR-1 expression in a similar manner to the results obtained in this study (387;516). This suggests that the reduction in VEGFR-1 and increase in VEGFR-2 expression may be associated with mature EC likely to proliferate in response to shear stress (a situation similar to angiogenesis) and indeed in the case of the PR_4 group a significant increase in cell metabolism or numbers can be seen which may become more apparent if longer term studies were carried out.

9.5 Conclusion

Although there is a great deal of future work necessary before conclusions can be drawn with confidence, the following work provides great importance and a

significant improvement in understanding cells genetic behaviour in contact with biomaterials.

In conclusion this investigation confirms previous findings regarding the potential benefits of preconditioning and demonstrates that preconditioning under the right conditions can result in a significant improvement in EC retention when EC are exposed to physiological flow. The study also builds upon the last chapters work examining gene expression on cylindrical conduits when exposed to flow and demonstrates, for the first time, that low flow preconditioning causes alterations in gene expression in this situation. It suggests that such alterations can be determined successfully and that further investigations into other potentially significant genes may well be of benefit in exploring further the potential mechanism by which preconditioning improves cell retention whilst studies into protein expression via techniques such as Western blotting would also be of interest. Such studies would also be valuable in determining the most effective method of preconditioning with regard to the optimal length of time for preconditioning and the potential advantages of a recovery period prior to exposure to physiological flow. Finally it also builds on previous studies and demonstrates further the suitability and potential of the POSS nanocomposite for future use in tissue engineered coronary artery bypass grafts.

10

Conclusion of thesis

10.1 Summary and conclusion

Synthetic grafts such as Dacron and ePTFE are satisfactory in replacement of larger vessels, however when dealing with smaller diameter (<6 mm) vessels in low flow states, the patency is far lower (8;32;53). This is because the biomaterials activate thrombus formation on its lumen while the differential compliance at the anastomotic site, contributes to the formation of intimal hyperplasia. As such, autologous grafts remain the gold standard for coronary artery replacement as they are both compliant and non-thrombogenic. However, large numbers of patients do not have suitable arteries or veins for coronary artery bypass surgery therefore there is a great demand of a synthetic alternative. Chapter 1 described the need for novel small diameter compliant coronary artery bypass grafts. The Biomaterials and Tissue Engineering Centre of the Royal Free and University College Medical School have developed a polymer intended for cardiovascular devices. This polymer material is based on covalently bonding polyurethane with a silsesquioxane 'nanomolecule' (52).

The aim of this thesis was to undergo the development of a small diameter synthetic coronary artery bypass graft with the aid of tissue engineering. To this end it employed the novel nanocomposite polymer for the development of a hybrid graft utilising human umbilical vein endothelial cells as a cell source. It further examined the alterations in

gene expression of the seeded endothelial cells under varying haemodynamic shear stress conditions.

The haemodynamic environment has shown to have significant effects *on* the function of endothelial cells (89). The endothelial lining of blood vessels is subjected to a wide range of haemodynamically-generated shear-stress forces throughout the vascular system. Chapter 2 described the *in vivo* and *in vitro*, endothelial cells changes in their morphology and biochemistry in response to shear stress in a force- and time-dependent way, or when a critical threshold is exceeded. It also discussed the lack of studies on the response of shear stress in cell seeded synthetic tubular grafts. Gene expression associated with cellular proliferation, adhesion and extracellular matrix formation have been poorly studied on cylindrical prosthetic grafts. A few studies exist on cell-material interaction but these are limited (314;315). Understanding the cellular response to a 'biomaterial' is fundamental. The investigation of gene expression patterns allows determining the molecular effects of cells are expressing.

One of the primary challenges in this thesis was encountered in Chapter 4. Prior to any cell-graft and haemodynamic shear stress studies the initial investigation was based on defining a suitable method for removing the seeded cells from the graft lumen for downstream applications. Various methods of RNA isolation was undertaken on seeded tubular polyurethane based grafts. At this stage, this study was undertaken on poly(carbonate-urea)urethane grafts as the nanocomposite polymer was under development in our laboratory. This preliminary study was vital to determine whether sufficient RNA yields could be obtained for gene expression studies as well as to produce a reliable and reproducible method in order to progress onto further work in this thesis. To this date, there have been no other published data (apart from this study) indicating the isolation of RNA from seeded grafts.

Three methods of cell/RNA isolation from the graft surface were analysed and demonstrated that there was no significance between cell scraping, direct lysing or trypsinising the cells from the graft prior to RNA extraction. Despite this trypsinisation was the best tool to use as no damage occurred on the graft compared to the other two methods and provided higher levels of RNA. Furthermore, the method of isolation did not affect RNA stability. The study highlighted a novel approach to the removal of the cells and the subsequent isolation of the RNA. It demonstrated that the study of gene expression is possible under such conditions. Efforts were made to ensure that this

technique utilised readily available techniques ensuring that this method is reproducible and could be readily employed by other groups. The key to the study of genes in this situation is that the isolation of the cells from the conduit should not alter the genes expressed in a significant way and this was demonstrated by this study.

In Chapter 5 the biocompatibility of the novel nanocomposite polymer for a tissue-engineering product was assessed for it to perform as a substrate that will support the appropriate cellular activity, including the facilitation of molecular and mechanical signalling systems, in order to optimise tissue regeneration, without eliciting any undesirable effects. It was anticipated that by seeding the grafts a further decrease in the risk that inclusions would occur would be achieved and that this would help prevent problems such as intimal hyperplasia developing. The ability of these conduits to be seeded with endothelial cells was then investigated. As the polymer had not been studied in this context before no data were available for the effects that it might have on the cells. The study analysed sheets of polymer showed that not only was it not toxic under the range of conditions used (including both direct exposure to the polymer itself and indirect exposure to cell culture medium conditioned with powdered polymer) but that cells attached readily to the polymer and could be maintained in culture for a period of time consistent with that needed for the study of gene expression under flow. This was confirmed by Alamar blue cell viability assays and cell proliferation pico green assays.
In conclusion the nanocomposite can be successfully seeded with endothelial cells and indicates that, once seeded; the endothelial cells remain viable and proliferate for a period of days. This combined with its other advantages suggests that nanocomposite is suitable for further development in the development of a coronary bypass graft.

Having confirmed the anti-cytotoxicity effects of the nanocomposite the next stage was to fabricate this polymer into compliant small diameter tubular conduits. Advanced novel fabrication methods were assessed to build three-dimensional conduits that have a porous internal structure that will enable the growth of cells. Two techniques, namely electrospraying and extrusion were considered as potential methods to produce conduits. In electrospraying, the polymer was sprayed from a needle with a highly charged electrode. This technique has been previously demonstrated to be an attractive method for the fabrication of small diameter grafts (476). Further to this step the graft was made porous by placing the electrospun or extruded polymer into a

coagulant-called phase-inversion. An *in vitro* flow circuit was used to test the compliance of these conduits. To measure the burst pressure conduits were placed in a high pressure syringe pump. Attempts at electrospraying the nanocomposite onto mandrels as a technique proved futile as polymer deposition was uneven. After phase-inversion the conduit was relatively weak. The conduits showed to burst when initial pressure was applied. When tested for compliance all the electrosprayed conduits failed within the initial application of physiological flow. The extrusion of the polymer solution into water was found to be the most effective method to create a suitable conduit. The compliance measured was found to be similar to native arteries. Studies carried out in parallel in our laboratory have demonstrated that such a conduit possessed the duel properties of strength and physiological compliance required for the purpose envisaged in this study. The high levels of structural integrity of the grafts produced by this method under flow and the physiological compliance it achieved make this an excellent subject for use in cardiac bypass grafts.

An important aspect of the development of a successful synthetic CABG is to investigate the possibility of carrying out EC seeding of an artificial conduit. Evidence for the requirement of a luminal EC lining is provided by the poor patency observed when unseeded synthetic grafts with diameters less then 6 mm are employed (486). In order to maximise the efficiency of the experiments and to minimise the requirements for large numbers of cells to seed the conduits, studies on seeding density and the optimum duration of seeding were conducted. Following on from Chapter 6, extruded conduits were seeded with endothelial cells at various concentrations and seeding times. Cells that were seeded on the graft for 4 hours did not result in many cells adhering over this period. As hypothesised the longer the seeding time the more adherence of cells. The nanocomposite demonstrated a time-dependant seeding efficiency requirement. Cells seeded at 1.2×10^4 cells/cm^2 with a 24 hour seeding time were considered the best condition. Whilst there was a slight increase in seeding efficiency for a higher density of cells, it was considered more attainable to use this amount. Furthermore, examination of RNA yield from these cells demonstrated it to be successful. Some reports suggest cells to be confluent on the polymer surface prior to investigations (314). Many researchers have allowed culturing of cells on the polymer surface over weeks two achieve confluency. A longer period of seeding time in this study would have allowed for possibly more adherence, this has yet to be counterbalanced by the need for medium

exchange over such a long period. This in itself could have disrupted the adhesion process. Furthermore, seeding a large density of cells to achieve a monolayer is relatively impossible. Firstly this would require extensive cell culturing in the laboratory for two-three months to achieve the amount of cells required to seed a length of vascular graft used clinically and thus hoping that most of the cells sufficiently adhere to the grafts.

Further to this study, the large number of cells needed to seed such grafts meant that alterations in phenotype were a concern. Primary cells in particular have a tendency to change in phenotype in a number of ways with an increasing number of passages. Gene expression is one of the factors that may be affected by changes over time in culture and can be further influenced by the conditions under which the cells are maintained. As with all gene expression studies another potential problem to be overcome was that the cells investigated may show different patterns of gene expression for each individual study. This can invalidate studies and shifts in the 'baseline' will make differences induced by models such as exposure to flow more difficult to monitor and interpret. In an effort to reduce the potential effect of such problems studies on the stability of the chosen genes over long periods of culture and successive passages were carried out and demonstrated that the culture conditions employed did not alter the gene expression under the conditions investigated. Such stability was also vitally important if sufficient cells were to be cultured to conduct the types of investigations carried out in this thesis. These is vital as it demonstrated that the conditions employed provided a stable and reproducible model and that the use of HUVEC for seeding was possible despite the need (to obtain adequate cell numbers for seeding) to combine several different cell isolations.

Addressing these issues, there is much literature to show that cells simply was off grafts when exposed to pulsatile flow and the high pressures of the arterial circulation (11;208). It is known that the mechanical stress orientates cells and the extracellular matrix both *in vitro* and *in vivo*. Pulsatile blood flow results in a mechanical stimulation composed of hydrostatic pressure, tangential shear stress and circumferential stretch-relaxation. EC because of their contact with flowing blood or medium are exposed to all three forces (517). Shear stress being the most relevant force has shown to enhance EC attachment, retention and differentiation as well as being a critical factor in their

biological regulatory function. Shear stress increases proliferation of EC and increase in production of extracellular matrix molecules like collagen.

In Chapter 8, the aim of the study was a first time assessment if the pattern of gene expression observed was altered under flow conditions in seeded nanocomposite grafts. Using these principles a flow circuit developed in our laboratory that is capable of simulating the pressures found in a native artery was used. This circuit was also used in compliance studies (Chapter 6) of the nanocomposite grafts. Cylindrical nanocomposite conduits were seeded with endothelial cells and subjected to physiological shear stress of ~14 dynes/cm^2. The genes chosen for study were transforming growth factor (TGF-β1), collagen-1 (COL-1) and platelet endothelial cell adhesion molecule-1 (PECAM-1). Changes in gene expression were observed in these studies and although only key genes could be measured these behaved in ways consistent with the expected results and those reported by other groups (375;392;502). In particular, changes were observed in a time-dependant manner as those encountered in studies where EC are exposed to shear stress (504). A decrese in cell viability from Alamar blue™ results was observed in nanocomposite grafts after four hours of physiological shear stress compared to those maintained under static. Increases in expression of structural and extracellular matrix genes were seen and are consistent with increased cellular attachment and a suspected change in phenotype form the resting cultured state to a more *in vivo* like gene expression.

At present, attempts to seed EC on vascular prosthesis materials are problematic with the major concern being the low number of EC that remain on the graft surface after exposure to *in vivo* shear stress. The decrease in cell viability and increased expression of the COL-1, PECAM-1 and TGF-β1 genes observed in the study in Chapter 8 may be related to the cells strengthening their attachment to the nanocomposite substrate under physiological levels of shear stress. Preconditioning has been shown to positively influence the development of tissue-engineered grafts (326;338;339). Therefore the final aim in this thesis was to address the effects of shear stress preconditioning on EC seeded on nancomposite conduits. The use of preconditioning with lower flow rates prior to physiological flow has been highlighted in many studies to promote continued cellular attachment and reduce cell loss upon exposure to physiological flow (338). This was confirmed in this study by the increase in cell viability observed after preconditioning compared to those exposed only to

physiological flow. The application of 1-2 dynes/cm2 shear stress for four hours prior to physiological shear stress increases in TGF-β1, whereas PECAM-1 expression remained relatively constant. A significant decrease in vascular endothelial growth factor receptor-1 (VEGFR-1) expression was observed in both one and four hour preconditioned cells when followed by immediate exposure to physiological flow. This situation was reversed in the case of vascular growth factor receptor-2 (VEGFR-2) where a significant increase of gene expression was observed in the preconditioned nanocomposite grafts. Both VEGFR-1 and VEGFR-2 are known to bind vascular endothelial growth factor (504) with high affinity and previous studies have shown that VEGFR-2 mediated signalling can result in significant changes in morphology together with alterations in actin organisation in EC with high expression levels of this receptor (387). Furthermore studies have shown that the expression of VEGFR-2 is induced by the application of shear stress associated with a reduction in VEGFR-1 expression in a similar manner to the results obtained in this study (387;516). This suggests that the reduction in VEGFR-1 and increase in VEGFR-2 expression may be associated with mature EC likely to proliferate in response to shear stress (a situation similar to angiogenesis). The data generated by this investigation showed that this was likely to be responsible for a rapid change in the gene expression of cells when exposed to low flow akin to that seen under physiological flow. That this occurs at low flow highlights that this is a likely mechanism for the promotions of attachment and in future may provide an insight into the importance of such promotion in the continued attachment of cells seeded on vascular conduits.

In conclusion this thesis has demonstrated that it is possible to produce and seed conduits made from a novel nanocomposite and that once seeded the cells remain adhered under physiological flow. Further it highlights the importance of preconditioning to promote gene upregulation of potentially significant adhesive proteins and the further promotion of extracellular matrix proteins. This study demonstrated the importance of gene studies not only as a potential tool to investigate promoting cell attachment but also to aid a better understanding of the process. By understanding the gene expression changes that cells undergo under flow it is hoped that further understanding of the process of intimal hyperplasia may be promoted. A limitation to this study has been the number and types of gene studied when seeded on the grafts. This work would be better afforded with playng particular attention to the

surface adhesion molecules that determine the migration and adhesiveness of ECs. Although VEGFR2 was a keen interest in this study, and could have a significant importance in manipulating growth of a new vessel, investigating the molecules involved in cell-cell and cell-ECM attachment (such cadherins, selectins and focal adhesion kinases) as would better our knowledge of increasing cell attachment to artificial substitutes. Thus the understanding of how ECs attach to the graft would better our kowledge in the lack of adhessivness of ECs seeded grafts and therefore provide a manipulative tool in enhancing cell adhesion to artificial grafts.

10.2 Future work

This thesis describes initial work that has been undertaken whereby early stages of developing a small diameter coronary artery bypass graft have been completed. There is continued research and development required for completion of this work;

1. *Animal studies: assess the long term patency of these hybrid grafts and look at the potential infiltration of host cells both helpful and harmful.*

Potential Advantages:	Long term studies possible
	Closest mimic to clinical environment
Difficulties to be overcome:	Different genes may be involved
	Initial cell isolation needs to be characterised

2. *Long term flow studies in vitro.*

Potential Advantages:	Development of existing model
	No animal use
	Genes in humans characterised
Difficulties to be overcome:	Long term studies prone to infection
	Shorter endpoints compared to animal work
	No host interaction

3. *Use of adult stem cells as a cell source (endothelial progenitor cells)*

Potential Advantages:	Better chance of clinically significant cell source
	Possible to study cellular interaction with graft
	Work already carried out by our group highlights the potential of these cells for such studies

Difficulties to be overcome: May require different genes to be studied and the amount of RNA extracted may be a problem
Cell attachment of these cells is yet to be characterise under flow

4. Surface modification of the polymer with peptides and other bioactive molecules

Potential Advantages: Potential for increased cell attachment or adherence and hence retention
Technology shows promise and indicates usefulness in Clinical studies but no gene studies yet
Possible to more closely mimic natural cell attachment

Difficulties to be overcome: Genetic alterations after interaction with such molecules would need to be characterised
Cell type would have to be identified for clinical use as different interactions would be anticipated with different cell types

11

Reference list

(1) Hooi JD, Kester AD, Stoffers HE, Rinkens PE, Knottnerus JA, van Ree JW. Asymptomatic peripheral arterial occlusive disease predicted cardiovascular morbidity and mortality in a 7-year follow-up study. J Clin Epidemiol 2004 Mar;57(3):294-300.

(2) Mayer B, Erdmann J, Schunkert H. Genetics and heritability of coronary artery disease and myocardial infarction. Clin Res Cardiol 2007 Jan;96(1):1-7.

(3) Cook S, Walker A, Hugli O, Togni M, Meier B. Percutaneous coronary interventions in Europe : Prevalence, numerical estimates, and projections based on data up to 2004. Clin Res Cardiol 2007 Apr 26.

(4) Kunlin J. The treatment of arterial obstruction by vein grafting. Arch Mal Coeur 1949;42:371-5.

(5) Berroeta C, Benbara A, Provenchere S, Ajzenberg N, Benessiano J, Depoix JP, et al. A comparison of bilateral with single internal mammary artery grafts on postoperative mediastinal drainage and transfusion requirement. Anesth Analg 2006 Dec;103(6):1380-5.

(6) Wang X, Lin P, Yao Q, Chen C. Development of small-diameter vascular grafts. World J Surg 2007 Apr;31(4):682-9.

(7) Ballotta E, Renon L, De RA, Barbon B, Terranova O, Da GG. Prospective randomized study on reversed saphenous vein infrapopliteal bypass to treat limb-threatening ischemia: common femoral artery versus superficial femoral or popliteal and tibial arteries as inflow. J Vasc Surg 2004 Oct;40(4):732-40.

(8) Klinkert P, van Dijk PJ, Breslau PJ. Polytetrafluoroethylene femorotibial bypass grafting: 5-year patency and limb salvage. Ann Vasc Surg 2003 Sep;17(5):486-91.

(9) Abbott WM, Megerman J, Hasson JE, L'Italien G, Warnock DF. Effect of compliance mismatch on vascular graft patency. J Vasc Surg 1987 Feb;5(2):376-82.

(10) Baird RN, Kidson IG, L'Italien GJ, Abbott WM. Dynamic compliance of arterial grafts. Am J Physiol 1977 Nov;233(5):H568-H572.

(11) Baird RN, Abbott WM. Pulsatile blood-flow in arterial grafts. Lancet 1976 Oct 30;2(7992):948-50.

(12) Rhee K, Lee SM. Effects of radial wall motion and flow waveform on the wall shear rate distribution in the divergent vascular graft. Ann Biomed Eng 1998 Nov;26(6):955-64.

(13) Salacinski HJ, Goldner S, Giudiceandrea A, Hamilton G, Seifalian AM, Edwards A, et al. The mechanical behavior of vascular grafts: a review. J Biomater Appl 2001 Jan;15(3):241-78.

(14) Sarkar S, Schmitz-Rixen T, Hamilton G, Seifalian AM. Achieving the ideal properties for vascular bypass grafts using a tissue engineered approach: a review. Med Biol Eng Comput 2007 Apr;45(4):327-36.

(15) Stewart SF, Lyman DJ. Effects of an artery/vascular graft compliance mismatch on protein transport: a numerical study. Ann Biomed Eng 2004 Jul;32(7):991-1006.

(16) Garcia MJ, Passer AA. Coronary-artery bypass surgery with internal-thoracic-artery grafts. N Engl J Med 1996 Jun 13;334(24):1609.

(17) Kitamura S, Kawachi K, Kawata T, Kobayashi S, Mizuguchi K, Kameda Y, et al. [Ten-year survival and cardiac event-free rates in Japanese patients with the left anterior descending artery revascularized with internal thoracic artery or saphenous vein graft: a comparative study]. Nippon Geka Gakkai Zasshi 1996 Mar;97(3):202-9.

(18) Esaki J, Koshiji T, Okamoto M, Tsukashita M, Ikuno T, Sakata R. Gastroepiploic artery grafting does not improve the late outcome in patients with bilateral internal thoracic artery grafting. Ann Thorac Surg 2007 Mar;83(3):1024-9.

(19) Fusejima K, Takahara Y, Sudo Y, Murayama H, Masuda Y, Inagaki Y. Comparison of coronary hemodynamics in patients with internal mammary artery and saphenous vein coronary artery bypass grafts: a noninvasive approach using combined two-dimensional and Doppler echocardiography. J Am Coll Cardiol 1990 Jan;15(1):131-9.

(20) 2007. Ref Type: Internet Communication, http://www.sts.org/index.html

(21) Lytle BW, Loop FD, Cosgrove DM, Ratliff NB, Easley K, Taylor PC. Long-term (5 to 12 years) serial studies of internal mammary artery and saphenous vein coronary bypass grafts. J Thorac Cardiovasc Surg 1985 Feb;89(2):248-58.

(22) Loop FD, Lytle BW, Cosgrove DM, Stewart RW, Goormastic M, Williams GW, et al. Influence of the internal-mammary-artery graft on 10-year survival and other cardiac events. N Engl J Med 1986 Jan 2;314(1):1-6.

(23) Moore HD. The replacement of blood vessels by polythene tubes. Surg Gynecol Obstet 1950 Nov;91(5):593-600.

(24) Voorhees AB, Jr., Jaretzki A, III, Blakemore AH. The use of tubes constructed from vinyon "N" cloth in bridging arterial defects. Ann Surg 1952 Mar;135(3):332-6.

(25) Blakemore AH, Voorhees AB, Jr. The use of tubes constructed from vinyon N cloth in bridging arterial defects; experimental and clinical. Ann Surg 1954 Sep;140(3):324-34.

(26) Hess F. History of (micro) vascular surgery and the development of small-caliber blood vessel prostheses (with some notes on patency rates and re-endothelialization). Microsurgery 1985;6(2):59-69.

(27) Deterling RA, Jr., Bhonslay SB. An evaluation of synthetic materials and fabrics suitable for blood vessel replacement. Surgery 1955 Jul;38(1):71-91.

(28) Ishida T, Kurosawa H, Nishida H, Aomi S, Endo M. Sequential bypass using the right gastroepiploic artery for coronary artery bypass grafting. Jpn J Thorac Cardiovasc Surg 2003 Jul;51(7):277-81.

(29) Hehrlein FW, Schlepper M, Loskot F, Scheld HH, Walter P, Mulch J. The use of expanded polytetrafluoroethylene (PTFE) grafts for myocardial revascularization. J Cardiovasc Surg (Torino) 1984 Nov;25(6):549-53.

(30) Matsumoto H, Hasegawa T, Fuse K, Yamamoto M, Saigusa M. A new vascular prosthesis for a small caliber artery. Surgery 1973 Oct;74(4):519-23.

(31) Lyman DJ, Fazzio FJ, Voorhees H, Robinson G, Albo D, Jr. Compliance as a factor effecting the patency of a copolyurethane vascular graft. J Biomed Mater Res 1978 May;12(3):337-45.

(32) Hallman GL, Cooley DA, Mcnamara DG, Latson JR. Single left coronary artery with fistula to right ventricle: reconstruction of two-coronary system with dacron graft. Circulation 1965 Aug;32:293-7.

(33) Sauvage LR, Schloemer R, Wood SJ, Logan G. Successful interposition synthetic graft between aorta and right coronary artery. Angiographic follow-up to sixteen months. J Thorac Cardiovasc Surg 1976 Sep;72(3):418-21.

(34) Chard RB, Johnson DC, Nunn GR, Cartmill TB. Aorta-coronary bypass grafting with polytetrafluoroethylene conduits. Early and late outcome in eight patients. J Thorac Cardiovasc Surg 1987 Jul;94(1):132-4.

(35) Yokoyama T, Gharavi MA, Lee YC, Edmiston WA, Kay JH. Aorta--coronary artery revascularization with an expanded polytetrafluoroethylene vascular graft. A preliminary report. J Thorac Cardiovasc Surg 1978 Oct;76(4):552-5.

(36) Rashid ST, Salacinski HJ, Button MJ, Fuller B, Hamilton G, Seifalian AM. Cellular engineering of conduits for coronary and lower limb bypass surgery: role of cell attachment peptides and pre-conditioning in optimising smooth muscle cells (SMC) adherence to compliant poly(carbonate-urea)urethane (MyoLink) scaffolds. Eur J Vasc Endovasc Surg 2004 Jun;27(6):608-16.

(37) Sonoda H, Takamizawa K, Nakayama Y, Yasui H, Matsuda T. Coaxial double-tubular compliant arterial graft prosthesis: time-dependent morphogenesis and compliance changes after implantation. J Biomed Mater Res A 2003 May 1;65(2):170-81.

(38) Hari PR, Ajithkumar B, Sharma CP. Hydrogen grafted polymer surfaces: interaction and morphology of platelets. J Biomater Appl 1993 Oct;8(2):174-82.

(39) Orang F, Plummer CJ, Kausch HH. Effects of processing conditions and in vitro ageing on the physical properties of Biomer. Biomaterials 1996 Mar;17(5):485-90.

(40) Belanger MC, Marois Y, Roy R, Mehri Y, Wagner E, Zhang Z, et al. Selection of a polyurethane membrane for the manufacture of ventricles for a totally implantable artificial heart: blood compatibility and biocompatibility studies. Artif Organs 2000 Nov;24(11):879-88.

(41) Eberhart A, Zhang Z, Guidoin R, Laroche G, Guay L, De La FD, et al. A new generation of polyurethane vascular prostheses: rara avis or ignis fatuus? J Biomed Mater Res 1999;48(4):546-58.

(42) Ota K, Kawai T, Teraoka S, Sasaki Y, Nakagawa Y. Clinical application of a self-sealing poly(ether-urethane) graft applicable to blood access for hemodialysis. Artif Organs 1989 Dec;13(6):498-503.

(43) Nakagawa Y, Ota K, Sato Y, Fuchinoue S, Teraoka S, Agishi T. Complications in blood access for hemodialysis. Artif Organs 1994 Apr;18(4):283-8.

(44) Brothers TE, Rios GA, Robison JG, Elliot BM. Justification of intervention for limb-threatening ischemia: a surgical decision analysis. Cardiovasc Surg 1999 Jan;7(1):62-9.

(45) Szycher M, Reed AM, Siciliano AA. In vivo testing of a biostable polyurethane. J Biomater Appl 1991 Oct;6(2):110-30.

(46) Edwards A, Carson RJ, Bowald S, Quist WC. Development of a microporous compliant small bore vascular graft. J Biomater Appl 1995 Oct;10(2):171-87.

(47) Aldenhoff YB, van D, V, ter WJ, Habets J, Poole-Warren LA, Koole LH. Performance of a polyurethane vascular prosthesis carrying a dipyridamole (Persantin) coating on its lumenal surface. J Biomed Mater Res 2001 Feb;54(2):224-33.

(48) Dempsey DJ, Phaneuf MD, Bide MJ, Szycher M, Quist WC, LoGerfo FW. Synthesis of a novel small diameter polyurethane vascular graft with reactive binding sites. ASAIO J 1998 Sep;44(5):M506-M510.

(49) Wetzels GM, Koole LH. Photoimmobilisation of poly(N-vinylpyrrolidinone) as a means to improve haemocompatibility of polyurethane biomaterials. Biomaterials 1999 Oct;20(20):1879-87.

(50) Fields C, Cassano A, Allen C, Meyer A, Pawlowski KJ, Bowlin GL, et al. Endothelial cell seeding of a 4-mm I.D. polyurethane vascular graft. J Biomater Appl 2002 Jul;17(1):45-70.

(51) Tang YW, Labow RS, Santerre JP. Enzyme-induced biodegradation of polycarbonate-polyurethanes: dependence on hard-segment chemistry. J Biomed Mater Res 2001 Dec 15;57(4):597-611.

(52) Kannan RY, Salacinski HJ, De GJ, Clatworthy I, Bozec L, Horton M, et al. The antithrombogenic potential of a polyhedral oligomeric silsesquioxane (POSS) nanocomposite. Biomacromolecules 2006 Jan;7(1):215-23.

(53) Abbott WM, Callow A, Moore W, Rutherford R, Veith F, Weinberg S. Evaluation and performance standards for arterial prostheses. J Vasc Surg 1993 Apr;17(4):746-56.

(54) Abbott WM, Vignati JJ. Prosthetic grafts: when are they a reasonable alternative? Semin Vasc Surg 1995 Sep;8(3):236-45.

(55) Yaginuma G, Abe K, Ottomo M, Okada Y, Ota K, Fujimori S, et al. [Use of the radial artery graft in coronary artery bypass grafting: harvesting technique and spasm prevention]. Kyobu Geka 1998 Sep;51(10):823-8.

(56) Nollert G, Amend J, Reichart B. Use of the internal mammary artery as a graft in emergency coronary artery bypass grafting after failed PTCA. Thorac Cardiovasc Surg 1995 Jun;43(3):142-7.

(57) Salacinski HJ, Tai NR, Carson RJ, Edwards A, Hamilton G, Seifalian AM. In vitro stability of a novel compliant poly(carbonate-urea)urethane to oxidative and hydrolytic stress. J Biomed Mater Res 2002 Feb;59(2):207-18.

(58) 2007.Ref Type: Internet Communication, www.heartsts.org

(59) Thomas AC, Campbell GR, Campbell JH. Advances in vascular tissue engineering. Cardiovasc Pathol 2003 Sep;12(5):271-6.

(60) Kubik T, Bogunia-Kubik K, Sugisaka M. Nanotechnology on duty in medical applications. Curr Pharm Biotechnol 2005 Feb;6(1):17-33.

(61) Ghalanbor Z, Marashi SA, Ranjbar B. Nanotechnology helps medicine: nanoscale swimmers and their future applications. Med Hypotheses 2005;65(1):198-9.

(62) Habal MB. The biologic basis for the clinical application of the silicones. A correlate to their biocompatibility. Arch Surg 1984 Jul;119(7):843-8.

(63) Labow RS, Meek E, Santerre JP. Hydrolytic degradation of poly(carbonate)-urethanes by monocyte-derived macrophages. Biomaterials 2001 Nov;22(22):3025-33.

(64) Capone CD. Biostability of a non-ether polyurethane. J Biomater Appl 1992 Oct;7(2):108-29.

(65) Mathur AB, Collier TO, Kao WJ, Wiggins M, Schubert MA, Hiltner A, et al. In vivo biocompatibility and biostability of modified polyurethanes. J Biomed Mater Res 1997 Aug;36(2):246-57.

(66) Hergenrother RW, Yu XH, Cooper SL. Blood-contacting properties of polydimethylsiloxane polyurea-urethanes. Biomaterials 1994 Jun;15(8):635-40.

(67) Park JH, Park KD, Bae YH. PDMS-based polyurethanes with MPEG grafts: synthesis, characterization and platelet adhesion study. Biomaterials 1999 May;20(10):943-53.

(68) Rhodes NP, Bellon JM, Bujan MJ, Soldani G, Hunt JA. Inflammatory response to a novel series of siloxane-crosslinked polyurethane elastomers having controlled biodegradation. J Mater Sci Mater Med 2005 Dec;16(12):1207-11.

(69) Joshi M, Butola BS. Polymeric Nanocomposites - Polyhedral Oligomeric Silsesquioxanes (POSS) as Hybrid Nanofiller. Polymer Reviews, 2007;44(4):389-410.

(70) Kannan RY, Salacinski HJ, Odlyha M, Butler PE, Seifalian AM. The degradative resistance of polyhedral oligomeric silsesquioxane nanocore integrated polyurethanes: an in vitro study. Biomaterials 2006 Mar;27(9):1971-9.

(71) Langer R, Vacanti JP. Tissue engineering. Science 1993 May 14;260(5110):920-6.

(72) MacArthur BD, Oreffo RO. Bridging the gap. Nature 2005 Jan 6;433(7021):19.

(73) Berger K, Sauvage LR, Rao AM, Wood SJ. Healing of arterial prostheses in man: its incompleteness. Ann Surg 1972 Jan;175(1):118-27.

(74) Furchgott RF, Zawadzki JV. The obligatory role of endothelial cells in the relaxation of arterial smooth muscle by acetylcholine. Nature 1980 Nov 27;288(5789):373-6.

(75) Autio I, Malo-Ranta U, Kallioniemi OP, Nikkari T. Cultured bovine aortic endothelial cells secrete factor(s) chemotactic for aortic smooth muscle cells. Artery 1989;16(2):72-83.

(76) Cybulsky MI, Gimbrone MA, Jr. Endothelial expression of a mononuclear leukocyte adhesion molecule during atherogenesis. Science 1991 Feb 15;251(4995):788-91.

(77) Casscells W. Migration of smooth muscle and endothelial cells. Critical events in restenosis. Circulation 1992 Sep;86(3):723-9.

(78) Vanhoutte PM. Endothelium and control of vascular function. State of the Art lecture. Hypertension 1989 Jun;13(6 Pt 2):658-67.

(79) Marsden PA, Goligorsky MS, Brenner BM. Endothelial cell biology in relation to current concepts of vessel wall structure and function. J Am Soc Nephrol 1991 Jan;1(7):931-48.

(80) Galley HF, Webster NR. Physiology of the endothelium. Br J Anaesth 2004 Jul;93(1):105-13.

(81) Cines DB, Pollak ES, Buck CA, Loscalzo J, Zimmerman GA, McEver RP, et al. Endothelial cells in physiology and in the pathophysiology of vascular disorders. Blood 1998 May 15;91(10):3527-61.

(82) Dejana E. Endothelial cell-cell junctions: happy together. Nat Rev Mol Cell Biol 2004 Apr;5(4):261-70.

(83) Sadler JE. Biochemistry and genetics of von Willebrand factor. Annu Rev Biochem 1998;67:395-424.

(84) De ML, Girolami A, Russell S, Ruggeri ZM. Interaction of asialo von Willebrand factor with glycoprotein Ib induces fibrinogen binding to the glycoprotein IIb/IIIa complex and mediates platelet aggregation. J Clin Invest 1985 Apr;75(4):1198-203.

(85) Weinbaum S, Tarbell JM, Damiano ER. The structure and function of the endothelial glycocalyx layer. Annu Rev Biomed Eng 2007;9:121-67.

(86) Weinbaum S, Zhang X, Han Y, Vink H, Cowin SC. Mechanotransduction and flow across the endothelial glycocalyx. Proc Natl Acad Sci U S A 2003 Jun 24;100(13):7988-95.

(87) Hu X, Weinbaum S. A new view of Starling's hypothesis at the microstructural level. Microvasc Res 1999 Nov;58(3):281-304.

(88) Thi MM, Tarbell JM, Weinbaum S, Spray DC. The role of the glycocalyx in reorganization of the actin cytoskeleton under fluid shear stress: a "bumper-car" model. Proc Natl Acad Sci U S A 2004 Nov 23;101(47):16483-8.

(89) Nerem RM. Hemodynamics and the vascular endothelium. J Biomech Eng 1993 Nov;115(4B):510-4.

(90) Palmer RM, Ferrige AG, Moncada S. Nitric oxide release accounts for the biological activity of endothelium-derived relaxing factor. Nature 1987 Jun 11;327(6122):524-6.

(91) Bredt DS. Endogenous nitric oxide synthesis: biological functions and pathophysiology. Free Radic Res 1999 Dec;31(6):577-96.

(92) Hickey MJ. Role of inducible nitric oxide synthase in the regulation of leucocyte recruitment. Clin Sci (Lond) 2001 Jan;100(1):1-12.

(93) Rees DD, Palmer RM, Moncada S. Role of endothelium-derived nitric oxide in the regulation of blood pressure. Proc Natl Acad Sci U S A 1989 May;86(9):3375-8.

(94) Chen G, Yamamoto Y, Miwa K, Suzuki H. Hyperpolarization of arterial smooth muscle induced by endothelial humoral substances. Am J Physiol 1991 Jun;260(6 Pt 2):H1888-H1892.

(95) Dzau VJ. Multiple pathways of angiotensin production in the blood vessel wall: evidence, possibilities and hypotheses. J Hypertens 1989 Dec;7(12):933-6.

(96) Katusic ZS, Vanhoutte PM. Superoxide anion is an endothelium-derived contracting factor. Am J Physiol 1989 Jul;257(1 Pt 2):H33-H37.

(97) Yanagisawa M, Kurihara H, Kimura S, Tomobe Y, Kobayashi M, Mitsui Y, et al. A novel potent vasoconstrictor peptide produced by vascular endothelial cells. Nature 1988 Mar 31;332(6163):411-5.

(98) Dohi Y, Hahn AW, Boulanger CM, Buhler FR, Luscher TF. Endothelin stimulated by angiotensin II augments contractility of spontaneously hypertensive rat resistance arteries. Hypertension 1992 Feb;19(2):131-7.

(99) Taddei S, Favilla S, Duranti P, Simonini N, Salvetti A. Vascular renin-angiotensin system and neurotransmission in hypertensive persons. Hypertension 1991 Sep;18(3):266-77.

(100) Kato T, Iwama Y, Okumura K, Hashimoto H, Ito T, Satake T. Prostaglandin H2 may be the endothelium-derived contracting factor released by acetylcholine in the aorta of the rat. Hypertension 1990 May;15(5):475-81.

(101) Aird WC. Vascular bed-specific thrombosis. J Thromb Haemost 2007 Jul;5 Suppl 1:283-91.

(102) Stern DM, Esposito C, Gerlach H, Gerlach M, Ryan J, Handley D, et al. Endothelium and regulation of coagulation. Diabetes Care 1991 Feb;14(2):160-6.

(103) Ware JA, Heistad DD. Seminars in medicine of the Beth Israel Hospital, Boston. Platelet-endothelium interactions. N Engl J Med 1993 Mar 4;328(9):628-35.

(104) Pearson JD. Endothelial cell function and thrombosis. Baillieres Best Pract Res Clin Haematol 1999 Sep;12(3):329-41.

(105) Dusting GJ, Moncada S, Vane JR. Prostacyclin: its biosynthesis, actions, and clinical potential. Adv Prostaglandin Thromboxane Leukot Res 1982;10:59-106.

(106) Schr+Âder H, Schr+Âr K. Prostacyclin-dependent cyclic AMP formation in endothelial cells. Naunyn-Schmiedeberg's Archives of Pharmacology 1993 Jan 1;347(1):101-4.

(107) Bajaj MS, Birktoft JJ, Steer SA, Bajaj SP. Structure and biology of tissue factor pathway inhibitor. Thromb Haemost 2001 Oct;86(4):959-72.

(108) Gajdusek C, Carbon S, Ross R, Nawroth P, Stern D. Activation of coagulation releases endothelial cell mitogens. J Cell Biol 1986 Aug;103(2):419-28.

(109) Macfarlane RG. An Enzyme Cascade in the Blood Clotting Mechanism, and its Function as a Biochemical Amplifier. Nature 1964 May 2;202(4931):498-9.

(110) Dahlback B, Villoutreix BO. The anticoagulant protein C pathway. FEBS Lett 2005 Jun 13;579(15):3310-6.

(111) Rigby AC, Grant MA. Protein S: a conduit between anticoagulation and inflammation. Crit Care Med 2004 May;32(5 Suppl):S336-S341.

(112) Gerlach H, Esposito C, Stern DM. Modulation of endothelial hemostatic properties: an active role in the host response. Annu Rev Med 1990;41:15-24.

(113) Kooistra T, Schrauwen Y, Arts J, Emeis JJ. Regulation of endothelial cell t-PA synthesis and release. Int J Hematol 1994 Jun;59(4):233-55.

(114) Ulfhammer E, Larsson P, Karlsson L, Hrafnkelsdottir T, Bokarewa M, Tarkowski A, et al. TNF-alpha mediated suppression of tissue type plasminogen activator expression in vascular endothelial cells is NF-kappaB- and p38 MAPK-dependent. J Thromb Haemost 2006 Aug;4(8):1781-9.

(115) Dano K, Andreasen PA, Grondahl-Hansen J, Kristensen P, Nielsen LS, Skriver L. Plasminogen activators, tissue degradation, and cancer. Adv Cancer Res 1985;44:139-266.

(116) Meier P, Finch A, Evan G. Apoptosis in development. Nature 2000 Oct 12;407(6805):796-801.

(117) Adams JM, Huang DC, Puthalakath H, Bouillet P, Vairo G, Moriishi K, et al. Control of apoptosis in hematopoietic cells by the Bcl-2 family of proteins. Cold Spring Harb Symp Quant Biol 1999;64:351-8.

(118) Kerr JF, Wyllie AH, Currie AR. Apoptosis: a basic biological phenomenon with wide-ranging implications in tissue kinetics. Br J Cancer 1972 Aug;26(4):239-57.

(119) Baffert F, Le T, Sennino B, Thurston G, Kuo CJ, Hu-Lowe D, et al. Cellular changes in normal blood capillaries undergoing regression after inhibition of VEGF signaling. Am J Physiol Heart Circ Physiol 2006 Feb 1;290(2):H547-H559.

(120) Segure INMA, Serrano ANTO, De Buitrago GG, Gonzalez MA, Abad JL, Claveria CRIS, et al. Inhibition of programmed cell death impairs in vitro

vascular-like structure formation and reduces in vivo angiogenesis. FASEB J 2002 Jun 1;16(8):833-41.

(121) Duval H, Harris M, Li J, Johnson N, Print C. New insights into the function and regulation of endothelial cell apoptosis. Angiogenesis 2003;6(3):171-83.

(122) Szebenyi G, Fallon JF. Fibroblast growth factors as multifunctional signaling factors. Int Rev Cytol 1999;185:45-106.

(123) Tilly JL, Billig H, Kowalski KI, Hsueh AJ. Epidermal growth factor and basic fibroblast growth factor suppress the spontaneous onset of apoptosis in cultured rat ovarian granulosa cells and follicles by a tyrosine kinase-dependent mechanism. Mol Endocrinol 1992 Nov;6(11):1942-50.

(124) Aharoni D, Meiri I, Atzmon R, Vlodavsky I, Amsterdam A. Differential effect of components of the extracellular matrix on differentiation and apoptosis. Current Biology 1997 Jan;7(1):43-51.

(125) Amsterdam A, Gold RS, Hosokawa K, Yoshida Y, Sasson R, Jung Y, et al. Crosstalk Among Multiple Signaling Pathways Controlling Ovarian Cell Death. Trends in Endocrinology and Metabolism 1999 Sep 1;10(7):255-62.

(126) Nobes CD, Hall A. Rho GTPases control polarity, protrusion, and adhesion during cell movement. J Cell Biol 1999 Mar 22;144(6):1235-44.

(127) Ridley AJ. Rho-related proteins: actin cytoskeleton and cell cycle. Curr Opin Genet Dev 1995 Feb;5(1):24-30.

(128) Folkman J. Angiogenesis: an organizing principle for drug discovery? Nat Rev Drug Discov 2007 Apr;6(4):273-86.

(129) Hillen F, Griffioen AW. Tumour vascularization: sprouting angiogenesis and beyond. Cancer Metastasis Rev 2007 Dec;26(3-4):489-502.

(130) Shima DT, Adamis AP, Ferrara N, Yeo KT, Yeo TK, Allende R, et al. Hypoxic induction of endothelial cell growth factors in retinal cells: identification and characterization of vascular endothelial growth factor (VEGF) as the mitogen. Mol Med 1995 Jan;1(2):182-93.

(131) Morisada T, Kubota Y, Urano T, Suda T, Oike Y. Angiopoietins and Angiopoietin-Like Proteins in Angiogenesis.

(132) Rofstad EK, Henriksen K, Galappathi K, Mathiesen B. Antiangiogenic Treatment with Thrombospondin-1 Enhances Primary Tumor Radiation Response and Prevents Growth of Dormant Pulmonary Micrometastases after Curative Radiation Therapy in Human Melanoma Xenografts. Cancer Res 2003 Jul 15;63(14):4055-61.

(133) Ferrara N, Gerber HP, LeCouter J. The biology of VEGF and its receptors. Nat Med 2003 Jun;9(6):669-76.

(134) Parenti A, Bellik L, Brogelli L, Filippi S, Ledda F. Endogenous VEGF-A is responsible for mitogenic effects of MCP-1 on vascular smooth muscle cells. Am J Physiol Heart Circ Physiol 2004 May 1;286(5):H1978-H1984.

(135) Liang D, Chang JR, Chin AJ, Smith A, Kelly C, Weinberg ES, et al. The role of vascular endothelial growth factor (VEGF) in vasculogenesis, angiogenesis, and hematopoiesis in zebrafish development. Mechanisms of Development 2001 Oct;108(1-2):29-43.

(136) Takahashi H, Shibuya M. The vascular endothelial growth factor (VEGF)/VEGF receptor system and its role under physiological and pathological conditions. Clin Sci 2005 Sep 1;109(3):227-41.

(137) Zilberberg L, Shinkaruk S, Lequin O, Rousseau B, Hagedorn M, Costa F, et al. Structure and inhibitory effects on angiogenesis and tumor development of a new vascular endothelial growth inhibitor. J Biol Chem 2003 Sep 12;278(37):35564-73.

(138) Shibuya M. Vascular endothelial growth factor receptor-1 (VEGFR-1/Flt-1): a dual regulator for angiogenesis. Angiogenesis 2006;9(4):225-30.

(139) Goumans MJ, Valdimarsdottir G, Itoh S, Rosendahl A, Sideras P, ten DP. Balancing the activation state of the endothelium via two distinct TGF-beta type I receptors. EMBO J 2002 Apr 2;21(7):1743-53.

(140) Watabe T, Nishihara A, Mishima K, Yamashita J, Shimizu K, Miyazawa K, et al. TGF-{beta} receptor kinase inhibitor enhances growth and integrity of embryonic stem cell-derived endothelial cells. J Cell Biol 2003 Dec 22;163(6):1303-11.

(141) Yamagami S, Yokoo S, Mimura T, Amano S. Effects of TGF-{beta}2 on Immune Response-Related Gene Expression Profiles in the Human Corneal Endothelium. Invest Ophthalmol Vis Sci 2004 Feb 1;45(2):515-21.

(142) Cook-Mills JM, Deem TL. Active participation of endothelial cells in inflammation. J Leukoc Biol 2005 Apr 1;77(4):487-95.

(143) Pober JS, Cotran RS. The role of endothelial cells in inflammation. Transplantation 1990 Oct;50(4):537-44.

(144) Wheelock MJ, Johnson KR. Cadherin-mediated cellular signaling. Current Opinion in Cell Biology 2003 Oct;15(5):509-14.

(145) Stevens T, Garcia JGN, Shasby DM, Bhattacharya J, Malik AB. Mechanisms regulating endothelial cell barrier function. Am J Physiol Lung Cell Mol Physiol 2000 Sep 1;279(3):L419-L422.

(146) Dudek SM, Garcia JGN. Cytoskeletal regulation of pulmonary vascular permeability. J Appl Physiol 2001 Oct 1;91(4):1487-500.

(147) Martin-Padura I, Lostaglio S, Schneemann M, Williams L, Romano M, Fruscella P, et al. Junctional Adhesion Molecule, a Novel Member of the

Immunoglobulin Superfamily That Distributes at Intercellular Junctions and Modulates Monocyte Transmigration. J Cell Biol 1998 Jul 13;142(1):117-27.

(148) Nitta T, Hata M, Gotoh S, Seo Y, Sasaki H, Hashimoto N, et al. Size-selective loosening of the blood-brain barrier in claudin-5-deficient mice. J Cell Biol 2003 May 12;161(3):653-60.

(149) Matter K, Balda MS. Signalling to and from tight junctions. Nat Rev Mol Cell Biol 2003 Mar;4(3):225-37.

(150) Stevenson BR, Siliciano JD, Mooseker MS, Goodenough DA. Identification of ZO-1: a high molecular weight polypeptide associated with the tight junction (zonula occludens) in a variety of epithelia. J Cell Biol 1986 Sep 1;103(3):755-66.

(151) Nawroth R, Poell G, Ranft A, Kloep S, Samulowitz U, Fachinger G, et al. VE-PTP and VE-cadherin ectodomains interact to facilitate regulation of phosphorylation and cell contacts. EMBO J 2002 Sep 16;21(18):4885-95.

(152) Takeichi M. Cadherins: a molecular family important in selective cell-cell adhesion. Annu Rev Biochem 1990;59:237-52.

(153) Salomon D, Ayalon O, Patel-King R, Hynes RO, Geiger B. Extrajunctional distribution of N-cadherin in cultured human endothelial cells. J Cell Sci 1992 May 1;102(1):7-17.

(154) Liaw CW, Cannon C, Power MD, Kiboneka PK, Rubin LL. Identification and cloning of two species of cadherins in bovine endothelial cells. EMBO J 1990 Sep;9(9):2701-8.

(155) Lorenzon P, Vecile E, Nardon E, Ferrero E, Harlan JM, Tedesco F, et al. Endothelial Cell E- and P-Selectin and Vascular Cell Adhesion Molecule-1 Function as Signaling Receptors. J Cell Biol 1998 Sep 7;142(5):1381-91.

(156) Kameda H, Morita I, Handa M, Kaburaki J, Yoshida T, Mimori T, et al. Re-expression of functional P-selectin molecules on the endothelial cell surface by repeated stimulation with thrombin. Br J Haematol 1997 May;97(2):348-55.

(157) Gotsch U, Jager U, Dominis M, Vestweber D. Expression of P-selectin on endothelial cells is upregulated by LPS and TNF-alpha in vivo. Cell Adhes Commun 1994 Apr;2(1):7-14.

(158) Armstead VE, Minchenko AG, Schuhl RA, Hayward R, Nossuli TO, Lefer AM. Regulation of P-selectin expression in human endothelial cells by nitric oxide. Am J Physiol 1997 Aug;273(2 Pt 2):H740-H746.

(159) Minamino T, Kitakaze M, Sanada S, Asanuama H, Kurotobi T, Koretsune Y, et al. Increased Expression of P-Selectin on Platelets Is a Risk Factor for Silent Cerebral Infarction in Patients With Atrial Fibrillation : Role of Nitric Oxide. Circulation 1998 Oct 27;98(17):1721-7.

(160) Spertini O, Cordey AS, Monai N, Giuffre L, Schapira M. P-selectin glycoprotein ligand 1 is a ligand for L-selectin on neutrophils, monocytes, and CD34+ hematopoietic progenitor cells. J Cell Biol 1996 Oct 1;135(2):523-31.

(161) Sheppard D. Endothelial integrins and angiogenesis: not so simple anymore. J Clin Invest 2002 Oct;110(7):913-4.

(162) Lampugnani MG, Resnati M, Dejana E, Marchisio PC. The role of integrins in the maintenance of endothelial monolayer integrity. J Cell Biol 1991 Feb 1;112(3):479-90.

(163) Clark EA, Brugge JS. Integrins and signal transduction pathways: the road taken. Science 1995 Apr 14;268(5208):233-9.

(164) Humphries MJ. Integrin structure. Biochem Soc Trans 2000;28(4):311-39.

(165) Tuckwell D, Humphries M. Integrin-collagen binding. Seminars in Cell & Developmental Biology 1996 Oct;7(5):649-57.

(166) Languino LR, Gehlsen KR, Wayner E, Carter WG, Engvall E, Ruoslahti E. Endothelial cells use alpha 2 beta 1 integrin as a laminin receptor. J Cell Biol 1989 Nov 1;109(5):2455-62.

(167) Faull RJ, Kovach NL, Harlan JM, Ginsberg MH. Affinity modulation of integrin alpha 5 beta 1: regulation of the functional response by soluble fibronectin. J Cell Biol 1993 Apr 1;121(1):155-62.

(168) Lee EC, Lotz MM, Steele GD, Jr., Mercurio AM. The integrin alpha 6 beta 4 is a laminin receptor. J Cell Biol 1992 May;117(3):671-8.

(169) Hodivala-Dilke K. [alpha]v[beta]3 integrin and angiogenesis: a moody integrin in a changing environment. Current Opinion in Cell Biology 2008 Oct;20(5):514-9.

(170) Wight TN. The extracellular matrix and atherosclerosis. Curr Opin Lipidol 1995 Oct;6(5):326-34.

(171) Hutchings HELE, Ortega NATH, Plouet JEAN. Extracellular matrix-bound vascular endothelial growth factor promotes endothelial cell adhesion, migration, and survival through integrin ligation. FASEB J 2003 Aug 1;17(11):1520-2.

(172) Takai E, Landesberg R, Katz RW, Hung CT, Guo XE. Substrate modulation of osteoblast adhesion strength, focal adhesion kinase activation, and responsiveness to mechanical stimuli. Mol Cell Biomech 2006 Mar;3(1):1-12.

(173) Jockusch BM, Bubeck P, Giehl K, Kroemker M, Moschner J, Rothkegel M, et al. The molecular architecture of focal adhesions. Annu Rev Cell Dev Biol 1995;11:379-416.

(174) Juliano RL, Reddig P, Alahari S, Edin M, Howe A, Aplin A. Integrin regulation of cell signalling and motility. Biochem Soc Trans 2004 Jun;32(Pt3):443-6.

(175) Jones JL, Walker RA. Integrins: a role as cell signalling molecules. Mol Pathol 1999 Aug;52(4):208-13.

(176) Brummendorf T, Rathjen FG. Cell adhesion molecules. 1: immunoglobulin superfamily. Protein Profile 1994;1(9):951-1058.

(177) Luscinskas FW, Cybulsky MI, Kiely JM, Peckins CS, Davis VM, Gimbrone MA, Jr. Cytokine-activated human endothelial monolayers support enhanced neutrophil transmigration via a mechanism involving both endothelial-leukocyte adhesion molecule-1 and intercellular adhesion molecule-1. J Immunol 1991 Mar 1;146(5):1617-25.

(178) Barreiro O, Yanez-Mo M, Serrador JM, Montoya MC, Vicente-Manzanares M, Tejedor R, et al. Dynamic interaction of VCAM-1 and ICAM-1 with moesin and ezrin in a novel endothelial docking structure for adherent leukocytes. J Cell Biol 2002 Jun 24;157(7):1233-45.

(179) Carman CV, Jun CD, Salas A, Springer TA. Endothelial Cells Proactively Form Microvilli-Like Membrane Projections upon Intercellular Adhesion Molecule 1 Engagement of Leukocyte LFA-1. J Immunol 2003 Dec 1;171(11):6135-44.

(180) Su WH, Chen Hi, Jen CJ. Differential movements of VE-cadherin and PECAM-1 during transmigration of polymorphonuclear leukocytes through human umbilical vein endothelium. Blood 2002 Nov 15;100(10):3597-603.

(181) Feng D, Nagy JA, Pyne K, Dvorak HF, Dvorak AM. Neutrophils Emigrate from Venules by a Transendothelial Cell Pathway in Response to FMLP. J Exp Med 1998 Mar 16;187(6):903-15.

(182) Feng D, Nagy JA, Dvorak HF, Dvorak AM. Ultrastructural studies define soluble macromolecular, particulate, and cellular transendothelial cell pathways in venules, lymphatic vessels, and tumor-associated microvessels in man and animals. Microsc Res Tech 2002 Jun 1;57(5):289-326.

(183) Rossetti G, Collinge M, Bender JR, Molteni R, Pardi R. Integrin-dependent regulation of gene expression in leukocytes. Immunol Rev 2002 Aug;186:189-207.

(184) Delisser HM, Newman PJ, Albelda SM. Platelet endothelial cell adhesion molecule (CD31). Curr Top Microbiol Immunol 1993;184:37-45.

(185) Delisser HM, Newman PJ, Albelda SM. Molecular and functional aspects of PECAM-1/CD31. Immunol Today 1994 Oct;15(10):490-5.

(186) Ilan N, Madri JA. PECAM-1: old friend, new partners. Curr Opin Cell Biol 2003 Oct;15(5):515-24.

(187) Newman PJ, Newman DK. Signal transduction pathways mediated by PECAM-1: new roles for an old molecule in platelet and vascular cell biology. Arterioscler Thromb Vasc Biol 2003 Jun 1;23(6):953-64.

(188) Sauvage LR, Berger K, Beilin LB, Smith JC, Wood SJ, Mansfield PB. Presence of endothelium in an axillary-femoral graft of knitted Dacron with an external velour surface. Ann Surg 1975 Dec;182(6):749-53.

(189) Tiwari A, Kidane A, Salacinski H, Punshon G, Hamilton G, Seifalian AM. Improving endothelial cell retention for single stage seeding of prosthetic grafts: use of polymer sequences of arginine-glycine-aspartate. Eur J Vasc Endovasc Surg 2003 Apr;25(4):325-9.

(190) Kobashi T, Matsuda T. Fabrication of branched hybrid vascular prostheses. Tissue Eng 1999 Dec;5(6):515-24.

(191) Doi K, Matsuda T. Significance of porosity and compliance of microporous, polyurethane-based microarterial vessel on neoarterial wall regeneration. J Biomed Mater Res 1997 Dec 15;37(4):573-84.

(192) Doi K, Matsuda T. Enhanced vascularization in a microporous polyurethane graft impregnated with basic fibroblast growth factor and heparin. J Biomed Mater Res 1997 Mar 5;34(3):361-70.

(193) Ratcliffe A. Tissue engineering of vascular grafts. Matrix Biol 2000 Aug;19(4):353-7.

(194) Miwa H, Matsuda T. An integrated approach to the design and engineering of hybrid arterial prostheses. J Vasc Surg 1994 Apr;19(4):658-67.

(195) Herring M, Gardner A, Glover J. A single-staged technique for seeding vascular grafts with autogenous endothelium. Surgery 1978 Oct;84(4):498-504.

(196) Zilla P, Fasol R, Deutsch M, Fischlein T, Minar E, Hammerle A, et al. Endothelial cell seeding of polytetrafluoroethylene vascular grafts in humans: a preliminary report. J Vasc Surg 1987 Dec;6(6):535-41.

(197) Seifalian AM, Tiwari A, Hamilton G, Salacinski HJ. Improving the clinical patency of prosthetic vascular and coronary bypass grafts: the role of seeding and tissue engineering. Artif Organs 2002 Apr;26(4):307-20.

(198) Bordenave L, Remy-Zolghadri M, Fernandez P, Bareille R, Midy D. Clinical performance of vascular grafts lined with endothelial cells. Endothelium 1999;6(4):267-75.

(199) Salacinski HJ, Tai NR, Punshon G, Giudiceandrea A, Hamilton G, Seifalian AM. Optimal endothelialisation of a new compliant poly(carbonate-urea)urethane vascular graft with effect of physiological shear stress. Eur J Vasc Endovasc Surg 2000 Oct;20(4):342-52.

(200) Tiwari A, Salacinski HJ, Hamilton G, Seifalian AM. Tissue engineering of vascular bypass grafts: role of endothelial cell extraction. Eur J Vasc Endovasc Surg 2001 Mar;21(3):193-201.

(201) Zilla P, Fasol R, Dudeck U, Siedler S, Preiss P, Fischlein T, et al. In situ cannulation, microgrid follow-up and low-density plating provide first passage

endothelial cell masscultures for in vitro lining. J Vasc Surg 1990 Aug;12(2):180-9.

(202) Hess F, Steeghs S, Jerusalem R, Reijnders O, Jerusalem C, Braun B, et al. Patency and morphology of fibrous polyurethane vascular prostheses implanted in the femoral artery of dogs after seeding with subcultivated endothelial cells. European Journal of Vascular Surgery 1993 Jul;7(4):402-8.

(203) Koveker GB, Graham LM, Burkel WE, Sell R, Wakefield TW, Dietrich K, et al. Extracellular matrix preparation of expanded polytetrafluoroethylene grafts seeded with endothelial cells: influence on early platelet deposition, cellular growth, and luminal prostacyclin release. Surgery 1991 Mar;109(3 Pt 1):313-9.

(204) Seeger JM, Klingman N. Improved endothelial cell seeding with cultured cells and fibronectin-coated grafts. Journal of Surgical Research 1985 Jun;38(6):641-7.

(205) Teebken OE, Puschmann C, Aper T, Haverich A, Mertsching H. Tissue-Engineered Bioprosthetic Venous Valve: a Long-Term Study in Sheep. European Journal of Vascular and Endovascular Surgery 2003 Apr;25(4):305-12.

(206) Noishiki Y, Tomizawa Y, Yamane Y, Matsumoto A. The vicious cycle of nonhealing neointima in fabric vascular prostheses. Artif Organs 1995 Jan;19(1):7-16.

(207) Noishiki Y, Yamane Y, Ichikawa Y, Yamazaki I, Yamamoto K, Kosuge T, et al. Age Dependency of Neointima Formation on Vascular Prostheses in Dogs. Artificial Organs 2000;24(9):718-28.

(208) Giudiceandrea A, Seifalian AM, Krijgsman B, Hamilton G. Effect of prolonged pulsatile shear stress in vitro on endothelial cell seeded PTFE and compliant polyurethane vascular grafts. European Journal of Vascular and Endovascular Surgery 1998 Feb;15(2):147-54.

(209) Herring M, Gardner A, Glover J. Seeding human arterial prostheses with mechanically derived endothelium. The detrimental effect of smoking. J Vasc Surg 1984 Mar;1(2):279-89.

(210) Zilla P, Siedler S, Fasol R, Sharefkin JB. Reduced reproductive capacity of freshly harvested endothelial cells in smokers: a possible shortcoming in the success of seeding? J Vasc Surg 1989 Aug;10(2):143-8.

(211) Anders E, Alles JU, Delvos U, Potzsch B, Preissner KT, Muller-Berghaus G. Microvascular endothelial cells from human omental tissue: Modified method for long-term cultivation and new aspects of characterization. Microvascular Research 1987 Sep;34(2):239-49.

(212) Jarrell BE, Williams SK, Stokes G, Hubbard FA, Carabasi RA, Koolpe E, et al. Use of freshly isolated capillary endothelial cells for the immediate establishment of a monolayer on a vascular graft at surgery. Surgery 1986 Aug;100(2):392-9.

(213) Kesler KA, Herring MB, Arnold MP, Glover JL, Park HM, Helmus MN, et al. Enhanced strength of endothelial attachment on polyester elastomer and polytetrafluoroethylene graft surfaces with fibronectin substrate. J Vasc Surg 1986 Jan;3(1):58-64.

(214) Tiwari A, Salacinski HJ, Punshon G, Hamilton G, Seifalian AM. Development of a hybrid cardiovascular graft using a tissue engineering approach. FASEB J 2002 Jun;16(8):791-6.

(215) Salacinski HJ, Tiwari A, Hamilton G, Seifalian AM. Cellular engineering of vascular bypass grafts: Role of chemical coatings for enhancing endothelial cell attachment. Medical and Biological Engineering and Computing 2001 Nov 12;39(6):609-18.

(216) Bos GW, Scharenborg NM, Poot AA, Engbers GH, Beugeling T, van Aken WG, et al. Endothelialization of crosslinked albumin-heparin gels. Thromb Haemost 1999 Dec;82(6):1757-63.

(217) Bos GW, Scharenborg NM, Poot AA, Engbers GH, Terlingen JG, Beugeling T, et al. Adherence and proliferation of endothelial cells on surface-immobilized albumin-heparin conjugate. Tissue Eng 1998;4(3):267-79.

(218) Budd JS, Bell PR, James RF. Attachment of indium-111 labelled endothelial cells to pretreated polytetrafluoroethylene vascular grafts. Br J Surg 1989 Dec;76(12):1259-61.

(219) Itoh H, Aso Y, Furuse M, Noishiki Y, Miyata T. A Honeycomb Collagen Carrier for Cell Culture as a Tissue Engineering Scaffold. Artificial Organs 2001;25(3):213-7.

(220) Dalsing MC, Kevorkian M, Raper B, Nixon C, Lalka SG, Cikrit DF, et al. An experimental collagen-impregnated Dacron graft: potential for endothelial seeding. Ann Vasc Surg 1989 Apr;3(2):127-33.

(221) Goissis G, Suzigan S, Parreira DR, Maniglia JV, Braile DM, Raymundo S. Preparation and Characterization of Collagen-Elastin Matrices From Blood Vessels Intended as Small Diameter Vascular Grafts. Artificial Organs 2000;24(3):217-23.

(222) Marois Y, Sigot-Luizard MF, Guidoin R. Endothelial cell behavior on vascular prosthetic grafts: effect of polymer chemistry, surface structure, and surface treatment. ASAIO J 1999 Jul;45(4):272-80.

(223) Kumar TR, Krishnan LK. A stable matrix for generation of tissue-engineered nonthrombogenic vascular grafts. Tissue Eng 2002 Oct;8(5):763-70.

(224) Schneider A, Melmed RN, Schwalb H, Karck M, Vlodavsky I, Uretzky G. An improved method for endothelial cell seeding on polytetrafluoroethylene small caliber vascular grafts. J Vasc Surg 1992 Apr;15(4):649-56.

(225) Ye Q, Zund G, Jockenhoevel S, Schoeberlein A, Hoerstrup SP, Grunenfelder J, et al. Scaffold precoating with human autologous extracellular matrix for

improved cell attachment in cardiovascular tissue engineering. ASAIO J 2000 Nov;46(6):730-3.

(226) Shi Q, Bhattacharya V, Hong-De Wu M, Sauvage LR. Utilizing Granulocyte Colony--stimulating Factor to Enhance Vascular Graft Endothelialization from Circulating Blood Cells. Annals of Vascular Surgery 2002 May;16(3):314-20.

(227) McMillan R, Meeks B, Bensebaa F, Deslandes Y, Sheardown H. Cell adhesion peptide modification of gold-coated polyurethanes for vascular endothelial cell adhesion. J Biomed Mater Res 2001 Feb;54(2):272-83.

(228) Bach AD, Bannasch H, Galla TJ, Bittner KM, Stark GB. Fibrin glue as matrix for cultured autologous urothelial cells in urethral reconstruction. Tissue Eng 2001 Feb;7(1):45-53.

(229) Haegerstrand A, Bengtsson L, Gillis C. Serum proteins provide a matrix for cultured endothelial cells on expanded polytetrafluoroethylene vascular grafts. Scand J Thorac Cardiovasc Surg 1993;27(1):21-6.

(230) Deutsch M, Meinhart J, Fischlein T, Preiss P, Zilla P. Clinical autologous in vitro endothelialization of infrainguinal ePTFE grafts in 100 patients: A 9-year experience. Surgery 1999 Nov;126(5):847-55.

(231) Lehle K, Buttstaedt J, Birnbaum DE. Expression of adhesion molecules and cytokines in vitro by endothelial cells seeded on various polymer surfaces coated with titaniumcarboxonitride. J Biomed Mater Res A 2003 Jun 1;65(3):393-401.

(232) Chandy T, Das GS, Wilson RF, Rao GHR. Use of plasma glow for surface-engineering biomolecules to enhance bloodcompatibility of Dacron and PTFE vascular prosthesis. Biomaterials 2000 Apr;21(7):699-712.

(233) Miller DC, Thapa A, Haberstroh KM, Webster TJ. Endothelial and vascular smooth muscle cell function on poly(lactic-co-glycolic acid) with nano-structured surface features. Biomaterials 2004 Jan;25(1):53-61.

(234) Seliktar D, Nerem RM, Galis ZS. Mechanical strain-stimulated remodeling of tissue-engineered blood vessel constructs. Tissue Eng 2003 Aug;9(4):657-66.

(235) Chello M, Mastroroberto P, Frati G, Patti G, D'Ambrosio A, Di Sciascio G, et al. Pressure distension stimulates the expression of endothelial adhesion molecules in the human saphenous vein graft. The Annals of Thoracic Surgery 2003 Aug;76(2):453-8.

(236) Fields RC, Solan A, McDonagh KT, Niklason LE, Lawson JH. Gene therapy in tissue-engineered blood vessels. Tissue Eng 2003 Dec;9(6):1281-7.

(237) George SJ, Williams A, Newby AC. An essential role for platelet-derived growth factor in neointima formation in human saphenous vein in vitro. Atherosclerosis 1996 Feb;120(1-2):227-40.

(238) Kroll MH, Hellums JD, McIntire LV, Schafer AI, Moake JL. Platelets and shear stress. Blood 1996 Sep 1;88(5):1525-41.

(239) Turitto VT. Blood viscosity, mass transport, and thrombogenesis. Prog Hemost Thromb 1982;6:139-77.

(240) Chien S. Shear dependence of effective cell volume as a determinant of blood viscosity. Science 1970 May 22;168(934):977-9.

(241) Rodkiewicz CM, Sinha P, Kennedy JS. On the application of a constitutive equation for whole human blood. J Biomech Eng 1990 May;112(2):198-206.

(242) Wootton DM, Ku DN. Fluid mechanics of vascular systems, diseases, and thrombosis. Annu Rev Biomed Eng 1999;1:299-329.

(243) Gotlieb AI, Langille BL. The role of rheology in atherosclerotic coronary artery disease. In: Fuster V, Ross R, Topol EJ, editors. Atherosclerosis and Coronary Artery Disease.Philadelphia: Lippincott-Raven; 1996. p. 595-606.

(244) Golledge J, Turner RJ, Harley SL, Springall DR, Powell JT. Circumferential deformation and shear stress induce differential responses in saphenous vein endothelium exposed to arterial flow. J Clin Invest 1997 Jun 1;99(11):2719-26.

(245) Zamir M. Shear forces and blood vessel radii in the cardiovascular system. J Gen Physiol 1977 Apr;69(4):449-61.

(246) Nerem RM. Vascular fluid mechanics, the arterial wall, and atherosclerosis. J Biomech Eng 1992 Aug;114(3):274-82.

(247) Fry DL. Acute vascular endothelial changes associated with increased blood velocity gradients. Circ Res 1968 Feb;22(2):165-97.

(248) Ruggeri ZM. Mechanisms initiating platelet thrombus formation. Thromb Haemost 1997 Jul;78(1):611-6.

(249) Friedman MH, Hutchins GM, Bargeron CB, Deters OJ, Mark FF. Correlation between intimal thickness and fluid shear in human arteries. Atherosclerosis 1981 Jun;39(3):425-36.

(250) Ku DN, Giddens DP, Zarins CK, Glagov S. Pulsatile flow and atherosclerosis in the human carotid bifurcation. Positive correlation between plaque location and low oscillating shear stress. Arteriosclerosis 1985 May;5(3):293-302.

(251) Cunningham KS, Gotlieb AI. The role of shear stress in the pathogenesis of atherosclerosis. Lab Invest 2005 Jan;85(1):9-23.

(252) Helmlinger G, Geiger RV, Schreck S, Nerem RM. Effects of pulsatile flow on cultured vascular endothelial cell morphology. J Biomech Eng 1991 May;113(2):123-31.

(253) Kosaki K, Ando J, Korenaga R, Kurokawa T, Kamiya A. Fluid shear stress increases the production of granulocyte-macrophage colony-stimulating factor

by endothelial cells via mRNA stabilization. Circ Res 1998 Apr 20;82(7):794-802.

(254) Garcia-Cardena G, Comander J, Anderson KR, Blackman BR, Gimbrone MA, Jr. Biomechanical activation of vascular endothelium as a determinant of its functional phenotype. Proc Natl Acad Sci U S A 2001 Apr 10;98(8):4478-85.

(255) Patrick CW, Jr., McIntire LV. Shear stress and cyclic strain modulation of gene expression in vascular endothelial cells. Blood Purif 1995;13(3-4):112-24.

(256) Davies PF. Flow-mediated endothelial mechanotransduction. Physiol Rev 1995 Jul;75(3):519-60.

(257) Kataoka N, Ujita S, Sato M. Effect of flow direction on the morphological responses of cultured bovine aortic endothelial cells. Med Biol Eng Comput 1998 Jan;36(1):122-8.

(258) Nerem RM, Levesque MJ, Cornhill JF. Vascular endothelial morphology as an indicator of the pattern of blood flow. J Biomech Eng 1981 Aug;103(3):172-6.

(259) Barbee KA, Davies PF, Lal R. Shear stress-induced reorganization of the surface topography of living endothelial cells imaged by atomic force microscopy. Circ Res 1994 Jan;74(1):163-71.

(260) Chien S, Li S, Shyy YJ. Effects of mechanical forces on signal transduction and gene expression in endothelial cells. Hypertension 1998 Jan;31(1 Pt 2):162-9.

(261) Gimbrone MA, Jr., Resnick N, Nagel T, Khachigian LM, Collins T, Topper JN. Hemodynamics, endothelial gene expression, and atherogenesis. Ann N Y Acad Sci 1997 Apr 15;811:1-10.

(262) Ishida T, Takahashi M, Corson MA, Berk BC. Fluid shear stress-mediated signal transduction: how do endothelial cells transduce mechanical force into biological responses? Ann N Y Acad Sci 1997 Apr 15;811:12-23.

(263) Chen BP, Li YS, Zhao Y, Chen KD, Li S, Lao J, et al. DNA microarray analysis of gene expression in endothelial cells in response to 24-h shear stress. Physiol Genomics 2001 Oct 10;7(1):55-63.

(264) McCormick SM, Eskin SG, McIntire LV, Teng CL, Lu CM, Russell CG, et al. DNA microarray reveals changes in gene expression of shear stressed human umbilical vein endothelial cells. Proc Natl Acad Sci U S A 2001 Jul 31;98(16):8955-60.

(265) Wasserman SM, Mehraban F, Komuves LG, Yang RB, Tomlinson JE, Zhang Y, et al. Gene expression profile of human endothelial cells exposed to sustained fluid shear stress. Physiol Genomics 2002 Dec 26;12(1):13-23.

(266) Folkman J, D'Amore PA. Blood vessel formation: what is its molecular basis? Cell 1996 Dec 27;87(7):1153-5.

(267) Partanen J, Dumont DJ. Functions of Tie1 and Tie2 receptor tyrosine kinases in vascular development. Curr Top Microbiol Immunol 1999;237:159-72.

(268) Hsieh HJ, Li NQ, Frangos JA. Shear stress increases endothelial platelet-derived growth factor mRNA levels. Am J Physiol 1991 Feb;260(2 Pt 2):H642-H646.

(269) Asakura T, Karino T. Flow patterns and spatial distribution of atherosclerotic lesions in human coronary arteries. Circ Res 1990 Apr;66(4):1045-66.

(270) Kanse SM, Benzakour O, Kanthou C, Kost C, Lijnen HR, Preissner KT. Induction of vascular SMC proliferation by urokinase indicates a novel mechanism of action in vasoproliferative disorders. Arterioscler Thromb Vasc Biol 1997 Nov;17(11):2848-54.

(271) Clowes AW, Clowes MM, Au YP, Reidy MA, Belin D. Smooth muscle cells express urokinase during mitogenesis and tissue-type plasminogen activator during migration in injured rat carotid artery. Circ Res 1990 Jul;67(1):61-7.

(272) Sokabe T, Yamamoto K, Ohura N, Nakatsuka H, Qin K, Obi S, et al. Differential regulation of urokinase-type plasminogen activator expression by fluid shear stress in human coronary artery endothelial cells. Am J Physiol Heart Circ Physiol 2004 Nov;287(5):H2027-H2034.

(273) Noris M, Morigi M, Donadelli R, Aiello S, Foppolo M, Todeschini M, et al. Nitric oxide synthesis by cultured endothelial cells is modulated by flow conditions. Circ Res 1995 Apr;76(4):536-43.

(274) Brooks AR, Lelkes PI, Rubanyi GM. Gene expression profiling of human aortic endothelial cells exposed to disturbed flow and steady laminar flow. Physiol Genomics 2002;9(1):27-41.

(275) Negishi M, Lu D, Zhang YQ, Sawada Y, Sasaki T, Kayo T, et al. Upregulatory expression of furin and transforming growth factor-beta by fluid shear stress in vascular endothelial cells. Arterioscler Thromb Vasc Biol 2001 May;21(5):785-90.

(276) Sumpio BE, Du W, Galagher G, Wang X, Khachigian LM, Collins T, et al. Regulation of PDGF-B in endothelial cells exposed to cyclic strain. Arterioscler Thromb Vasc Biol 1998 Mar;18(3):349-55.

(277) Passerini AG, Milsted A, Rittgers SE. Shear stress magnitude and directionality modulate growth factor gene expression in preconditioned vascular endothelial cells. J Vasc Surg 2003 Jan;37(1):182-90.

(278) Malek AM, Gibbons GH, Dzau VJ, Izumo S. Fluid shear stress differentially modulates expression of genes encoding basic fibroblast growth factor and platelet-derived growth factor B chain in vascular endothelium. J Clin Invest 1993 Oct;92(4):2013-21.

(279) Ohura N, Yamamoto K, Ichioka S, Sokabe T, Nakatsuka H, Baba A, et al. Global analysis of shear stress-responsive genes in vascular endothelial cells. J Atheroscler Thromb 2003;10(5):304-13.

(280) von Offenberg SN, Cummins PM, Birney YA, Cullen JP, Redmond EM, Cahill PA. Cyclic strain-mediated regulation of endothelial matrix metalloproteinase-2 expression and activity. Cardiovasc Res 2004 Sep 1;63(4):625-34.

(281) Sampath R, Kukielka GL, Smith CW, Eskin SG, McIntire LV. Shear stress-mediated changes in the expression of leukocyte adhesion receptors on human umbilical vein endothelial cells in vitro. Ann Biomed Eng 1995 May;23(3):247-56.

(282) Nagel T, Resnick N, Atkinson WJ, Dewey CF, Jr., Gimbrone MA, Jr. Shear stress selectively upregulates intercellular adhesion molecule-1 expression in cultured human vascular endothelial cells. J Clin Invest 1994 Aug;94(2):885-91.

(283) Tsuboi H, Ando J, Korenaga R, Takada Y, Kamiya A. Flow stimulates ICAM-1 expression time and shear stress dependently in cultured human endothelial cells. Biochem Biophys Res Commun 1995 Jan 26;206(3):988-96.

(284) Chiu JJ, Chen LJ, Lee PL, Lee CI, Lo LW, Usami S, et al. Shear stress inhibits adhesion molecule expression in vascular endothelial cells induced by coculture with smooth muscle cells. Blood 2003 Apr 1;101(7):2667-74.

(285) Chiu JJ, Wung BS, Hsieh HJ, Lo LW, Wang DL. Nitric oxide regulates shear stress-induced early growth response-1. Expression via the extracellular signal-regulated kinase pathway in endothelial cells. Circ Res 1999 Aug 6;85(3):238-46.

(286) Hsieh HJ, Li NQ, Frangos JA. Pulsatile and steady flow induces c-fos expression in human endothelial cells. J Cell Physiol 1993 Jan;154(1):143-51.

(287) Awolesi MA, Sessa WC, Sumpio BE. Cyclic strain upregulates nitric oxide synthase in cultured bovine aortic endothelial cells. J Clin Invest 1995 Sep;96(3):1449-54.

(288) Fisslthaler B, Popp R, Michaelis UR, Kiss L, Fleming I, Busse R. Cyclic stretch enhances the expression and activity of coronary endothelium-derived hyperpolarizing factor synthase. Hypertension 2001 Dec 1;38(6):1427-32.

(289) Shyy YJ, Hsieh HJ, Usami S, Chien S. Fluid shear stress induces a biphasic response of human monocyte chemotactic protein 1 gene expression in vascular endothelium. Proc Natl Acad Sci U S A 1994 May 24;91(11):4678-82.

(290) Chiu JJ, Chen LJ, Chen CN, Lee PL, Lee CI. A model for studying the effect of shear stress on interactions between vascular endothelial cells and smooth muscle cells. J Biomech 2004 Apr;37(4):531-9.

(291) Iba T, Sumpio BE. Tissue plasminogen activator expression in endothelial cells exposed to cyclic strain in vitro. Cell Transplant 1992;1(1):43-50.

(292) Diamond SL, Sharefkin JB, Dieffenbach C, Frasier-Scott K, McIntire LV, Eskin SG. Tissue plasminogen activator messenger RNA levels increase in cultured human endothelial cells exposed to laminar shear stress. J Cell Physiol 1990 May;143(2):364-71.

(293) Nguyen KT, Frye SR, Eskin SG, Patterson C, Runge MS, McIntire LV. Cyclic strain increases protease-activated receptor-1 expression in vascular smooth muscle cells. Hypertension 2001 Nov;38(5):1038-43.

(294) Kohler TR, Kirkman TR, Kraiss LW, Zierler BK, Clowes AW. Increased blood flow inhibits neointimal hyperplasia in endothelialized vascular grafts. Circ Res 1991 Dec;69(6):1557-65.

(295) Geary RL, Kohler TR, Vergel S, Kirkman TR, Clowes AW. Time course of flow-induced smooth muscle cell proliferation and intimal thickening in endothelialized baboon vascular grafts. Circ Res 1994 Jan;74(1):14-23.

(296) Fisher SA, Langille BL, Srivastava D. Apoptosis during cardiovascular development. Circ Res 2000 Nov 10;87(10):856-64.

(297) Cho A, Mitchell L, Koopmans D, Langille BL. Effects of changes in blood flow rate on cell death and cell proliferation in carotid arteries of immature rabbits. Circ Res 1997 Sep;81(3):328-37.

(298) Cho A, Courtman DW, Langille BL. Apoptosis (programmed cell death) in arteries of the neonatal lamb. Circ Res 1995 Feb;76(2):168-75.

(299) Berceli SA, Davies MG, Kenagy RD, Clowes AW. Flow-induced neointimal regression in baboon polytetrafluoroethylene grafts is associated with decreased cell proliferation and increased apoptosis. J Vasc Surg 2002 Dec;36(6):1248-55.

(300) Kenagy RD, Fischer JW, Davies MG, Berceli SA, Hawkins SM, Wight TN, et al. Increased plasmin and serine proteinase activity during flow-induced intimal atrophy in baboon PTFE grafts. Arterioscler Thromb Vasc Biol 2002 Mar 1;22(3):400-4.

(301) Kenagy RD, Fischer JW, Lara S, Sandy JD, Clowes AW, Wight TN. Accumulation and loss of extracellular matrix during shear stress-mediated intimal growth and regression in baboon vascular grafts. J Histochem Cytochem 2005 Jan;53(1):131-40.

(302) Hamdan AD, Aiello LP, Quist WC, Ozaki CK, Contreras MA, Phaneuf MD, et al. Isolation of genes differentially expressed at the downstream anastomosis of prosthetic arterial grafts with use of mRNA differential display. J Vasc Surg 1995 Feb;21(2):228-34.

(303) Cordero JA, Jr., Quist WC, Hamdan AD, Phaneuf MD, Contreras MA, LoGerfo FW. Identification of multiple genes with altered expression at the distal anastomosis of healing polytetrafluoroethylene grafts. J Vasc Surg 1998 Jul;28(1):157-66.

(304) Stone DH, Sivamurthy N, Contreras MA, Fitzgerald L, LoGerfo FW, Quist WC. Altered ubiquitin/proteasome expression in anastomotic intimal hyperplasia. J Vasc Surg 2001 Dec;34(6):1016-22.

(305) Willis DJ, Kalish JA, Li C, Deutsch ER, Contreras MA, LoGerfo FW, et al. Temporal gene expression following prosthetic arterial grafting. J Surg Res 2004 Jul;120(1):27-36.

(306) Geary RL, Wong JM, Rossini A, Schwartz SM, Adams LD. Expression profiling identifies 147 genes contributing to a unique primate neointimal smooth muscle cell phenotype. Arterioscler Thromb Vasc Biol 2002 Dec 1;22(12):2010-6.

(307) Kalish JA, Willis DJ, Li C, Link JJ, Deutsch ER, Contreras MA, et al. Temporal genomics of vein bypass grafting through oligonucleotide microarray analysis. J Vasc Surg 2004 Mar;39(3):645-54.

(308) Isoda K, Nishikawa K, Kamezawa Y, Yoshida M, Kusuhara M, Moroi M, et al. Osteopontin plays an important role in the development of medial thickening and neointimal formation. Circ Res 2002 Jul 12;91(1):77-82.

(309) van der Loop FT, Gabbiani G, Kohnen G, Ramaekers FC, van Eys GJ. Differentiation of smooth muscle cells in human blood vessels as defined by smoothelin, a novel marker for the contractile phenotype. Arterioscler Thromb Vasc Biol 1997 Apr;17(4):665-71.

(310) Sapienza P, di Marzo L, Cucina A, Corvino V, Mingoli A, Giustiniani Q, et al. Release of PDGF-BB and bFGF by human endothelial cells seeded on expanded polytetrafluoroethylene vascular grafts. J Surg Res 1998 Feb 15;75(1):24-9.

(311) Clowes AW, Kirkman TR, Reidy MA. Mechanisms of arterial graft healing. Rapid transmural capillary ingrowth provides a source of intimal endothelium and smooth muscle in porous PTFE prostheses. Am J Pathol 1986 May;123(2):220-30.

(312) Pitsch RJ, Minion DJ, Goman ML, van Aalst JA, Fox PL, Graham LM. Platelet-derived growth factor production by cells from Dacron grafts implanted in a canine model. J Vasc Surg 1997 Jul;26(1):70-8.

(313) Jeon BH, Chang SJ, Kim JW, Hong YM, Yoon SY, Choe IS. Effect of high blood flow on the expression of endothelial constitutive nitric oxide synthase in rats with femoral arteriovenous shunts. Endothelium 2000;7(4):243-52.

(314) Zhang JY, Beckman EJ, Piesco NP, Agarwal S. A new peptide-based urethane polymer: synthesis, biodegradation, and potential to support cell growth in vitro. Biomaterials 2000 Jun;21(12):1247-58.

(315) Menconi MJ, Owen T, Dasse KA, Stein G, Lian JB. Molecular approaches to the characterization of cell and blood/biomaterial interactions. J Card Surg 1992 Jun;7(2):177-87.

(316) Li S, Lao J, Chen BP, Li YS, Zhao Y, Chu J, et al. Genomic analysis of smooth muscle cells in 3-dimensional collagen matrix. FASEB J 2003 Jan;17(1):97-9.

(317) Vailhe B, Vittet D, Feige JJ. In vitro models of vasculogenesis and angiogenesis. Lab Invest 2001 Apr;81(4):439-52.

(318) Ueda A, Koga M, Ikeda M, Kudo S, Tanishita K. Effect of shear stress on microvessel network formation of endothelial cells with in vitro three-dimensional model. Am J Physiol Heart Circ Physiol 2004 Sep;287(3):H994-1002.

(319) Montesano R, Vassalli JD, Baird A, Guillemin R, Orci L. Basic fibroblast growth factor induces angiogenesis in vitro. Proc Natl Acad Sci U S A 1986 Oct;83(19):7297-301.

(320) Milkiewicz M, Brown MD, Egginton S, Hudlicka O. Association between shear stress, angiogenesis, and VEGF in skeletal muscles in vivo. Microcirculation 2001 Aug;8(4):229-41.

(321) Gloe T, Sohn HY, Meininger GA, Pohl U. Shear stress-induced release of basic fibroblast growth factor from endothelial cells is mediated by matrix interaction via integrin alpha(v)beta3. J Biol Chem 2002 Jun 28;277(26):23453-8.

(322) Lu X, Wang R. [Culture and identify the endothelial cells of human umbilical vein]. Wei Sheng Yan Jiu 2001 May;30(3):188-9, back.

(323) Rosenman JE, Kempczinski RF, Pearce WH, Silberstein EB. Kinetics of endothelial cell seeding. J Vasc Surg 1985 Nov;2(6):778-84.

(324) Schnittler HJ, Franke RP, Fuhrmann R ea. Influence of various substrates on the actin filament system of cultured human vascular endothelial cells exposed to fluid shear stress. 2005.

(325) Kaehler J, Zilla P, Fasol R, Deutsch M, Kadletz M. Precoating substrate and surface configuration determine adherence and spreading of seeded endothelial cells on polytetrafluoroethylene grafts. J Vasc Surg 1989 Apr;9(4):535-41.

(326) Baguneid M, Murray D, Salacinski HJ, Fuller B, Hamilton G, Walker M, et al. Shear-stress preconditioning and tissue-engineering-based paradigms for generating arterial substitutes. Biotechnol Appl Biochem 2004 Apr;39(Pt 2):151-7.

(327) Xiao L, Shi D. Role of precoating in artificial vessel endothelialization. Chin J Traumatol 2004 Oct;7(5):312-6.

(328) Fernandez P, Deguette A, Pothuaud L, Belleannee G, Coste P, Bordenave L. Quality control assessment of ePTFE precoating procedure for in vitro endothelial cell seeding. Biomaterials 2005 Aug;26(24):5042-7.

(329) Meinhart JG, Deutsch M, Fischlein T, Howanietz N, Froschl A, Zilla P. Clinical autologous in vitro endothelialization of 153 infrainguinal ePTFE grafts. Ann Thorac Surg 2001 May;71(5 Suppl):S327-S331.

(330) Lamm P, Juchem G, Milz S, Schuffenhauer M, Reichart B. Autologous endothelialized vein allograft: a solution in the search for small-caliber grafts in coronary artery bypass graft operations. Circulation 2001 Sep 18;104(12 Suppl 1):I108-I114.

(331) Kumar TR, Krishnan LK. Fibrin-mediated endothelial cell adhesion to vascular biomaterials resists shear stress due to flow. J Mater Sci Mater Med 2002 Aug;13(8):751-5.

(332) Yu H, Wang Y, Eton D, Rowe VL, Terramani TT, Cramer DV, et al. Dual cell seeding and the use of zymogen tissue plasminogen activator to improve cell retention on polytetrafluoroethylene grafts. J Vasc Surg 2001 Aug;34(2):337-43.

(333) Clowes MM, Lynch CM, Miller AD, Miller DG, Osborne WR, Clowes AW. Long-term biological response of injured rat carotid artery seeded with smooth muscle cells expressing retrovirally introduced human genes. J Clin Invest 1994 Feb;93(2):644-51.

(334) Geary RL, Clowes AW, Lau S, Vergel S, Dale DC, Osborne WR. Gene transfer in baboons using prosthetic vascular grafts seeded with retrovirally transduced smooth muscle cells: a model for local and systemic gene therapy. Hum Gene Ther 1994 Oct;5(10):1211-6.

(335) Yu H, Dai W, Yang Z, Kirkman P, Weaver FA, Eton D, et al. Smooth muscle cells improve endothelial cell retention on polytetrafluoroethylene grafts in vivo. J Vasc Surg 2003 Sep;38(3):557-63.

(336) Huber TS, Welling TH, Sarkar R, Messina LM, Stanley JC. Effects of retroviral-mediated tissue plasminogen activator gene transfer and expression on adherence and proliferation of canine endothelial cells seeded onto expanded polytetrafluoroethylene. J Vasc Surg 1995 Dec;22(6):795-803.

(337) Dunn PF, Newman KD, Jones M, Yamada I, Shayani V, Virmani R, et al. Seeding of vascular grafts with genetically modified endothelial cells. Secretion of recombinant TPA results in decreased seeded cell retention in vitro and in vivo. Circulation 1996 Apr 1;93(7):1439-46.

(338) Dardik A, Liu A, Ballermann BJ. Chronic in vitro shear stress stimulates endothelial cell retention on prosthetic vascular grafts and reduces subsequent in vivo neointimal thickness. J Vasc Surg 1999 Jan;29(1):157-67.

(339) Ott MJ, Ballermann BJ. Shear stress-conditioned, endothelial cell-seeded vascular grafts: improved cell adherence in response to in vitro shear stress. Surgery 1995 Mar;117(3):334-9.

(340) Ballermann BJ, Ott MJ. Adhesion and differentiation of endothelial cells by exposure to chronic shear stress: a vascular graft model. Blood Purif 1995;13(3-4):125-34.

(341) Schneider PA, Hanson SR, Price TM, Harker LA. Durability of confluent endothelial cell monolayers on small-caliber vascular prostheses in vitro. Surgery 1988 Apr;103(4):456-62.

(342) Sentissi JM, Ramberg K, O'Donnell TF, Jr., Connolly RJ, Callow AD. The effect of flow on vascular endothelial cells grown in tissue culture on polytetrafluoroethylene grafts. Surgery 1986 Mar;99(3):337-43.

(343) Kraiss LW, Kirkman TR, Kohler TR, Zierler B, Clowes AW. Shear stress regulates smooth muscle proliferation and neointimal thickening in porous polytetrafluoroethylene grafts. Arterioscler Thromb 1991 Nov;11(6):1844-52.

(344) Gulbins H, Dauner M, Petzold R, Goldemund A, Anderson I, Doser M, et al. Development of an artificial vessel lined with human vascular cells. J Thorac Cardiovasc Surg 2004 Sep;128(3):372-7.

(345) Gulbins H, Pritisanac A, Petzold R, Goldemund A, Doser M, Dauner M, et al. A low-flow adaptation phase improves shear-stress resistance of artificially seeded endothelial cells. Thorac Cardiovasc Surg 2005 Apr;53(2):96-102.

(346) Lee YS, Park DK, Kim YB, Seo JW, Lee KB, Min BG. Endothelial cell seeding onto the extracellular matrix of fibroblasts for the development of a small diameter polyurethane vessel. ASAIO J 1993 Jul;39(3):M740-M745.

(347) Fridman R, Alon Y, Doljanski F, Fuks Z, Vlodavsky I. Cell interaction with the extracellular matrices produced by endothelial cells and fibroblasts. Exp Cell Res 1985 Jun;158(2):461-76.

(348) Miyata T, Conte MS, Trudell LA, Mason D, Whittemore AD, Birinyi LK. Delayed exposure to pulsatile shear stress improves retention of human saphenous vein endothelial cells on seeded ePTFE grafts. J Surg Res 1991 May;50(5):485-93.

(349) Fillinger MF, Sampson LN, Cronenwett JL, Powell RJ, Wagner RJ. Coculture of endothelial cells and smooth muscle cells in bilayer and conditioned media models. J Surg Res 1997 Feb 1;67(2):169-78.

(350) Seliktar D, Nerem RM, Galis ZS. The role of matrix metalloproteinase-2 in the remodeling of cell-seeded vascular constructs subjected to cyclic strain. Ann Biomed Eng 2001 Nov;29(11):923-34.

(351) Stegemann JP, Nerem RM. Phenotype modulation in vascular tissue engineering using biochemical and mechanical stimulation. Ann Biomed Eng 2003 Apr;31(4):391-402.

(352) Feugier P, Black RA, Hunt JA, How TV. Attachment, morphology and adherence of human endothelial cells to vascular prosthesis materials under the action of shear stress. Biomaterials 2005 May;26(13):1457-66.

(353) Wolf S, Werthessen NT. Dynamics of arterial flow. Adv Exp Med Biol 1979;115:1-472.

(354) Pratt KJ, Williams SK, Jarrell BE. Enhanced adherence of human adult endothelial cells to plasma discharge modified polyethylene terephthalate. J Biomed Mater Res 1989 Oct;23(10):1131-47.

(355) Dewey CF, Jr., Bussolari SR, Gimbrone MA, Jr., Davies PF. The dynamic response of vascular endothelial cells to fluid shear stress. J Biomech Eng 1981 Aug;103(3):177-85.

(356) Langille LB. Integrity of arterial endothelium following acute exposure to high shear stress. Biorheology 1984;21(3):333-46.

(357) Reutelingsperger C, Van Goll R, Heijnen V, Frederik P, Lindhout T. The rotating disc as a device to study the adhesive properties of endothelial cells under differential shear stresses. 5, 361-367. 2005. Ref Type: Generic

(358) Dunkern TR, Paulitschke M, Meyer R, Buttemeyer R, Hetzer R, Burmester G, et al. A novel perfusion system for the endothelialisation of PTFE grafts under defined flow. Eur J Vasc Endovasc Surg 1999 Aug;18(2):105-10.

(359) Pratt KJ, Jarrell BE, Williams SK, Carabasi RA, Rupnick MA, Hubbard FA. Kinetics of endothelial cell-surface attachment forces. J Vasc Surg 1988 Apr;7(4):591-9.

(360) Ott MJ, Olson JL, Ballermann BJ. Chronic in vitro flow promotes ultrastructural differentiation of endothelial cells. Endothelium: Journal of Endothelial Cell Research 1995;3(1):21-30.

(361) Baldwin HS, Shen HM, Yan HC, Delisser HM, Chung A, Mickanin C, et al. Platelet endothelial cell adhesion molecule-1 (PECAM-1/CD31): alternatively spliced, functionally distinct isoforms expressed during mammalian cardiovascular development. Development 1994 Sep;120(9):2539-53.

(362) Pinter E, Barreuther M, Lu T, Imhof BA, Madri JA. Platelet-endothelial cell adhesion molecule-1 (PECAM-1/CD31) tyrosine phosphorylation state changes during vasculogenesis in the murine conceptus. Am J Pathol 1997 May;150(5):1523-30.

(363) Bogen S, Pak J, Garifallou M, Deng X, Muller WA. Monoclonal antibody to murine PECAM-1 (CD31) blocks acute inflammation in vivo. J Exp Med 1994 Mar 1;179(3):1059-64.

(364) Nakada MT, Amin K, Christofidou-Solomidou M, O'Brien CD, Sun J, Gurubhagavatula I, et al. Antibodies against the first Ig-like domain of human platelet endothelial cell adhesion molecule-1 (PECAM-1) that inhibit PECAM-1-dependent homophilic adhesion block in vivo neutrophil recruitment. J Immunol 2000 Jan 1;164(1):452-62.

(365) Newton-Nash DK, Newman PJ. A new role for platelet-endothelial cell adhesion molecule-1 (CD31): inhibition of TCR-mediated signal transduction. J Immunol 1999 Jul 15;163(2):682-8.

(366) Prager E, Staffler G, Majdic O, Saemann M, Godar S, Zlabinger G, et al. Induction of hyporesponsiveness and impaired T lymphocyte activation by the CD31 receptor:ligand pathway in T cells. J Immunol 2001 Feb 15;166(4):2364-71.

(367) Mahooti S, Graesser D, Patil S, Newman P, Duncan G, Mak T, et al. PECAM-1 (CD31) expression modulates bleeding time in vivo. Am J Pathol 2000 Jul;157(1):75-81.

(368) Patil S, Newman DK, Newman PJ. Platelet endothelial cell adhesion molecule-1 serves as an inhibitory receptor that modulates platelet responses to collagen. Blood 2001 Mar 15;97(6):1727-32.

(369) Ferrero E, Ferrero ME, Pardi R, Zocchi MR. The platelet endothelial cell adhesion molecule-1 (PECAM1) contributes to endothelial barrier function. FEBS Lett 1995 Nov 6;374(3):323-6.

(370) Carmeliet P, Jain RK. Angiogenesis in cancer and other diseases. Nature 2000 Sep 14;407(6801):249-57.

(371) Zhou Z, Christofidou-Solomidou M, Garlanda C, Delisser HM. Antibody against murine PECAM-1 inhibits tumor angiogenesis in mice. Angiogenesis 1999;3(2):181-8.

(372) Kim CS, Wang T, Madri JA. Platelet endothelial cell adhesion molecule-1 expression modulates endothelial cell migration in vitro. Lab Invest 1998 May;78(5):583-90.

(373) Schimmenti LA, Yan HC, Madri JA, Albelda SM. Platelet endothelial cell adhesion molecule, PECAM-1, modulates cell migration. J Cell Physiol 1992 Nov;153(2):417-28.

(374) Yang S, Graham J, Kahn JW, Schwartz EA, Gerritsen ME. Functional roles for PECAM-1 (CD31) and VE-cadherin (CD144) in tube assembly and lumen formation in three-dimensional collagen gels. Am J Pathol 1999 Sep;155(3):887-95.

(375) Delisser HM, Christofidou-Solomidou M, Strieter RM, Burdick MD, Robinson CS, Wexler RS, et al. Involvement of endothelial PECAM-1/CD31 in angiogenesis. Am J Pathol 1997 Sep;151(3):671-7.

(376) Halama T, Groger M, Pillinger M, Staffler G, Prager E, Stockinger H, et al. Platelet endothelial cell adhesion molecule-1 and vascular endothelial cadherin cooperatively regulate fibroblast growth factor-induced modulations of adherens junction functions. J Invest Dermatol 2001 Jan;116(1):110-7.

(377) Sheibani N, Newman PJ, Frazier WA. Thrombospondin-1, a natural inhibitor of angiogenesis, regulates platelet-endothelial cell adhesion molecule-1 expression and endothelial cell morphogenesis. Mol Biol Cell 1997 Jul;8(7):1329-41.

(378) Imbert E, Poot AA, Figdor CG, Feijen J. Expression of leukocyte adhesion molecules by endothelial cells seeded on various polymer surfaces. J Biomed Mater Res 2001 Sep 5;56(3):376-81.

(379) Muller WA. The role of PECAM-1 (CD31) in leukocyte emigration: studies in vitro and in vivo. J Leukoc Biol 1995 Apr;57(4):523-8.

(380) Cenni E, Granchi D, Ciapetti G, Verri E, Cavedagna D, Gamberini S, et al. Expression of adhesion molecules on endothelial cells after contact with knitted Dacron. Biomaterials 1997 Mar;18(6):489-94.

(381) Vaporciyan AA, Delisser HM, Yan HC, Mendiguren II, Thom SR, Jones ML, et al. Involvement of platelet-endothelial cell adhesion molecule-1 in neutrophil recruitment in vivo. Science 1993 Dec 3;262(5139):1580-2.

(382) Grimmond S, Lagercrantz J, Drinkwater C, Silins G, Townson S, Pollock P, et al. Cloning and characterization of a novel human gene related to vascular endothelial growth factor. Genome Res 1996 Feb;6(2):124-31.

(383) Lee J, Gray A, Yuan J, Luoh SM, Avraham H, Wood WI. Vascular endothelial growth factor-related protein: a ligand and specific activator of the tyrosine kinase receptor Flt4. Proc Natl Acad Sci U S A 1996 Mar 5;93(5):1988-92.

(384) Achen MG, Jeltsch M, Kukk E, Makinen T, Vitali A, Wilks AF, et al. Vascular endothelial growth factor D (VEGF-D) is a ligand for the tyrosine kinases VEGF receptor 2 (Flk1) and VEGF receptor 3 (Flt4). Proc Natl Acad Sci U S A 1998 Jan 20;95(2):548-53.

(385) Shibuya M, Yamaguchi S, Yamane A, Ikeda T, Tojo A, Matsushime H, et al. Nucleotide sequence and expression of a novel human receptor-type tyrosine kinase gene (flt) closely related to the fms family. Oncogene 1990 Apr;5(4):519-24.

(386) Matthews W, Jordan CT, Gavin M, Jenkins NA, Copeland NG, Lemischka IR. A receptor tyrosine kinase cDNA isolated from a population of enriched primitive hematopoietic cells and exhibiting close genetic linkage to c-kit. Proc Natl Acad Sci U S A 1991 Oct 15;88(20):9026-30.

(387) Mustonen T, Alitalo K. Endothelial receptor tyrosine kinases involved in angiogenesis. J Cell Biol 1995 May;129(4):895-8.

(388) Thomas KA. Vascular endothelial growth factor, a potent and selective angiogenic agent. J Biol Chem 1996 Jan 12;271(2):603-6.

(389) Shalaby F, Rossant J, Yamaguchi TP, Gertsenstein M, Wu XF, Breitman ML, et al. Failure of blood-island formation and vasculogenesis in Flk-1-deficient mice. Nature 1995 Jul 6;376(6535):62-6.

(390) Pepper MS, Ferrara N, Orci L, Montesano R. Potent synergism between vascular endothelial growth factor and basic fibroblast growth factor in the induction of angiogenesis in vitro. Biochem Biophys Res Commun 1992 Dec 15;189(2):824-31.

(391) Hanahan D, Folkman J. Patterns and emerging mechanisms of the angiogenic switch during tumorigenesis. Cell 1996 Aug 9;86(3):353-64.

(392) Ghosh J, Murphy MO, Turner N, Khwaja N, Halka A, Kielty CM, et al. The role of transforming growth factor beta1 in the vascular system. Cardiovasc Pathol 2005 Jan;14(1):28-36.

(393) Heimark RL, Twardzik DR, Schwartz SM. Inhibition of endothelial regeneration by type-beta transforming growth factor from platelets. Science 1986 Sep 5;233(4768):1078-80.

(394) Muller G, Behrens J, Nussbaumer U, Bohlen P, Birchmeier W. Inhibitory action of transforming growth factor beta on endothelial cells. Proc Natl Acad Sci U S A 1987 Aug;84(16):5600-4.

(395) Majack RA. Beta-type transforming growth factor specifies organizational behavior in vascular smooth muscle cell cultures. J Cell Biol 1987 Jul;105(1):465-71.

(396) Battegay EJ, Raines EW, Seifert RA, Bowen-Pope DF, Ross R. TGF-beta induces bimodal proliferation of connective tissue cells via complex control of an autocrine PDGF loop. Cell 1990 Nov 2;63(3):515-24.

(397) Pepper MS, Vassalli JD, Orci L, Montesano R. Biphasic effect of transforming growth factor-beta 1 on in vitro angiogenesis. Exp Cell Res 1993 Feb;204(2):356-63.

(398) Pepper MS. Transforming growth factor-beta: vasculogenesis, angiogenesis, and vessel wall integrity. Cytokine Growth Factor Rev 1997 Mar;8(1):21-43.

(399) Ohno M, Cooke JP, Dzau VJ, Gibbons GH. Fluid shear stress induces endothelial transforming growth factor beta-1 transcription and production. Modulation by potassium channel blockade. J Clin Invest 1995 Mar;95(3):1363-9.

(400) Lum RM, Wiley LM, Barakat AI. Influence of different forms of fluid shear stress on vascular endothelial TGF-beta1 mRNA expression. Int J Mol Med 2000 Jun;5(6):635-41.

(401) Barber RD, Harmer DW, Coleman RA, Clark BJ. GAPDH as a housekeeping gene: analysis of GAPDH mRNA expression in a panel of 72 human tissues. Physiol Genomics 2005 May 11;21(3):389-95.

(402) Zhang Z, Xiao Z, Diamond SL. Shear stress induction of C-type natriuretic peptide (CNP) in endothelial cells is independent of NO autocrine signaling. Ann Biomed Eng 1999 Jul;27(4):419-26.

(403) Sakai K, Mohtai M, Iwamoto Y. Fluid shear stress increases transforming growth factor beta 1 expression in human osteoblast-like cells: modulation by cation channel blockades. Calcif Tissue Int 1998 Dec;63(6):515-20.

(404) Huddleson JP, Srinivasan S, Ahmad N, Lingrel JB. Fluid shear stress induces endothelial KLF2 gene expression through a defined promoter region. Biol Chem 2004 Aug;385(8):723-9.

(405) Houston P, Dickson MC, Ludbrook V, White B, Schwachtgen JL, McVey JH, et al. Fluid shear stress induction of the tissue factor promoter in vitro and in vivo is mediated by Egr-1. Arterioscler Thromb Vasc Biol 1999 Feb;19(2):281-9.

(406) Schubert A, Cattaruzza M, Hecker M, Darmer D, Holtz J, Morawietz H. Shear stress-dependent regulation of the human beta-tubulin folding cofactor D gene. Circ Res 2000 Dec 8;87(12):1188-94.

(407) Thi MM, Kojima T, Cowin SC, Weinbaum S, Spray DC. Fluid shear stress remodels expression and function of junctional proteins in cultured bone cells. Am J Physiol Cell Physiol 2003 Feb;284(2):C389-C403.

(408) Huddleson JP, Ahmad N, Srinivasan S, Lingrel JB. Induction of KLF2 by fluid shear stress requires a novel promoter element activated by a phosphatidylinositol 3-kinase-dependent chromatin-remodeling pathway. J Biol Chem 2005 Jun 17;280(24):23371-9.

(409) Greisler HP, Johnson S, Joyce K, Henderson S, Patel NM, Alkhamis T, et al. The effects of shear stress on endothelial cell retention and function on expanded polytetrafluoroethylene. Arch Surg 1990 Dec;125(12):1622-5.

(410) Walpola PL, Gotlieb AI, Cybulsky MI, Langille BL. Expression of ICAM-1 and VCAM-1 and monocyte adherence in arteries exposed to altered shear stress. Arterioscler Thromb Vasc Biol 1995 Jan;15(1):2-10.

(411) Frangos JA, Eskin SG, McIntire LV, Ives CL. Flow effects on prostacyclin production by cultured human endothelial cells. Science 1985 Mar 22;227(4693):1477-9.

(412) Young C, Jarrell BE, Hoying JB, Williams SK. A porcine model for adipose tissue-derived endothelial cell transplantation. Cell Transplant 1992;1(4):293-8.

(413) Solomon DE. The seeding of human aortic endothelial cells on the extra-cellular matrix of human umbilical vein endothelial cells. Int J Exp Pathol 1992 Aug;73(4):491-501.

(414) Goldman S, Copeland J, Moritz T, Henderson W, Zadina K, Ovitt T, et al. Saphenous vein graft patency 1 year after coronary artery bypass surgery and effects of antiplatelet therapy. Results of a Veterans Administration Cooperative Study. Circulation 1989 Nov;80(5):1190-7.

(415) Herring MB, Dilley R, Jersild RA, Jr., Boxer L, Gardner A, Glover J. Seeding arterial prostheses with vascular endothelium. The nature of the lining. Ann Surg 1979 Jul;190(1):84-90.

(416) Grenier G, Remy-Zolghadri M, Guignard R, Bergeron F, Labbe R, Auger FA, et al. Isolation and culture of the three vascular cell types from a small vein biopsy sample. In Vitro Cell Dev Biol Anim 2003 Mar;39(3-4):131-9.

(417) Pearce WH, Rutherford RB, Whitehill TA, Rosales C, Bell KP, Patt A, et al. Successful endothelial seeding with omentally derived microvascular endothelial cells. J Vasc Surg 1987 Jan;5(1):203-6.

(418) Arts CH, Hedeman Joosten PP, Blankensteijn JD, Staal FJ, Ng PY, Heijnen-Snyder GJ, et al. Contaminants from the transplant contribute to intimal hyperplasia associated with microvascular endothelial cell seeding. Eur J Vasc Endovasc Surg 2002 Jan;23(1):29-38.

(419) Hewett PW, Murray JC. Immunomagnetic purification of human microvessel endothelial cells using Dynabeads coated with monoclonal antibodies to PECAM-1. Eur J Cell Biol 1993 Dec;62(2):451-4.

(420) Vici M, Pasquinelli G, Preda P, Martinelli GN, Gibellini D, Freyrie A, et al. Electron microscopic and immunocytochemical profiles of human subcutaneous fat tissue microvascular endothelial cells. Ann Vasc Surg 1993 Nov;7(6):541-8.

(421) Curti T, Pasquinelli G, Preda P, Freyrie A, Laschi R, D'Addato M. An ultrastructural and immunocytochemical analysis of human endothelial cell adhesion on coated vascular grafts. Ann Vasc Surg 1989 Oct;3(4):351-63.

(422) Salacinski HJ, Punshon G, Krijgsman B, Hamilton G, Seifalian AM. A hybrid compliant vascular graft seeded with microvascular endothelial cells extracted from human omentum. Artif Organs 2001 Dec;25(12):974-82.

(423) Hernando A, Garcia-Honduvilla N, Bellon JM, Bujan J, Navlet J. Coatings for vascular prostheses: mesothelial cells express specific markers for muscle cells and have biological activity similar to that of endothelial cells. Eur J Vasc Surg 1994 Sep;8(5):531-6.

(424) Morganti M, Budianto D, Takiy BA, Henze U, Mittermayer C, Sagripanti A, et al. Detection of minimal but significant amount of von Willebrand factor in human omentum mesothelial cell cultures. Biomed Pharmacother 1996;50(8):369-72.

(425) Pasic M, Muller-Glauser W, von Segesser L, Odermatt B, Lachat M, Turina M. Endothelial cell seeding improves patency of synthetic vascular grafts: manual versus automatized method. Eur J Cardiothorac Surg 1996;10(5):372-9.

(426) Clarke JM, Pittilo RM, Nicholson LJ, Woolf N, Marston A. Seeding Dacron arterial prostheses with peritoneal mesothelial cells: a preliminary morphological study. Br J Surg 1984 Jul;71(7):492-4.

(427) Sterpetti AV, Hunter WJ, Schultz RD, Sugimoto JT, Blair EA, Hacker K, et al. Seeding with endothelial cells derived from the microvessels of the omentum and from the jugular vein: a comparative study. J Vasc Surg 1988 May;7(5):677-84.

(428) Pasic M, Muller-Glauser W, von Segesser LK, Lachat M, Mihaljevic T, Turina MI. Superior late patency of small-diameter Dacron grafts seeded with omental microvascular cells: an experimental study. Ann Thorac Surg 1994 Sep;58(3):677-83.

(429) Verhagen HJ, Blankensteijn JD, de Groot PG, Heijnen-Snyder GJ, Pronk A, Vroom TM, et al. In vivo experiments with mesothelial cell seeded ePTFE vascular grafts. Eur J Vasc Endovasc Surg 1998 Jun;15(6):489-96.

(430) Ivarsson ML, Holmdahl L, Falk P, Molne J, Risberg B. Characterization and fibrinolytic properties of mesothelial cells isolated from peritoneal lavage. Scand J Clin Lab Invest 1998 May;58(3):195-203.

(431) Van Horn DL, Hanna C, Schultz RO. Corneal cryopreservation. II. Ultrastructural and viability changes. Arch Ophthalmol 1970 Nov;84(5):655-67.

(432) Hartmann C, Rieck P. A new test for endothelial viability. The Janus green photometry technique. Arch Ophthalmol 1989 Oct;107(10):1511-5.

(433) Poole CA, Brookes NH, Clover GM. Keratocyte networks visualised in the living cornea using vital dyes. J Cell Sci 1993 Oct;106 (Pt 2):685-91.

(434) Wilhelm F, Melzig M, Gorscher T, Franke G. [Differential value of various vital stains of corneal endothelium]. Ophthalmologe 1995 Aug;92(4):496-8.

(435) Lindstrom RL, Doughman DJ, Van Horn DL, Dancil D, Harris JE. A metabolic and electron microscopic study of human organ-cultured cornea. Am J Ophthalmol 1976 Jul;82(1):72-82.

(436) Mosmann T. Rapid colorimetric assay for cellular growth and survival: application to proliferation and cytotoxicity assays. J Immunol Methods 1983 Dec 16;65(1-2):55-63.

(437) Lin HB, Sun W, Mosher DF, Garcia-Echeverria C, Schaufelberger K, Lelkes PI, et al. Synthesis, surface, and cell-adhesion properties of polyurethanes containing covalently grafted RGD-peptides. J Biomed Mater Res 1994 Mar;28(3):329-42.

(438) Scudiero DA, Shoemaker RH, Paull KD, Monks A, Tierney S, Nofziger TH, et al. Evaluation of a soluble tetrazolium/formazan assay for cell growth and drug sensitivity in culture using human and other tumor cell lines. Cancer Res 1988 Sep 1;48(17):4827-33.

(439) Nikolaychik VV, Samet MM, Lelkes PI. A new method for continual quantitation of viable cells on endothelialized polyurethanes. J Biomater Sci Polym Ed 1996;7(10):881-91.

(440) Lindstrom RL, Kaufman HE, Skelnik DL, Laing RA, Lass JH, Musch DC, et al. Optisol corneal storage medium. Am J Ophthalmol 1992 Sep 15;114(3):345-56.

(441) Kempermann G, Gage FH. New nerve cells for the adult brain. Sci Am 1999 May;280(5):48-53.

(442) Skehan P, Storeng R, Scudiero D, Monks A, McMahon J, Vistica D, et al. New colorimetric cytotoxicity assay for anticancer-drug screening. J Natl Cancer Inst 1990 Jul 4;82(13):1107-12.

(443) Papadimitriou E, Lelkes PI. Measurement of cell numbers in microtiter culture plates using the fluorescent dye Hoechst 33258. J Immunol Methods 1993 Jun 4;162(1):41-5.

(444) Seifalian AM, Salacinski HJ, Punshon G, Krijgsman B, Hamilton G. A new technique for measuring the cell growth and metabolism of endothelial cells seeded on vascular prostheses. J Biomed Mater Res 2001 Jun 15;55(4):637-44.

(445) Ahmed SA, Gogal RM, Jr., Walsh JE. A new rapid and simple non-radioactive assay to monitor and determine the proliferation of lymphocytes: an

alternative to [3H]thymidine incorporation assay. J Immunol Methods 1994 Apr 15;170(2):211-24.

(446) Salacinski HJ, Hancock S, Seifalian AM, inventors; Polymer for use in conduits and medical devices.0401204. 2005.

(447) Shahan TA, Siegel PD, Sorenson WG, Kuschner WG, Lewis DM. A sensitive new bioassay for tumor necrosis factor. J Immunol Methods 1994 Oct 14;175(2):181-7.

(448) Farinelli SE, Greene LA. Cell cycle blockers mimosine, ciclopirox, and deferoxamine prevent the death of PC12 cells and postmitotic sympathetic neurons after removal of trophic support. J Neurosci 1996 Feb 1;16(3):1150-62.

(449) Baker CN, Banerjee SN, Tenover FC. Evaluation of Alamar colorimetric MIC method for antimicrobial susceptibility testing of gram-negative bacteria. J Clin Microbiol 1994 May;32(5):1261-7.

(450) Pfaller MA, Barry AL. Evaluation of a novel colorimetric broth microdilution method for antifungal susceptibility testing of yeast isolates. J Clin Microbiol 1994 Aug;32(8):1992-6.

(451) Fields RD, Lancaster MV. Dual-attribute continuous monitoring of cell proliferation/cytotoxicity. Am Biotechnol Lab 1993 Mar;11(4):48-50.

(452) Ahn SJ, Costa J, Emanuel JR. PicoGreen quantitation of DNA: effective evaluation of samples pre- or post-PCR. Nucleic Acids Res 1996 Jul 1;24(13):2623-5.

(453) Marois Y, Guidoin R, Roy R, Vidovsky T, Jakubiec B, Sigot-Luizard MF, et al. Selecting valid in vitro biocompatibility tests that predict the in vivo healing response of synthetic vascular prostheses. Biomaterials 1996 Oct;17(19):1835-42.

(454) Korzeniewski C, Callewaert DM. An enzyme-release assay for natural cytotoxicity. J Immunol Methods 1983 Nov 25;64(3):313-20.

(455) Decker T, Lohmann-Matthes ML. A quick and simple method for the quantitation of lactate dehydrogenase release in measurements of cellular cytotoxicity and tumor necrosis factor (TNF) activity. J Immunol Methods 1988 Nov 25;115(1):61-9.

(456) Thompson CA, Colon-Hernandez P, Pomerantseva I, MacNeil BD, Nasseri B, Vacanti JP, et al. A novel pulsatile, laminar flow bioreactor for the development of tissue-engineered vascular structures. Tissue Eng 2002 Dec;8(6):1083-8.

(457) Hoerstrup SP, Sodian R, Sperling JS, Vacanti JP, Mayer JE, Jr. New pulsatile bioreactor for in vitro formation of tissue engineered heart valves. Tissue Eng 2000 Feb;6(1):75-9.

(458) Sodian R, Lemke T, Fritsche C, Hoerstrup SP, Fu P, Potapov EV, et al. Tissue-engineering bioreactors: a new combined cell-seeding and perfusion system for vascular tissue engineering. Tissue Eng 2002 Oct;8(5):863-70.

(459) Sodian R, Lemke T, Loebe M, Hoerstrup SP, Potapov EV, Hausmann H, et al. New pulsatile bioreactor for fabrication of tissue-engineered patches. J Biomed Mater Res 2001;58(4):401-5.

(460) Hoerstrup SP, Zund G, Sodian R, Schnell AM, Grunenfelder J, Turina MI. Tissue engineering of small caliber vascular grafts. Eur J Cardiothorac Surg 2001 Jul;20(1):164-9.

(461) Punshon G, Vara DS, Sales KM, Kidane AG, Salacinski HJ, Seifalian AM. Interactions between endothelial cells and a poly(carbonate-silsesquioxane-bridge-urea)urethane. Biomaterials 2005 Nov;26(32):6271-9.

(462) Oluwole BO, Du W, Mills I, Sumpio BE. Gene regulation by mechanical forces. Endothelium 1997;5(2):85-93.

(463) Bottaro DP, Liebmann-Vinson A, Heidaran MA. Molecular signaling in bioengineered tissue microenvironments. Ann N Y Acad Sci 2002 Jun;961:143-53.

(464) Bissell MJ, Radisky D. Putting tumours in context. Nat Rev Cancer 2001 Oct;1(1):46-54.

(465) Cukierman E, Pankov R, Stevens DR, Yamada KM. Taking cell-matrix adhesions to the third dimension. Science 2001 Nov 23;294(5547):1708-12.

(466) Breen EC, Fu Z, Normand H. Calcyclin gene expression is increased by mechanical strain in fibroblasts and lung. Am J Respir Cell Mol Biol 1999 Dec;21(6):746-52.

(467) Lafrenie RM, Bernier SM, Yamada KM. Adhesion to fibronectin or collagen I gel induces rapid, extensive, biosynthetic alterations in epithelial cells. J Cell Physiol 1998 May;175(2):163-73.

(468) Lam K, Zhang L, Yamada KM, Lafrenie RM. Adhesion of epithelial cells to fibronectin or collagen I induces alterations in gene expression via a protein kinase C-dependent mechanism. J Cell Physiol 2001 Oct;189(1):79-90.

(469) Gerritsen ME, Soriano R, Yang S, Zlot C, Ingle G, Toy K, et al. Branching out: a molecular fingerprint of endothelial differentiation into tube-like structures generated by Affymetrix oligonucleotide arrays. Microcirculation 2003 Jan;10(1):63-81.

(470) Song RH, Kocharyan HK, Fortunato JE, Glagov S, Bassiouny HS. Increased flow and shear stress enhance in vivo transforming growth factor-beta1 after experimental arterial injury. Arterioscler Thromb Vasc Biol 2000 Apr;20(4):923-30.

(471) Seifalian AM, Salacinski HJ, Tiwari A, Edwards A, Bowald S, Hamilton G. In vivo biostability of a poly(carbonate-urea)urethane graft. Biomaterials 2003 Jun;24(14):2549-57.

(472) Passerini AG, Polacek DC, Shi C, Francesco NM, Manduchi E, Grant GR, et al. Coexisting proinflammatory and antioxidative endothelial transcription profiles in a disturbed flow region of the adult porcine aorta. Proc Natl Acad Sci U S A 2004 Feb 24;101(8):2482-7.

(473) Ota T, Fujii M, Sugizaki T, Ishii M, Miyazawa K, Aburatani H, et al. Targets of transcriptional regulation by two distinct type I receptors for transforming growth factor-beta in human umbilical vein endothelial cells. J Cell Physiol 2002 Dec;193(3):299-318.

(474) Kirkpatrick JE. Symptoms in peripheral artery disease. J Insur Med 1999;31(1):37-8.

(475) Inoguchi H, Kwon IK, Inoue E, Takamizawa K, Maehara Y, Matsuda T. Mechanical responses of a compliant electrospun poly(L-lactide-co-epsilon-caprolactone) small-diameter vascular graft. Biomaterials 2006 Mar;27(8):1470-8.

(476) Khorasani MT, Shorgashti S. Fabrication of microporous polyurethane by spray phase inversion method as small diameter vascular grafts material. J Biomed Mater Res A 2006 May;77(2):253-60.

(477) Zdrahala RJ. Small caliber vascular grafts. Part II: Polyurethanes revisited. J Biomater Appl 1996 Jul;11(1):37-61.

(478) Kannan RY, Salacinski HJ, Edirisinghe MJ, Hamilton G, Seifalian AM. Polyhedral oligomeric silsequioxane-polyurethane nanocomposite microvessels for an artificial capillary bed. Biomaterials 2006 Sep;27(26):4618-26.

(479) Chen JH, Laiw RF, Jiang SF, Lee YD. Microporous segmented polyetherurethane vascular graft: I. Dependency of graft morphology and mechanical properties on compositions and fabrication conditions. J Biomed Mater Res 1999;48(3):235-45.

(480) White R, Goldberg L, Hirose F, Klein S, Bosco P, Miranda R, et al. Effect of healing on small internal diameter arterial graft compliance. Biomater Med Devices Artif Organs 1983;11(1):21-9.

(481) Tai NR, Salacinski HJ, Edwards A, Hamilton G, Seifalian AM. Compliance properties of conduits used in vascular reconstruction. Br J Surg 2000 Nov;87(11):1516-24.

(482) Charlesworth D, White ET, Kent.S, inventors;US2,130,521B. 1985.

(483) Keener J, Sned J. Mathematical Physiology. Springer-Verlag: New York; 1998.

(484) Walden R, L'Italien GJ, Megerman J, Abbott WM. Matched elastic properties and successful arterial grafting. Arch Surg 1980 Oct;115(10):1166-9.

(485) Greenwald SE, Berry CL. Improving vascular grafts: the importance of mechanical and haemodynamic properties. J Pathol 2000 Feb;190(3):292-9.

(486) Cameron A, Davis KB, Green G, Schaff HV. Coronary bypass surgery with internal-thoracic-artery grafts--effects on survival over a 15-year period. N Engl J Med 1996 Jan 25;334(4):216-9.

(487) Zilla P, Deutsch M, Meinhart J, Puschmann R, Eberl T, Minar E, et al. Clinical in vitro endothelialization of femoropopliteal bypass grafts: an actuarial follow-up over three years. J Vasc Surg 1994 Mar;19(3):540-8.

(488) Coulomb B, Dubertret L. Skin cell culture and wound healing. Wound Repair Regen 2002 Mar;10(2):109-12.

(489) Jones I, Currie L, Martin R. A guide to biological skin substitutes. Br J Plast Surg 2002 Apr;55(3):185-93.

(490) Boyce ST. Design principles for composition and performance of cultured skin substitutes. Burns 2001 Aug;27(5):523-33.

(491) Shimizu T, Yamato M, Kikuchi A, Okano T. Cell sheet engineering for myocardial tissue reconstruction. Biomaterials 2003 Jun;24(13):2309-16.

(492) Ochoa ER, Vacanti JP. An overview of the pathology and approaches to tissue engineering. Ann N Y Acad Sci 2002 Dec;979:10-26.

(493) Yang S, Leong KF, Du Z, Chua CK. The design of scaffolds for use in tissue engineering. Part I. Traditional factors. Tissue Eng 2001 Dec;7(6):679-89.

(494) Lu L, Zhu X, Valenzuela RG, Currier BL, Yaszemski MJ. Biodegradable polymer scaffolds for cartilage tissue engineering. Clin Orthop Relat Res 2001 Oct;(391 Suppl):S251-S270.

(495) Feng Z, Yamato M, Akutsu T, Nakamura T, Okano T, Umezu M. Investigation on the mechanical properties of contracted collagen gels as a scaffold for tissue engineering. Artif Organs 2003 Jan;27(1):84-91.

(496) Lee CR, Grodzinsky AJ, Spector M. The effects of cross-linking of collagen-glycosaminoglycan scaffolds on compressive stiffness, chondrocyte-mediated contraction, proliferation and biosynthesis. Biomaterials 2001 Dec;22(23):3145-54.

(497) Wang XH, Li DP, Wang WJ, Feng QL, Cui FZ, Xu YX, et al. Crosslinked collagen/chitosan matrix for artificial livers. Biomaterials 2003 Aug;24(19):3213-20.

(498) Illi B, Nanni S, Scopece A, Farsetti A, Biglioli P, Capogrossi MC, et al. Shear stress-mediated chromatin remodeling provides molecular basis for flow-dependent regulation of gene expression. Circ Res 2003 Jul 25;93(2):155-61.

(499) Wasserman SM, Topper JN. Adaptation of the endothelium to fluid flow: in vitro analyses of gene expression and in vivo implications. Vasc Med 2004 Feb;9(1):35-45.

(500) Vara DS, Punshon G, Sales KM, Salacinski HJ, Dijk S, Brown RA, et al. Development of an RNA isolation procedure for the characterisation of human endothelial cell interactions with polyurethane cardiovascular bypass grafts. Biomaterials 2005 Jun;26(18):3987-93.

(501) Vara DS, Punshon G, Sales KM, Hamilton G, Seifalian AM. The effect of shear stress on human endothelial cells seeded on cylindrical viscoelastic conduits: an investigation of gene expression. Biotechnol Appl Biochem 2006 Nov;45(Pt 3):119-30.

(502) Cucina A, Sterpetti AV, Borrelli V, Pagliei S, Cavallaro A, D'Angelo LS. Shear stress induces transforming growth factor-beta 1 release by arterial endothelial cells. Surgery 1998 Feb;123(2):212-7.

(503) Fujiwara K, Masuda M, Osawa M, Kano Y, Katoh K. Is PECAM-1 a mechanoresponsive molecule? Cell Struct Funct 2001 Feb;26(1):11-7.

(504) Li YS, Haga JH, Chien S. Molecular basis of the effects of shear stress on vascular endothelial cells. J Biomech 2005 Oct;38(10):1949-71.

(505) Mitola S, Brenchio B, Piccinini M, Tertoolen L, Zammataro L, Breier G, et al. Type I collagen limits VEGFR-2 signaling by a SHP2 protein-tyrosine phosphatase-dependent mechanism 1. Circ Res 2006 Jan 6;98(1):45-54.

(506) Wang N, Miao H, Li YS, Zhang P, Haga JH, Hu Y, et al. Shear stress regulation of Kruppel-like factor 2 expression is flow pattern-specific. Biochem Biophys Res Commun 2006 Mar 24;341(4):1244-51.

(507) Fawcett J, Buckley C, Holness CL, Bird IN, Spragg JH, Saunders J, et al. Mapping the homotypic binding sites in CD31 and the role of CD31 adhesion in the formation of interendothelial cell contacts. J Cell Biol 1995 Mar;128(6):1229-41.

(508) Korshunov VA, Berk BC. Flow-induced vascular remodeling in the mouse: a model for carotid intima-media thickening. Arterioscler Thromb Vasc Biol 2003 Dec;23(12):2185-91.

(509) Jockenhoevel S, Zund G, Hoerstrup SP, Schnell A, Turina M. Cardiovascular tissue engineering: a new laminar flow chamber for in vitro improvement of mechanical tissue properties. ASAIO J 2002 Jan;48(1):8-11.

(510) Ueba H, Kawakami M, Yaginuma T. Shear stress as an inhibitor of vascular smooth muscle cell proliferation. Role of transforming growth factor-beta 1 and tissue-type plasminogen activator. Arterioscler Thromb Vasc Biol 1997 Aug;17(8):1512-6.

(511) Medhurst AD, Harrison DC, Read SJ, Campbell CA, Robbins MJ, Pangalos MN. The use of TaqMan RT-PCR assays for semiquantitative analysis of gene expression in CNS tissues and disease models. J Neurosci Methods 2000 May 15;98(1):9-20.

(512) Gibson UE, Heid CA, Williams PM. A novel method for real time quantitative RT-PCR. Genome Res 1996 Oct;6(10):995-1001.

(513) Lion T. Control genes in reverse transcriptase-polymerase chain reaction assays. Leukemia 1996 Sep;10(9):1527-8.

(514) Magid R, Murphy TJ, Galis ZS. Expression of matrix metalloproteinase-9 in endothelial cells is differentially regulated by shear stress. Role of c-Myc. J Biol Chem 2003 Aug 29;278(35):32994-9.

(515) Kannan RY, Salacinski HJ, Butler PE, Hamilton G, Seifalian AM. Current status of prosthetic bypass grafts: a review. J Biomed Mater Res B Appl Biomater 2005 Jul;74(1):570-81.

(516) Shay-Salit A, Shushy M, Wolfovitz E, Yahav H, Breviario F, Dejana E, et al. VEGF receptor 2 and the adherens junction as a mechanical transducer in vascular endothelial cells. Proc Natl Acad Sci U S A 2002 Jul 9;99(14):9462-7.

(517) Sumpio BE. Hemodynamic forces and vascular cell biology. RG Landes Co; 1993.